United States Department of Agriculture

August 2016

Hydrology Technical Note No. 4

Hydrologic Analyses of Post-Wildfire Conditions

Natural Resources Conservation Service

August 2016

Cover photo: Nabours Mountain directly east of Glenwood, NM. Photo courtesy of USDA Forest Service, Gila National Forest, Silver City, NM

Acknowledgments

This technical note was developed, as noted, by **Dan Moore**, Hydraulic Engineer, West National Technology Support Center, NRCS, Portland, OR, (Case Study 4: Whitewater Creek; Gila Wilderness, NM); **Nathaniel Todea**, Hydraulic Engineer, NRCS, Salt Lake City, UT, (Case Study 5: Saratoga Springs Wildfire, UT); **Geoff Cerrelli**, retired, Hydraulic Engineer, NRCS, (Case Study 2: Bitterroot Wildfires, MT); **Steven Yochum**, Hydrologist, U.S. Forest Service, Fort Collins, CO, (formerly NRCS, Lakewood, CO), (Case Study 1: High Park Fire, CO, and Case Study 3: West Fork Complex Fire, CO); **John B. Norman, III**, Soil Scientist, Major Land Resource Area, Soil Survey Office, NRCS, Fort Collins, CO (Case Study 3: West Fork Complex Fire, CO); and **Claudia Hoeft**, National Hydraulic Engineer, NRCS, Washington DC.

Table of Contents

Appendix A: Case Study 1, High Park Fire, Colorado

Appendix B: Case Study 2, Bitterroot Wildfires, Montana

Appendix C: Case Study 3, West Force Complex Fire, Colorado

Appendix D: Case Study 4, Whitewater Creek, Gila Wilderness, New Mexico

Appendix E: Case Study 5, Saratoga Springs, Utah

Figures

Appendix A Figures

Appendix B Figures

Appendix C Figures

Appendix D Figures

Appendix E Figures

Tables

Appendix Tables

Hydrologic Analyses of Post-Wildfire Conditions

Introduction

Periodic wildfires occur naturally in forests of the Western United States. Whether natural or human-caused, wildfire changes the landscape immediately, extensively, and with long-term effects. One of the most significant effects is the removal of protective vegetation, resulting in more rapid runoff. Wildfire also frequently inhibits soil infiltration, resulting in larger runoff volumes. The radically changed hydrologic response of burned watersheds also causes post-wildfire runoff events to excessively erode streambanks and transport high loads of sediment and debris.

Hydrologists can help communities prepare for post-wildfire conditions using predictive rainfall-runoff models. Runoff and erosion expected after a fire can be estimated, along with the probabilities of various flood levels. These models also assist in planning revegetation efforts in burned watersheds by revealing areas that will provide the greatest benefit from the application of conservation activities.

This technical note provides hydrologic guidance for analysis of burned watersheds. It discusses specific impacts of wildfire on the runoff process, with detailed information on modeling the rainfall runoff process in burned watersheds. Various hydrologic models and analysis techniques may be profitably used to estimate post-wildfire flooding and sedimentation. Five case studies document these techniques, modeling actual wildfire-burned watersheds.

The Role of NRCS in Post-Fire Assessments and Modeling

Many Federal agencies provide assistance related to wildfire (table 1). In contrast to the public-land focus of many agencies, NRCS helps private landowners with conservation practices that promote good land management. As individual landowners seek to take advantage of the benefits of conservation, they rely on NRCS' technical expertise in agronomy, soils, rangeland management, nutrient and pesticide management, biology, and hydrology, among other disciplines. After a fire, NRCS can provide rapid assessments of expected increased flood peaks, sediment flow in streams, and other hazards on the watershed. As post-fire spatial data becomes available, NRCS can provide downstream communities with more thorough technical analyses of ongoing streamflow and sedimentation potential. NRCS assistance may augment that of the USDA Forest Service (FS), as discussed below, or it may serve as the only Federal technical assistance available.

The FS is authorized to carry out burned area emergency response (BAER) assessments to identify imminent post-wildfire threats to human life and safety, property, and critical natural or cultural resources on National Forest System (NFS) lands and to take immediate actions to manage unacceptable risks. The FS typically organizes the BAER process, but other Federal, Tribal, State, and local agencies often participate to cover other Federal and non-Federal lands adjacent to or intermingled with NFS lands in the event of fires exceeding defined thresholds for size, severity, and/or soil resource damage (Safford, et al. 2008).

The intent of the BAER program is to determine whether wildfire-caused changes in soil hydrologic function result in hazardous conditions that threaten life, health, property, or critical cultural and natural resources due to flooding, erosion, and debris flows. BAER teams often provide immediate hydrologic assessments. Communities value these rapid assessments precisely because they provide some gauge of the sudden and new vulnerability of the watershed. However, rapid production of assessments may entail a sacrifice in accuracy. Additionally, fires that do not occur on the NFS are not authorized to receive a BAER response.

Table 1 Federal agencies and their roles concerning wildfire events

Agency	Roles
USDA Forest Service	
Pre-event	Forest management, information dissemination, training, fire tower lookout staffing, status monitoring
During-event	Infrastructure protection
Post-event	Damage assessment, emergency watershed protection, burned area emergency response (BAER Teams)
National Interagency Fire Center*	
Pre-event	Info dissemination, training, agency coordination
During-event	Fire-fight coordination
U.S. National Weather Service	
During-event	Forecasting fire conditions
Post-event	Flash flood warnings
U.S. Geological Survey	
Pre-event	Data collection through gage network
Post-event	Short-term gage installation and data collection, research on hazards caused by wildfire
Federal Emergency Management Agency	
Pre-event	Disaster preparedness, information dissemination
Post-event	Financial assistance
U.S. Bureau of Land Management	
Pre-event	Federal rangeland management

*Sponsoring Federal agencies include USDA Forest Service, Bureau of Land Management, National Oceanic and Atmospheric Administration (NOAA) National Weather Service, National Park Service, Bureau of Indian Affairs, U.S. Fish and Wildlife Service, and U.S. Fire Administration—FEMA.

The congressionally authorized Emergency Watershed Protection (EWP) Program encourages implementation of emergency measures after a natural disaster to help protect against imminent hazards to life and property. Through EWP, NRCS shares the cost of remedial actions and provides technical assistance for such measures, which may include upland mulching, construction of debris and sediments basins, removal of debris and/or excess sediment from streambeds, establishment of cover on critically eroding lands or streambanks, repair of conservation practices, and purchase of floodplain easements.

Important Terms and Terminology

Because wildfire affects a watershed in more aspects than hydrology, the terminology used by professionals can sometimes be confusing. The ecosystem response, for example, may include soil erosion, vegetation regeneration, microbial community structure restoration, faunal recolonization, and invasive species introduction (Keeley 2009). As specifically related to hydrologic response, a short list of terms and definitions follows. The National Wildfire Coordinating Group (NWCG 2006), among others, provides glossaries of wildland fire terminology larger in scope than hydrology, some of which are available on the Web. Parsons, et al. (2010) contains similar clarifications of wildfire terminology.

Agencies and personnel involved with wildfires use the following terms extensively. These relate to the driving mechanisms of hydrologic modeling and to pertinent GIS spatial data.

Burned Area Reflectance Classification (BARC)

The BARC process is a spatial data analysis technique for creating GIS layers of soil burn severity by comparing the reflectance difference in certain wavelengths between pre- and post-fire aerial images (Safford et al. 2008). BARC informs BAER decisions about locations requiring field visits. The imagery processing is also called "Landsat differenced Normalized Burn Ratio" or dNBR, which is defined below. Comparison with field-collected data has shown that BARC products tend to be more indicative of post-fire vegetative condition than of soil condition, especially in low to moderately burned areas (Hudak et al. 2004).

Burn Severity

Burn severity is a qualitative assessment of the heat pulse directed toward the ground during a fire. It relates to soil heating, large fuel and duff consumption, consumption of the litter and organic layer beneath trees and isolated shrubs, and mortality of buried plant parts (NWCG 2006). Burn severity is subdivided into two indices, one for soil and one for vegetation. Figure 1 illustrates a comparison between burn severity and the term fire intensity.

Observations of the following changes in soil characteristics (Parsons et al. 2010) form the basis for soil burn-severity evaluations:

- Loss of effective ground cover due to consumption of litter and duff
- Surface color change due to char, ash cover, or soil oxidation
- Loss of soil structure due to consumption of soil organic matter
- Consumption of fine roots in the surface soil horizon
- Formation of water repellent layers that reduce infiltration

Fire Intensity

Fire intensity (fig. 1) is a description of the physical combustion process of energy release from organic matter and represents the energy released during various phases of a wildfire (Keeley 2009). The concept applies to various aspects of a currently ongoing wildfire event, such as fire line intensity, which is the rate of heat transfer per unit length of the fire line. By contrast, burn severity is a post-fire condition.

Figure 1 Differentiating between fire intensity and burn severity (Parsons, et al. 2010)

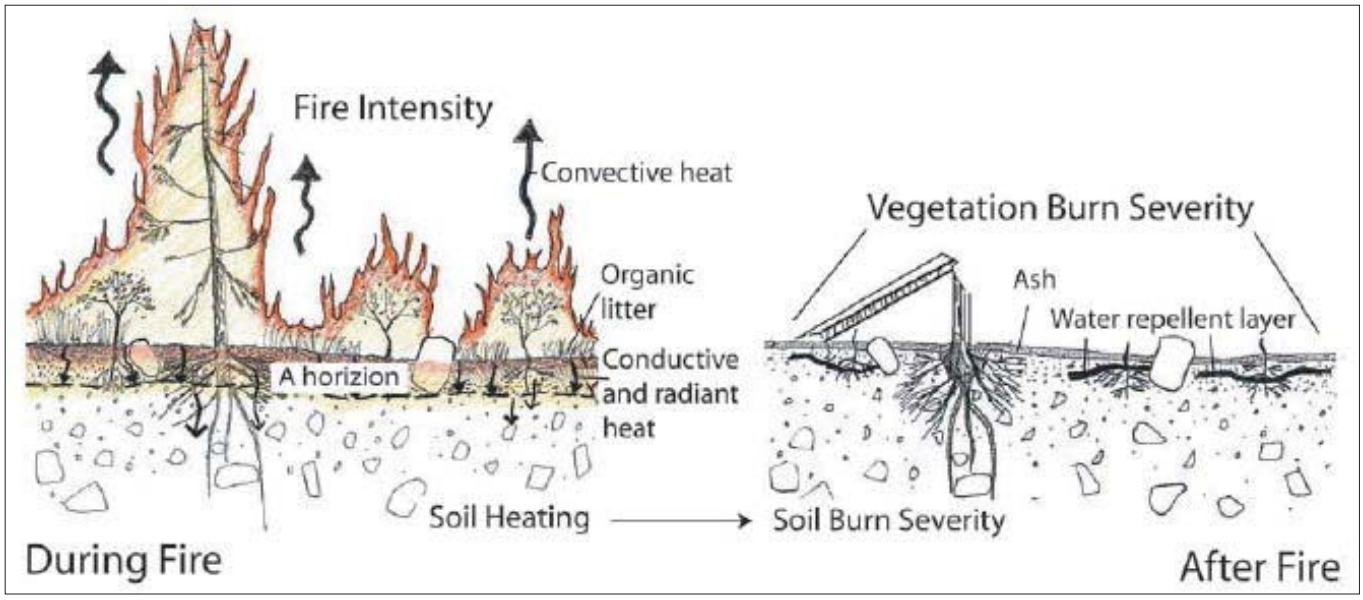

Fire Severity

The term "fire severity" is most commonly used in empirical studies to refer to the immediate impact on soil and vegetation of heat pulses above and below ground, particularly by indexing the degree of organic matter consumed (Keeley 2009). This term is very similar to the term burn severity, which is preferred by BAER specialists.

Hydrophobicity or Soil Water Repellency

A characteristic of soil generally related to organic matter, soil hydrophobicity is the tendency of the soil to resist wetting or infiltration of moisture. A relatively thin hydrophobic layer can form in an unburned forest, due to the leaching of organic matter from the duff into the soil. During wildfire, the hydrophobic layer can shift downward in the soil and increase in thickness. The intense heat of the wildfire produces a marked temperature gradient in the upper soil layer because dry soil is a poor heat conductor (DeBano 1981). That temperature gradient tends to transport vaporized organic matter downward in the soil column until cooler layers can condense it. Subsequent organic coating of soil particles results in a water repellent layer. Refer to figure 2 for a schematic between unburned and burned condition. DeBano 2000a and 2000b also provide a review of this topic.

Figure 2 Soil-water repellency (hydrophobicity) as altered by wildfire (DeBano 2000b)

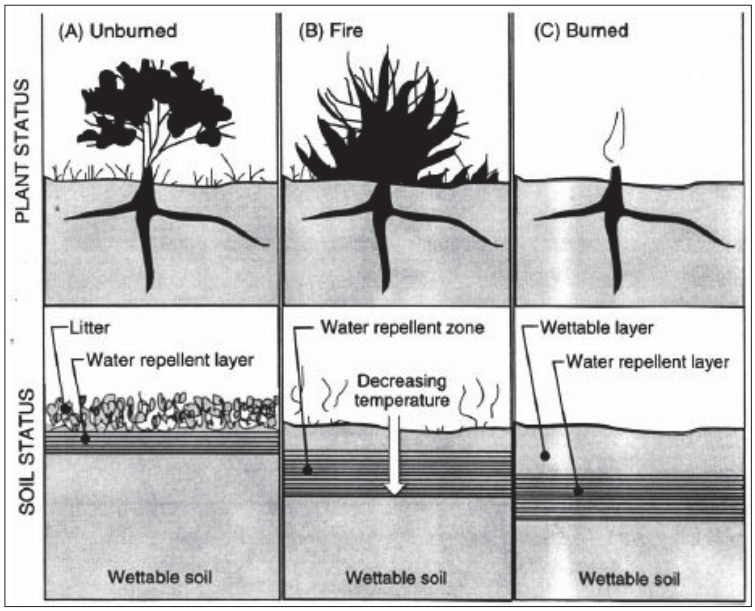

Landsat Differenced Normalized Burn Ratio (dNBR)

By comparing pre-fire and post-fire Landsat imagery, the differenced normalized burn ratio, or dNBR, analysis enables classification of burn severity. The BARC classification for soil burn severity uses this process. A modification of dNBR called RdNBR, where R stands for relative, is used to assign vegetation burn severity. Comparing the absolute difference in images using dNBR tends to assign too much weight to pre-burn vegetation conditions. The relative version, RdNBR, removes this bias (Safford, et al. 2008; Miller and Thode 2007).

Rapid Assessments of Vegetation Condition After Wildfire (RAVG)

A process used by FS specialists to prepare spatial mapping of wildfire effects on vegetation, rapid assessments of vegetation condition after wildfire (RAVG) uses Landsat thematic map images and accounts for before and after wildfire conditions. The reduction of vegetation due to wildfire is indexed by basal area loss, where basal area is a forest management term referring to the sum of cross-sectional areas of

trees and stems at breast-height for a given section of land. Although the BAER teams generally focus on rapid assessment of soil burn severity using BARC, the RAVG project creates maps of wildfire impact on vegetation, usually within 30 days of fire containment.

Soil Burn Severity Mapping

The FS BAER teams assess soil burn severity and produce high-resolution GIS-based maps. The process uses remote sensing (BARC) with field verification (Parsons et al. 2010). The GIS soil burn severity layers generally use three categories that are defined as follows (Parsons et al. 2010):

- **Low Soil Burn Severity**.—Surface organic layers are not completely consumed and roots are generally unchanged, due to minimal heat penetration of the soil. While exposed mineral soil may appear lightly charred, the canopy and understory vegetation generally appears unchanged.
- **Moderate Soil Burn Severity.—**Up to 80 percent of the pre-fire ground cover may be consumed. Roots may be scorched but generally not completely consumed, and soil structure is unchanged.
- **High Soil Burn Severity.—**All or nearly all of the pre-fire ground cover is generally consumed, along with roots up to 0.1 inches (0.25 cm) in diameter. Charring may be visible on larger roots. Significant bare or ash-covered soil is exposed and soil structure is less stable due to loss of root mass.

Wildfire Impacts on Watershed Hydrology

A diagram of the hydrologic cycle succinctly shows water processes of Earth and transport mechanisms (fig. 3, NASA 2012). For example, evaporation changes the water phase from liquid to vapor, while transporting it from the surface to the atmosphere.

For wildfire-impacted watersheds, the most pertinent parts of the hydrologic cycle are driven by rising land elevations. Clouds moving moisture from lower elevations lose holding capacity over higher elevations. The returning rainfall has gained potential energy and must infiltrate or run off as gravity draws it back to the ocean sink. Wildfire tends to speed up this return and proportion more to runoff rather than to infiltration.

As a highly effective solvent and with considerable momentum and energy, liquid water begins the erosive process upon first contact with the Earth's surface—as raindrops impact bare soil. Concentrating flows, whether in small rivulets or larger streams, easily entrain silt, sand, and clay particles, leaving erosion

Figure 3 The hydrologic cycle (NASA 2012)

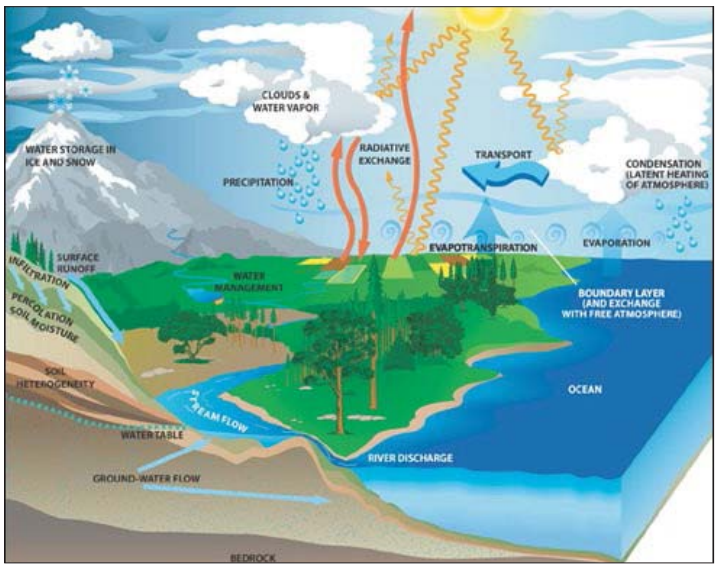

scars on land surfaces and stream banks. Vegetation offers some protection, shielding the soil surface from raindrop impact, holding soil in place with root structures, and impeding flow with branches and leaves. Forest litter can also help protect the soil surface. Plants help the soil resist the erosive forces of flowing water both within overland pathways as well as within stream corridors.

Destruction of vegetation removes the natural surface roughness that slows runoff and allows more infiltration. Hydrophobic soil decreases infiltration by blocking pores. Together, these typical post-fire conditions tend to increase runoff volume, flow velocity, and erosivity. Consequently, the healing of a watershed after a fire depends on the return of vegetation to pre-fire conditions and the breakdown of soil hydrophobicity. Over the course of several years, these processes gradually diminish elevated runoff volume, velocity, and erosivity to pre-fire levels. One study found that 10-year rainfall events on a wildfire-impacted landscape resulted in 100-year or 200-year peak floods (Conedera et al. 2003). Another study found that wildfire increased runoff proportionally more for smaller watersheds than for larger ones (Stoof et al. 2011).

Assessment of Post-fire Soil and Vegetation Conditions

One of the most convenient ways to assess the post-fire runoff surface condition is to use soil burn severity mapping (fig. 4) derived by the BARC process. Using this product, the hydrologist can determine vegetation loss as a percentage of drainage area for any drainage subarea. Another useful spatial data product, derived through the RAVG process, are maps that relate specifically to vegetation rather than soil condition. Historical information on vegetation effects is available through the cooperative project "Monitoring Trends in Burn Severity" (MTBS) available on the Web.

Figure 4 Example of burn severity mapping

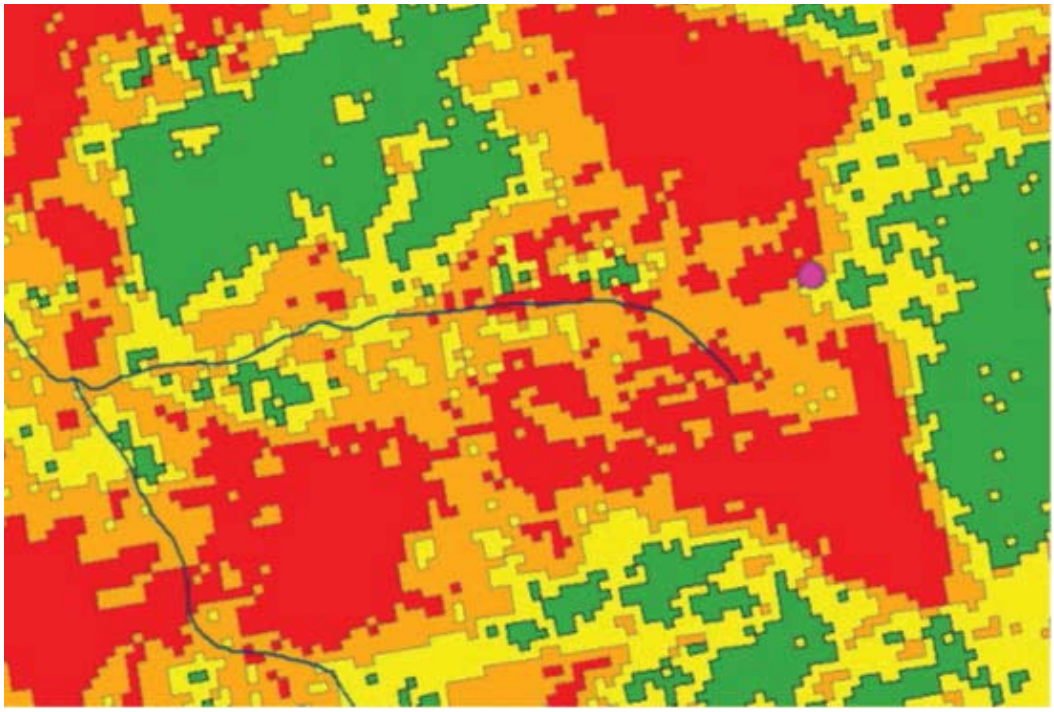

(red=high, orange=medium, yellow=low, green=no burn)

Another useful data product (fig. 5) is from a Federal mapping initiative called LandFire (2010). Also known as Landscape Fire and Resource Management Planning Tools, this initiative was established by the U.S. Department of Interior and the FS, with the goal of providing "a comprehensive, consistent, scientifically credible suite of spatial data layers for the entire United States" (LandFire 2010), including vegetation types, forest canopy, canopy heights, fire regime classes, and more. Subdivided by geographic region, these high-resolution maps are available through the LandFire Web site.

Figure 5 Oregon vegetation types, as mapped by LandFire (2010)

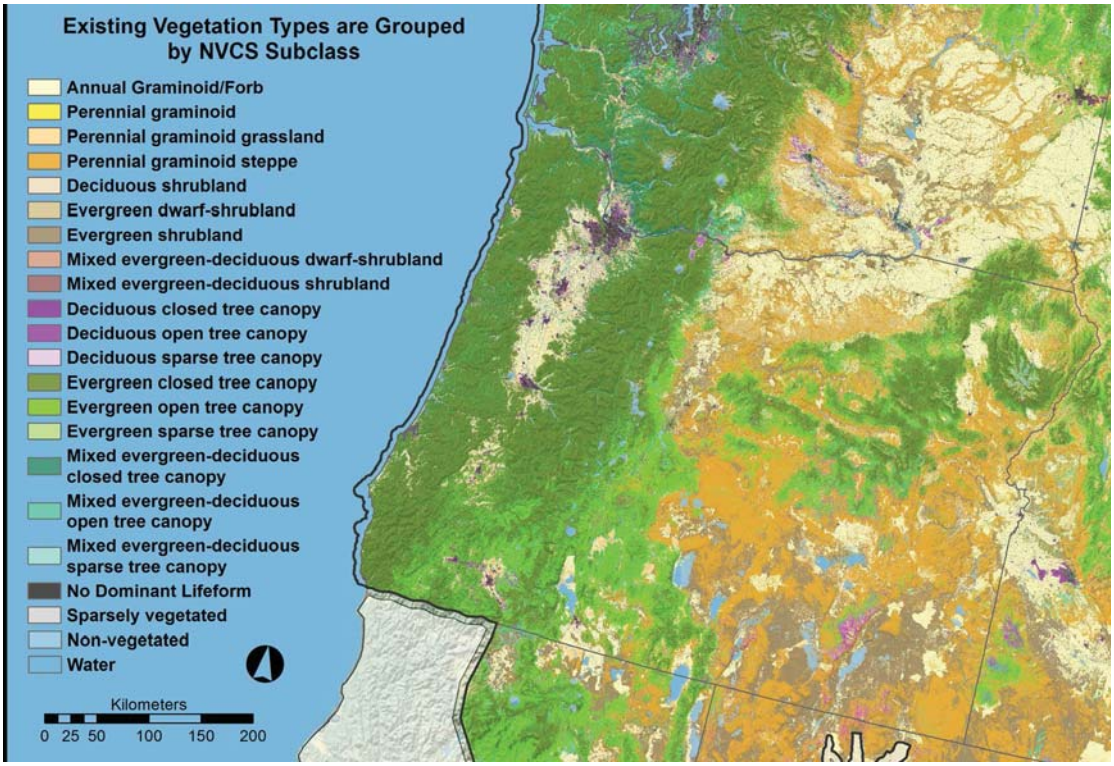

Assessment of Post-Fire Soil Hydrophobic Conditions

The development of soil hydrophobicity is multifactored and does not necessarily correlate well with soil burn severity (Parsons et al. 2010). The depth and thickness of wildfire-induced soil hydrophobicity is dependent upon vegetation type, amount of soil organic matter, soil texture, fire residence time, and burn temperature (DeBano 1981, Huffman et al. 2001). An important precondition is that organic matter must exist for the wildfire to vaporize, leading to condensation of the hydrophobic compounds within the soil profile (DeBano et al. 1967).

Greater water repellency is generally associated with coarse-grained soil texture. Given a limited supply of condensing hydrophobic substances, the smaller surface areas of coarse-grained soils are more completely covered than the greater surface area of silts and clays (Doerr et al. 2000).

In addition, the susceptibility of a soil to hydrophobicity may be related to hydrologic soil group classification (MacDonald et al. 2000). The four hydrologic soil groups (HSGs) are a standard parameter of the NRCS soil survey, fully described in USDA-NRCS 2009b. The soils of HSG A typically have less than 10 percent clay and more than 90 percent sand or gravel. The soils of HSG B typically have 50 to 90 percent sand, whereas HSGs C and D have less than 50 percent sand content. The coarseness of HSGs A and B gives them a greater tendency toward hydrophobicity, while the higher silt and clay content of HSGs C and D renders them less susceptible to hydrophobicity. However, HSG is specifically assigned based on saturated hydraulic

conductivity of the least transmissive soil layer, not to particle size or hydrophobic susceptibility, and should not be considered a definitive precursor for water repellency. (USDA-NRCS 2009b.)

Hydrophobicity of the upper mineral soil layer can be determined in the field through a simple procedure:

1. Scrape away any ash layer.
2. Place several individual drops of water on the air-dried surface.
3. Soil layer is considered hydrophobic if drops remain after 1 minute (fig. 6).

The depth of the water repellent layer can depend on fire temperature. Less severe burning may produce hydrophobicity of the soil surface. Locations of greater burn severity may result in the top of the hydrophobic layer being at some depth, say 0.5 to 3 inches. Recognizing this possibility, test the lower layers if the top layer is not water repellent. Scrape away 0.5 to 1 inch of soil depth and repeat the water drop test. By continuing this procedure, both the depth of the top and bottom of the hydrophobic layer may be determined for that location. Repeat this field procedure over time to investigate hydrophobicity persistence. Expect considerable spatial variability in hydrophobicity.

Figure 6 Water droplets resist infiltration into soil due to extreme hydrophobicity (Doerr et al. 2000)

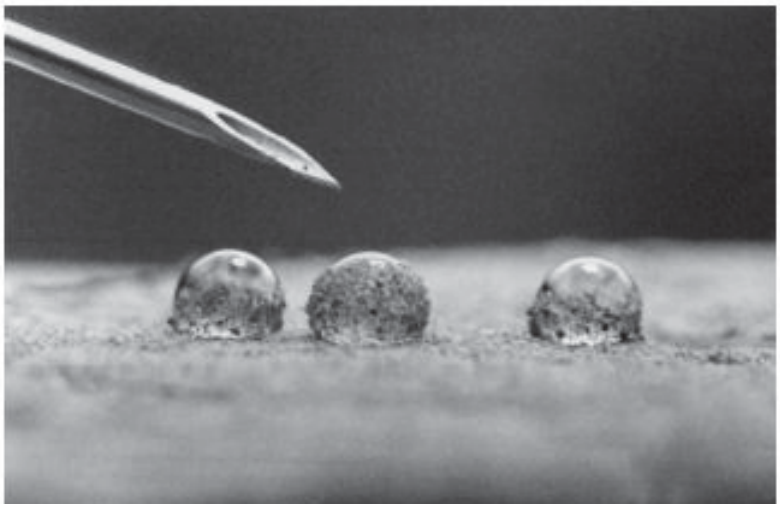

More extensive field procedures are available to quantify the degree of hydrophobicity, such as measuring the water drop penetration time (WDPT). For more severe hydrophobicity, ethanol drops are sometimes used in a critical surface tension (CST) test. Huffman et al. (2001), Scott (2000), Doerr (1998), and Robichaud et al. (2008) discuss these and other more extensive procedures.

The persistence of hydrophobicity is dependent upon several factors, including wetting-drying cycles, and both physical and biological action (Huffman et al. 2001 and DeBano 1981).

Contact by moisture is a factor in the breakdown of hydrophobicity. Although first contact with moisture is repelled, when the soil moisture threshold is exceeded, the layer will allow some infiltration. Upon drying, the layer may again become hydrophobic. This wetting and drying process, along with other physical and biological factors, removes hydrophobicity over time. Among the other factors that help break down hydrophobicity are impact of wildlife treading, impact of falling vegetation such as branches, root penetration of the water repellent layer, and the freeze-thaw process. The hydrophobicity may be minimized in as short a time as a few months (Huffman et al. 2001), but more extensive hydrophobic layers can persist for up to 6 years (Dyrness 1976).

Hydrologic Modeling of Burned Watersheds

Methods and Models

Numerous methods and computer programs, varying in complexity, are available for modeling rainfall-runoff processes. In general, these models account for the pertinent aspects of the landscape, including land cover, soils, elevation, slope, subbasin shape, vegetation character, and flow time of concentration. Meteorology is characterized using either actual storm hyetographs of one or more precipitation gages, or theoretical less-frequent event storms, such as the 100-year, 24-hour storm. Hypothetical precipitation totals are distributed over time using predetermined synthetic storm distribution curves that define rainfall intensity throughout the storm. The shape of the runoff hydrograph is often estimated using one of several possible unit-hydrograph estimation methods. For larger watersheds flow routing may be needed to transform and attenuate flow through stream systems.

Several commonly used computer models for rainfall-runoff analysis are listed in table 2. Continuous simulation models, such as Agricultural Non-Point-Source Pollution Model (AGNPS, USDA-ARS, 2013a) and the Soil and Water Assessment Tool (SWAT, USDA-ARS, 2013b) help analyze runoff, sedimentation, and water quality issues over long time periods, such as decades. Post wildfire runoff events are due to the rainfall of a single storm or short-term rainfall. Commonly used computer models are the U.S. Army Corps of Engineers program Hydrologic Engineering Center – Hydrologic Modeling System (HEC-HMS, USACE-HEC, 2013); and the NRCS models, Computer Program for Project Formulation – Hydrology (WinTR-20, USDA-NRCS 2004c), and Small Watershed Hydrology (WinTR-55, USDA-NRCS 2009a). BAER teams also use WILDCAT (Hawkins and Greenberg 1990). The ARS program, KINEROS2 (A Kinematic Runoff and Erosion Model, Smith et al. 2005, Canfield and Goodrich 2005) is also used for wildfire area runoff simulation through the Automated Geospatial Watershed Assessment (AGWA) GIS-based tool for watershed assessments. The AGWA tool is a GIS interface that automates the parameterization and execution of the SWAT and KINEROS2 models.

Table 2 Computer models for rainfall-runoff analysis

Acronym	Name	Reference
AGNPS	Agricultural Non-Point Source Pollution Model	USDA-ARS 2013a
SWAT	Soil and Water Assessment Tool	USDA-ARS 2013b
HecHMS	Hydrologic Engineering Center – Hydrologic Modeling System	USACE-HEC 2013
WinTR-20	Computer Program for Project Formulation – Hydrology	USDA-NRCS 2004c
WinTR-55	Small Watershed Hydrology	USDA-NRCS 2009a
Wildcat4	WILDCAT4 flow model	Hawkins & Greenberg 1990
KINEROS2	Kinematic Runoff and Erosion Model	Smith, et al. 2005
AGWA	Automated Geospatial Watershed Assessment Tool	Canfield and Goodrich 2005

In modeling a storm event, given precipitation volume distributed over time (a hyetograph), the hydrologist must determine what fraction infiltrates and/or is stored in surface depressions. The models of table 2 handle these phenomena in one of two general ways: the NRCS curve number (CN) method or physically based methods, such as Green and Ampt (GA). However, runoff analysis is not complete with either the CN or GA methods. The CN runoff method provides a total runoff volume estimate at a watershed outlet, but nothing about peak flow rate or hydrograph shape. The GA method provides the fraction of precipitation that infiltrates, leaving that which is ready to runoff, but does not route that runoff to the outlet.

With the NRCS models, WinTR-20 and WinTR-55, runoff volume is computed using the NRCS runoff CN method. Runoff hydrographs are developed by applying the runoff volume, estimated using the CN method, and time of concentration to a dimensionless unit hydrograph. Infiltration methods, such as GA, available in models such as HEC-HMS, do not employ runoff CNs (although HEC-HMS also has a CN option).

Several case studies presented in this technical note as appendices A through E illustrate the use of these models individually or various combinations of these models. Case studies 1 (appendix A) and 3 (appendix C) illustrate the use of HEC-HMS with the runoff CN method. Case study 2 (appendix B) illustrates the use of the fire hydrology, or FIRE HYDRO, spreadsheet, an adaptation of the runoff CN method. Case study 4 (appendix D) illustrates the use of HEC-HMS with a GIS-derived unit hydrograph, and the Green and Ampt infiltration method. Finally, case study 5 (appendix E) illustrates the use of AGWA and WinTR-20.

Adjustment of Event-Based Runoff Modeling Components for Burned Areas

The phenomena of rainfall, interception, surface storage, infiltration, and runoff transformation are discussed in hydrology textbooks, such as Bendient, Huber, and Vieux (2012). To use any of the computer models in table 2 for post-wildfire hydrology, the analyst should understand the impact of fire on these various physical processes. Adjustment of hydrologic model features allows comparison of pre-fire versus post-fire estimates of runoff peaks and hydrograph shapes.

Accounting for changes in runoff hydrology due to wildfire is generally a matter of determining the extent to which runoff has accelerated due to the loss of vegetation or the lack of infiltration due to soil hydrophobicity. Wildfire may alter any or all of several runoff modeling components. The following sections provide detailed information about adjusting CNs, times of concentration, flow travel times, Manning's roughness coefficients, soil infiltration characteristics, and unit hydrographs.

Runoff CNs

Title 210, National Engineering Handbook (NEH), Part 630, Chapter 9, "Hydrologic Soil-Cover Complexes" (USDA-NRCS 2004a), documents the general process of determining CNs, providing tables of CNs for agricultural lands and for arid and semi-arid rangelands (table 3). Figure 7 provides a graphical solution of the CN equation used to compute Q, runoff volume. The CN method depends on the determination of the CN index for a given watershed and given hydrologic condition. Hydrologic condition is based on a combination of vegetation and land surface characteristics as they affect infiltration. The tables also demonstrate the variance of CN with hydrologic soil group.

Existing methods for adjusting runoff CNs to account for wildfire effects are for the most part based heavily upon the hydrologic judgment of practitioners who have studied burned watersheds. A number of publications, including Foltz et al. (2009) have documented these methods. For a synopsis of the state of the art, research issues related to post-wildfire runoff and erosion processes, and suggested areas needing further work, see Moody et al. (2013).

Table 3 Runoff CNs for arid and aemiarid rangelands (USDA-NRCS 2004a)

Cover type	Hydrologic condition[1]	A[2]	B	C	D
Herbaceous-mixture of grass, weeds, and low-growing brush, with brush the minor element	poor	-	80	87	93
	fair	-	71	81	89
	good	-	62	74	85
Oak-aspen-mountain brush mixture of oak brush, aspen, mountain mahogany, bitter brush, maple, and other brush	poor	-	66	74	79
	fair	-	48	57	63
	good	-	30	41	48
Pinyon-juniper-pinyon, juniper, or both; grass understory	poor	-	75	85	89
	fair	-	58	73	80
	good	-	41	61	71
Sagebrush with grass understory	poor	-	67	80	86
	fair	-	51	63	70
	good	-	35	47	55
Desert shrub-major plants include saltbush greasewood, creosotebush, blackbrush, bursage, palo verde, mesquite, and cactus	poor	63	77	85	88
	fair	55	72	81	86
	good	49	68	79	84

[1.] Hydrologic conditions defined as
- poor: < 30 percent ground cover (litter, grass, and brush overstory)
- fair: 30 to 70 percent ground cover
- good: >70 percent ground cover

[2.] Average runoff conditions (group A only developed for desert shrub).

Figure 7 Graphical solution of the CN runoff equation (USDA-NRCS 2004b)

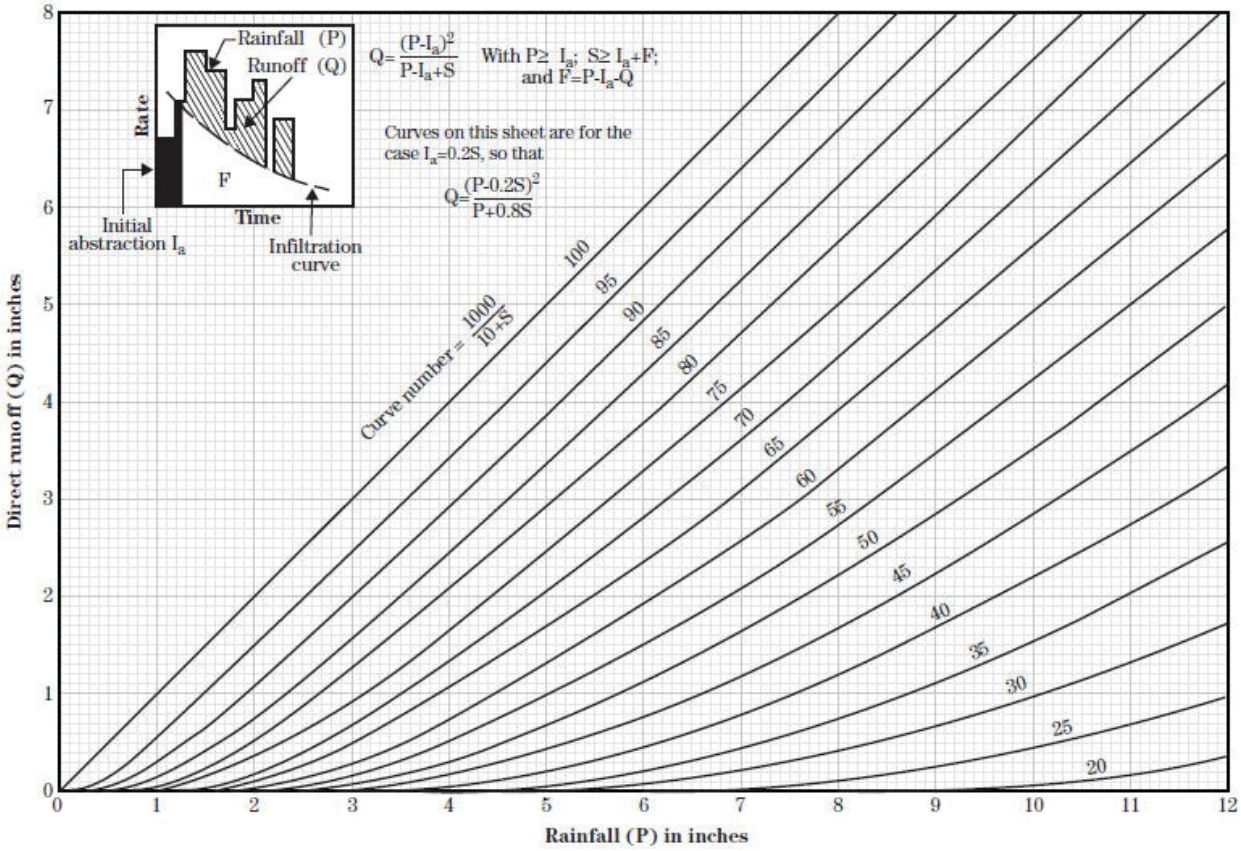

Adjustment of CNs for Wildfire Effects

One of the first efforts to establish some methodology for adjustment of runoff CNs for the effects of wildfire was Cerrelli (2005). Studying Montana wildfire events in 2000 and 2001, Cerrelli created an Excel spreadsheet that computes watershed CNs for four conditions: 1) pre-fire, 2) early post-fire with possible hydrophobicity, 3) medium term post-fire with hydrophobicity no longer in effect, but little re-emergent vegetation, and 4) later post-fire, after one growing season. For high burn severity areas, the investigation included a table of wildfire affected CNs (table 4). The Fire Hydrology, or FIRE HYDRO, spreadsheet and user notes are available at the NRCS Web site.

Table 4 Suggested runoff CNs for burned areas from Cerrelli (2005)

Hydrologic soil group	High burn severity CN
A	64
B	78
C	85
D	88

In addition, the guidance for moderate burn severity is to use the published CN tables, but with cover type in fair condition and for low burn severity, to adjust the CN to the aspect of the fire-burned slopes. For low burn severity, with north and east facing slopes, the guidance is to use cover type good condition, and for south and west facing slopes to use a CN between cover type fair and good condition.

Case study 2 of this technical note documents Cerrelli's investigation, method development, and use on the Montana Bitterroot wildfires of 2000.

The USDA FS provides Web-based guidance for determination of wildfire affected runoff CNs (USDA FS 2015), which includes Cerrelli (2005). Tables 5 and 6 show post-fire runoff CNs suggested by two different investigators (Story 2003 and Stuart 2000) for FS Region 1. (See figure 8 for a map of the USDA FS Regions.)

Table 5 Forest Region 1 CNs (Story 2003)

Post-fire condition	CN range
High burn severity, with hydrophobic soils	93–98
High burn severity, without hydrophobic soils	90–95

Table 6 Forest Region 1 CNs (Stuart 2000)

Post-fire condition	CN range
Moderate burn severity	80
Low burn severity	70–72
Unburned	60–64
Moderate burn severity, with BAER treatments	75
Moderate burn severity, with BAER treatments	66

Figure 8 USDA Forest Service regions

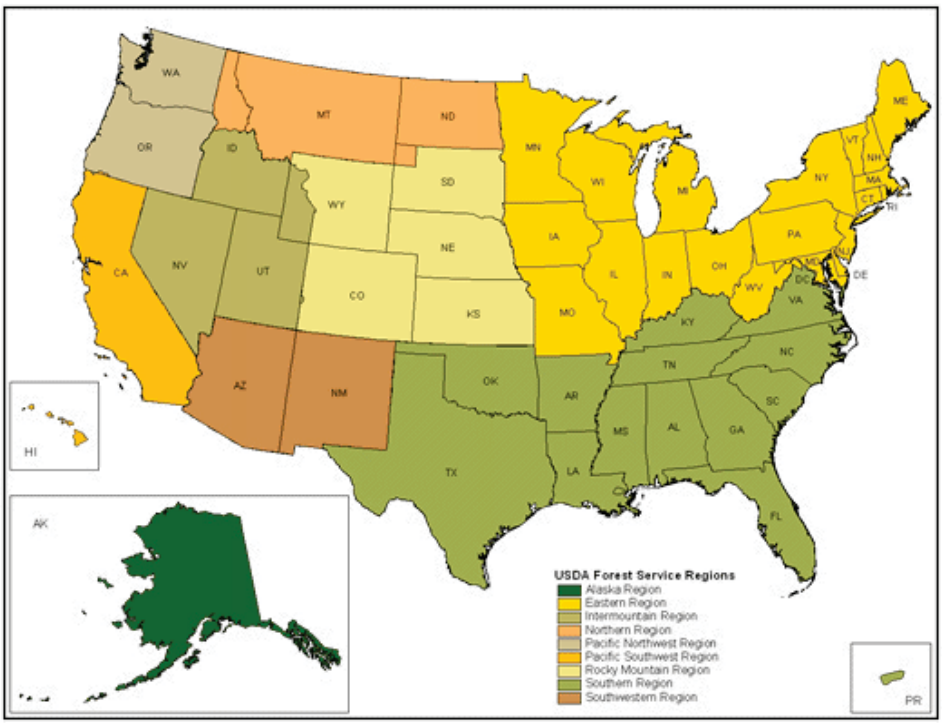

USDA Forest Service

Tables 7 and 8 show CNs suggested by FS hydrologists for FS Region 3 (Arizona and New Mexico).

Table 7 Forest Region 3 CNs (Livingston and others 2005)

Post-fire condition	CN range
High burn severity, with hydrophobic soils	95
High burn severity, without hydrophobic soils	92
Moderate burn severity, with hydrophobic soils	89
Moderate burn severity, without hydrophobic soils	87
Low burn severity	80–83
Unburned	55–75

Table 8 Forest Region 3 CNs (USDA Forest Service 2015)

Post-fire condition	CN range
High burn severity, with hydrophobic soils	95
High burn severity, without hydrophobic soils	90–91
Moderate burn severity, with hydrophobic soils	90
Moderate burn severity, without hydrophobic soils	85
Low burn severity	$CN_{pre\text{-}fire} + 5$
Straw mulch with good coverage	60
Seeding with log erosion barriers, 1-year post-fire	75
Log erosion barriers without hydrophobic soils	85

Another investigation by the FS produced a table comparing pre-fire to post-fire runoff CNs for the 2003 Aspen fire in Arizona (table 9). Although these FS studies generally use NRCS hydrology models, Case study 1 in this technical note demonstrates the use of CNs within the HEC-HMS model.

Table 9 Forest Region 3 pre-fire and post-fire CNs (USDA Forest Service 2015)

Hydrologic soil group	$CN_{pre\text{-}fire}$	$CN_{post\text{-}fire}$		
		Low burn severity	Moderate burn severity	High burn severity
B	56	65	–	–
C	67	70–75	80	90
D	77	80–85	90	95

Limitations of the CN Method

The lack of field data in burned catchments and related research to verify the effect on CN hampers post-fire runoff modeling with CNs. There is little research adequate to determine best-fit runoff CNs, even for unburned mountain and forested watersheds. One study of ten Appalachian forested watersheds that did use measured data found that measured CNs varied significantly from published suggested values (Tedela et al. 2012). The study also found very wide confidence limits for the measured values. One watershed, with a measured mean CN of 57, had 95-percent confidence interval of 32 to 83. Other studies also found inability to achieve a stable CN value (Hawkins 1993, and Springer and Hawkins 2005).

Hydrologists modeling forested watersheds should understand the difference between two major runoff-generating processes and their likelihood during storms of different magnitudes pre-fire versus post-fire. Forested watersheds in unburned conditions may tend toward saturation-excess overland flow, with runoff generated from relatively small fractions of the subareas, where rainfall depths exceed the soil capacity to retain water. Newly burned watersheds, however, may tend toward more significant infiltration-excess (also called Hortonian) overland flow, with surface runoff due to rainfall intensities exceeding soil infiltration rate (fig. 9).

Figure 9 Runoff generating processes, hillslope terminating at a watercourse (Garen and Moore 2005)

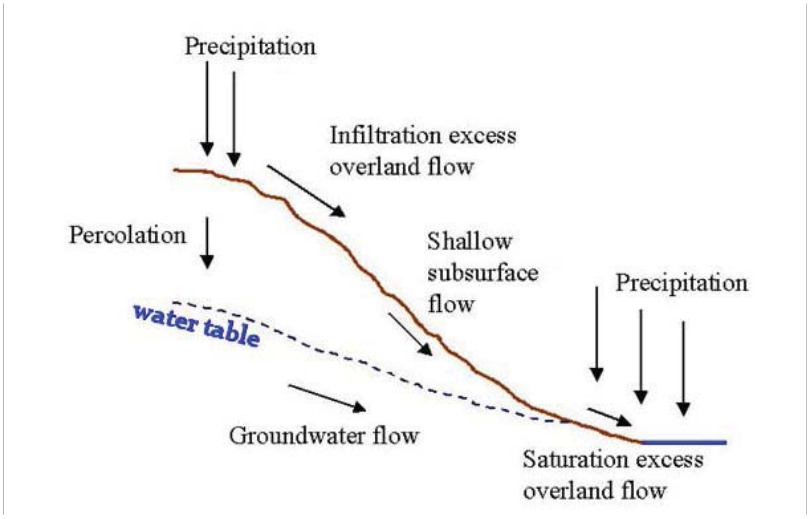

Time of Concentration

Watershed time of concentration (T_c) is defined as the time required for runoff to flow from the most hydraulically remote point in the watershed to its outlet. In hydrograph analysis, T_c is considered a representation of the time from the end of excess rainfall to the point of inflection on the receding limb. Watershed lag time is defined as the time from the center of excess rainfall to the hydrograph peak. Both lag and T_c are shown on the dimensionless unit hydrograph schematic, figure 16. These definitions and methods of computation are discussed in 210-NEH, Part 630, Chapter 15, "Time of Concentration," (USDA-NRCS 2010).

The estimation of T_c is often accomplished using either the watershed lag method or the velocity method.

Watershed Lag Method

Time of concentration can be estimated using the following equation, called the watershed lag method.

$$T_c = \frac{l^{0.8}\left(\frac{1000}{CN} - 9\right)^{0.7}}{1140Y^{0.5}} \qquad \text{eq. 1}$$

where—

T_c = time of concentration (hr)

l = flow length (ft)

CN = curve number (dimensionless)

Y = average land slope (percent)

Velocity Method

Another way to estimate T_c described in 210-NEH, Part 630, Chapter 15, is the velocity method. This method equates T_c to the sum of estimated flow times for three types of flow from the hydraulically most distant point in the watershed, namely, sheet flow, shallow concentrated flow, and channel flow. Note that the NRCS term "sheet flow" is also called "overland flow" since such flow is not always over a planar surface. The following equation for sheet flow travel time, provided in 210-NEH, Part 630, Chapter 15, was derived from the kinematic wave equation:

$$T_{sheet} = \frac{0.007(nl)^{0.8}}{P^{0.5}S^{0.4}} \qquad \text{eq. 2}$$

where—

T_{sheet} = travel time (hr)

n = Manning's roughness coefficient for overland flow, obtained from table 10

l = sheet flow length (ft < 100)

P = 2-year, 24-hour rainfall (in)

S = land slope (ft/ft)

Table 10 Manning's roughness coefficients for sheet flow (depth generally ≤ 0.1 ft)

Surface description	Manning's *n* value
Smooth (concrete, asphalt, gravel, or bare soil)	0.011
Fallow fields (no residue)	0.05
Cultivated soil, with residue <= 20%	0.06
Cultivated soil, with residue > 20%	0.17
Short-grass prairie	0.15
Dense grasses	0.24
Bermuda grass	0.41
Natural rangeland	0.13
Woods with light underbrush	0.40
Woods with dense underbrush	0.80

For the shallow concentrated flow and channel flow segments, the following equations may be used. For shallow concentrated flow, velocity may be estimated using table 11. Channel velocity may be estimated with Manning's equation (eq. 4).

$$T_{shallow} = \frac{l_{shallow}}{3600V_{shallow}} \qquad T_{channel} = \frac{l_{channel}}{3600V_{channel}} \qquad \text{eq. 3}$$

where—

$T_{shallow}$ = travel time, shallow concentrated flow (hr)

$T_{channel}$ = travel time, channel flow (hr)

$l_{shallow}$ = flow length, shallow concentrated flow (ft, generally less than 1,000)

$l_{channel}$ = flow length, channel flow (ft)

$V_{shallow}$ = flow velocity, shallow concentrated flow (ft/sec)

$V_{channel}$ = flow velocity, channel flow (ft/sec)

Table 11 Shallow concentrated flow velocity equations, where *S*=flow slope in ft/ft

Flow type	Manning's n value	Velocity equation (ft/sec)
Pavement and small upland gullies	0.025	$V_{shallow} = 20.328\sqrt{S}$
Grassed waterways	0.050	$V_{shallow} = 16.135\sqrt{S}$
Nearly bare/untilled or alluvial fan flow	0.051	$V_{shallow} = 9.965\sqrt{S}$
Cultivated straight row crops	0.058	$V_{shallow} = 8.762\sqrt{S}$
Short-grass pasture	0.073	$V_{shallow} = 6.962\sqrt{S}$
Minimum tillage cultivation, contoured or strip-cropped, or woodlands	0.101	$V_{shallow} = 5.032\sqrt{S}$
Forest with heavy ground litter or hay meadows	0.202	$V_{shallow} = 2.516\sqrt{S}$

$$V_{channel} = \frac{1.486R^{2/3}S^{1/2}}{n} \qquad \text{eq. 4}$$

where—

$V_{channel}$ = average cross-sectional flow velocity (ft/sec)

R = hydraulic radius (ft) = $A/P_{w,}$ where—

A = cross-sectional flow area, ft^2

P_w = wetted perimeter, ft

S = flow slope (ft/ft)

n = Manning's n value for channel flow

Adjustment of Runoff Flow Time for Wildfire Effects

For the watershed lag method, post-wildfire effects are entirely accounted for by adjusting the CN. See the section "Adjustment of Curve Number for Wildfire Effects."

For the sheet flow portion of the velocity method, post-wildfire effects are entirely accounted for using Manning's roughness coefficient. The analyst must decide whether and how much to reduce the *n*-value, based on reduction of vegetation caused by the fire. Using table 10, for example, a pre-fire condition might justify an *n*-value of 0.13 or 0.15, associated with natural range or short-grass prairie, reduced to a post-fire *n*-value of 0.05 or 0.011, associated with fallow ground or smooth surface, caused by total burning of vegetation.

Hydrologists should also keep in mind that Manning's roughness coefficients are of a different scale between overland flow and channel flow, due to the phenomenon of relative roughness, which is a measure of flow depth (or hydraulic radius) over surface roughness height. Given a homogeneous surface, the Manning's roughness value will not necessarily be the same at all depths. For very shallow flow, at or near the boundary roughness height, Manning's *n*-value will be larger. At depths much greater than roughness height, Manning's *n*-value will tend to settle to a single value (for a homogeneous surface).

Overland flow generally has a larger relative roughness than channel flow. The effects of wildfire tend to lower both relative roughness and Manning's *n*-value for overland flow, while raising them for collector channels. Early post-fire overland flow roughness values may be set to that of bare soil. Moody and Kinner (2006) suggest that wildfire basically results in overland flow Manning's roughness values near that of bare soil and that minor variation from this value (0.011) has much less effect on model results than changes in effective rainfall. In addition, the effect of hydrophobicity can be accounted for by lower overland flow roughness values, near those of rough concrete. Canfield et al. (2005), using measured rainfall and runoff at Starmer Canyon, NM (part of the Cerro Grande wildfire of 2000), found that, to model the observed, overland flow roughness values varied significantly with surface condition (fig. 10).

Channels clogged with post-fire debris or sediment have higher Manning's roughness values than their pre-fire condition. The modeler should consider that, immediately post-fire, channels have elevated roughness values due to transport of significant newly available sediment and debris. With time, these channel roughness values change, although return to pre-fire roughness may take many years. Smaller channels, such as collectors, may take the longest to return to pre-fire roughness conditions, due to lack of streampower to move fire-related sediment and debris.

Research has shown that steep mountain streams have significantly higher roughness values than lower elevation streams, with Manning's *n*-values often ranging from 0.1 to 0.2 (Yochum et al. 2012). These higher values are due to the presence of large cobbles and boulders, relative to stream cross-section size, as well as step-pools, instream wood, and extreme variability along the longitudinal profile. A single large boulder can sometimes so restrict flow area that significantly greater out of bank flow occurs only for a short section.

References for selection of roughness values for high gradient streams include both photographic guidance (Barnes 1967, Aldridge and Garrett 1973, Hicks and Mason 1998, Yochum and Bledsoe 2010, Yochum et al. 2014) and quantitative prediction tools (Limerinos 1970, Hey 1979, Jarrett 1984, Bathurst 1985, Yochum et al. 2012).

Figure 10 KINEROS model hydrographs, using measured data from the same Starmer Canyon hillslope, with surface conditions varying from bare soil to forested (Canfield et al. 2005)

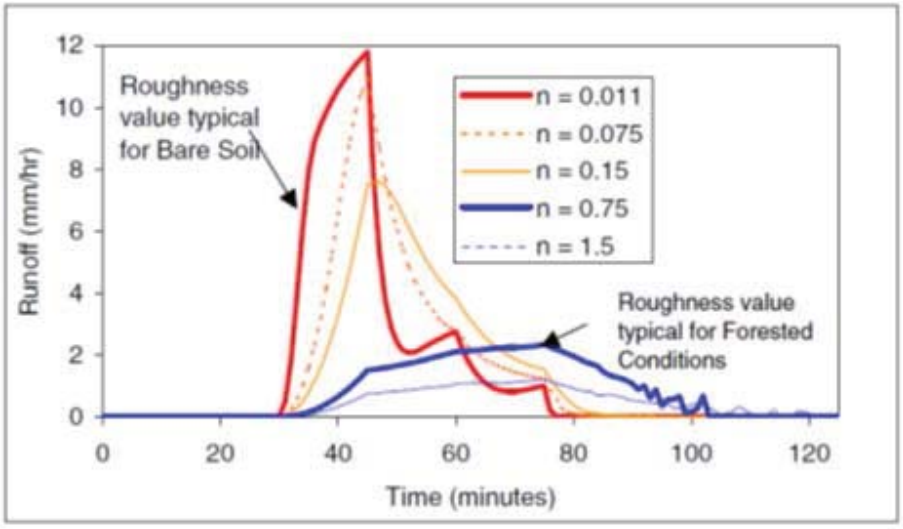

Hydrologic modeling of conditions both pre-fire and post-fire may benefit from a more extensive examination of subbasin drainage by development of time-area histograms. These are derived using GIS, and can verify whether the estimated longest path in a partially burned watershed is truly the longest, time wise, rather than lengthwise. The time-area histogram also helps determine hydrograph peaking factors for the use of unit hydrograph transformations. (See the "Unit Hydrographs" section.)

Infiltration Parameters

Physically-based infiltration methods, such as GA, do not attempt to index overall watershed conditions, but rather assume that physical processes at a given point on the landscape may be applied at a wider spatial scale. The GA method is a simplification of infiltration equations that incorporate soil characteristics, such as hydraulic conductivity, and physical aspects such as pressure of surface water and matric suction of the soil (due to capillary action). The GA method represents infiltration as a depth of wetted soil, with moisture gradually moving downward in the soil column as a front, and that this movement can be estimated using soil porosity, soil hydraulic conductivity, initial soil water content, and the soil matric suction at the wetted front. Figure 11 shows the Green-Ampt conception of the soil column.

Figure 11 Green-ampt infiltration into the soil column

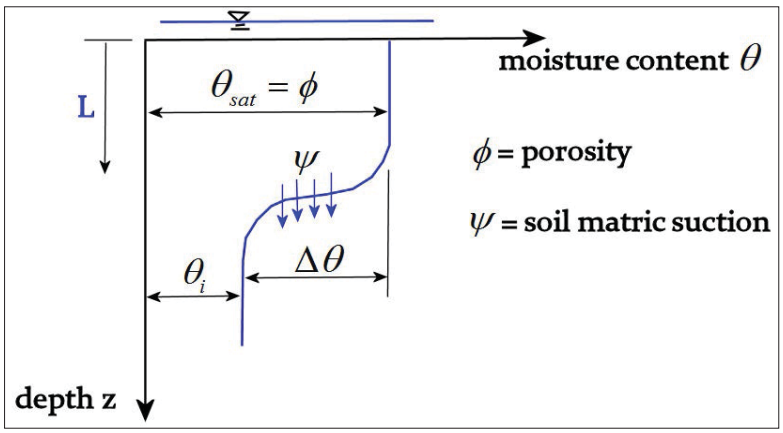

The GA method is a simplification of Richard's equation (USACE-HEC, 2013) for infiltration that has a limited number of parameters that can be reasonably estimated using soils data. As discussed in the HEC-HMS Technical Reference Manual (USACE-HEC 2013), GA infiltration is estimated using equation 5, with parameters correlated with soil texture (table 12).

$$f_t = K\left[\frac{1+(\phi-\theta_i)S_f}{F_t}\right] \qquad \text{eq. 5}$$

where—

f_t = loss during time period, t

K = saturated hydraulic conductivity

ϕ = effective soil porosity (volume air/volume soil)

θ_i = initial soil water content (volume water/volume soil)

S_f = wetting front suction

F_t = cumulative loss at time t

Initial soil water content, in equation 5, ranges between zero (a completely dry soil) and the effective porosity. The user estimates this value using an antecedent soil moisture index and values from table 12 for field capacity and wilting point.

Table 12 Green Ampt parameters for soil texture classes (Rawls et al. 1983, Saxton et al. 1986)

Texture	Horizon	*φeffective*	K_{sat}	S_f	*θ*field cap	θwiltingPt
		(cm³/cm³)	(cm/hr)	(cm)	(cm³/cm³)	(cm³/cm³)
sand	combined	0.417	23.56	4.95	0.13	0.06
	A	0.431	-	5.34	-	-
	B	0.421	-	6.38	-	-
	C	0.408	-	2.07	-	-
loamy sand	combined	0.401	5.98	6.13	0.15	0.07
	A	0.424	-	6.01	-	-
	B	0.412	-	4.21	-	-
	C	0.385	-	5.16	-	-
sandy loam	combined	0.412	2.18	11.01	0.20	0.09
	A	0.469	-	15.24	-	-
	B	0.428	-	8.89	-	-
	C	0.389	-	6.79	-	-
loam	combined	0.434	0.68	8.89	0.26	0.12
	A	0.476	-	10.01	-	-
	B	0.489	-	6.40	-	-
	C	0.382	-	9.27	-	-
silt loam	combined	0.486	1.30	16.68	0.29	0.11
	A	0.514	-	10.91	-	-
	B	0.515	-	7.21	-	-
	C	0.460	-	12.62	-	-
sandy clay loam	combined	0.330	0.30	21.85	0.26	0.16
	B	0.330	-	26.10	-	-
	C	0.332	-	23.90	-	-
clay loam	combined	0.309	0.20	20.88	0.33	0.19
	A	0.430	-	27.00	-	-
	B	0.397	-	18.52	-	-
	C	0.400	-	15.21	-	-
silty clay loam	combined	0.432	0.20	27.30	0.37	0.19
	A	0.477	-	13.97	-	-
	B	0.441	-	18.56	-	-
	C	0.451	-	21.54	-	-
sandy clay	combined	0.321	0.12	23.90	0.35	0.25
	B	0.335	-	36.74	-	-
silty clay	combined	0.423	0.10	29.22	0.42	0.26
	B	0.424	-	30.66	-	-
	C	0.416	-	45.65	-	-
silty clay	combined	0.385	0.06	31.63	0.48	0.35
	B	0.412	-	27.72	-	-
	C	0.419	-	54.65	-	-

Adjustment of Infiltration Parameters for Wildfire Effects

When wildfire results in hydrophobic soil, the spatial extent is generally not over the entire drainage area. The extent to which the hydrophobicity has reduced infiltration also varies from place to place. Along with soil burn severity mapping, field investigation may give the hydrologist considerable insight as to the extent of infiltration reduction caused by hydrophobicity. However, since it is impossible to visit and test every square foot of ground, the hydrologist must estimate the widespread effect of hydrophobicity, and the rate infiltration returns to normal as water repellency breaks down over time.

Three modeling options are available to account for hydrophobicity. The hydraulic conductivity may be reduced (GA method), the percentage of impervious area may be increased, or if using the CN method, increase the CN to the high 90s. Canfield et al. (2005), in their field studies of post-wildfire conditions, examined of the effect on saturated hydraulic conductivity. The increase over time of K_{sat} (fig. 12) may be an indication of the breakdown of hydrophobicity and return of vegetation. In the HEC-HMS model, the first two options are available in the same interface, as shown in figure 13, implementing GA infiltration.

Figure 12 Optimal hillslope hydraulic conductivity, Cerro Grande, NM, fire (Canfield et al. 2005)

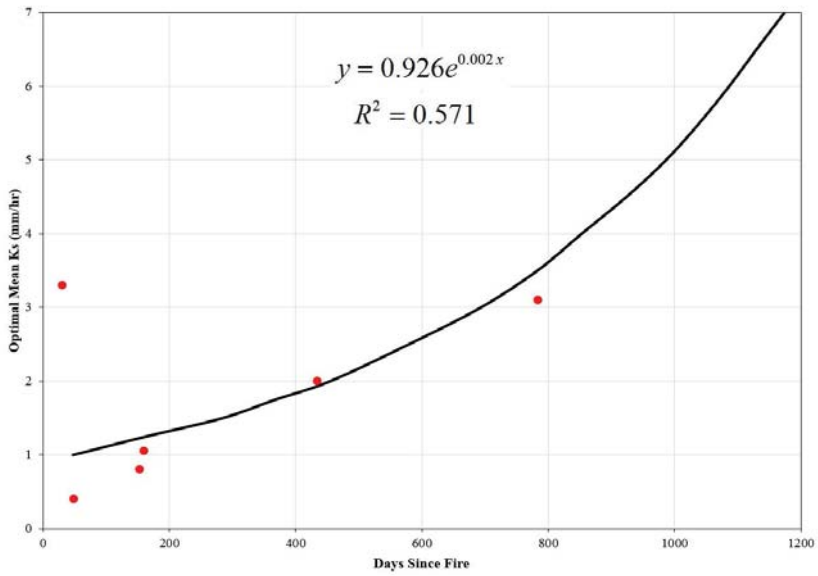

Figure 13 HEC-HMS Green and Ampt input interface (USACE-HEC 2013)

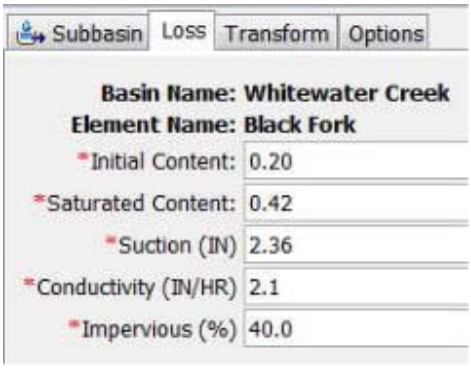

Unit Hydrographs

The process of converting a runoff volume to a hydrograph shape is called transformation. Several of the computer models in table 2 perform the transformation of spatially distributed runoff to an outlet using some variation of unit hydrograph (UH) theory. UH theory, advanced by L.K. Sherman in the 1930s, suggests that the runoff behavior of a watershed can be typed, given its physical characteristics, so that whenever a unit of direct runoff is produced in a watershed over a given duration, the hydrograph peak and shape at the outlet will be that of the unit hydrograph. If a rainfall event produces more than one unit of direct runoff, then the outlet hydrograph can be computed by multiplying each ordinate of the UH by the amount of runoff in that duration.

The following list details a number of assumptions inherent in the theory:

- A given subbasin has a different unit hydrograph for each possible duration of direct runoff.
- The effective rainfall, defined as the rainfall that becomes direct runoff, occurs uniformly over the subbasin.
- The shape and duration of the UH are independent of the effective rainfall intensity, which only effects the magnitude of flow in each UH time interval.

- If a given rainfall event is divided into subsequent 30-minute intervals of effective rainfall, a 30-minute UH is applied to each interval of effective rainfall, to obtain an outflow for that time interval. The total outflow is the sum of the runoff hydrographs produced from each time interval. This is called the superposition principle (fig. 14).
- The S curve, derived by summing a series of UHs of a given duration, each shifted by that duration, allows for the computation of runoff hydrographs from a single curve regardless of effective rainfall duration (fig. 15).

Figure 14 Runoff hydrographs by convolution and superposition, using 30-minute unit hydrograph

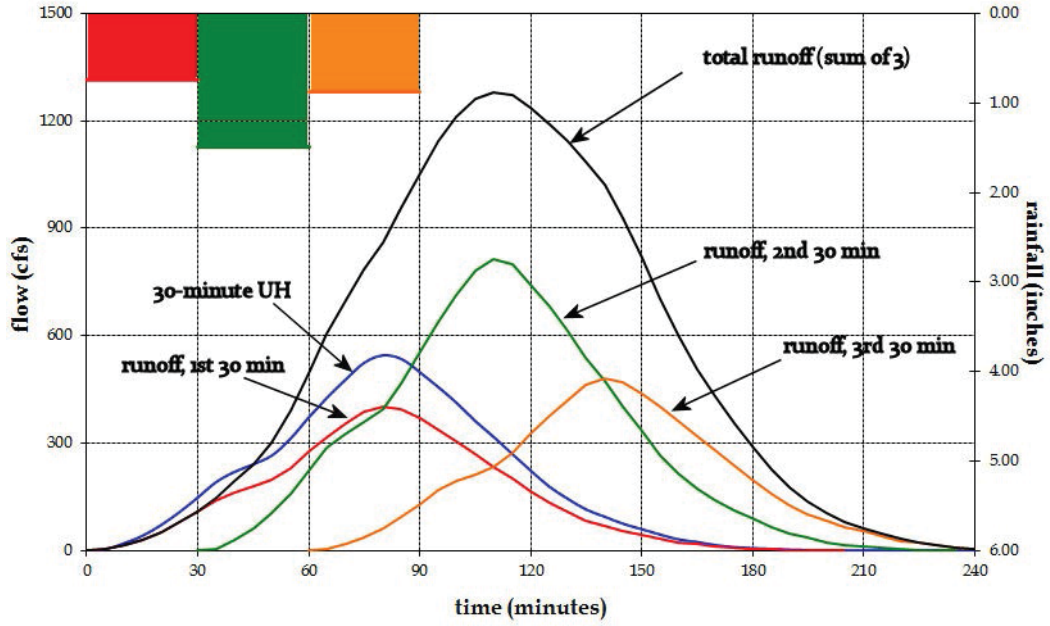

Figure 15 S-curve developed from 30-minute unit hydrograph

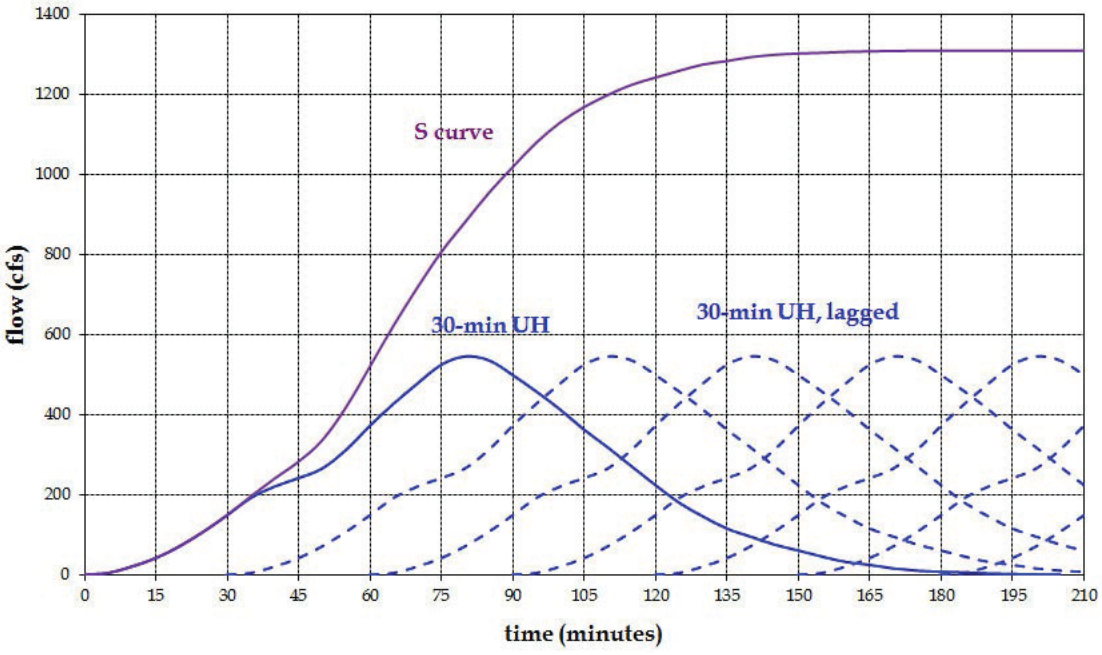

NRCS dimensionless unit hydrograph

As documented in the 210-NEH, Part 630, Hydrology, Chapter 16, Hydrographs (USDA-NRCS 2007), the NRCS approach is to use a standard dimensionless curvilinear hydrograph estimation (fig. 16).

Figure 16 Dimensionless unit hydrograph, with time of concentration and lag (USDA-NRCS 2010)

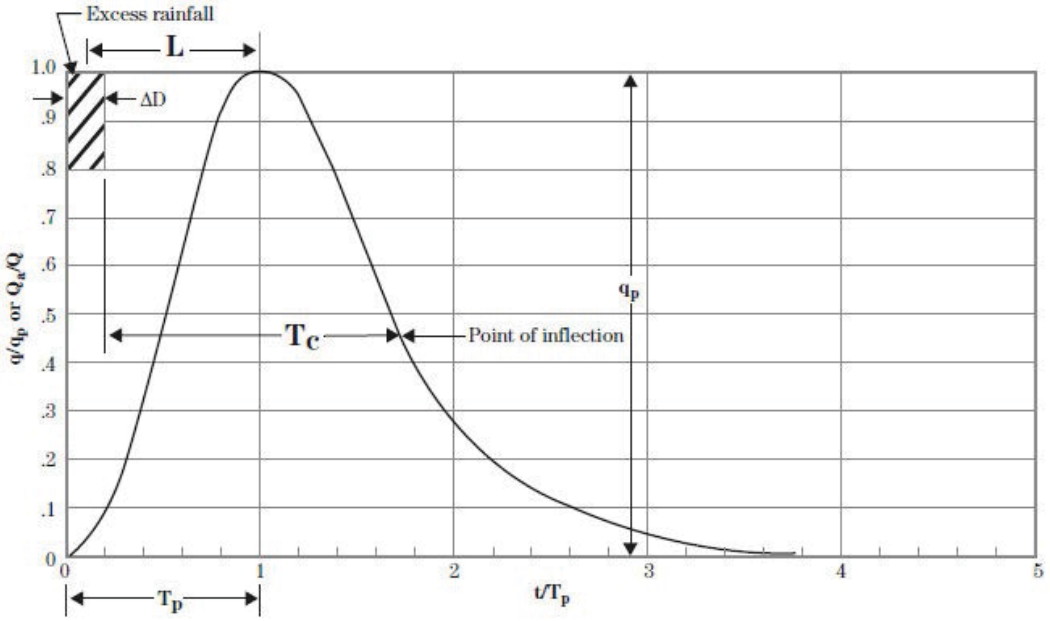

$$T_p = 0.667 T_c \qquad \text{eq. 6}$$

$$q_p = \frac{484 A Q}{0.667 T_c} \qquad \text{eq. 7}$$

where—

L = Lag (hr)

T_c = time of concentration (hr)

T_p = time to peak (hr)

ΔD = duration of excess rainfall (hr)

t/Tp = ratio between time interval and time to peak (dimensionless)

q = discharge rate at time t (ft^3/sec)

q_p = UH peak discharge rate at time T_p, (ft^3/sec)

Q_a = runoff volume up to t (in)

A = watershed drainage area ($mi^{2)}$

Q = total runoff volume (in)

The coefficient 484 in equation 7 is called the peak rate factor (PRF). The PRF is a ratio of the runoff under the rising limb of the unit hydrograph to the total time base. For the default PRF of 484, the rising side of the dimensionless unit hydrograph represents 37.5 percent of the total runoff volume. The NRCS reference shows that the PRF may be estimated using time to peak and time of recession. A factor K is given (eq. 8), which relates to PRF as shown in equation 9.

$$K = \frac{2}{1 + \frac{T_r}{T_p}} = \frac{2T_p}{T_p + T_r} \qquad \text{eq. 8}$$

$$PRF = 645.33K = \frac{1291T_p}{T_p + T_r} \qquad \text{eq. 9}$$

where—

T_p = time to peak = 1 hour for the dimensionless unit hydrograph

T_r = time of recession

Since the PRF is dependent on the timing of watershed drainage, it is also dependent on such factors as watershed slope and landscape features, such as wetlands, that would detain runoff. Flatter sloped watersheds with more storage effects tend to have lower PRFs, whereas steeper watersheds with fewer storage effects tend to have higher PRFs. For example, one southwest Florida watershed had peak rate factors ranging from between 188 to 257 and another ranging from between 302 to 390 (Dendy 1987). On the other hand, Whitewater Creek in New Mexico (case study 4, appendix D) in this technical note) was found to have PRFs over 700.

Note that the curvilinear UH of figure 16 was developed graphically and not an equation, but is a smooth curve fitted to the triangular estimation, achieving a natural hydrograph shape. If a different PRF is used, the curvilinear UH has a different shape. The reference appendix 16B (USDA-NRCS 2007) provides tables of dimensionless UHs for several other peak rate factors.

The NRCS hydrology models, such as WinTR-20, assume the default PRF of 484. The user can use a different PRF, but must take additional steps to load the applicable dimensionless unit hydrograph. The HEC-HMS model gives the user several options for runoff transformation, including the NRCS dimensionless UH. HEC-HMS version 4.1 provides the ability to vary the PRF to values other than 484.

Adjustment of Unit Hydrograph for Wildfire Effects

Generally, the hydrologist does not have the benefit of data from studies and instrumentation from burned watersheds. The best option for estimation of timing is hydrologic judgement of changes in Manning's roughness, changes in watershed storage, and changes in peak factor. Of these, general watershed storage effects may be the least important. Steeper mountainous watersheds do not tend to have significant wetland or ponding areas. If they do, then the effect of wildfire may be minimal, except that sedimentation would tend to somewhat reduce storage effects. The HEC-HMS user manual states, "…many studies have found that the storage coefficient, divided by the sum of the time of concentration and storage coefficient, is reasonably constant over a region." However, the hydrologist working with a burned watershed will generally discover that no such regionally derived storage coefficients exist.

For steeper watersheds, such as those of the Western United States, which experience wildfire, the peak rate factor should be estimated, rather than assuming the default. Figure 17 shows an example from case study 4. The pre-fire PRF was already above 600, but the wildfire effect was to raise it further. While the PRF can

be estimated using times to peak and recession (equation 9) the availability of GIS layers may facilitate a better estimate using time-area histograms.

The HEC-HMS model offers several synthetic UH transformation methods, which, similarly to the NRCS dimensionless unit hydrograph, require some estimate of the magnitude and timing of the UH peak. To use the Snyder UH, for example, HEC-HMS requires input of standard lag and peaking coefficient. For the Clark UH, the model requires input of time of concentration and storage coefficient. For the NRCS dimensionless UH, time of concentration is required, along with UH peak discharge computed from equation 7 (with the option to use a different peak factor than the standard).

Similarly, to the NRCS peak rate factor, the HEC-HMS Snyder synthetic unit hydrograph peaking constant has no small effect on the hydrograph. The HEC-HMS user manual (USACE 2013) states that "it ranges from 0.4 to 0.8, with lower values associated with steep-rising hydrographs." The user manual also states that the peaking constant "is estimated using the best judgment of the user, or possibly from locally-developed relationships to watershed physical features."

While the NRCS hydrology program WinTR-20 facilitates the use of unit hydrographs up to 600 in peak rate factor (see appendix 16B of USDA-NRCS 2007), the HEC-HMS model accepts input of user-derived unit hydrographs and S-curves. See case study 4, appendix D, in this technical note.

Figure 17 Baldy Creek pre-fire and post-fire 30-minute unit hydrographs

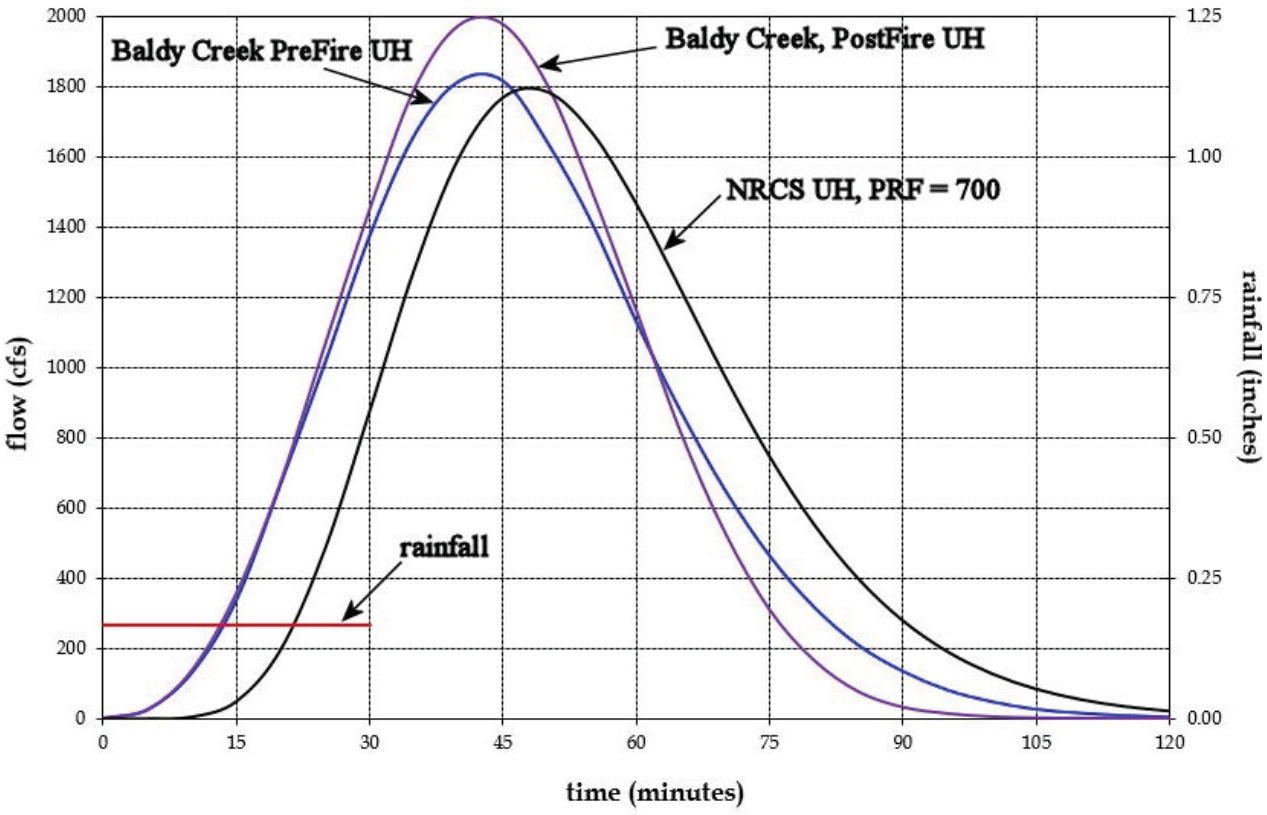

Kinematic Wave Transformation

The models KINEROS2 and AGWA perform runoff transformation using kinematic wave transform. HEC-HMS also offers the kinematic wave transform as an option. The kinematic wave model refers to an approximation of the full unsteady flow routing equations of Saint Venant. A number of variations on these equations exist based on ignoring terms that, in certain applications, are considered negligible (see Ponce and Simons 1977). The kinematic wave model retains only one of four terms, and thus cannot accommodate diffusion of hydrograph peaks. For watershed hydrology applications, the kinematic wave transform is considered perfectly adequate. For further discussion of applicability, see the HEC-HMS Technical Reference Manual (USACE 2013). See also MacArthur and DeVries (1993).

The kinematic wave technique performs time-step calculations using differential equations for flow on various land surface types (overland, collector channels, and stream channels). Ponce (1991) suggested that the kinematic wave transform not be applied to subareas larger than one square mile because larger areas subject the differential equation solutions to artificial numerical effects. However, Woolhiser (1992) and Goodrich (1992) point out that difficulties with numerical stability do not render a model inapplicable to larger watersheds. Goodrich had, at the time, successfully modeled subbasins up to 2.5 square miles. These discussions alert the user to be aware of numerical stability issues related to drainage area.

As discussed in the HEC-HMS Technical Reference Manual (USACE 2013), the equations used in the kinematic wave transform reduce to various approximations of Manning's equation. The user, then, must provide estimations of n-value for the various surfaces (for which tables 10 and 11 may be referenced).

Adjustment of Kinematic Wave Transformation Parameters for Wildfire Effects

Whether direct runoff is transformed into an outlet hydrograph using unit hydrographs or kinematic wave equations, the hydrologist must assess the post-fire change in runoff travel time. The alteration of Manning's roughness coefficient is one consideration. Hydrophobicity may also speed up overland flow runoff. By limiting infiltration, water repellency deepens the flow on the overland surface, while also tending to smooth it. Transport of loose soil above the hydrophobic layer, however, tends to raise roughness coefficient.

Time-Area Histogram Synthetic Unit Hydrograph Development

Unit hydrographs may be developed using streamflow and precipitation records, but gages for the pre-fire condition may not exist. Even if they do, the records will not facilitate development of a post-fire UH. Another option is to develop a synthetic unit hydrograph using estimated time-area histograms of runoff from the burned watersheds. The procedure can also be used to estimate peak rate factors or to develop dimensionless unit hydrographs for use in NRCS computer models.

To develop this terrain-based synthetic unit hydrograph, the user creates GIS raster information that ultimately allows the estimation of time-bands of raster cells, each band defining the area of a subbasin that drains to the outlet in the same time interval. To obtain flow velocity, the user develops a Manning's roughness raster, based on whether the cell contains overland (sheet flow), shallow-concentrated, or channel flow (fig. 18). Other factors taken into account in the derivation of the roughness layer are soil types, vegetation types, and burn severity. Figure 19 shows a subbasin raster of high burn severity locations. A flow slope raster can also be developed from the DEM layer (fig. 20). Details on the creation of these raster layers with ArcMap (ESRI 2010) is provided with case study 4, "Whitewater Creek, Gila Wilderness, New Mexico," in appendix D of this technical note.

Figure 18 Example of an *n*-value raster, with progressively higher roughness with darker color

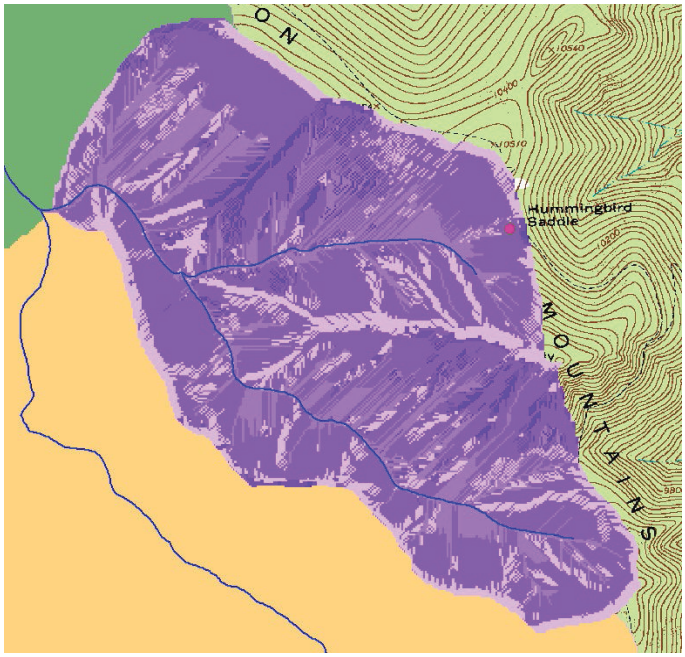

Figure 19 Example of high burn severity raster (red pixels)

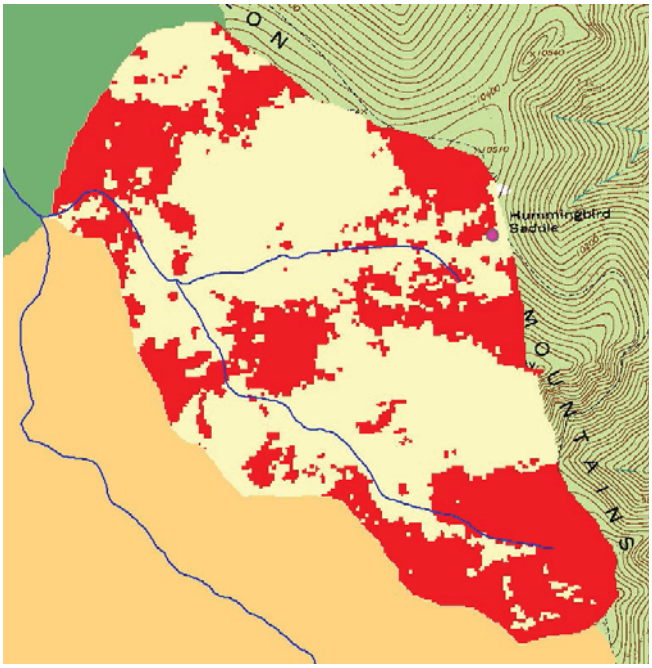

Figure 20 Example of flow slope raster, progressively steeper with darker color

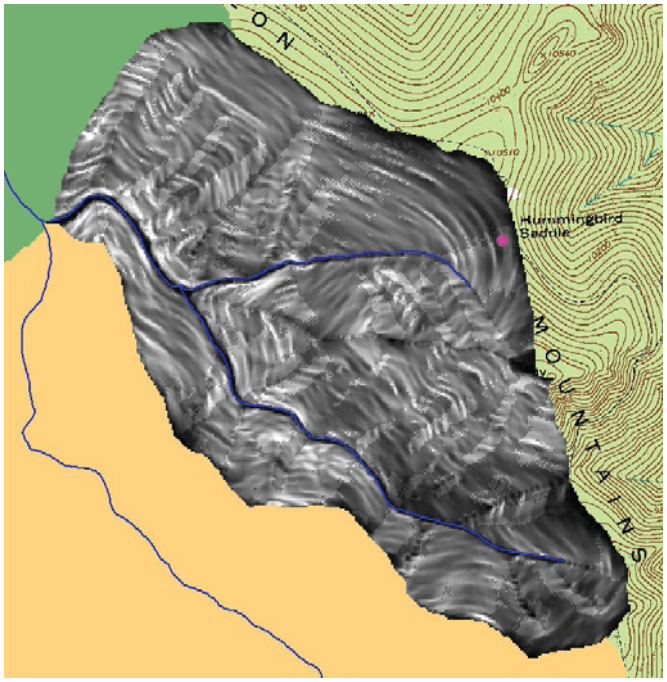

Flow velocity relationships may be derived from equations 2, 3, and 4 above. Case study 4 shows the use of similar flow velocity equations developed with reference to kinematic wave routing theory. Note that Manning's roughness values vary significantly between overland flow and channel values, as shown in tables 10 and 11. Further guidance on selection of post-wildfire roughness coefficients is provided in the section on adjustment of runoff flow time for wildfire effects.

In addition, the Manning's equation for stream velocity estimation (eq. 4) is dependent on flow cross-sectional area (within the hydraulic radius term). One way to estimate this parameter for any location in a watershed is to use hydraulic geometry relations of, say, bankfull flow area as a function of drainage area. Case study 4 provides further details on these procedures. Since a hydrograph runs through a range of flow depths and velocities, the use of bankfull parameters may result in low velocity estimates if the runoff being modeled is a rare event. Recall, however, that UH theory assumes the timing is identical no matter the intensity of effective rainfall.

From the velocity, raster a drainage time raster can be created to determine the number of cells that drain to the outlet in successive time bands of, say, 5 minutes. This velocity raster enables the derivation of a time-area histogram of the watershed. Standard hydrology textbooks such as Bedient, Huber, and Vieux (2012) show how a unit hydrograph can be easily created in a spreadsheet, using a time-area histogram. Case study 4 demonstrates the derivation of synthetic unit hydrographs by this methodology.

Sedimentation Estimation

Estimation of flow rates and velocities of clear streamflow (free of sediment and debris) benefits from the fact that liquid water has very stable properties, such as density, viscosity, incompressibility, and homogeneity. Predicting the movement of woody debris is difficult because the size, shape, and availability of any given mass is random. With sediment, unit weight is not highly variable, but the range of particle sizes and cohesiveness is extremely wide, from micron-sized cohesive clays, through the range of silts and sands, to gravel, to enormous boulders. The susceptibility of gravels and cobbles to the lift and drag forces of streamflow partly depend on imbrication, or shielding, provided by other larger particles. Once in motion, the distance a particle will travel depends on the energy of the stream current, which varies longitudinally with drainage slope and transversely in a flow cross-section both horizontally and vertically.

Increased sediment transport by floodwater after watershed burn is common and often damaging, as shown in figure 21. The steepness of mountain streams provides energy to move sediment. Whenever some physical attribute of the stream lessens its ability to carry sediment, the stream responds by depositing whatever it can no longer transport. Figure 22 shows the result of a steep stream emerging from a canyon onto a plain. No longer confined by canyon walls, the stream may break out in various directions across an alluvial fan. In any of its chosen paths across the alluvial fan, the sediment-transport capability is greatly reduced, compared to that in the canyon from which it emerged. Resulting deposition creates the fan itself, but the location of flood channels from any given event varies significantly over time.

Figure 21 2010 post-wildfire debris flow from San Gabriel Mountains, CA

Photo by Robert Looper, U.S. Geological Survey (USGS)

Figure 22 Alluvial fan, Death Valley National Park

Photo by Marli Bryant Miller, (marlimillerphoto.com)

Rivers in unburned watersheds transport sediment via natural channel processes, depending on stream type. A number of stream classification systems exist, which evaluate river geomorphology based on channel size, shape, slope, and bed material. While the velocity and sediment transport capacity of a stream can vary significantly along its profile, it can also vary considerably within a single cross-section. The fastest flow is not usually on the surface, but at about three-quarters of the maximum depth over the thalweg (fig. 23). Velocity is reduced toward the flow boundaries, especially in the presence of vegetation.

Figure 23 A stream cross-section with isolines of velocity, maximized over the thalweg

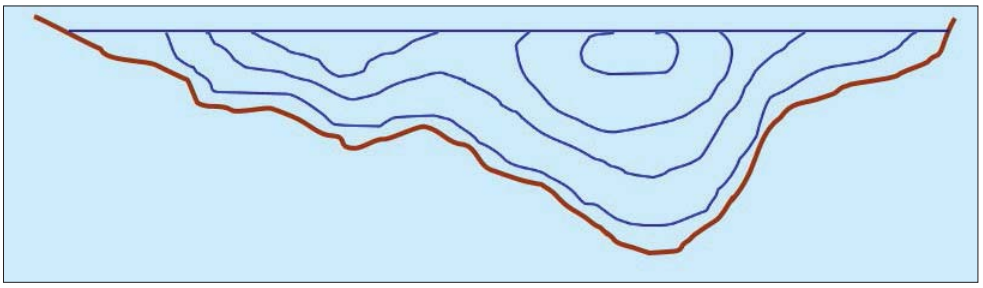

Velocity currents flow not only longitudinally, downstream, but also circulate sideways, in what are termed transverse or secondary currents. This phenomenon is responsible for the meandering behavior of rivers (fig. 24), as downwelling tends to scour out pools on the outside of bends, while gravel and sand deposition forms bars on the inside of bends.

Figure 24 Riffle-pool morphology

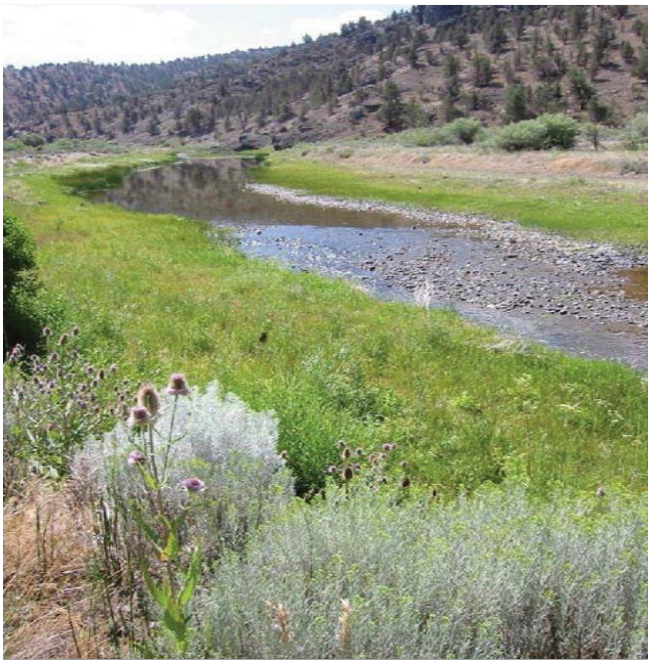

Wildfire destroys the erosion protection of vegetation, leaving watersheds vulnerable to not only elevated sediment-transport levels in otherwise clear streamflow, but also to debris flows and mudflows. Vegetation removal leaves overland flow slopes highly vulnerable to erosion, swales and gullies clog with sediment and debris, and hydrophobic soil at a depth of as little as 2 inches leaves the unconsolidated soil above it vulnerable to erosive flow. With wildfire, not only is sediment more vulnerable to erosion, but debris such as logs and partially burned branches are often washed into the streams. Sometimes the flowing water is so clogged with sediment, that the flowing mass is termed mudflow or debris flow. Having a higher density and viscosity than clear water flow, debris flows can be extremely dangerous.

Santi et al. (2006) define debris flow as "the rapid flow of saturated material consisting of more than 20 percent gravel and coarse material through a steep channel or over steep hillsides." Because the volume of debris flows can often be correlated with property damage and other hazards, a number of studies have examined size classification (Jakob 2005) and prediction (Santi and Morandi 2012, Prochaska et al. 2008) (table 13). Concerning post-wildfire recovery in the Western United States, Santi and Morandi (2012) state: "...there is a clear progression in decreasing volume of debris flows as basins recover from the wildfire: it takes approximately 1 year, or at a few locations, as much as 3 years, for debris production to return to pre-fire rates." Note that accelerated sediment transport rates, as opposed to debris flows, may persist much longer.

Another finding from Santi et al. (2006) is that "the majority of material in post-fire debris flows is eroded from the channels—only a small percentage of the total volume is contributed from hillslope rilling and sheetwash." Again, the analyst must distinguish between the much more sediment-bulked debris flow events and rainfall-runoff events with elevated sediment transport. The latter may well originate on hillslopes subjected to vegetation removal and hydrophobic soils associated with wildfire.

Concerning sediment, the design or evaluation of engineering structures in wildfire-impacted areas may take a number of approaches. Hydrographs modeled as clear flow are often increased by considering the bulking effect of entrained sediment. A specific sediment-transport computer model may be used to estimate locations and magnitudes of sediment aggradation or degradation. Debris flow or mud flow may be estimated or modeled. The USACE hydraulic model HEC-RAS has sediment transport modeling capability, but the available empirical sediment transport equations come with significant uncertainties and generally require calibration. Considerable field measurements of sediment supply and channel geometry are required.

Table 13 Size classification and potential consequences of debris flows (Santi and Morandi 2012)

Size class	Volume (m^3)	Potential consequences
1	<100	localized damage, small buildings, known to have killed foresters in small gullies
2	100–1000	could bury cars, destroy small wooden buildings, break trees, block culverts, derail trains
3	1000–10^4	could destroy larger buildings, damage concrete bridge piers, damage highways or pipelines
4	10^4–10^5	could block creeks, destroy parts of villages, destroy bridges, damage infrastructure corridors
5	10^5–10^6	could destroy larger urban areas, dam up creeks and small rivers
6–10	>10^6	generally restricted to volcanic events, capable of destroying entire cities, damming large rivers

Although the two-dimensional flood-routing model FLO-2D (O'Brien et al. 1993) has been used to model debris flow (Elliott et al. 2005) rapid post-wildfire assessments generally preclude its use due to extensive input requirements and model complexity. For estimation of debris flow impacts, the analyst should consider storm event frequency, source material availability, and location of concern relative to location of source material. Modeling debris flow generally requires a less frequent (higher rainfall peak) storm, such as a 50-year event, although immediately after the wildfire a 2-year event may suffice. Availability of source material can be assessed by field observations of channel conditions, primarily, but also steep hillslope conditions. The further the location of concern from the source material the less likely the effect of debris flow (as differentiated from sediment-bulked flow). Cannon et al. (2003), for example, found that the relative degree of debris flow hazard could be assessed by examining the abundance of colluvium available in stream channels, the degree of channel confinement, and channel gradient. The study concluded that further research is needed.

Models for Estimating Sediment Transport

For estimating elevated sediment transport, as opposed to debris flow, three models are discussed: GeoWEPP, AGWA, and RUSLE2.

GeoWEPP is a geospatial interface for the Water Erosion Prediction Project (WEPP) model (Flanagan et al. 2001). Both WEPP and GeoWEPP for ArcGIS are available on the Web. WEPP is a continuous simulation process-based model, applicable to hillslope erosion processes (sheet and rill erosion). It uses stochastically derived climate data from the CLIGEN model (Zhang and Garbrecht 2003). WEPP has two distinct disadvantages. First, WEPP is designed for continuous simulation. As a result, it is less applicable to storm events, which tend to drive post-fire runoff and sediment transport. Second, existing climate generator models such as CLIGEN and GEM6 are not designed to produce less frequent storm event peaks (Theurer et al. 2010) but rather the day-to-day kinds of rainfall events evaluated by continuous simulation models.

KINEROS2 (Kinematic Runoff and Erosion Model, Canfield, Goodrich, and Burns 2005) is an event-oriented, physically based model describing the processes of interception, infiltration, surface runoff and erosion from small agricultural watersheds. KINEROS2 may be run independently, or as an option within the Automated Geospatial Watershed Assessment (AGWA) modeling tool (Goodrich et al. 2005). AGWA is a GIS-based hydrologic modeling tool using standardized datasets to develop input parameter files for KINEROS2 and SWAT. The KINEROS model is applicable to storm events. AGWA has had improvements for post-wildfire use (Canfield and Goodrich 2005 and Burns 2005). The KINEROS2 model is available as a separate download from the USDA-Agricultural Research Service (ARS), Southwest Watershed Research Center (SWRC). AGWA modeling tool and documentation are also available from USDA-ARS-SWRC. See case study 5 for an example of the use of AGWA.

Another model sometimes used for post-fire sedimentation estimation is RUSLE2. This planning-level erosion model, according to the ARS documentation (USDA-NRCS 2013d), is used to estimate rill and interrill erosion where mineral soil is exposed to the erosive forces of impacting raindrops, water falling from vegetation, and surface runoff produced by Hortonian overland flow. The document states that RUSLE2 is applicable to forestlands; however, the model is intended to estimate annual average erosion from the above sources rather than event-based erosion. In fact, long-term datasets of stochastically generated climate variables used in the model tend to represent day-to-day conditions rather than the rarer storm events such as that of a 100-year recurrence (Theurer et al. 2010). The simplicity of the model and its conduciveness to spatial estimation using GIS, make RUSLE2 a possible tool for evaluating sedimentation due to wildfire. See case study 3 of this technical note for example. Theobald et al. (2010) documents the GIS manipulations involved and Litschert et al. (2014) applies RUSLE2 and GIS to wildfire in the Southern Rockies Ecoregion.

Adjustments for Modeling Sediment Transport From Burned Areas

Regardless of which estimation methods or models are applied, the modeler is advised to pay attention to burn severity. One study (Benavides-Solorio and MacDonald 2001) in Colorado found relatively small differences in runoff rates as a function of burn severity, but a much higher correlation for sediment yield. That study stated, "...percent ground cover accounted for 81 percent of the observed variability in sediment yields" and "...large differences in sediment yields with burn severity should be attributed primarily to

the differences in ground cover rather than the differences in runoff, water repellency, or antecedent soil moisture." These results imply that watershed recovery and return of sediment yield to unburned rates should be a function of vegetation and ground cover, and the study indicates that full recovery may take from 3 to 9 years.

Sediment Bulking

The post-fire hydrographs produced by the models previously discussed do not account for the phenomenon of sediment bulking. This term refers to the overall raising of hydrograph flows and stages due to significant sediment load. Many flood flows in unburned watersheds carry sediment, with normally minimal effect on hydrographs. At the other end of the spectrum, watersheds denuded of vegetation by fire or volcanic action can produce runoff so laden with sediment that it is referred to as mudflow or debris flow. As defined in the previous section, debris flow is considered that which entrains at least 20 percent gravel and coarse material. Elliott et al. (2005) delineates hyperconcentrated flows as ranging from 20 to 47 percent sediment concentration and mudflows as having a greater than 47 percent sediment concentration.

Post-wildfire flows that do not reach the 20-percent threshold nevertheless transport considerable sediment loads. This entrained sediment raises (or bulks) the overall flow rate and, at any particular location, raises the flood depth. For a hydrograph, the total bulked flow rate is the sum of the water discharge and the sediment discharge.

$$Q_{bulked} = Q_w + Q_{sed} \qquad \text{eq. 10}$$

One way to account for sediment bulking in post-wildfire hydrograph analyses is to apply a bulking factor to the flood peak (O'Brien and Fullerton 1989, Elliott et al. 2005):

$$BF = \frac{Q_w + Q_{sed}}{Q_w} = \frac{1}{1 + C_v} \qquad \text{eq. 11}$$

where C_v is the maximum sediment concentration by volume in percent.

As discussed in Elliott et al. (2005), if the event contains a sediment concentration just under hyperconcentrated (20 percent) then, using equation 10, the resulting bulking factor is 1.25.

Sediment concentration varies during a storm and generally peaks before that of the water discharge. One way researchers estimate sediment discharge over time is to measure data and derive simple regression equations. For example, Moody and Martin (2001) found, for two recently burned Colorado watersheds:

$$Q_{sed} = 4.4 Q_w^{1.5} \qquad \text{eq. 12}$$

$$Q_{sed} = 23 Q_w^{1.3} \qquad \text{eq. 13}$$

where—

Q_w = water flow (m^3/s)

Q_{sed} = sediment flow (m^3/s)

The study reported statistical correlations of r^2=0.89 for equation 11, and r^2=0.96 for equation 12. Using a hypothetical storm hydrograph, with a peak of about 580 cfs in the second watershed, and translating both discharges into cfs, a bulk factor for the peak of 1.06 is derived (fig. 25).

For post-fire hydrologic analyses, if previous studies for the watershed of concern exist, then maximum sediment concentrations and bulk factors are better estimated. The bulk factor can be much higher than the hypothetical one from above. For example, LACDPW (2006) has compiled curves for debris production and bulk factors for the Los Angeles River, Santa Clara River, and Antelope Valley watersheds, with wide variation from place to place. Figure 26 shows the data for one of their lower debris production areas with bulking factors near 1.5.

Figure 25 Hypothetical storm using equation 12 (all discharges converted to cfs)

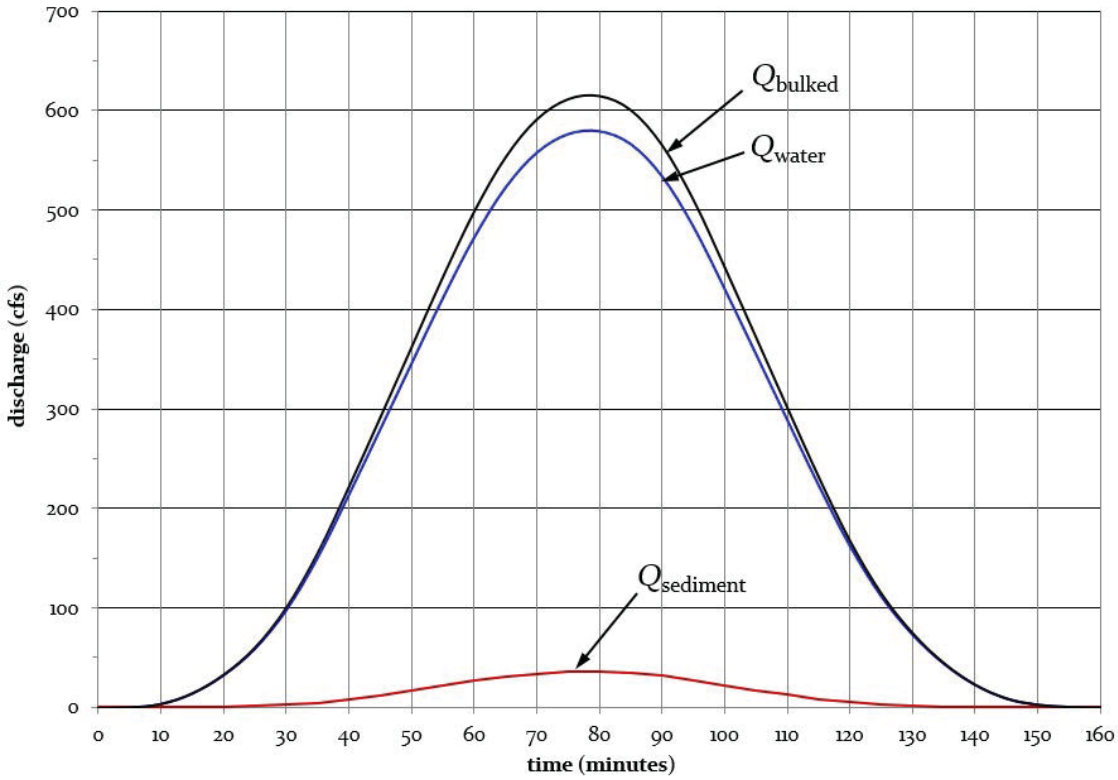

Figure 26 Sediment production and bulking factors for debris production area 7 (LACDPW 2006)

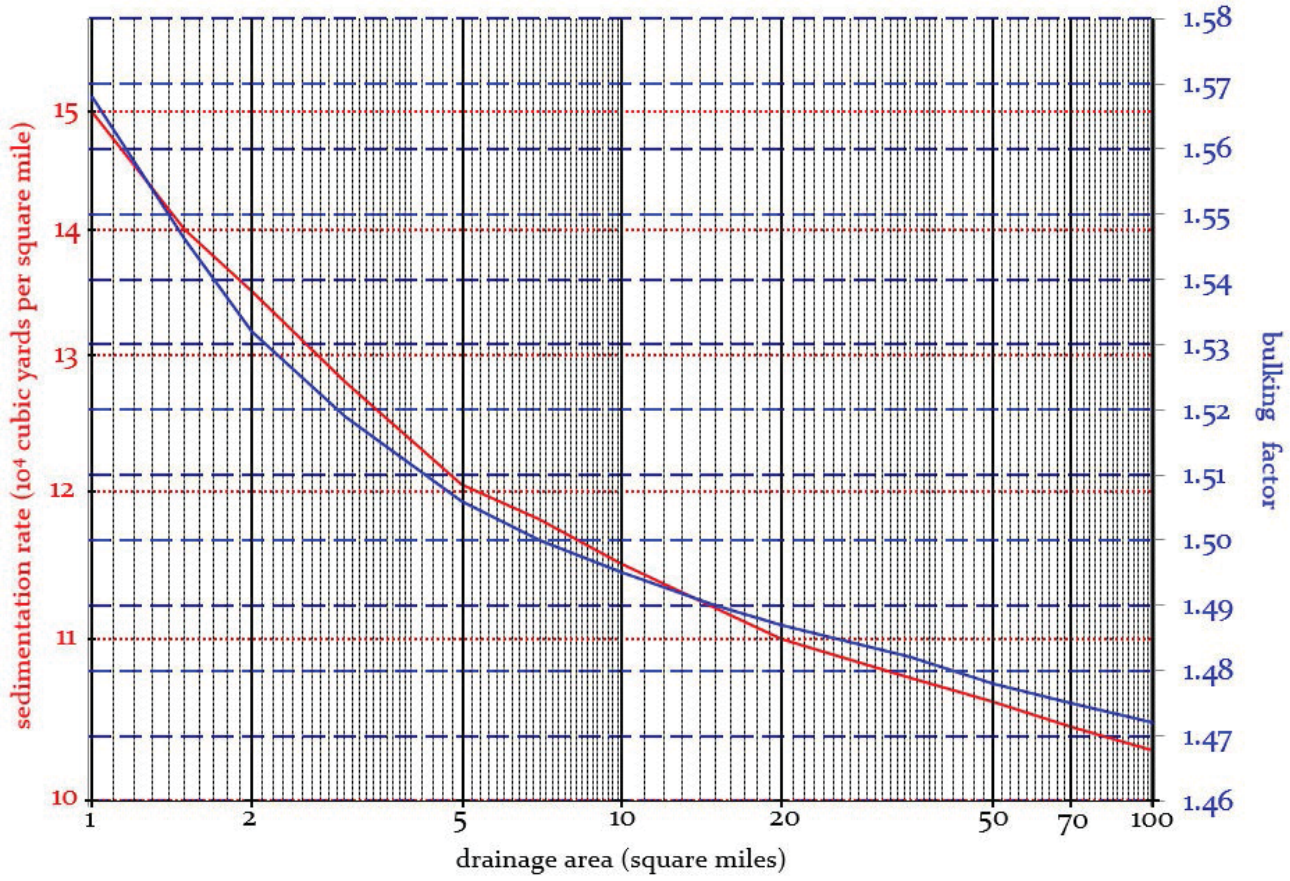

A factsheet from the USGS (Pierson 2005) provides guidance on field investigations to distinguish between debris flows and normal flow sediment deposits. The reference suggests that normal suspended sediment concentrations are 5 to 10 percent by volume, but that even with hyperconcentrated flow (volumes between 20 and 60 percent) the flow behavior is controlled by water, whereas mud flows (even higher sediment concentrations) have behavior controlled by the entrained sediment.

Field indicators listed for water flow deposits are that most grains are rounded, beds are stratified with good sorting both horizontally and vertically, with loose consistency when dry. Debris flow deposits, on the other hand, tend to be angular sand and fine gravel (indicating a hillslope source), nonstratified, and extremely poorly sorted, with coherent consistency rather than loose.

Note that when using post-wildfire streamflow records to calibrate modeled hydrographs these measurements are already bulked. When sediment load is high enough to be considered hyperconcentrated, flow gages will likely be either destroyed or unable to measure properly. For guidance on the timing of rainfall events that may produce debris flow, consider a flood of rare recurrence interval, such as the 50-year event, occurring shortly after wildfire. One study (Cannon et al. 2003) found significant post-wildfire debris flows occurring with storms as frequent as the 2-year event. The study suggests that the generation of high sediment concentrated flows is possible by progressive sediment bulking over time. In other words, smaller events can deposit sediment from burned slopes into upper basin channels. A subsequent larger event may then be significantly bulked because of the availability of this temporarily stored sediment. Another study (Giraud and McDonald, 2007) found that debris flows tend to result from channel incision rather than hillslope erosion, but agree with Cannon et al. (2003) that smaller events, merely bulked rather than hyperconcentrated, may contribute to later debris flow events.

Model Uncertainties, Calibration, Validation

The ideal watershed for rainfall-runoff process modeling has an extensive spatially distributed data collection network. The instrumentation would provide the hydrologist a historic record of rainfall amounts in time and space, soil moisture levels, baseflow levels, and sedimentation rates. However, even with a spatially dense network of instruments, say every half mile, considerable uncertainty remains, since conditions at points other than the station locations would have to be assumed. As discussed in Beven (2001), for example, the use of distributed hydrologic models for prediction of future states suffers a number of limitations, namely, problems of nonlinearity, scale, uniqueness, equifinality, and uncertainty. Other researchers suggest, more generally, that verification and validation of numerical models of natural systems is impossible (Oreskes, Shrader-Frechette, and Belitz 1994).

In the real world, the number of data collection stations in a watershed never comes close to true spatial adequacy. The watershed model is inherently an open system, subject to equifinality—that a given end state (say, a certain magnitude storm runoff peak at the outlet) can be caused by many potential combinations of circumstances (say, storms of similar intensity but different areal extent, centered over different points in the basin). Even if such an extensive data station network existed, the radical and sudden change wrought by wildfire renders the historical dataset inapplicable.

Although calibration and validation are not possible with post wildfire hydrologic modeling, the hydrologist should at least report sources of known uncertainty. If hydrophobicity exists, the hydrologist should report the evidence of spatial extent or persistence of significant water repellent layering, and by what means they attempted to accounted for it in the model. If data stations are installed after a fire, this recorded evidence of post-fire events may be used to show the reasonability of the hydrologic model. Such data does not generally support claims of calibration or validation, since scarcity of stations leaves open the possibility of more than one spatial layout of storms having the same impact at the stations. However, one or more hypothetical storm distributions, which reproduce the measured data, could be modeled to show whether the model responds reasonably. Case study 4 demonstrates this approach.

References

Aldridge, B. N., and J. M. Garrett, 1973. Roughness coefficients for stream channels in Arizona. U.S. Geological Survey Open-File Report, Tucson, AZ.

Bathurst, J.C. 1985. Flow resistance estimation in mountain rivers. Journal of Hydraulic Engineering 111(4), 625–643.

Bedient, P.B., W.C. Huber, and B.E. Vieux. 2012. Hydrology and Floodplain Analysis, Prentice Hall, NJ, 5th Edition, 801 pages.

Benavides-Solario, J.D., and L.H. MacDonald. 2001. Post-fire runoff and erosion from simulated rainfall on small plots, Colorado Front Range. Hydrological Processes, 15, 2931–2952.

Beven, K.J. 1989. Changing ideas in hydrology -- the case of physically-based models. Journal of Hydrology 105, 157–172.

Beven, K.J. 2001. How far can we go in distributed hydological modelling? Hydrology and Earth System Sciences 5, 1–12.

Canfield, H.E., Goodrich, D.C. 2005. Suggested changes to AGWA to account for fire (V. 2.1). Southwest Watershed Research Center, USDA-ARS, Tucson, AZ.

Canfield, H.E., D.C. Goodrich, and I.S. Burns. 2005. Selection of parameters values to model post-fire runoff and sediment transport at the watershed scale in Southwestern forests.

Cannon, S.H., J.E. Gartner, C. Parrett, and M. Parise. 2003. Wildfire-related debris-flow generation through episodic progressive sediment-bulking processes, western USA. In Proceedings: Debris-Flow Hazards Mitigation: Mechanics, Prediction, and Assessment.

Cerrelli, G.A. 2005. FIRE HYDRO, a simplified method for predicting peak discharges to assist in the design of flood protection measures western wildfires. In Proceedings of the ASCE 2005 Watershed Management Conference, July 2005, Williamsburg, VA. pp. 935–941.

CFR (Code of Federal Regulations), 2005. Emergency watershed protection program. 7 CFR Part 624.4.

Chen, L., M. Berli, C. Karletta. 2013. Examining modeling approaches for the rainfall-runoff process in wildfire-affected watersheds: using San Dimas Experimental Forest. Journal of the American Water Resources Association 1–16.

Conedera, M., L. Peter, P. Marxer, F. Forster, D. Rickenmann, L. Re. 2003. Consequences of forest fires on the hydrogeological response of mountain catchments: a case study of the Riale Buffaga, Ticino, Switzerland. Earth Surface Processes and Landforms 28, 117–129.

Debano, L.F., J.F. Osborn, J.S. Krammes, J. Letey. 1967. Soil wettability and wetting agents: our current knowledge of the problem. USDA Forest Service Research Paper PSW-43: 13.

DeBano, L.F. 2000a. Water repellency in soils: a historical overview. Journal of Hydrology, 231–232, 4-32.

DeBano, L.F. 2000b. The role of fire and soil heating on water repellency in wildland environments: a review. Journal of Hydrology, 231-232, 195–206.

DeBano, L.F. 1981. Water repellent soils: a state-of-the art. USDA Forest Service, General Technical Report PSW-46.

Dendy, G.S. 1987. A 24-hour rainfall distribution and peak rate factors for use in Southwest Florida. Masters Thesis, University of Central Florida, Orlando, FL, 172 pages.

Doerr, S.H. 1998. On standardizing the 'Water Drop Penetration Time' and the 'Molarity of an Ethanol Droplet' techniques to classify soil hydrophobicity: A case study using medium textured soils. Earth Surface Processes and Landforms 23, 663–668.

Doerr. S.H., R.A. Shakesby, R.P.D. Walsh. 2000. Soil water repellency: its causes, characteristics and hydro-geomorphological significance. Earth Science Reviews, 51, 33–65.

Dyrness, C.T. 1976. Effect of wildfire on soil wettability in the high cascades of Oregon. USDA Forest Service, Pacific Northwest Research Station, Research Paper PNW-202, 19 p.

Elliott, J.G., M.E. Smith, M.J. Friedel, M.R. Stevens, C.R. Bossong, D.W. Litke, R.S. Parker, C. Costello, J. Wagner, S.J. Char, M.A. Bauer, and S.R. Wilds. 2005. Analysis and mapping of post-fire hydrologic hazards for the 2002 Hayman, Coal Seam, and Missionary Ridge wildfires, Colorado. USGS Scientific Investigations Report 2004-5300, 80 pages.

Engman, E.T. 1986. Roughness coefficients for routing surface runoff. Journal of Irrigation and Drainage Engineering 112 (1). Amer. Soc. of Civil Eng., New York, NY. pp. 39–53.

ESRI (Environmental Systems Resource Institute). 2010. ArcMap 10.0 ESRI, Redlands, CA.

Fang, X., et al. 2005. Revisit of NRCS unit hydrograph procedures. In Proceedings of the ASCE Texas Section Spring Meeting, Austin, TX, April 2005, 21 pages.

Flanagan, D.C., et al. 2001. Chapter 7: The Water Erosion Prediction Project (WEPP) model. In Landscape Erosion and Evolution Modeling. Kluwer Academic Publishers, Norwell, MA. 51 pages.

Folmar, N.D., and A.C. Miller. 2008. Development of an empirical lag time equation. ASCE Journal of Irrigation and Drainage Engineering 112(1), pp. 39–53.

Foltz, R.B., P.R. Robichaud, and H. Rhee. 2009. A synthesis of post-fire road treatments for BAER teams: methods, treatment effectiveness, and decisionmaking tools for rehabilitation. USDA Forest Service General Technical Report RMRS-GTR-228.

Garen, D.C., D.S. Moore. 2005 Curve number hydrology in water quality modeling: uses, abuses and future directions. Journal of the American Water Resources Association 42(2), 377–388.

Giraud, R.E., and G.N. McDonald. 2007. The 2000-2004 fire-related debris flows in northern Utah. In: Proceedings 1st North American Landslide Conference, AEG Special Publication 23, 1522–1531.

Goodrich, D.C. 1992. Discussion of "The kinematic wave controversy" by Victor M. Ponce (April, 1991, Vol. 117, No. 4). ASCE Journal of Hydraulic Engineering 118(9): 1334–1335.

Goodrich, D.C., et al. 2005. Rapid post-fire hydrologic watershed assessment using the AGUA GIS-based hydrologic modeling tool. In Proceedings of the ASCE 2005 Watershed Management Conference, July 2005, Williamsburg, VA, pp. 1–12.

Hawkins, R.H., D.E. Woodward, A.T. Hjelmfelt, J.A. Van Mullem, and Q.D. Quan. 2002. Runoff curve number method: examination of the initial abstraction ratio. Proceedings Federal Interagency Hydrologic Modeling Conference, Las Vegas, NV, 12pp.

Hawkins, R.H. 1993 Asymptotic determination of runoff curve numbers from data. Journal of Irrigation and Drainage Engineering 119, 334–345.

Hawkins, R.H., R.J. Greenberg. 1990. WILDCAT4 flow model. School of Renewable Natural Resources, University of Arizona, Tucson, AZ, BLM contact: Dan Muller, Denver, CO.

Henkle, J.E., E. Wohl, N. Beckman. 2011. Locations of channel heads in the semiarid Colorado Front Range, USA Geomorphology 129, 309–319.

Hey, R.D. 1979. Flow resistance in gravel bed rivers, ASCE Journal of the Hydraulics Division, 105(4), 365–379.

Hicks, D.M., P.D. Mason. 1998. Roughness characteristics of New Zealand rivers, 2nd Edition, Water Resource Publications.

Hudak, A.T., P.R. Robichaud, J.S. Evans, J. Clark, K. Lannom, P. Morgan, C. Stone. 2004. Field validation of burned area reflectance classification (BARC) products for post fire assessment. Remote Sensing for Field Users: Proceedings of the Tenth Forest Service Remote Sensing Applications Conference, Salt Lake City, UT, April 5–9 2004.

Huffman, E.L., L.H. MacDonald, and J.D. Stednick. 2001. Strength and persistence of fire-induced soil hydrophobicity under ponderosa and lodgepole pine, Colorado Front Range. Hydrologic Processes, 15, 2877–2892.

Jakob, M. 2005. A size classification for debris flows. Engineering Geology, 79, 151–161.

Jarrett, R.D. 1984. Hydraulics of high-gradient streams. Journal of Hydraulic Engineering 110 (11), 1519–1539.

Keeley, J.E. 2009. Fire intensity, fire severity and burn severity: a brief review and suggested usage. International Journal of Wildland Fire, 18, 116–126.

LACDPW (Los Angeles County Department of Public Works), 2006. Sedimentation Manual, 2nd Edition.

LandFire 2010. LandFire Fact Sheet, http://www.landfire.gov/.

Lawrence, D. S. L. 1997. Macroscale surface roughness and frictional resistance in overland flow. Earth Surface Processes and Landforms 22: 365–382.

Limerinos J.T. 1970. Determination of the Manning coefficient from measured bed roughness in natural channels. U.S. Geological Survey Water Supply Paper 1898-B, 52 pages.

Litschert, S.E., D.M. Theobald, and T.C. Brown. 2014. Effects of climate change and wildfire on soil loss in Southern Rockies Ecoregion. Catena 118, 206–219.

Livingston, R.K., T.A. Earles, and K.R. Wright. 2005. Los Alamos post-fire watershed recovery: a curve-number-based evaluation. In Proceedings of the ASCE 2005 Watershed Management Conference, July 2005, Williamsburg, VA, pp. 471–481.

MacArthur, R., and J.J. DeVries. (1993) Introduction and application of kinematic wave routing techniques using HEC-1. U.S. Army Corps of Engineers Hydrologic Engineering Center, Davis, CA, 68 pages.

MacDonald, L.H., R.N. Sampson, D. Brady, L. Juarros, and D. Martin. Predicting Post-Fire Erosion and Sedimentation Risk on a Landscape Scale: A Case Study from Colorado, pp. 57-87. Chapter 4 in Mapping Wildfire Hazards and Risks, edited by Sampson, R.N., Atkinson, R.D., and Lewis, J.W. Journal of Sustainable Forestry, Vol. 11, 1/2, 2000.

Maidment, D.R. 1992. Handbook of Hydrology McGraw-Hill, Inc.

McCuen, R.H. and T.R. Bondelid. 1983. Estimating Unit Hydrograph Peak Rate Factors. ASCE Journal of Irrigation and Drainage Engineering 109(2), 238–250.

Miller, J.D., and A.E. Thode. 2007. Quantifying burn severity in a heterogeneous landscape with a relative version of the delta Normalized Burn Ratio (dNBR). Remote Sensing of Environment 109, 66–80.

Moody, J.A., et al. 2013. Current research issues related to post-wildfire runoff and erosion processes. Earth Science Reviews, (in publication).

Moody, J.A., and D.A. Martin. 2009. Synthesis of sediment yields after wildfire in different rainfall regimes in the Western United States. International Journal of Wildland Fire, 18, 96–115.

Moody, J. A., and D.A. Kinner. 2006. Spatial structure of stream and hillslope drainage networks following gully erosion after wildfire. Earth Surface Processes and Landforms 31(3): 319–337.

Moody, J.A., and D.A. Martin. 2001. Hydrologic and sedimentologic response of two burned watersheds in Colorado, USGS Water-Resources Investigations Report 01-4122, 146 pages.

NASA 2012. NOAA National Aeronautics and Space Administration , Water and Energy Cycle Web site: http://science.nasa.gov/earth-science/oceanography/ocean-earth-system/ocean-water-cycle/

NWCG 2006. Glossary of wildland fire terminology. National Wildfire Coordinating Group, Incident Operations Standards Working Team.

O'Brien, J. S., P.T. Julien, and W.T. Fullerton. (1993). Two-dimensional water flood and mudflow simulation. ASCE Journal of Hydraulic Engineering 119(2): 244–261.

O'Brien, J.S., and W.T. Fullerton. 1989. Hydraulic and sediment transport study of Crown Pointe flood wall: Breckenridge, Colo., Lenzotti and Fullerton Consulting Engineers, Inc., 34 p.

Oreskes, N., K. Shrader-Frechette, and K. Belitz. (1994) Verification, validation, and confirmation of numerical models in the earth sciences. Science 263, 641–646.

Parsons, A., S.A. Lewis, C. Napper, and J.T. Clark. 2010. Field guide for mapping post-fire soil burn severity. USDA Forest Service General Technical Report RMRS-GTR-243, 49 pages.

Pierson, T.C. 2005. Distinguishing between debris flows and floods from field evidence in small watersheds. USGS factsheet 2004-3142.

Ponce, V.M. 1991. The kinematic wave controversy. ASCE Journal of Hydraulic Engineering 117(4): 511–525.

Ponce, V.M., and D.B. Simons. 1977. Shallow wave propogation in open channel flow. ASCE Journal of Hydraulic Engineering 103: 1461–1476.

Prochaska, A.B., P.M. Santi, J.D. Higgins, and S.H. Cannon. 2008. Debris-flow runout predictions based on the average channel slope (ACS). Engineering Geology, 98, 29–40.

Rallison, R.E. 1980. Origin and evolution of the SCS runoff equation. Proceedings of the Symposium on Watershed Management; American Society of Civil Engineers, Boise, ID.

Rallison, R.E., and N. Miller. 1982. Past, present, and future SCS runoff procedure. In Rainfall-Runoff Relationships, V.P. Singh, ed., Water Resources Publ., Littleton, CO, pp. 353–364.

Rawls, W.J., D.L. Brakensiek, and N. Miller. 1983. Green-Ampt infiltration parameters from soils data. ASCE Journal of Hydraulic Engineering. 109: 62–70.

Robichaud, P.R., S.A. Lewis, L.E. Ashmum. 2008. New procedure for sampling infiltration to assess post-fire soil water repellency. USDA Forest Service, Rocky Mountain Research Station, Research Note RMRS-RN-33.

Safford, H.D., et al. 2008. BAER Soil Burn Severity Maps Do Not Measure Fire Effects to Vegetation: A Comment on Odion and Hanson (2006). Ecosystems, 11:1, 1–11.

Santi, P. and L. Morandi. 2012. Comparison of debris-flow volumes from burned and un-burned areas. Landslides, 9, 1-13.

Santi, P. et al. 2006. Evaluation of post-wildfire debris flow mitigation methods and development of decision-support tools. Report to USGS and the Joint Fire Science Program, 78 pages.

Saxton, K.E., W.J. Rawls, J.S. Romberger, and R.I. Papendick. (1986) Estimating generalized soil-water characteristics from texture. Transactions of the American Society of Agricultural Engineers 50(4): 1031–1035.

Scott, D.F. 2000. Soil wettability in forested catchments of South Africa; as measured by different methods and as affected by vegetation cover and soil characteristics. Journal of Hydrology 231–232, 87–104.

Smith, R.E., D.C. Goodrich, D.A. Woolhiser, C.L. Unkrich. 2005. KINEROS – A kinematic runoff and erosion model. In: Computer Models of Watershed Hydrology, V.J. Singh (Editor). Water Resource Publications, Highland Ranch, CO, pp. 597–632.

Springer, E.P., R.H. Hawkins. 2005. Curve number and peakflow responses following the Cerro Grande Fire on a small watershed. In: Moglen, G.E., ed. Proceedings of Managing Watersheds for Human and Natural Impacts: Engineering, Ecological, and Economic Challenges, July 19–22, 2005, Williamsburg, VA, USA. American Society of Civil Engineers, Alexandria, VA.

Stoof, C.R., R.W. Vervoort, J. Iwema, E. van den Elsen, A.J.D. Ferreira, C.J. Ritsema. 2011. Hydrological response of a small catchment burned by an experimental fire. Hydrology and Earth System Sciences Discussions 8, 4053–4098.

Story, M. 2003. Cited by USDA Forest Service BAER Tools Web page.

Stuart, B. 2000. Maudlow Fire, Burned Area Emergency Rehabilitation (BAER) plan. Townend MT: USDA Forest Service, Northern Region, Helena National Forest.Cited by USDA Forest Service BAER Tools Web page.

Tedela, N.H., S.C. McCutcheon, T.C. Rasmussen, R.H. Hawkins, W.T. Swank, J.L. Campbell, M.B. Adams, C.R. Jackson, and E.W. Tollner. 2012. Runoff curve numbers for 10 small forested watersheds in the mountains of the Eastern United States. ASCE Journal of Hydrologic Engineering, 17, 1188–1198.

Theobald, D.M., D.M. Merritt, and J.B. Norman, III. 2010. Assessment of threats to riparian ecosystems in the Western U.S. A report presented to The Western Environmental Threats Assessment Center, Prineville, OR, by the USDA Stream Systems Technology Center and Colorado State University, Fort Collins, 61p.

Theurer, F.D., D.S. Moore, W.H. Merkel, Q.D. Quan, H.F. Moody, R.L. Bingner, J. Bonta, and D. Flanagan. 2010. Comparison of historical versus synthetic weather inputs to watershed models and their effect on pollutant loads. In Proceedings of the 2nd Joint Federal Interagency Conference, Las Vegas, NV, 12pp.

USACE-HEC (U.S. Army Corps of Engineers, Hydrologic Engineering Center), 2013. Hec-HMS.

USDA-ARS (U.S. Department of Agriculture-Agricultural Research Service), 2013a. AGNPS.

National Sedimentation Laboratory, ARS, USDA, Oxford, MS.

USDA-ARS (U.S. Department of Agriculture-Agricultural Research Service), 2013b. Soil and Water Assessment Tool: SWAT. Grassland Soil and Water Research Laboratory, ARS, USDA, Temple, TX.

USDA-ARS (U.S. Department of Agriculture-Agricultural Research Service), 2013c. The Soil Infiltration Model in KINEROS2. Southwest Watershed Research Center, Tucson, AZ.

USDA-ARS (U.S. Department of Agriculture-Agricultural Research Service), 2013d. Science Documentation Revised Universal Soil Loss Equation Version 2 (RUSLE2) ARS Washington, DC. 355pp.

USDA Forest Service (U.S. Department of Agriculture) 2015. Burned Area Emergency Response Tools Web page.

USDA-NRCS (U.S. Department of Agriculture-Natural Resources Conservation Service), 2004a. NRCS National Engineering Handbook, Part 630 Hydrology, Chapter 9, Hydrologic soil cover complexes. Accessed in April 2013.

USDA-NRCS (U.S. Department of Agriculture-Natural Resources Conservation Service), 2004b. NRCS National Engineering Handbook, Part 630 Hydrology, Chapter 10, Estimation of direct runoff from storm rainfall. Accessed in April 2013.

USDA-NRCS (U.S. Department of Agriculture-Natural Resources Conservation Service), 2004c. WinTR-20 User Guide. Accessed in April 2013.

USDA-NRCS (U.S. Department of Agriculture-Natural Resources Conservation Service), 2009a. Small Watershed Hydrology WinTR-55 User Guide. Accessed in April 2013.

USDA-NRCS (U.S. Department of Agriculture-Natural Resources Conservation Service), 2009b. NRCS National Engineering Handbook, Part 630 Hydrology, Chapter 7, Hydrologic Soil Groups. Accessed in April 2013.

USDA-NRCS (U.S. Department of Agriculture-Natural Resources Conservation Service), 2010. NRCS National Engineering Handbook, Part 630 Hydrology, Chapter 15, Time of Concentration. Accessed in April 2013.

USDA-NRCS (U.S. Department of Agriculture-Natural Resources Conservation Service), 2007. NRCS National Engineering Handbook, Part 630 Hydrology, Chapter 16, Hydrographs. Accessed in April 2013.

USDA-SCS (U.S. Department of Agriculture-Soil Conservation Service), 1991. Engineering Field Handbook, Chapter 2, Estimating Runoff. Accessed in April 2013.

Woolhiser, D.A. 1992. Discussion of "The kinematic wave controversy" by Victor M. Ponce (April, 1991, Vol. 117, No. 4). ASCE Journal of Hydraulic Engineering 118(9): 1337–1339.

Yochum, S., B. Bledsoe. 2010. Flow resistance estimation in high-gradient streams. 2nd Joint Federal Interagency Conference, Las Vegas, NV, June 27– July 1.

Yochum, S.E., B.P. Bledsoe, G.C.L. David, E. Wohl. 2012. Velocity prediction in high-gradient channels. Journal of Hydrology. 424–425, 84–98, doi:10.1016/j.jhydrol.2011.12.031.

Yochum, S.E., F. Comiti, E. Wohl, G.C. L. David, L. Mao. 2014. Photographic guidance for selecting flow resistance coefficients in high-gradient channels. U.S. Department of Agriculture, Forest Service, Rocky Mountain Research Station, General Technical Report RMRS-GTR-323.

Zhang, X.C. and J.D. Garbrecht. 2003. Evaluation of CLIGEN precipitation parameters and their implication on WEPP runoff and erosion prediction. In Transactions of the American Society of Agricultural Engineers, 46, 311–320.

Appendix A: Case Study 1

High Park Fire, Colorado

Background

The High Park fire, in the foothills west of Fort Collins, CO (fig. A–1 and A–2), burned within an area of 88,600 acres between June 9 and July 1, 2012. The fire burned primarily in steep, forested terrain, with average slopes ranging from 14 to 49 percent and elevations ranging from 5,300 to 10,200 feet. It was a fast burning fire, with about 37,000 acres burned in the first 3 days, and a "dirty burn," with a substantial amount of unburned area (21,100 acres, 23 percent) distributed as a patchy mosaic throughout the fire extent. Of the impacted area, 9,800 acres burned at high soil burn severity (11 percent), 36,300 acres burned at moderate severity (40 percent), and 21,300 acres burned at low severity (23 percent).

Figure A–1 Sunset through smoke plumes, from Fort Collins on day 1 of the High Park fire

Figure A–2 Aerial extent and soil burn severity of the High Park fire, based on a BARC image

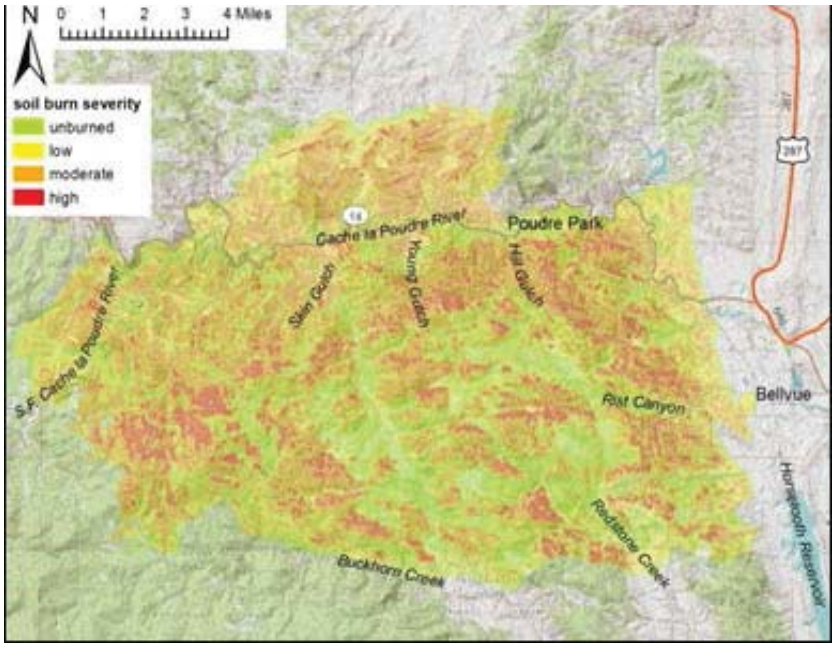

Just as wildfire containment was achieved, the summer monsoon season started. Increased flooding and debris flows were observed in streams draining numerous portions of the fire, with local residents noting that some of these floods were the most severe since the Big Thomson Flood of 1976. Ash mobilized due to the enhanced runoff flowed into the Cache la Poudre River, a primary source of drinking and irrigation water for the northern Colorado Front Range. Since part of the Horsetooth Reservoir watershed was also burned, water supply storage in this reservoir was threatened with contamination.

As expected, the most severe flooding was in catchments with the highest percentages of high soil burn severity. In these areas the vegetation cover and soil litter were consumed, leaving surfaces dominated by a bare mineral condition, reduced surface roughness, and possible hydrophobicity. These high severity burn areas also likely had substantial destruction of seed banks, forcing longer vegetative recovery rates and resulting in longer periods of enhanced flooding. Increased flood peaks, flow volumes, sediment transport, nutrient enrichment, and stream channel destabilization are expected for a number of years in many streams draining the fire area, threatening life, property, infrastructure, and water quality.

An initial hydrologic analysis was provided by a Burned Area Emergency Response (BAER) report for the large catchments draining this fire. Local and State officials, however, concerned with increased flood hazard potential and noting the preliminary nature of the BAER report, requested assistance from NRCS. Of particular interest were flow frequency estimates for post-fire conditions. This case study provides an overview of the analyses performed to provide these estimates.

Methods

A rainfall-runoff model was developed to simulate the expected runoff response for both pre- and post-fire conditions, for the 2-, 10-, 25-, 50-, and 100-year 1-hour rainfall events. Hydrologic modeling was performed using the program HEC-HMS (version 3.5), developed by the USACE Hydrologic Engineering Center. The NRCS curve number (CN) technique for estimating direct runoff from rain events was used in this analysis. As quality control, peak flows estimated using USGS regression equations (Capesius and Stephens 2009), embedded in USGS Streamstats, were compared to the CN runoff results for unburned conditions.

The BAER assessment led by the FS provided initial peak flow estimates used for post-fire flood mitigation planning activities (BAER 2012). This hydrologic analysis used the WILDCAT model (Hawkins and Greenberg 1990), which also relies on the CN method. The analysis was constrained to a deadline of 1 week after fire containment, per FS requirements. Hence, the modeling was relatively coarse and neglected relevant hydrologic mechanisms such as variability in lag time between pre- and post-fire conditions, vegetation type, differences in runoff between moderate and high soil burn severity areas, as well as flood attenuation in larger catchments. Additionally, the BAER modeling used relatively large catchments in some areas, which, given the large burn area of the High Park fire, added to the courseness of the BAER results. For example, the modeling was less able to account for flood wave attenuation. NRCS initiated a more detailed hydrologic analysis of streams draining the High Park fire area, likely enhancing the accuracy of predictions for flood mitigation efforts. Initial results of this modeling were obtained for key catchments just before the monsoon season started in early July, which provide preliminary flooding estimates to local and State officials. These results were refined throughout the summer and the analysis expanded to provide flood estimates for most streams draining the fire extent (Yochum 2012a, Yochum 2012b). While the results provide reasonable estimates of the increased flooding expected from the burned watershed, further monitoring and research underway in some areas may enable future modeling refinements. These could employ, for example, more mechanistic rainfall-runoff simulations than the CN method. Hence, post-wildfire flood simulation modeling, especially large events involving substantial private land ownership, more dense settlement, and higher risks to life, property, and infrastructure, should be viewed as an iterative process with models of varying complexity developed over time to satisfy specific needs.

The NRCS model estimated runoff using the CN procedure documented in "Estimation of Direct Runoff from Storm Rainfall" (USDA-NRCS 2004b). The CN is a simple catchment-scale method that gives estimates of flood peaks and volumes at watershed outlets, with more accurate results expected for larger, higher-intensity rain events. The method is also discussed in Hydrologic Soil Cover Complexes (USDA-NRCS

2004b), Rallison (1980), and numerous other publications. However, little quantitative information has been published of the database on which it was developed (Maidment 1992) and many of the curves used in the development have been lost (Woodward 2005). In general, the method was developed for rural watersheds in various parts of the United States, within 24 States, was developed for single storms, not continuous or partial storm simulation, and was not intended to recreate a specific response from an actual storm (Rallison 1980).

Catchments and modeled stream channels implemented in the analyses are presented in figure A–3. Overall, 105 delineated catchments were utilized in the modeling. The average catchment area was 1.6 square miles, with the individual sizes determined by required computation points (to provide needed flood predictions at roadway crossing, homes at risk, etc.), catchment morphologic characteristics, and the need for simulating flood routing and attenuation in the modeled stream channels

Runoff CN Estimation

CNs were assigned to the modeled catchments according to hydrologic soil group, vegetative type, soil burn severity, and ground cover condition (percent cover). The average catchment CN was computed using an aerial averaging methodology in GIS, with more than 51,000 polygons computed for the entire modeled extent.

Soil burn severity (fig. A–3) is the principle driver for increasing flow in runoff predictions. For this modeling, soil burn severity was measured using the Burned Area Reflectance Classification (BARC) process from satellite data collected on 7/20/2012, by researchers at Colorado State University (CSU). BARC uses reflectance recorded in satellite images to quantify soil burn severity. For defining soil burn severity, BARC images have the advantage of being comprehensive and relatively-rapidly developable. However,

Figure A–3 Modeled basins and channels, flow computation points, soil burn severity

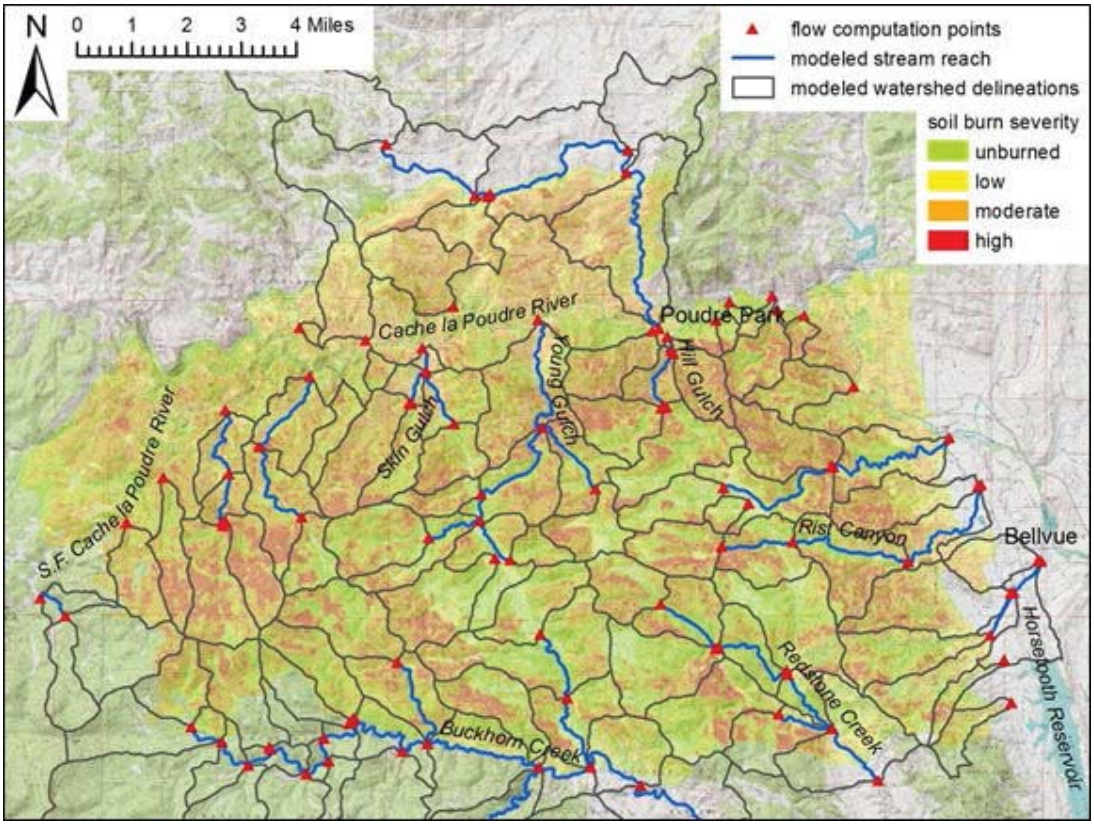

comparison with field-collected data has indicated that this remotely-sensed product can be more indicative of post-fire vegetative condition than soil condition, especially in low to moderately burned areas (Hudak et al. 2004). Qualitative field assessment of the High Park fire BARC image indicated a reasonable prediction of burn severity in high and moderate areas. The soil burn severity imagery depicted in figure A–3 was developed by the USGS Earth Resources Observation and Science Center (from the same 7/20 satellite data), rather than the CSU interpretation implemented in the hydrologic modeling. This BARC interpretation was not available at the time of the analysis, though the burn severity estimates are relatively comparable and substantial variations in flood peaks are not expected.

Hydrologic soil group (HSG) classification was selected using soils data published in the NRCS SSURGO (Soil Survey Geographic) database. Two soil surveys cover the fire extent: NRCS Larimer County survey (CO644), published in 1980, and USFS Arapahoe-Roosevelt survey (CO 645), published in 2001. The USFS survey covers the western one-third of the fire area.

Vegetation type, from Southwest Regional Gap Analysis Project (SWReGAP) land cover mapping, was included in the CN assignments used for the modeling. The dominant vegetation types within the fire boundary were lodgepole, mixed conifer, ponderosa, shrubs, and grass.

The assigned CN values are provided in table A–1. Using a fair ground cover condition, NRCS recommended values (USDA-NRCS 2004a) were applied by hydrologic soil group for unburned conditions. The CN values for low, moderate and high severity burn areas, at the four hydrologic conductivity classifications, were estimated based on CN values developed from post-fire runoff measurements (Livingston et al. 2005), with additional guidance from Wright et al. (2005) and Goodrich et al. (2005).

Rainfall

Since the High Park fire area is most susceptible to flooding from relatively short duration monsoonal rain events, a 1-hour storm duration was implemented. Rainfall depths were extracted from NOAA Atlas 2, Volume 3 (Miller et al. 1973) for the 2-, 10-, 25-, 50-, and 100-year rainfall events. The rainfall duration and distribution was identical to that used in the BAER modeling (BAER 2012) and is provided in the project report (Yochum 2012b). For catchments with drainages areas ≥ 6 square miles, an areal reduction factor

Table A–1 CN assignments implemented in High Park fire hydrologic modeling (highlighted columns indicate values extracted from USDA-NRCS 2004a)

Cover Description	**A** HSG				**B** HSG				**C** HSG				**D** HSG			
	Unburned	Low	Moderate	High	Unburned	Low	Moderate	High	Unburned	Low	Moderate	High	Unburned	Low	Moderate	High
Herbaceous, pasture, alpine meadow, park	49	55	67	77	61*	68*	80	86	74*	81	88	89	82*	86*	92*	95
Oak-aspen—mountain brush mixture of oak brush, aspen, mountain mahogany, bitter brush, maple, and other brush	45*	52*	65	77	48	55	65	86	57	70*	80*	89	63	70	80	92
Ponderosa pine-juniper (grass understory)	49*	57*	65	77	58	65	75	86	73	78*	83*	89	80	85	90	92
Sagebrush (grass understory)	46*	54*	65	77	51	60	75	86	63	70	80*	89	70	75	85	92
Lodgepole pine forest	49*	57*	65	77	60	65	70	86	71	78*	83*	89	79	83*	87*	92
Bare soil	77	77	77	77	86	86	86	86	91	91	91	91	94	94	94	94
Wetland	98	98	98	98	98	98	98	98	98	98	98	98	98	98	98	98

* Updated value based on Black Forest and West Fork Complex wildfires. Not as implemented in High Park analysis.

was applied as detailed in Miller et al. (1973). Reduction varied from 0.95 to 0.78. When applied, this area reduction was implemented in all catchments; flow may be underpredicted in the smaller, upper catchments of such drainages.

Lag Time

Lag time (*L*) was computed using the watershed lag method (USDA-NRCS 2010). This equation is—

$$L = \frac{l^{0.8}\left(S+1\right)^{0.7}}{1900Y^{0.5}} \qquad \text{eq. A–1}$$

where *l* is flow length (ft), *Y* is average watershed land slope (%), and *S* is maximum potential retention (in). S may be calculated from equation A–2:

$$S = \frac{1000}{cn'} - 10 \qquad \text{eq. A–2}$$

where *cn'* is the retardance factor and is approximately equal to the *CN*. This method allows the computation of differing lag times for pre- and post-fire simulations, reflecting the actual physical mechanism of more rapid flow response during post-fire conditions. The method was developed under a wide range of conditions, including steep, heavily forested watersheds (USDA-NRCS 2010). Equation A–1 was developed similarly to the time of concentration equation in the technical note (eq. 1). Lag is considered to be 0.6 of the time of concentration.

Flow Routing

A Muskingum-Cunge procedure was used to route flow from upper catchments to stream outlets, along the modeled stream reaches (fig. A–3). This one-dimensional method simulates flow attenuation but does not provide a numerical solution of the full unsteady flow routing equations, as provided in such computational models as HEC-RAS. Instead, in each reach flow routing was estimated using a single simplified cross section, channel slope, and Manning's *n* estimate. Photographic guidance (Yochum and Bledsoe 2010) was used to help select flow resistance coefficients, and these values were checked by inspecting the model solutions to verify that the selected Manning's *n* values resulted in subcritical or approximately critical flow velocity. Hence, it was assumed that bedform development prevents reach-average supercritical flow in these alluvial channels.

Sediment Bulking

A simple multiplication factor was applied to the post-fire flood predictions to account for sediment bulking in the debris flows. For burned catchments, this multiplication factor was assumed to be 1.25 if the (severe + moderate) soil burn severity aerial extent was greater than 50 percent, and 1.1 for catchments with between 10 and 50 percent (severe + moderate) soil burn severity.

StreamStats

The regional USGS regression equations for peak flow prediction (Capesius and Stephens 2009), embedded in Streamstats, were used to assess the reasonableness of pre-fire peak flow predictions. The predictions use input of drainage area and the 6-hour, 100-year precipitation depth to provide expected runoff from rain events, reflecting the expectation that floods result from summer monsoons. The error bars associated with these predictions are substantial—typically about 140 percent.

These predictions are based on streamgage data and, hence, provide a level of ground truthing, but this method accounts for only drainage area and precipitation regime. Other physical characteristics and processes that are relevant in runoff processes, such as infiltration capacity, vegetative type, ground cover condition, watershed shape, and flow attenuation, are not accounted for. However, due to its foundation

in field-collected data within similar watersheds, this method is valuable for assessing the general reasonableness of the model predictions for pre-fire conditions.

Results and Discussion

Hydrologic modeling was performed to develop estimates of increased flood hazard and potential threats to life and property along streams draining the High Park fire. For several key catchments, at locations of threats to residences, example hydrographs (fig. A–4) show the expected response to a 10-year rainfall depth over each entire catchment. Substantially increased flow peaks and runoff volumes were estimated. The simplicity of a map presentation style (fig. A–5) facilitated use by planners, designers, and emergency response officials. Results were provided at 96 computation points over the fire extent and also provided as attributes in ArcGIS shapefiles. In addition to simulated flood peaks, time-to-peak estimates were provided to give emergency response personnel estimates of the expected flood response times. For detailed results, refer to appendix A of the project report (Yochum 2012b) and the accompanying poster (Yochum 2012a).

Substantially higher peak flows and flood volumes are predicted for post-fire conditions. In many catchments, post fire conditions were predicted to cause a 50- or 100-year flood (pre-fire recurrence) to result from a 10-year rain event on burned landscapes, similar to measured fire runoff responses (Conedera et al. 2003). If it is estimated that the fire impacts on runoff in each of these catchments will be substantial for at least 5 years, the risk of a 10-year rainfall event over each point in these catchments over those 5 years of destabilization is 41 percent, with resulting 50- to 100-year floods (pre-fire recurrence). If a 10-year recovery period is assumed, the risk increases to 65 percent. However, the expected severity of flooding lowers with increasing catchment size, due to the small spatial extent of typical convective storms.

Due to their simplicity, peak flow enhancement ratios (*Qpost / Qpre*) may be a preferred method for communicating flood enhancement predictions. Predicted ratios for the 25-year rain event are provided (fig. A–6). Peak flow enhancement ratios are higher for more frequent rain events (2- and 10-year storms) and lower for less frequent events (50- and 100-year storms), with this same pattern observed with field-collected data (Moody and Martin 2001). This method only provides meaningful results where the pre-fire peak flow is greater than zero for the rainfall event of interest.

Figure A–4 Example estimated pre- and post-fire hydrographs for the 10-year rain event

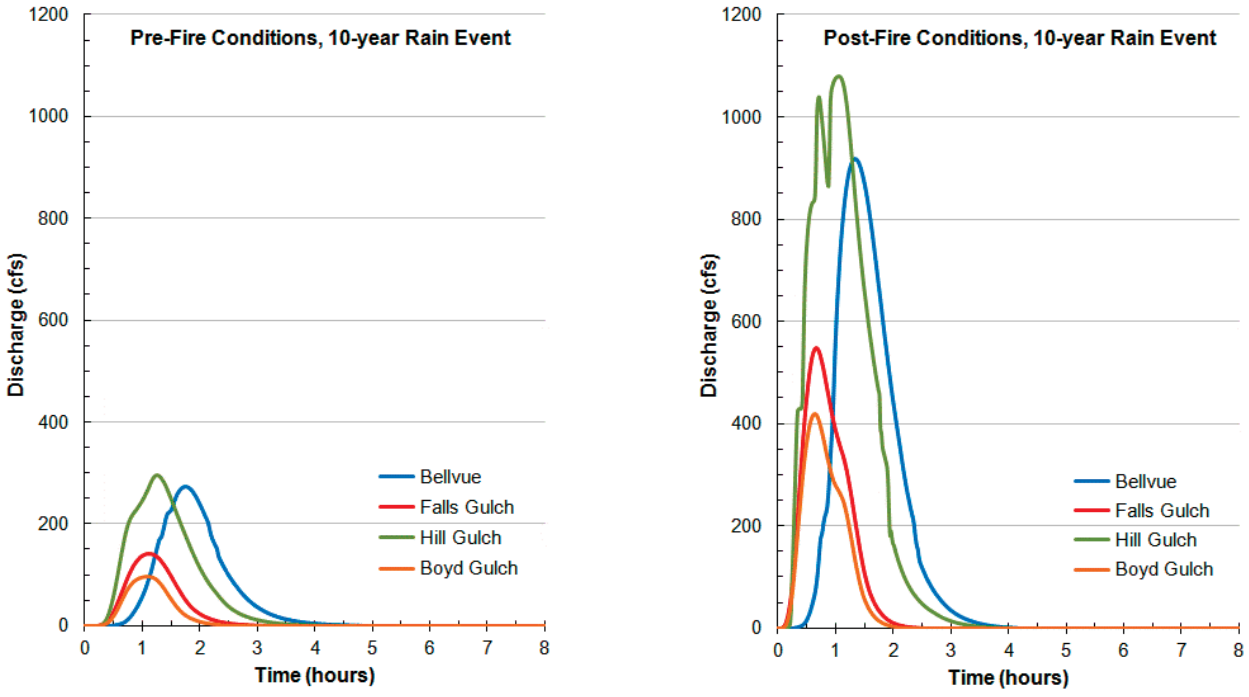

Figure A–5 Example map with pre- and post-fire flood prediction estimates for the Poudre Park area

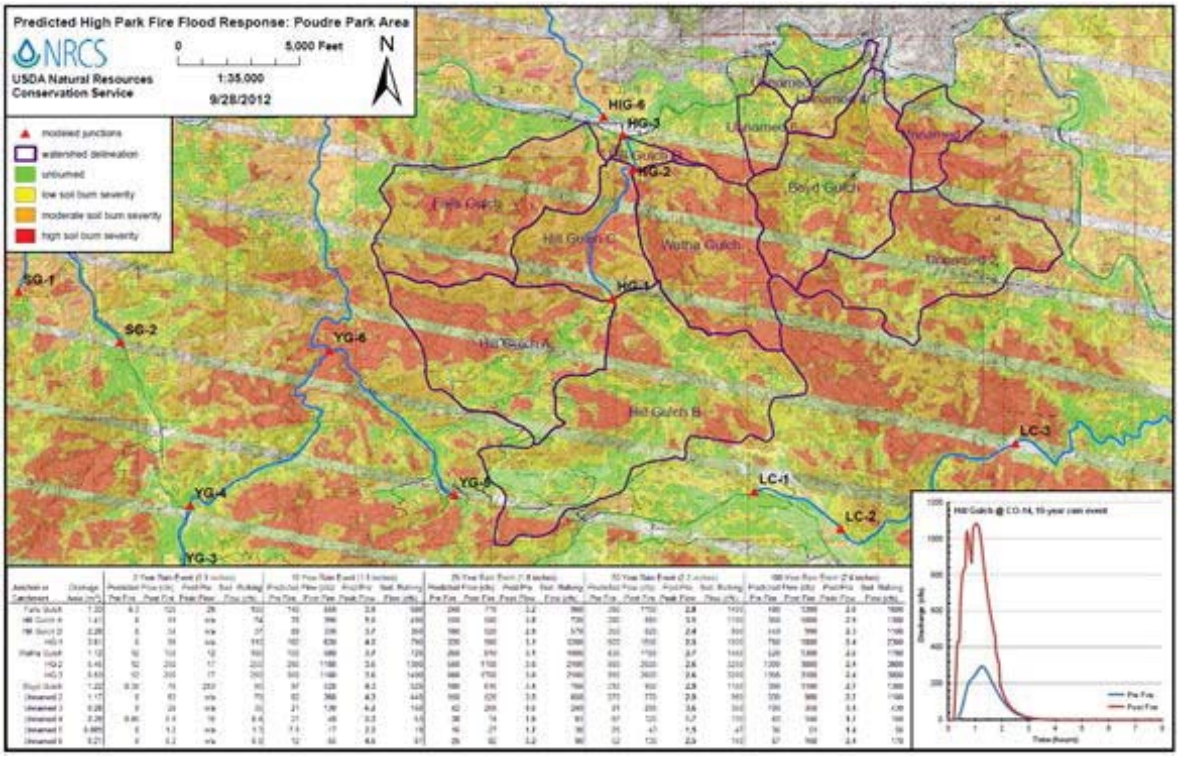

Figure A–6 Estimated 25-year peak flow enhancement ratios for the High Park fire

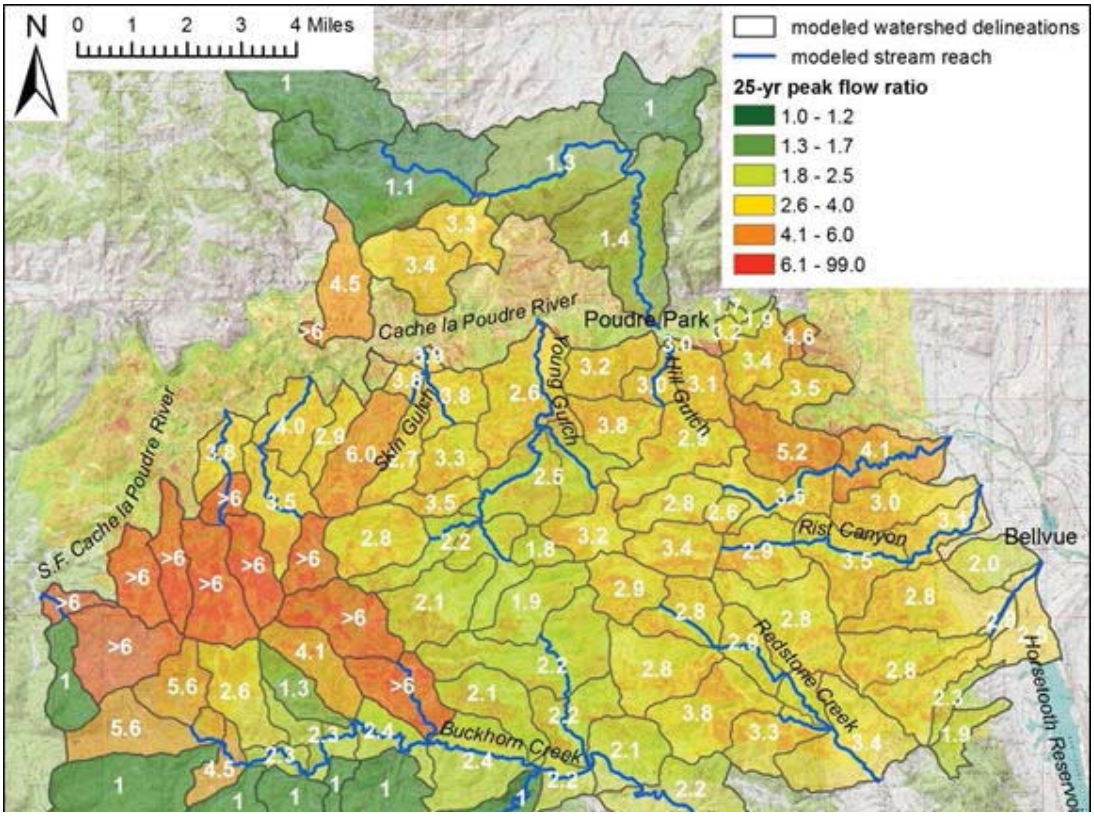

Comparison With Regression Predictions

Table A–2 illustrates USGS regression modeling results (from Streamstats) compared to CN modeling results at a number of locations, for the 10- and 25-year events. Considering the large expected prediction errors of the USGS regression equations in this area (typically 140 percent), the results are reasonably comparable. The greatest differences in prediction are typically in the largest catchments. Differences in the results are likely due to limited data available for selecting CN values for post-fire conditions, questionable CN model appropriateness in forested watersheds, and possible inaccurate rainfall depths and aerial reduction factors. Additionally, the regression technique does not account for relevant hydrologic processes, such as variable soil infiltration capacity, vegetative type, ground cover condition, and stream flow attenuation.

Accuracy and Limitations

As with all hydrologic modeling, the results provided by these simulations are approximate. Comparisons with flood peaks estimated using the USGS regression equations (table A–2) indicate that the pre-fire runoff simulations are more-or-less reasonable overall, but that the modeling often provides estimates that may be inaccurate, especially as catchment size increases. Post-fire runoff prediction using the CN technique is hampered by the very little available field data to enable reliable selection of CN values from measured rainfall and runoff in burned catchments. Additionally, the use of dated rainfall depths and areal reduction factors (Miller et al. 1973) in orographic-forced mountainous watersheds adds an additional layer of uncertainty to the estimates.

Additionally, greater infiltration is indicated by the USFS soil survey than the adjacent NRCS survey, with infiltration commonly increasing by a step at the survey boundary and a large area with HSG A indicated. In the most problematic areas zero runoff is predicted for pre-fire conditions in some catchments during the 10- and 25-year rain events. This problem may be due to shallow, permeable soils over bedrock dominating the USFS soil survey classification methodology, but the true reason for this inconsistency is unknown. As a result, the modeling may be underpredicting runoff and overestimating flood response ratios in catchments draining the Arapaho-Roosevelt soil survey area, especially for more frequent (shallower) rainfall events.

More fundamentally, the reliability of the CN method for predicting peak flow from forested, mountainous watersheds is questionable, due to doubtful appropriateness of the CN method and shifting streamflow generation processes between and pre- and post-fire conditions. This issue is discussed in the main body of this technical note under the section “Limitations of the CN Method.”

Despite these shortcomings, due to its relative simplicity and achievable data requirements for large scales, the CN method is a preferred tool for predicting flood responses of wildfire areas. The modeling performed

Table A–2 Comparison of CN modeling with USGS regression results from Streamstats

	Area	10-yr flow (cfs)		25-yr flow (cfs)			Area	10-yr flow		25-yr flow (cfs)	
Point	(mi^2)	CN	Reg	CN	Reg	Point	(mi^2)	CN	Reg	CN	Reg
MC-2	3.33	119	212	249	360	BG	1.22	97	95	177	151
MC-5	6.61	272	335	588	574	UN-3	0.28	21	40	42	61
BC-8	23.2	44	407	119	650	RdC-2	5.05	131	231	284	382
BC-13	42.9	244	599	474	974	RdC-5	13.2	180	445	479	764
BC-18	55.0	332	741	729	1230	RdC-6	16.2	168	512	478	885
HIG-3	10.9	207	248	446	387	RC-2	3.00	172	170	334	277
HIG-5	21.8	210	348	466	554	RC-4	8.16	282	316	549	531
LC-1	1.20	23	96	60	152	SG-1	3.09	103	120	216	183
LC-4	6.97	168	277	354	460	SG-2	1.19	45	73	96	111
CG	2.00	89	92	178	139	SG-4	5.99	191	182	395	283

for the High Park fire has substantial value for identifying areas of greatest threat to life, property, and infrastructure. Peak flow ratios provide an excellent tool for communicating expected increases in runoff with agencies, first responders, and the public. Peak flow and runoff volume estimates are also still required for sizing infrastructure improvements. The unknown extent of uncertainty in the estimates needs to be effectively communicated to provide assurances that involved parties use the estimates with caution. Research and technical guidance is needed to develop and communicate more robust methods for flood prediction from wildfire-impacted landscapes.

Conclusions

Using the NRCS CN method, peak flow predictions were made for streams draining the High Park fire area, for both pre-fire and post-fire conditions. Watershed maps for each modeled catchment were developed, illustrating computation points, peak discharges, peak flow enhancement ratios, soil burn severity, and stream outlet hydrographs. While many relevant hydrologic mechanisms were simulated, including rainfall depth and spatial extent, variation in runoff by soil burn severity, vegetation type and soil conductivity, variable lag times, and stream attenuation, the questionable reliability of the CN method in forested watersheds, for both post-fire and pre-fire conditions, adds varying uncertainty to the estimates. Research is needed to address this uncertainty, especially since lives are often at risk. In the meantime, wildfires will occur and methods need to be available to predict the expected flood response from burned watersheds. This case study provides an example of one such approach.

Acknowledgements

Appreciation is expressed to High Park fire BAER team for their initial analyses, Brandon Stone and Colorado State University for the utilized BARC soil burn severity interpretation, and Randy McKinley of the USGS and Eric Schroder of the USFS for the presented soil burn severity interpretation. Appreciation is also expressed to John Andrews for his contributions to the post-fire CN assignment compilation, John Norman for GIS analysis assistance and soils expertise, and Kari Sever and Sam Streeter for field data collection.

References

BAER 2012. High Park Fire Burned Area Emergency Response Report. USDA USFS and NRCS, Larimer County, CO, Department of Transporation.

Capesius, J.P., and V.C. Stephens. 2009. Regional Regression Equations for Estimation of Natural Streamflow Statistics in Colorado. U.S. Department of Interior, U.S. Geological Survey, Scientific Investigations Report 2009-5136.

Conedera, M., L. Peter, P. Marxer, F. Forster, D. Rickenmann, and L. Re. 2003. Consequences of forest fires on the hydrogeological response of mountain catchments: A case study of the Riale Buffaga, Ticino, Switzerland. Earth Surface Processes and Landforms 28, 117-129.

Garen, D.C., and D.S. Moore. 2005. Curve Number Hydrology in Water Quality Modeling: Uses, Abuses and Future Directions. Journal of the American Water Resources Association 42(2), 377-388.

Goodrich, D.C., H.E. Canfield, I.S. Burns, D.J. Semmens, S.N. Miller, M. Hernandez, L.R. Levick, D.P. Guertin, and W.G. Kepner. 2005. Rapid Post-Fire Hydrologic Watershed Assessment Using the AGWA GIS-Based Hydrologic Modeling Tool. In: Moglen, G.E., ed. Proceedings of Managing Watersheds for Human and Natural Impacts: Engineering, Ecological, and Economic Challenges, July 19-22, 2005, Williamsburg, VA, USA. American Society of Civil Engineers, Alexandria, VA.

Hawkins, R.H. 1993. Asymptotic Determination of Runoff Curve Numbers from Data. Journal of Irrigation and Drainage Engineering 119, 334-345.

Hawkins, R.H., R.J. Greenberg. 1990 WILDCAT4 Flow Model. School of Renewable Natural Resources, University of Arizona, Tucson, AZ. BLM contact: Dan Muller, Denver, CO.

Hudak, A.T., P.R. Robichaud, J.S. Evans, J. Clark, K. Lannom, P. Morgan, and C. Stone. 2004. Field Validation of Burned Area Reflectance Classification (BARC) Products for Post Fire Assessment. Remote Sensing for Field Users: Proceedings of the Tenth Forest Service Remote Sensing Applications Conference, Salt Lake City, Utah, April 5-9 2004.

Livingston, R.K., T.A. Earles, and K.R. Wright. 2005. Los Alamos Post-Fire Watershed Recovery: A Curve-Number-Based Evaluation. In: Moglen, G.E., ed. Proceedings of Managing Watersheds for Human and Natural Impacts: Engineering, Ecological, and Economic Challenges, July 19-22, 2005, Williamsburg, VA, USA. American Society of Civil Engineers, Alexandria, VA.

Maidment, D.R. 1992. Handbook of Hydrology McGraw-Hill, Inc.

Moody, J.A., and D.A. Martin. 2001. Post-Fire, Rainfall-Intensity-Peak Discharge Relations for Three Mountainous Watersheds in the Western USA. Hydrological Processes 15, 2981-2993.

Miller, J.F., R.H. Frederick, and R.J. Tracey. 1973. Precipitation-Frequency Atlas of the Western United States. U.S. Department of Commerce, National Oceanic and Atmospheric Administration, National Weather Service, NOAA Atlas 2, Vol 3, Silver Spring, MD.

Rallison, R.E. 1980. Origin and Evolution of the SCS Runoff Equation. Proceedings of the Symposium on Watershed Management; American Society of Civil Engineers, Boise, ID.

Springer, E.P., and R.H. Hawkins. 2005. Curve Number and Peakflow Responses Following the

Cerro Grande Fire on a Small Watershed. In: Moglen, G.E., ed. Proceedings of Managing

Watersheds for Human and Natural Impacts: Engineering, Ecological, and Economic Challenges, July 19-22, 2005, Williamsburg, VA, USA. American Society of Civil Engineers, Alexandria, VA.

Tedela, N.H., S.C. McCutcheon, T.C. Rasmussen, R.H. Hawkins, W.T. Swank, J.L. Campbell, M.B. Adams, C.R. Jackson, and E.W. Tollner. 2012. Runoff Curve Numbers for 10 Small Forested Watersheds in the Mountains of the Eastern United States. Journal of Hydrologic Engineering, 17(11), 1188-1198.

USDA-NRCS (U.S. Department of Agriculture-Natural Resources Conservation Service), 2004a.

NRCS National Engineering Handbook, Part 630 Hydrology, Chapter 9, Hydrologic Soil Cover Complexes.

USDA-NRCS (U.S. Department of Agriculture-Natural Resources Conservation Service), 2004b. NRCS National Engineering Handbook, Part 630 Hydrology, Chapter 10, Estimation of Direct Runoff from Storm Rainfall.

USDA-NRCS (U.S. Department of Agriculture-Natural Resources Conservation Service), 2010. NRCS National Engineering Handbook, Part 630 Hydrology, Chapter 15, Time of Concentration.

Woodward, D. 2005. Personal Communications (email). Retired National Hydraulic Engineer, USDA Natural Resources Conservation Service, Washington, DC.

Wright, K.R., T.A. Earles, and E. Pemberton. 2005. Mesa Verde Bircher Fire Hydrological Impact. In: Moglen, G.E., ed. Proceedings of Managing Watersheds for Human and Natural Impacts: Engineering, Ecological, and Economic Challenges, July 19-22, 2005, Williamsburg, VA, USA. American Society of Civil Engineers, Alexandria, VA.

Yochum, S.E. 2012a. Poster: Increased Flood Potential of Steams Draining the High Park Fire, with Ratios of Predicted Post/Pre Fire Peak Flows for the 1-Hour, 25-Year Rain Event. U.S. Department of Agriculture, Natural Resources Conservation Service, Colorado State Office.

Yochum, S.E. 2012b. High Park Fire: Increased Flood Potential Analysis. U.S. Department of Agriculture, Natural Resources Conservation Service, Colorado State Office.

Yochum, S., and B. Bledsoe. 2010. Flow resistance in high-gradient streams. Proceedings of 4th Interagency Hydraulic Modeling Conference, June 21 – July 1st, 2010, Las Vegas, NV, USA.

This page intentionally left blank

Appendix B: Case Study 2:
Bitterroot Wildfires, Montana

Background

Southwestern Montana endured severe climatic drought conditions in 2000. Late that summer, wildfires raged through the area with the Bitterroot National Forest hit particularly hard. See figures B–1 through B–3 for location and fire severity mapping.

Figure B–1 State of Montana, with inset of Bitterroot River Valley

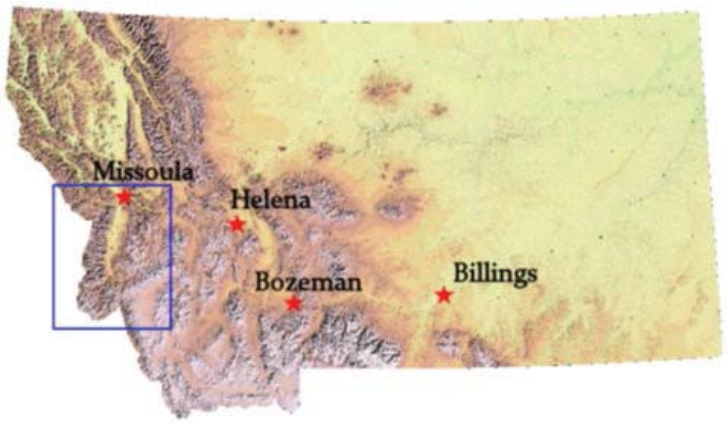

Figure B–2 Bitterroot River watershed with inset of area of the wildfires in the year 2000

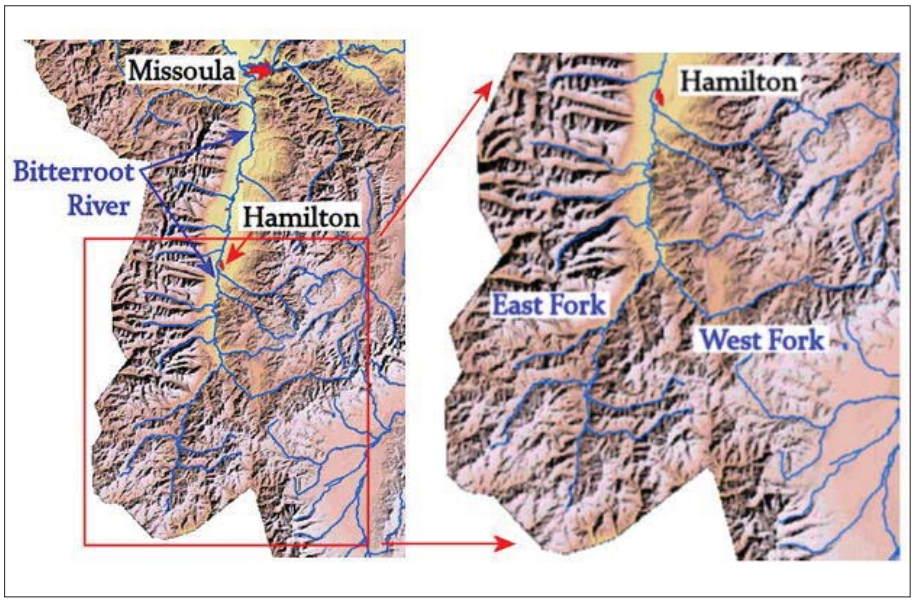

Figure B–3 Bitterroot fire severity for the fires of 2000 (Mahlum et al. 2011)

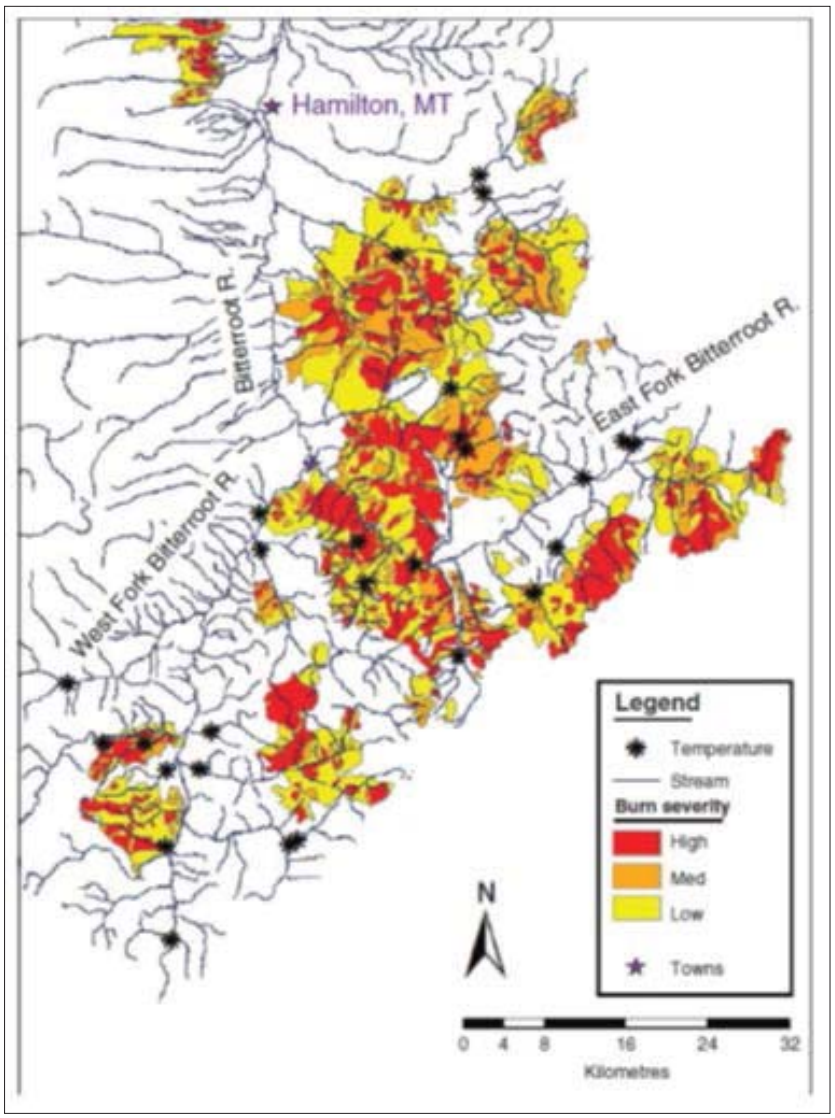

These fires were largely started by lightning strikes, as shown in figure B–4. The damaged area included 244,000 acres on USDA national forest lands and 49,000 acres of State-owned and private land. The severity of the fires ranged from low (some under-story destroyed, minimal impact on tree canopy) to high (complete destruction of all living plant material). See figure B–3 for fire severity and figure B–5 for photo of fire in progress.

After the fires, specialists from the USDA Forest Service (FS) and NRCS evaluated potential hydrologic impacts to area residents and infrastructure. The NRCS effort included the Emergency Watershed Protection Program (EWP). (For more detail on EWP, see section "The Role of NRCS in Post-Fire Assessments and Modeling" at the beginning of this technical note.) For the Bitterroot fires of 2000, an immediate technical challenge arose because traditional agency hydrologic methods were not designed to address post-wildfire conditions. A literature search for existing procedures yielded none that could be expeditiously applied. As a result, the NRCS Montana office developed a simple but accurate hydrologic evaluation method, that would be more broadly applicable to post-wildfire watershed protection projects. The spreadsheet tool FIRE HYDRO (Cerrelli 2005) resulted from this effort.

A key factor that made apparent the need for such a tool was the lack in existing NRCS engineering handbooks of guidance specifically related to post-wildfire conditions. The runoff curve number (CN)

Figure B–4 Lightning strikes, Bitterroot Valley, MT, initiating the wildfires of 2000

Figure B–5 One of the most poignant wildfire scenes ever captured, from Bitterroot in 2000

Photo by John McColgan, USDA Forest Service

methodology is described in Title 210, National Engineering Handbook (NEH), Part 630, Chapter 9, "Hydrologic Soil-Cover Complexes" (2004a); and Chapter 10, "Estimation of Direct Runoff from Storm Rainfall" (2004b). The new spreadsheet tool was to retain this guidance, given its familiarity to most NRCS engineers. However, the challenge was to provide correct CNs for the various land covers burned by wildfires of differing severities. Additionally, the analysis used to determine times of concentration for the burned areas needed to be examined for post-fire effects. As the FIRE HYDRO spreadsheet has been used by both NRCS and FS personnel after numerous wildfires since the year 2000, and in other States besides Montana, this case study will discuss its original development and use for evaluating the Bitterroot fires.

Methods

The envisioned goal of the spreadsheet tool was to provide a simplistic method, readily familiar to USDA field engineers, that could be run on laptop computers at remote locations. In evaluating a wildfire, NRCS field engineers must quickly determine appropriate conservation practices and areal extents that could be applied to reduce the impact of runoff and debris coming from the burn areas. The EWP and the Burn Area Emergency Rehabilitation Program (BAER) are administered for recovery work and typically activated quickly during, and shortly after an event. (See the technical note for more information on both EWP and BAER.) Within these programs, projects must be evaluated, designed, contracted, and constructed quickly or they will not be considered for agency funding.

The hydrologic principles found in the NRCS Engineering Field Handbook (EFH), Chapter 2, "Estimating Runoff" (USDA-NRCS 1989), were considered appropriate to meet the needs for this simple but accurate analysis of the wildfire areas. These procedures are abbreviated EFH-2.

At the time of this study (2000), EFH-2 was only available as a manual method that required the user to look to the tabular and graphical listings within the guidance to determine the runoff volume for the singular watershed under investigation. The EFH-2 peak discharge analysis requires the user to specify the design rainfall distribution type (defined by NRCS into four categories nationwide) that is appropriate for the project area under investigation. The NRCS Montana office has its own criteria for determining the appropriate selection of design rainfall distribution based on the project area's ratio of the 6-hour to 24-hour rainfall amounts for the desired recurrence event. The spreadsheet methodology was created in Microsoft Excel and named FIRE HYDRO, incorporating NRCS runoff CN technology and EFH-2 peak discharge graphical solution in conjunction with the NRCS Montana design rainfall selection criterion.

EFH-2 provides a set of curves for each rainfall distribution region in the United States. Each curve pertains to an I_a/P ratio (where I_a refers to the CN runoff initial abstraction and P is total rainfall, both units in inches). To obtain peak discharge, one selects the correct curve, given I_a/P, then enters the x-axis with time of concentration, and reads unit peak discharge on the y-axis. For FIRE HYDRO an algebraic function was derived for each of these curves and provided in the Excel file to solve for predicted peak discharge.

Among the technical issues that needed to be addressed in the creation of FIRE HYDRO were proper selection of burn area runoff CNs and times of concentration, and soil hydrophobicity. These issues will be discussed in greater detail below. The FIRE HYDRO methodology analyzes four different watershed conditions. They are as follows:

- Pre-fire—Watershed significantly healed from any previous fires
- Post-fire 1—Immediately after the event, with consideration of hydrophobic soil
- Post-fire 2—After some emergence of vegetation and loss of hydrophobicity
- Post-fire 3—After expected vegetation recovery in next growing season

These four conditions were evaluated to give the designer a greater feel for the range of runoff conditions that were, are, and will be present for the watershed being investigated. This information helps the designer better understand the change in relative risk over time on various alternative hydrologic control measures considered for installation, including the "do nothing" alternative.

For the Bitterroot fires, conditions were monitored for both immediately post-fire conditions and later post-fire conditions. Figure B–6 shows how runoff shortly after the burn eroded the soil surface and was retarded by the conservation practice of silt fencing.

Figure B–7 shows a watershed in the early stages of recovery. Figures B–8 and B–9 show Bitterroot watersheds after several years of recovery.

Figure B–6 Fully loaded silt fence placed after the 2000 Bitterroot Valley complex wildfire

Figure B–7 Laird Creek in 2001 within what was the Bitterroot Valley complex fire

Figure B–8 Glen Lake Trail in the summer of 2012

Figure B–9 The landscape around Glen Lake in the summer of 2012

Runoff CN Estimation for Burn Areas

The FIRE HYDRO method is used to evaluate individual watersheds by treating all land use and soil conditions as a composite homogeneous collection. This assumption contains inherent problems when widely varying runoff conditions exist in the watershed being modeled. A literature search for recommended runoff CNs for wildfire burn areas specifically related to climate and vegetation types of southwestern Montana yielded nothing. Consequently, select NRCS Montana engineers created the following guidance for selection of runoff CN based on burn severity and hydrologic soil grouping (HSG) specific to the Bitterroot wildfire vicinity (tables B–1 through B–4.)

Table B–1 Runoff CN for high severity burned areas of southwest Montana*

Hydrologic soil group	High burn severity CN
A	64
B	78
C	85
D	88

*High severity burn areas assumed to have attained a minimum of 30 percent ground cover consisting of vegetation, duff, thick ash, or woody debris by June of the following year.

Table B–2 Recommended runoff CN for moderate severity burned areas

Cover type	Runoff CN for given hydrologic soil group*			
	A	B	C	D
Herbaceous—mixture of grass, weeds, and low-growing brush, with brush the minor element	–	71	81	89
Oak-aspen—mountain brush mixture of oak brush, aspen, mountain mahogany, bitter brush, maple	–	48	57	63
Pinyon-juniper—pinyon, juniper or both, grass understory	–	58	73	80
Sagebrush—grass understory	–	51	63	71
Desert shrub—major plants include saltbush, greasewood, creosotebush, blackbrush, bursage, palo verde, mesquite, and cactus	55	72	81	86

* Moderate burn area runoff CNs are for cover types in fair condition. This table is from EFH-2, for arid and semiarid rangelands, which stated that CNs for HSG A were developed only for desert shrub cover type.

Table B–3 Runoff CNs for low severity burned and unburned areas with north- and east-facing slopes

Cover type	Runoff CN for given hydrologic soil group*			
	A	B	C	D
Herbaceous—mixture of grass, weeds, and low-growing brush, with brush the minor element	–	62	74	85
Oak-aspen—mountain brush mixture of oak brush, aspen, mountain mahogany, bitter brush, maple	–	30	41	48
Pinyon-juniper—pinyon, juniper or both, grass understory	–	41	61	71
Sagebrush—grass understory	–	35	47	55
Desert shrub—major plants include saltbush, greasewood, creosotebush, blackbrush, bursage, palo verde, mesquite, and cactus	49	68	79	84

* Low burn area runoff CNs are for cover types in good condition. This table is from EFH-2, for arid and semiarid rangelands, which stated that CNs for HSG A were developed only for desert shrub cover type.

Table B–4 Runoff CNs for low severity burned and unburned areas with south- and west-facing slopes

Cover type	Runoff CN for given hydrologic soil group*			
	A	B	C	D
Herbaceous—mixture of grass, weeds, and low-growing brush, with brush the minor element	–	67	78	87
Oak-aspen—mountain brush mixture of oak brush, aspen, mountain mahogany, bitter brush, maple	–	39	49	56
Pinyon-juniper—pinyon, juniper, or both, grass understory	–	50	67	76
Sagebrush—grass understory	–	45	55	63
Desert shrub—major plants include saltbush, greasewood, creosotebush, blackbrush, bursage, palo verde, mesquite, and cactus	52	70	80	85

*Low burn and unburned area runoff CNs are for cover types between fair and good condition, with values averaged from tables B–2 and B–3.

These recommended runoff CNs (for all burn severity types listed) were arrived at by consensus amongst three NRCS Montana engineers with hydrologic evaluation experience. See figures B–10 and B–11 for examples of data available for the Bitterroot fires that used in establishing the areal extent of different burn severities. The basic premise of the three NRCS Montana engineers was to establish a logical fit for burn area runoff CN values within the existing accepted NRCS runoff CN and land use table. There was no time between the fire occurrence and the need for installation of exigency runoff protection work for gauging or other verification procedures. Storms that occurred the following spring and summer, events of approximately 2-year to 5-year recurrence, 24-hour duration, did not produce runoff which led to the failure of any protection practices installed using these runoff CN values.

Figure B–10 Satellite imagery of burn severity of the 2000 Bitterroot Valley Complex wildfire

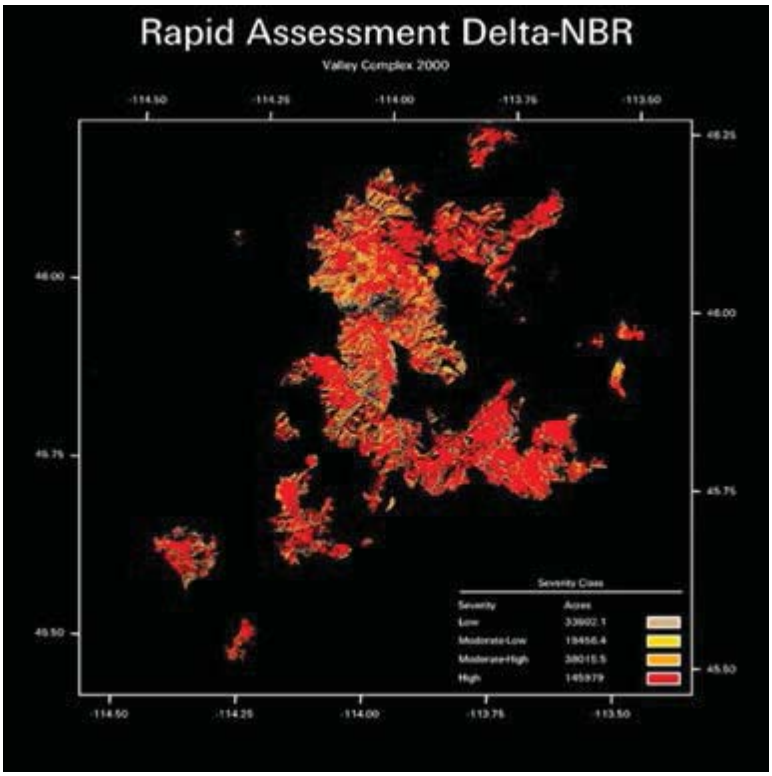

Figure B–11 Burn severity and rain gage data for storm event 1-year post-fire

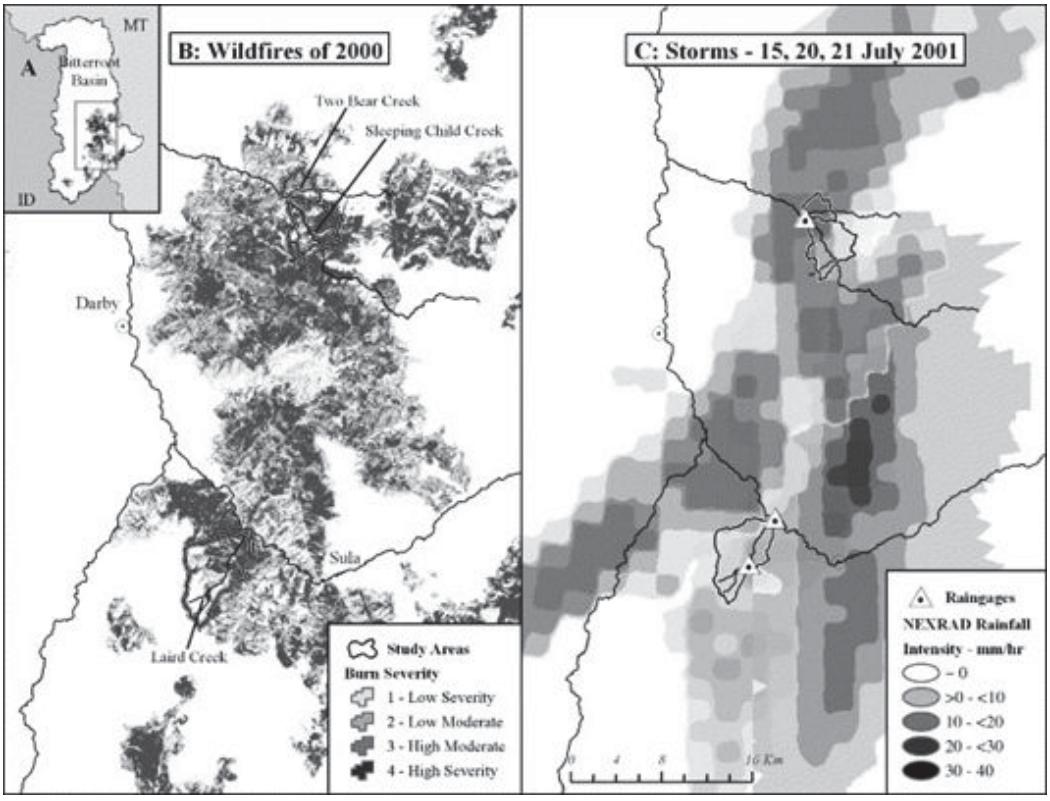

Hydrophobic Soils

Hydrophobicity in soils can be induced by wildfire. It requires certain soil textures and certain plant types to be burned in order to create this condition of significant water repellency. In brief, the condition can be found in more moderately coarse soils that have a deep plant litter mat and experience a severe burn. The resulting "waxy gas" that is created then permeates and coats the upper soil layer making it water repellent. More detail on soil hydrophobicity is provided in this technical note in sections "Hydrophobicity" and "Assessment of Post-Fire Soil Hydrophobic Conditions."

Runoff rates and volumes from hydrophobic soils can become extremely high. The engineer must make best estimates as to how widespread and persistent hydrophobicity exists after a fire. Assigning a design runoff CN to account for hydrophobicity also depends on the expected duration of this changed runoff condition. For example, the timing of next normal rain season compared to hydrophobic abatement recovery time should be considered. Field-testing is called for, which involves applying water to the mineral soil (below the ash layer) and checking for infiltration with time. See also this technical note in section "Accounting for Hydrophobicity With Infiltration Parameters." In addition, tables 7 and 8 previously in this technical note show FS-derived CNs in relation to soil hydrophobicity.

For the Bitterroot fires of 2000, the NRCS Montana engineers gave all hydrophobic soils an runoff CN of 94. It is important to consider the window of time to which hydrophobic conditions are expected to occur. Soil hydrophobicity tends to breakdown over time, as the water repellent layer is fractured through either plant growth activity or water action (freeze-thaw or dew and desiccation). These two processes occur very typically in Montana but may not be so prominent in other States.

Experience gained from the Bitterroot EWP effort, while considering hydrophobic soil properties for effective runoff CN assignment, yielded some interesting findings. Significant field reconnaissance, largely by FS personnel, was dedicated to evaluating the water-repellent properties of soils in the fire-affected watersheds. These investigations in the Bitterroot burn found areas with enough hydrophobicity to repel 50–70 percent of incoming water. It should be noted that even unburned forest soils can exhibit hydrophobicity. Tests in the Bitterroot fire area of adjacent unburned areas found that the soils would repel 40–60 percent of incoming water. It was thought that the drought that had been prevalent throughout the area in the summer of 2000 created a "tightening effect" of drought-affected soils, which created some water-repellency within the soil. Since the burned and unburned rates of water repellency seemed so similar, it was determined that the fire had not induced a significant increase in hydrophobicity. Therefore, the analysis of the Bitterroot fires using FIRE HYDRO shortly after the event did not use CNs that attempted to account for hydrophobic conditions. Observations of subsequent rainfall events tended to support the earlier suspicions, as large increases in runoff that might be expected from significantly hydrophobic areas was generally not in evidence.

Time of Concentration (T_c) and Assumed Watershed Shape

The engineers and technicians assigned to perform the watershed hydrologic evaluations of the Bitterroot wildfire area were not provided detailed topographic mapping of the site. They were provided GIS data that included total watershed area as well as percentages of which experienced low, moderate, or high severity burns along with soils data that included land slopes within the dominant soil classes found. It should be noted that, although today's engineers are often skilled GIS users, the rapid turnaround time for the Bitterroot fires of 2000 and the skill set of the engineers who happened to be available at the time precluded use of GIS to determine the longest flowpath lengths of subareas of the fire directly. Thus, an assumption was needed that would provide an estimate of watershed longest flow path based on drainage area. An assumed rectangular shape watershed with dimensions of one unit wide by two units long was made to produce the area stated for the watershed in the GIS data report. The longest flow path was taken as the longitudinal line down the center of this rectangle with a bend towards a corner at the upper third. The T_c was calculated using the Lag Method found in EFH-2. (See also the section "Watershed Lag Method" in this technical note.) This method used runoff CN, flow length, and average watershed slope (based on values from the soils data in the GIS data) as its basis. The post-fire T_c was assumed to stay equal to the pre-fire T_c even though there was a reduction in plant cover (therefore reduced flow friction leading to higher flow velocities) after the fire that should logically allow a faster T_c to develop. The assumption here though was that the excessive amount of available debris after the fire would cause blockages in the flowpath, a kind

of debris dam, which would serve to attenuate the flows. The degree of flow attenuation after a fire may vary tremendously from one area to another or one watershed to another, but it was felt that a reasonable estimate would be to use the same time of concentration for both pre-fire and post-fire conditions.

Results and Discussion

The FIRE HYDRO spreadsheet was frequently utilized by engineers and technicians involved with the 2000 Bitterroot wildfire recovery operations. NRCS personnel designed many runoff diversion practices to protect homes from the anticipated increased rainfall runoff brought about by changes in watershed conditions due to the wildfires. FS personnel used FIRE HYDRO to design for the enlargement of culverts to provide capacity for the anticipated increase in runoff and also to allow for fish passage. All of the practices designed using FIRE HYDRO were able to satisfactorily withstand rainfall-runoff events in the following years without any notable failures being reported.

It should be noted that many homes that benefitted from conservation practices after this event happened to be situated on the only reasonably flat land around, that being surrounded by steep mountainous land. Such land was near level because of being located on an alluvial fan created by deposition of sediments from previous historic wildfires. So, in effect, the homes were prime targets for heavy post-fire sediment and debris deposition, if not for the successful functioning of diversion practices (most typically in the form of concrete highway dividers placed slightly down the slope and above the area of interest).

One key feature that should be considered in establishing the proper design runoff CN for post-wildfire hydrologic evaluations is the anticipated recovery time of the watershed towards its pre-fire condition. Runoff CN increases as burn severity worsens. This leads to higher estimated runoff from the various design rainfalls used for sizing runoff control practices. These, in turn, lead to higher project costs. Nevertheless, in the seasons that follow, the wildfire landscape recovery tends to return hydrologic processes toward pre-fire conditions. The longer the healing time, the less the design runoff CN should diverge from that used immediately after the fire. It is incumbent upon the engineer in charge of assigning the recommended design runoff CNs for various land covers and burn severities to consider both the risk of failure versus storm frequency. Design runoff CNs based on recovery of the land cover can vary greatly in the seasons following a wildfire.

The Bitterroot fires of 2000 and the use of FIRE HYDRO to design conservation practices happened to coincide with disagreements among engineers about proper post-fire design storm recurrence intervals. The concern stemmed from the idea that the notable increase in runoff CN value as the result of a fire would be short-lived and ground cover recovery would decrease the runoff CN in the seasons following the wildfire. The EFH-2 method that FIRE HYDRO is based on is very sensitive to the selected design runoff CN. It was thought that if all designs, including those for low hazard structures, were based on the accepted storm recurrence interval (25-year for most practices) overly conservative and costly designs would result, since the watersheds would heal significantly in the early post-fire years. The NRCS Montana State conservation engineer issued a guidance letter to all EWP engineers and technicians relating to the selection of recurrence interval design storms to be used for the statewide EWP effort. Low hazard scenarios were to be designed for nondamaging passage of flows of the 25-year pre-fire peak discharge or post-fire 10-year peak, whichever was greater. High hazard scenarios were to be dealt with on a case-by-case basis, in consultation with the State engineer.

The assumption for using the same T_c both pre-fire and post-fire should be more thoroughly investigated to determine its validity. As previously mentioned, this assumption was based on the idea that the added debris and sediment load from the burn would create increased opportunity for flow blockages to occur, thereby slowing the runoff process from what might initially be expected from a higher runoff CN value. Improvements to post-fire hydrologic methods, such as FIRE HYDRO, would benefit from research in this area. Onsite inspection of the burn area during a prominent runoff event should provide evidence of the validity of the assumption that post-fire debris offsets the loss of vegetation in runoff speed. Evidence of flow blockages may exist and their potential to eventually breach after a storm. The ideal investigation would

gage rainfall and runoff both before and after a wildfire. This would provide the most accurate assessment of wildfire influence to T_c and storm runoff volume and rate.

Complex issues should be acknowledged when attempting to model post wildfire hydrology. One of the most impactful is the time variance of runoff CN value. Clearly, the effective runoff CN for burned watersheds will have increased drastically. As the watershed heals, however, the runoff CN reduces toward the pre-fire condition. At what rate is not necessarily easily determined. It might not be economically proper to assume the worst-case runoff CN (immediately after the fire) for all hydrologic modeling related to design of runoff control practices in these areas. An accurate assessment of runoff CN change with time would help decisionmakers develop a sensible strategy for setting proper design parameters. Peter Robichaud, USDA FS, has spent considerable time investigating and monitoring post-wildfire watersheds. His findings indicate a tremendous increase in sheet erosion taking place on the landscape the year following the fire but then cutting back drastically each year thereafter. Evidently, growth of grass on the bare ground provides abatement to raindrop impact on the soil thereby stemming erosion about a year or two after the fire. This technical note references Robichaud's work in three articles, (Foltz et al. 2009, Hudak et al. 2004, and Robichaud et al. 2008). The question remains as to whether the runoff amount has also significantly decreased in this timeframe. (The dominant driving mechanism of CN change over time may not be raindrop impact.)

Determining the reduction of post-wildfire runoff CNs over time to their pre-fire values may best be investigated by gaging the watershed runoff or possibly by documenting field indicators of stream flow levels along stream banks from various rainfall events. Optimally, these post-fire gage records would be compared to those kept from the same area prior to the fire.

One convenient option might be to gage watersheds for which good-quality USGS predictive regression equations (for, say, peak discharge) exist, and that have also experienced wildfire. These areas could then be similarly analyzed for newly developed equations to reveal what trends have become apparent. Runoff CNs could perhaps then be assigned within the NRCS hydrology models that produce results in line with the USGS gaged watersheds.

Limitations

Sound hydrologic judgment is called for in utilizing FIRE HYDRO. It is based on the NRCS CN runoff equation and subject to all of the assumptions pertaining to that method. The selection of appropriate (and likely weighted) runoff CN should be based on the best information available (pre-fire land cover and condition and fire severity distribution in the watershed being evaluated). The predicted peak discharges from this model are quite sensitive to the runoff CN used. The runoff CNs listed in this paper were refined from existing tables in EFH-2 and altered by the judgment of NRCS Montana engineers to address the conditions found in western Montana. Other areas may require similar scrutiny to best define appropriate runoff CN usage. The decision of whether or not it is appropriate to weigh the various runoff CN attributed subareas and treat them as one homogeneous area is left to the designer. A more refined modeling approach might be to use WinTR-20 (USDA-NRCS 2004c) or one of the hydrologic models discussed in the other case studies of this technical note. Consultation with experienced users of these programs is warranted to ensure accurate assessments.

Another way to handle nonhomogeneous watersheds with FIRE HYDRO would be to determine peak flow rates per unit area for various pre- and post-burn CNs for each of the various recurrence events. Watersheds that do not vary too widely could benefit by this procedure. For example, the watershed would be modeled in pre-fire condition and a pre-fire flow rate per unit area determined. Then only the area of the portion burned severely could be analyzed and a severe burn flow rate per unit area determined. If the burned area of this hypothetical watershed burn was severe only, then the total predicted peak would be the severe burn area times the severe flow rate per unit area, plus the unburned area times the unburned flow rate per unit area. Watersheds with a wide mosaic of burns (and resultant varying runoff CNs) would not be handled in this way, since they would not fit the homogenous assumption that the spreadsheet utilizes. Again, sound judgment by the designer is called for to ensure that accurate modeling procedures are followed.

Though the drainage area is limited to 2000 acres by the parent method (EFH-2) of FIRE HYDRO, some of the burn areas are much larger than this. The results of FIRE HYDRO were compared to those from a more detailed method (TR-20) and found to be reasonably close for watersheds in the 5–10 square mile range. Consequently, no limit on drainage area was imposed on FIRE HYDRO. The user is cautioned to exercise judgment in the appropriate use of FIRE HYDRO to make sure that sound principles of hydrology are being modeled properly for the conditions present in the watershed. The assumption of rectangular watershed shape, used in the T_c computation, should no longer be necessary, since today's widely available GIS programs generally produce longer flowpaths easily.

References

BAER 2012. High Park Fire Burned Area Emergency Response Report. USDA USFS and NRCS, Larimer County, CO, Department of Transportation.

Cerrelli, G.A. 2005. FIRE HYDRO, a simplified method for predicting peak discharges to assist in the design of flood protection measures western wildfires. In Proceedings of the ASCE 2005 Watershed Management Conference, July 2005, Williamsburg, VA. pp. 935-941.

Mahlum, S.K., L.A. Eby, M.K. Young, C.G. Clancy, and M. Jakober, 2011. Effects of wildfire on stream temperatures in the Bitterroot River Basin, Montana. International Journal of Wildland Fire, 20, 240-247.

USDA-NRCS (U.S. Department of Agriculture Natural Resources Conservation Service), 2004a. NRCS National Engineering Handbook, Part 630 Hydrology, Chapter 9, Hydrologic Soil Cover Complexes.

USDA-NRCS (U.S. Department of Agriculture-Natural Resources Conservation Service), 2004b. NRCS National Engineering Handbook, Part 630 Hydrology, Chapter 10, Estimation of Direct Runoff from Storm Rainfall.

USDA-NRCS (U.S. Department of Agriculture-Natural Resources Conservation Service), 2004c. WinTR-20 User Guide. Available at http://go.usa.gov/KoZ/. Accessed in April 2013.

USDA-NRCS (U.S. Department of Agriculture-Natural Resources Conservation Service), 1984. NRCS National Engineering Handbook, Part 650 Engineering Field Handbook, Chapter 2, Estimating Runoff.

This page intentionally left blank

Appendix C: Case Study 3:
West Fork Complex Fire, Colorado

Background

The West Fork Complex wildfire, in the San Juan Mountains west of the community of South Fork, burned more than 109,000 acres June 9 to July 12, 2013. See figure C–1 for the general location and figure C–2 for the area of the West Fork Complex fire.

Figure C–1 State of Colorado with zoom into the Upper Rio Grande watershed

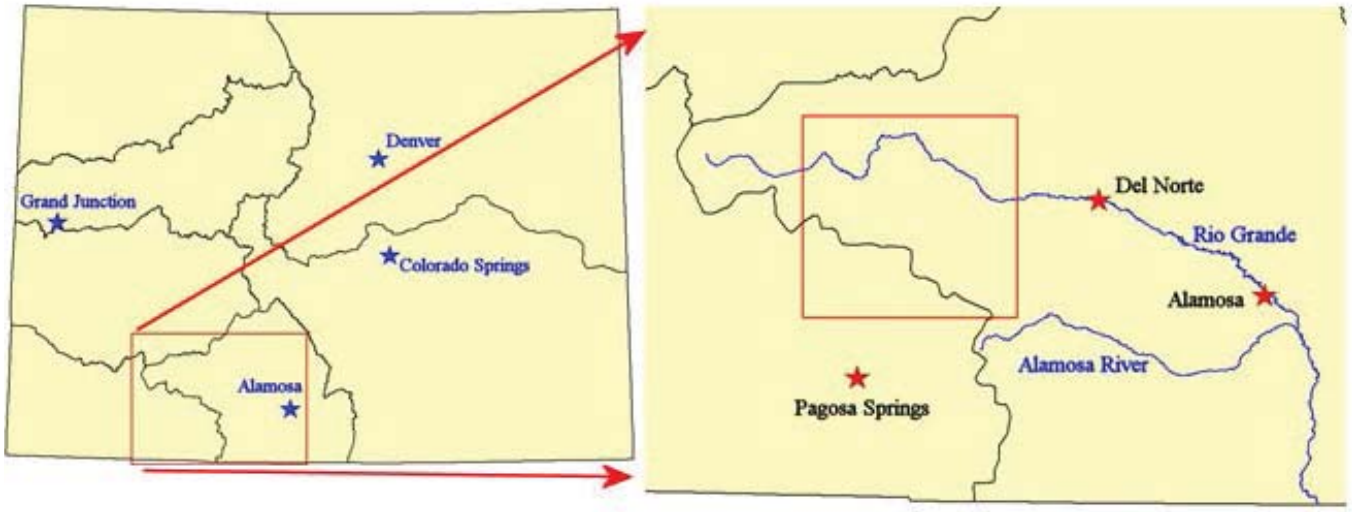

Figure C–2 Area of the West Fork Complex wildfire, west of South Fork, CO

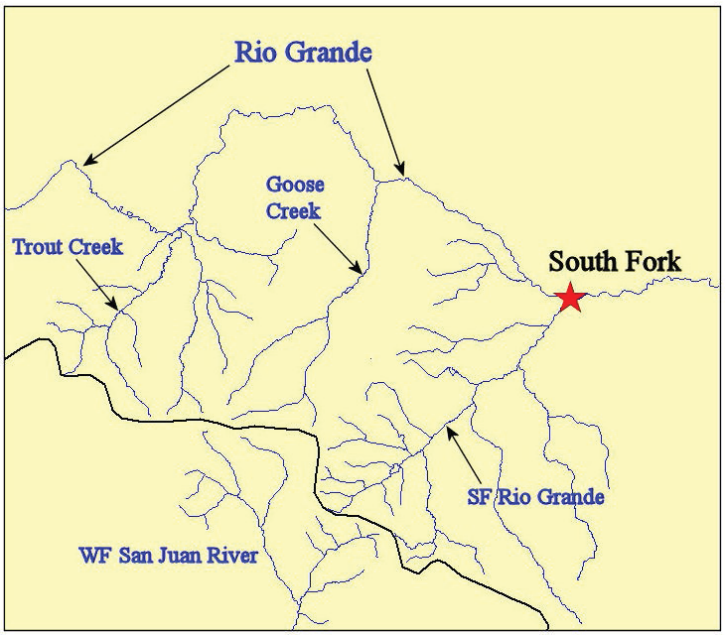

The fire area was composed of three separate fires: the Papoose fire in the Rio Grande watershed, the West Fork fire in the Rio Grande and San Juan watersheds, and the Windy Pass fire in the San Juan watershed. Together, these three fires are known as the West Fork Complex fire. See figure C–3 for the individual fire perimeters of the West Fork Complex.

Wildfires cause hydrologic shifts for a number of years. Substantially increased runoff and sediment production result from the loss of vegetation and soil cover, as well as from soil hydrophobicity. Lack of interception by vegetation, reduced soil infiltration, loss of surface roughness and ground litter, and increased hydrophobicity, all combine to shift the rainfall response from infiltration-dominated to surface runoff-dominated processes. For example, watershed impacts due to recent wildfire caused a Swiss catchment to produce runoff in the range of 100-year to 200-year recurrence interval from a 10-year rainfall event. This extreme runoff increase was due to changes in infiltration capacity (Conedera et al. 2003), although the phenomenon may have some scale dependency, with greater runoff enhancement in smaller catchments and tendencies towards overestimation in larger catchments (Stoof et al. 2011).

Hydrophobicity, which tends to be more prevalent with increased sand content and lower soil water content, has been found to weaken within a few months of a fire but persist for at least 22 months in ponderosa and lodgepole pine forests of the Colorado Front Range (Huffman et al. 2001). Post-fire sediment yield is most dependent on ground cover, with percent ground cover explaining more than 80 percent of the variability in sediment yield (Benavides-Solorio and MacDonald 2001). Accounting for soil burn severity is therefore fundamental for predicting sediment yield increases.

Figure C–3 Aerial extent of three fires known together as the West Fork Complex fire

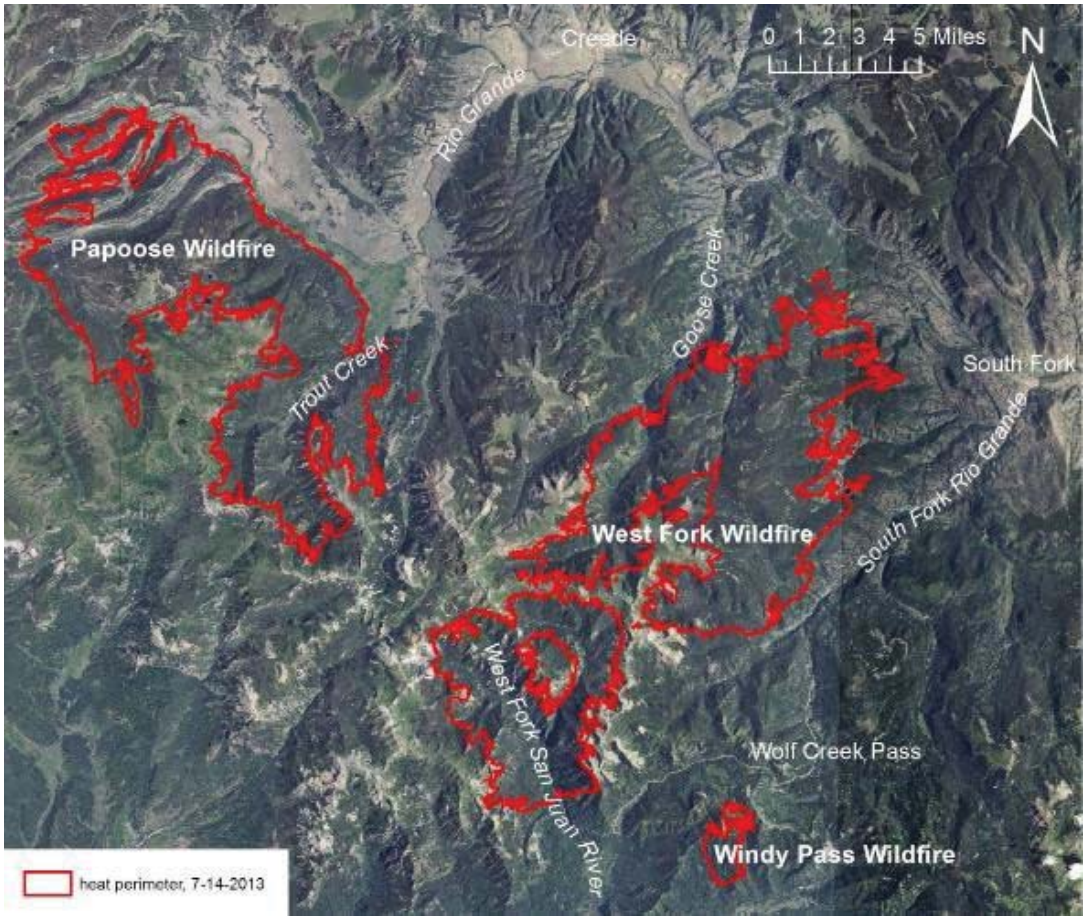

The West Fork Complex wildfire BAER report presented an initial hydrologic analysis of flood increases to be expected from the fire. However, this assessment was performed with a number of simplifications to meet the aggressive time line dictated by the BAER process. A more detailed peak flow analysis was performed to assess the variation and magnitude of increased flooding to be expected from the burned catchments. This analysis implemented the NRCS curve number (CN) runoff methodology.

Additionally, estimates of increased post-fire sediment yield help prioritize locations where hillslope and riparian mitigation may be needed. Such conservation practices minimize impacts of wildfire on such sensitive infrastructure as municipal water supply, irrigation diversions, and culvert conveyance. Predictions of post-fire sediment yield rely on mathematical models such as Revised Universal Soil Loss Equation (RUSLE) (Renard et al. 1997), Water Erosion Prediction Project (WEPP) (Elliot 2004), and GeoWEPP (Renschler 2003), as well as professional judgment (Robichaud et al. 2000). These methods have varying advantages and disadvantages for estimating the spatial distribution of post-fire soil loss, but all methods can require large amounts of time and energy to estimate soil loss and its associated risks over large spatial extents. With wildfires becoming more pronounced in the wildland-urban interface, rapid watershed management actions to protect sociological concerns, water quality, and ecosystem health are needed. This need for a rapid response to evaluate and manage post-fire soil loss has increased the interest in using GIS technology to spatially model post-fire sediment yields. Many toolsets have been produced that use the above models as engines to spatially estimate soil loss rates.

This case study details hydrologic analyses performed within the Rio Grande basin to assess the expected magnitude of flood increases in populated areas at risk of loss of life and property. Additionally, erosion modeling was performed to evaluate the expected increase in sediment expected from the burn areas. These results were provided to stakeholders to assist with planning and prioritizing recovery efforts.

Methods

Rainfall-runoff modeling was performed to simulate the expected flood response of the streams draining the wildfire areas. Additionally, predictions of post-fire sediment yield were also developed. The methods implemented to provide these predictions are presented below.

Hydrologic modeling for the West Fork Complex fire was performed using the program Hydrologic Engineering Center – Hydrologic Modeling System (HEC-HMS) from the U.S. Army Corps of Engineers Hydrologic Engineering Center. The NRCS curve number (CN) technique for estimating direct runoff from rain events, combined with the NRCS dimensionless unit hydrograph method, was used in this analysis. Catchments, modeled stream channels, and pour points are presented in figure C–4. The average modeled catchment size is 2.4 square miles.

The CN is a simple catchment-scale method that gives simplified results at a stream outlet, with more accurate results expected for larger, higher-intensity rain events. The method is documented in 210-NEH, Part 630, Hydrology, Chapters 9 and 10 (USDA-NRCS 2004a, USDA-NRCS 2004b), in Rallison (1980), as well as in numerous other publications. However, little quantitative information has been published of the database on which it was developed (Maidment 1992). In general, the method was developed for rural watersheds in various parts of the United States, within 24 States, was developed for single storms (not continuous or partial storm simulation), and was not intended to recreate a specific response from an actual storm (Rallison, 1980).

The initial abstraction (I_a) of the CN method has been traditionally assumed to be 0.2 of the storage coefficient, *S*. (For more on the CN method see "Runoff Curve Numbers" section of this document on page 10.) To reflect the decreased storage of a fire-impacted soil surface (due to a reduction of depression storage from the elimination of soil litter), the initial abstraction was assumed to be 0.1S for post-wildfire conditions in catchments that were substantially burned (>50 percent moderate + severe soil burn severity). Catchments that were not substantially burned were modeled with the standard I_a of 0.2S. Changes in I_a can alter CN assignments.

Figure C–4 Soil burn severity, model pour points, subwatersheds, and stream channels

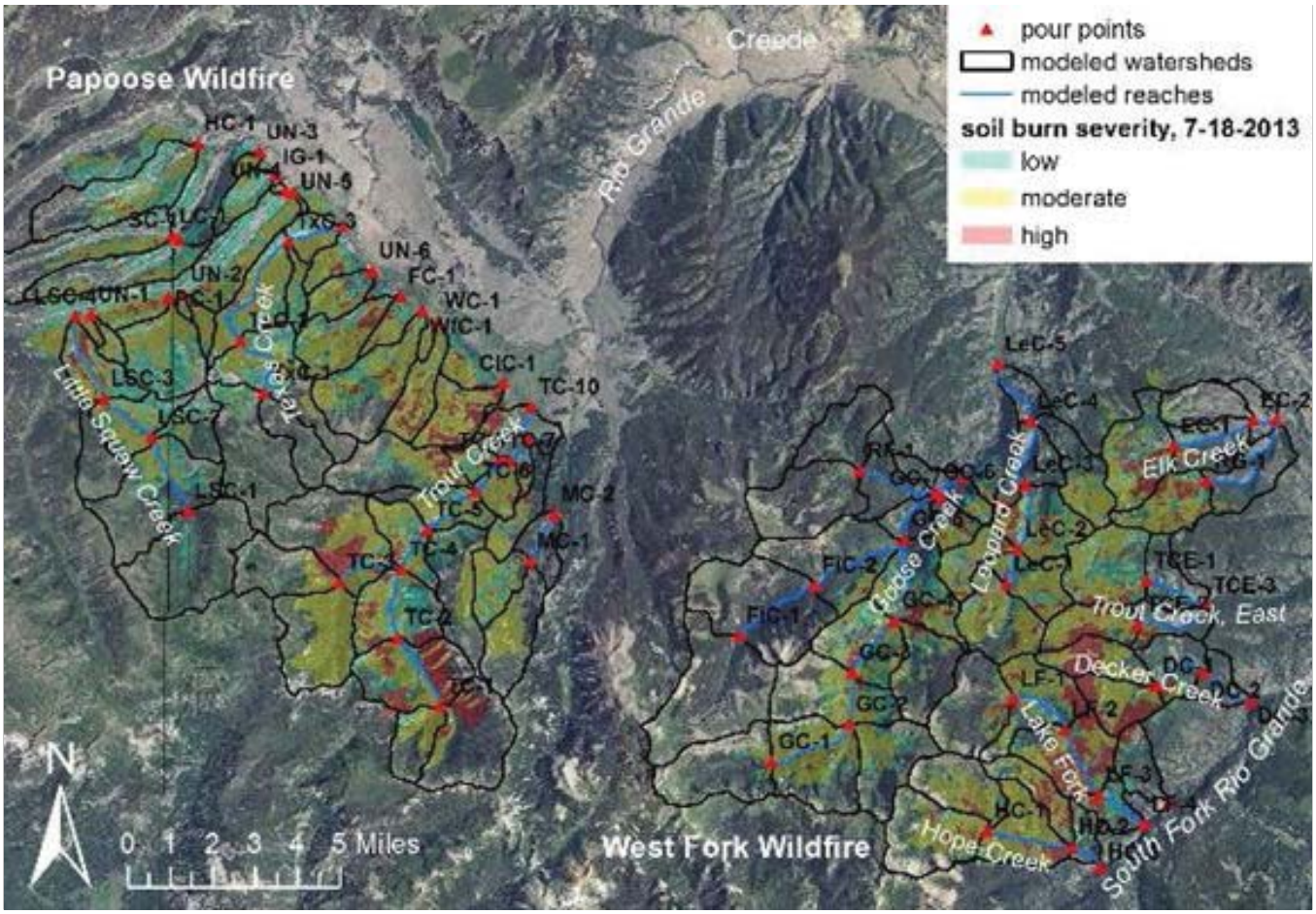

However, the impact of the I_a adjustment on CNs was disregarded; for the high CN post wildfire conditions, smaller shifts in CN due to changes in I_a can be expected (Woodward et al. 2003).

For the high CN post-wildfire conditions the impact on CNs of the I_a adjustment was ignored, since smaller shifts in CN due to changes in I_a can be expected (Woodward et al. 2003).

Runoff CN Estimation

CNs were assigned throughout the modeled catchments according to hydrologic soil group, vegetative type, and soil burn severity. Soil burn severity is a dominant factor in CN assignments in burned areas (see section "Runoff Curve Numbers" on page 10 of this technical note.) Hydrophobicity was assumed to be minimal, since the next substantial rain events (after this analysis was performed) would likely occur a year after the fire. The average catchment CN was computed using an aerial averaging methodology. Therefore, catchment size was limited to areas with similar runoff characteristics to provide the most reliable results. As catchment size increased, CNs were computed for adjacent and serial catchments, and flows were routed downstream and combined with lower catchments to predict flow at downstream points of interest. This was necessary due to the larger basins draining the fire areas, as well as to account for catchment shape and stream channel attenuation.

Soil burn severity is the principle driver for increasing flow in runoff predictions. For this modeling, soil burn severity was measured using the Burned Area Reflectance Classification (BARC) process from satellite data collected on July 18, 2013 (fig. C–4). BARC uses reflectance recorded in satellite images to quantify soil burn severity. For defining soil burn severity, BARC images have the advantage of being comprehensive and relatively rapidly developable. (See the technical note for more information on both BARC and soil burn severity.) However, comparison with field-collected data has indicated that this remotely sensed product can be more indicative of post-fire vegetative condition than soil condition, especially in low to moderately burned areas (Hudak et al. 2004).

Hydrologic soil group (HSG) classification was selected using soils data published in the NRCS SSURGO (Soil Survey Geographic) database. Using this method, soil are classified as being either A, B, C, or D type, where A allows the most infiltration and least runoff and D allows the least infiltration and greatest runoff. Type A soils are prevalent in many areas of the fire. Dual hydrologic groups (i.e., A/D or B/D) are indicated in portions of the catchments. These dual classifications are for certain wet soils that could be adequately drained, with the first letter indicating the wet condition and the second indicating the undrained condition. In these cases, an undrained condition was assumed.

Vegetation type, from the Southwest Regional Gap Analysis Project (SWReGAP) land cover mapping, was included in the assignment of CNs used for the modeling. The dominant vegetation types of the fire area catchments were spruce-fir, aspen, and alpine meadow and tundra.

CNs were assigned by polygons that had unique values of hydrologic soil group, vegetation type, and soil burn severity. Using primarily a compilation modified from the values used in the High Park (case study 1 of this technical note) and Black Forest Wildfire analyses, the implemented CN values are provided in table C–1. A fair ground cover condition was generally assumed for the unburned values abstracted from USDA-NRCS (2004a), though a good ground condition was assumed for herbaceous and grassland. The CN values for burned conditions were primarily compiled from various grey literature and unpublished sources; they should be considered approximate.

Table C–1 CN assignments implemented in West Fork Complex fire hydrologic modeling

Cover Desciption	**A** HSG				**B** HSG				**C** HSG				**D** HSG			
	Unburned	Low	Moderate	High	Unburned	Low	Moderate	High	Unburned	Low	Moderate	High	Unburned	Low	Moderate	High
Herbaceous, pasture, alpine meadow, park	49	55	67	77	61	68	80	86	74	81	88	89	82	86	92	95
Oak-aspen-mountain brush mixture of oak brush, aspen, mountain mahogany, bitter brush, maple, and other brush	45	52	65	77	48	55	65	86	57	70	80	89	63	70	80	92
Ponderosa pine-juniper (grass understory)	49	57	65	77	58	65	75	86	73	78	83	89	80	85	90	92
Sagebrush (grass understory)	46	54	65	77	51	60	75	86	63	70	80	89	70	75	85	92
Lodgepole pine forest	49	57	65	77	60	65	70	86	73	78	83	89	79	83	87	92
Bare soil	77	77	77	77	86	86	86	86	91	91	91	91	94	94	94	94
Wetland	98	98	98	98	98	98	98	98	98	98	98	98	98	98	98	98

Rainfall

Rainfall depths used in the modeling were extracted from NOAA Atlas 14, Vol 8 (Perica et al. 2013). Six-hour rainfall durations and NRCS Type II rainfall distributions were assumed. Three rainfall depths were used in the analysis, reflecting the variable spatial and elevation extent of the catchments draining the fire area. However, for each specific watershed analyzed, identical rainfall depths were used for all catchments. The specific rainfall depths for the 10-, 25-, 50- and 100-year floods are provided in table C–2. The implemented rainfall distributions for the 25-year event are shown in figure C–5. Note that the distribution places the majority of the 6-hour duration rainfall in 30 minutes.

For catchments with drainages areas greater than 11 square miles, an areal reduction factor was applied as detailed in Miller et al. (1973). Reduction varied from 0.98 (Elk Creek) to 0.94 (Trout Creek). When applied, this area reduction was implemented in all catchments; flow may be underpredicted in the smaller, upper catchments of such drainages.

Lag Time

Lag time (L), that is required to generate a hydrograph using the NRCS unit hydrograph methodology, was computed using the watershed lag method (USDA-NRCS 2010). This equation is—

$$L = \frac{l^{0.8}\left(S+1\right)^{0.7}}{1900Y^{0.5}} \qquad \text{eq. C–1}$$

where l is flow length (ft), Y is average watershed land slope (%), and S is maximum potential retention (in). S may be calculated from equation C–2:

$$S = \frac{1000}{cn'} - 10 \qquad \text{eq. C–2}$$

where *cn'* is the retardance factor and is approximately equal to the CN. This method allows the computation of differing lag times for pre- and post-fire conditions, reflecting the actual physical mechanism of more rapid flow response during post-fire conditions. Equation C–1 was developed similarly to the time of concentration equation earlier in this technical note (eq. 1). Lag is considered to be 0.6 of the time of concentration.

Table C–2 Rainfall depths (inches) implemented in the modeling

	Return Interval			
	10-year	**25-year**	**50-year**	**100-year**
Zone A	2.17	2.59	2.93	3.28
Zone B	1.79	2.18	2.48	2.77
Zone C	1.99	2.48	2.91	3.40

Figure C–5 Twenty-five-year cumulative rainfall distributions used in modeling

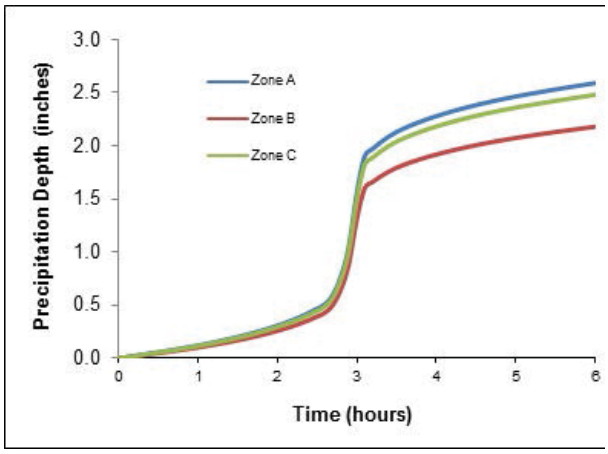

Flow Routing

A Muskingum-Cunge procedure was used to route flow from upper catchments to the stream outlets. This one-dimensional method, embedded in HEC-HMS, allows for flow attenuation in the computations but does not provide a numerical solution of the full unsteady flow routing equations, as provided in such computational models as HEC-RAS. In each reach, flow routing was estimated using a single simplified cross section, channel slope, and Manning's n roughness estimates. Manning's n was selected using a visual estimation procedure, with a quality control step to assure that subcritical or approximately critical velocity was maintained, reflecting an assumption that existing or new channel bedform development prevents reach-average supercritical flow.

Sediment Bulking

A simple multiplication factor was applied to the post-fire flood predictions to account for sediment bulking in the wildfire-induced floods. For burned catchments, this multiplication factor was assumed to be 1.25 if the severe + moderate soil burn severity aerial extent was greater than 50 percent, and 1.1 for catchments with between 15 and 50 percent soil burn severity.

Erosion Modeling

The Revised Universal Soil Loss Equation (RUSLE) model was chosen to estimate pre- and post-fire sediment related issues for the burn area because it is widely used, can be quick to execute with straight-forward factors, and has a large amount of supporting documentation. The RUSLE models (pre- and post-fire) are based on a spatial version of RUSLE outlined in the Assessment of Threats to Riparian Ecosystems in the Western United States (ATREW) (Theobald et al. 2010) report. More recently, Litschert et al. (2014) used similar methods to investigate climate change effects on wildfire frequency and soil loss in the Southern Rockies Ecoregion. The ATREW methods entail calculating RUSLE (eq. C–3) the standard way, using widely available fine resolution spatial datasets to approximate the six RUSLE factors. The ATREW report also provides guidance on parameterizing the RUSLE C and P factors based on commonly used landcover datasets (e.g., USGS National Landcover Dataset and USFS Existing Vegetation Dataset), as well as equations that scale GIS-based terrain analysis for the L and S factors.

$$A = R \cdot K \cdot L \cdot S \cdot C \cdot P \qquad \text{eq. C–3}$$

where—

A = average annual soil loss (tons/ha/yr).
R = rain erosivity factor (MJ mm/(ha h yr)).
K = soil erosivity factor (tons ha h/(ha MJ mm)).
LS = slope length and steepness factor.
C = cover management factor (>= 0).
P = management factor (>= 0).

The advantages of the ATREW approach are—

- The simple model parameterization uses nationwide spatial datasets.
- The sedimentation rate raster allows better spatial resolution of erosion estimation.
- Spatial evaluation of sediment yield helps prioritize soil treatment zones and emergency resource allocation.

The sediment modeling entailed four general steps:

1. Collection of geospatial dataset for the greater burn area (table C–3)
2. Development of spatial RUSLE factors for pre- and post-fire conditions
3. Calculation of RUSLE for pre- and post-fire scenarios (using ArcGIS Raster Calculator)
4. Attribution of computation points and values at risk with pre- and post-fire sedimentation rates.

Pre-fire and post-fire sedimentation rate estimates were executed in GIS using terrain analysis tools to calculate slope length and steepness (LS) jointly with simple map algebra statements. Computation of rainfall erosivity (R), soil erodibility (K) and cover management (C) factors used ancillary spatial datasets. The soil and cover management (P) factor was not incorporated into the analysis due to a lack of spatial information on management activity in the burn area. For each of the five RUSLE factors used, a 10-meter resolution raster dataset was generated. The five RUSLE factor rasters where multiplied together to calculate the local (cell level) sedimentation rate. These local rate values were accumulated downslope via a flow direction raster (fig. C–6) and averaged by the contributing area above each raster cell. This results in the final sedimentation rate raster with values representing the average cumulative sedimentation rate in tons per year over 30 years for each scenario.

Table C–3 Spatial datasets ssed for the six RUSLE factors

RUSLE factor	Web site	Description
R	http://www.epa.gov/esd/land-sci/emap_west_browser/pages/wemap_mm_sl_table.htm#mapnav	EPA EMAP RUSLE factors summarized to HUC 8 units for the Western United States.
K	http://datagateway.nrcs.usda.gov	NRCS SSURGO data downloaded for El Paso County, CO
LS	http://viewer.nationalmap.gov/viewer	10x10 meter elevation model downloaded for HUC 8 areas associated with the burn area
C	http://swregap.nmsu.edu/	30x30 meter landcover dataset for NV, AZ, UT, and CO
P	-	Parameter not used in analysis due to lack of good spatial data

Figure C–6 Flow direction raster cell example*

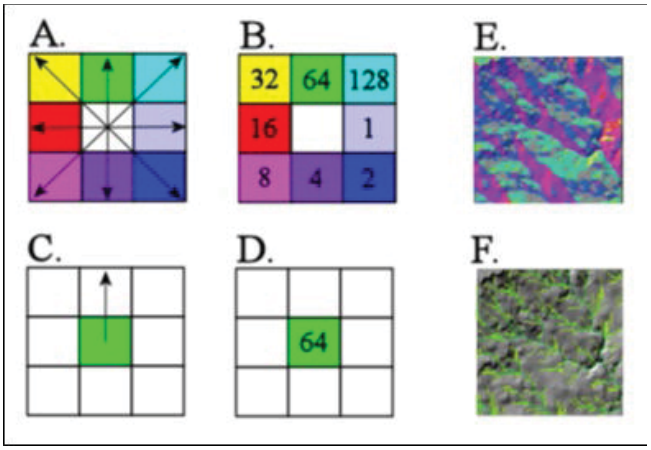

* A. Shows the eight directions of flow from center cell.
B. Shows the possible flow direction raster values.
C. Shows an example cell with a north flow direction.
D. Shows flow direction raster value of the cell in C.
E. Shows a flow direction grid with color scheme of A.
F. Shows a flow accumulation raster, with each cell encoding the number of cells that drain to it.

The rain erosivity (*R*) factor raster was generated by converting an EPA EMAP HUC 8 polygon shapefile to a raster containing *R* factor values. Due to a lack of information about how wildfire changes rain erosivity values and the *R* factor, raster was held constant between the pre- and post-fire scenarios. In addition, the EPA EMAP values are based on 30-year averages.

The development of soil erodibility (*K*) factor raster entailed summarizing KFFACT (SSURGO table attribute) to NRCS SSURGO map units and then rasterizing the map units in the same manner as the *R* factor. KFFACT (property of a soil horizon) was summarized to map unit delineations by calculating a depth and area weighted average based on horizon depths up to 15 centimeters and the component percent within a map unit. This was accomplished through queries developed in the SSURGO database downloaded from the USDA Geospatial Data Gateway Web site (see table C–3). The *K* factor raster was held constant for both pre- and post-fire scenarios even though burn severity alters soil erodibility. Altering soil erodibility based on burn severity between scenarios could be incorporated in future models but would require additional research and parameterization.

The *LS* factor was developed using basic terrain analysis methods outlined in Theobald et al. (2010) using a 10-meter elevation model. These methods include calculating a percent slope, aspect (radians), and accumulated upslope length. The accumulated upslope length process entailed accumulating number of contributing raster cells to a given cell based on the overland flow paths from the flow direction raster (fig. C–6). The resulting slope, aspect, and upslope length rasters were transformed using equations developed by Desmet and Grovers (1996) with Winchell et al. (2008) confirming the methodology by an analysis that compared GIS estimates with National Resources Inventory field observations, given herein as equation C–4, and Nearing (1997), given herein as equation C–6. These equations scale the values derived from the above terrain analysis to better fit within the framework of the RUSLE equation and ensure that the units are correct.

$$LS = S\left[\frac{\left(A + D^2\right)^{m+1} - A^{m+1}}{x^m * D^{m+2} * 22.13^m}\right] \qquad \text{eq. C–4}$$

where—

LS = transformed slope length and slope steepness at the given raster cell.
S = RUSLE slope steepness factor of the cell (equation C–7).
A = contributing drainage area to the cell (m2), D = raster cell size (10m).
x = aspect transformation (equation C–5).
m = percent slope transformation (equation C–6).

$$x = \sin\alpha + \cos\alpha \qquad \text{eq. C–5}$$

where α = land aspect of the raster cell in radians, clockwise from north

$$m = \frac{\beta}{1+\beta} \text{ where—} \qquad \beta = \frac{11.16\sin\theta}{3\sin\theta + 1.68} \qquad \text{eq. C–6}$$

and where θ = land slope (in percent).

The slope steepness (*S*) factor raster was developed using the Nearing (1997) equation (given herein as equation C–7) in conjunction with equations C–5 and C–6, which use aspect and slope dynamics to adjust for inaccuracies caused by scale. This is necessary because the raster values of the area draining to each cell (*A*, in square meters) can get very large and inflate sedimentation estimates. The raster for *S* factor was developed by transforming percent slope using equation C–7. That equation scales slope values to reduce inflated soil loss calculations, especially for slopes greater than 20 percent. The *LS* factor raster was calculated (eq. C–4) using the ArcGIS Raster Calculator. As with the *R* and *K* factors the *LS* factor was held constant between the pre- and post-fire models.

$$S = 1.5 + \frac{17}{1 + e^{(2.3 - 6.1 \sin \theta)}} \qquad \text{eq. C–7}$$

where θ = land slope (in percent).

The *C* factor parameterization for the pre- and post-fire scenarios was developed using various source tables from different documents related to RUSLE. The pre-fire scenario parameterization involved developing a lookup table that assigns the existing landcover types (Southwest ReGAP) within the greater burn area to their associated *C* factors (see table C–4). The table was compiled by Theobald et al. (2010) for the ATREW report and provides a broad spectrum of landcovers found in most landcover datasets and can be modified based on local knowledge. The post-fire *C* factor parameterization entailed modifying the pre-burn *C* factor raster based on burn severity classes derived from the BARC image. This process consisted of assigning the BARC burn severity classes *C* factor values (low burn = 1.03, moderate burn = 2.25, and high burn = 3.75) (Larsen et al. 2007) that were then used to modify the pre-fire *C* factors by summing the two rasters together. Larsen et al. (2007) estimated that high burn severity area *C* factors changed by 400 percent but didn't estimate moderate and low burn severity changes. For these, *C* factors changes were estimated using professional judgment.

Table C–4 *C* Factors for common land covers (Theobald et al. 2010)

Land cover	*C* factor	Citation
Barren	1.0000	Toy and Foster 1998
Coniferous forest	0.0020	Breiby 2006
Deciduous forest	0.0010	Breiby 2006
Deciduous shrubland	0.0250	Breiby 2006
Dense grassland	0.0800	Dawen et al. 2003
Floodplain forest	0.0100	Breiby 2006
Lowland coniferous forest	0.0025	Breiby 2006
Lowland deciduous forest	0.0015	Breiby 2006
Marsh/riparian/wetland	0.0010	Breiby 2006
Medium-tall grassland	0.0120	Breiby 2006
Mixed forest	0.0010	Breiby 2006
Mixed forest woodland	0.0020	Breiby 2006
Open water/exposed rock	0.0000	Breiby 2006; McCuen 1998
Shrubland other	0.0290	McQuen 1998
Snow field	0.0010	Dawen et al. 2003
Sparse grassland	0.2000	Dawen et al. 2003
Aggregate mining	1.0000	Guobin et al. 2006
Asphalt	0.0001	Toy and Foster, 1998
Cultivated crops irrigated	0.2400	McCuen, 1998
Developed general	0.0030	Guobin et al. 2006
Developed suburban	0.0020	Guobin et al. 2006
Developed urban	0.0010	Guobin et al. 2006
Fallow	1.0000	McCuen, 1998
General cropland	0.5000	Dawen et al., 2003
Gravel	0.2000	Toy and Foster, 1998
Industrial	0.0050	Guobin et al. 2006
Mixed urban	0.0040	Guobin et al. 2006
Paddy field	0.1000	Dawen et al., 2003
Pasture hay	0.1400	McCuen, 1998
Recreational grasses	0.0080	McCuen, 1998
Small grains	0.2300	McCuen, 1998

The final estimates of sedimentation rate for the pre- and post-fire scenarios were generated by multiplying the five factors, accumulating those values downslope by way of the flow direction raster, and calculating an area-weighted sedimentation rate. The latter is determined by dividing the accumulated sedimentation rate by the total accumulated drainage area. Figure C–7 shows how sediment yield varies in different zones on a hillslope. The transport of sediment from areas where it originates (steep slopes or burned areas) dampens with decrease in slope, increase in flow distance, or interruption by unburned areas. Figure C–8 is an example of an area-weighted sediment yield raster, showing that the high loss areas (red) dampened with flattening slope and distance.

Figure C–7 Conceptual diagram of sediment yield estimation on hillslope zone breaks

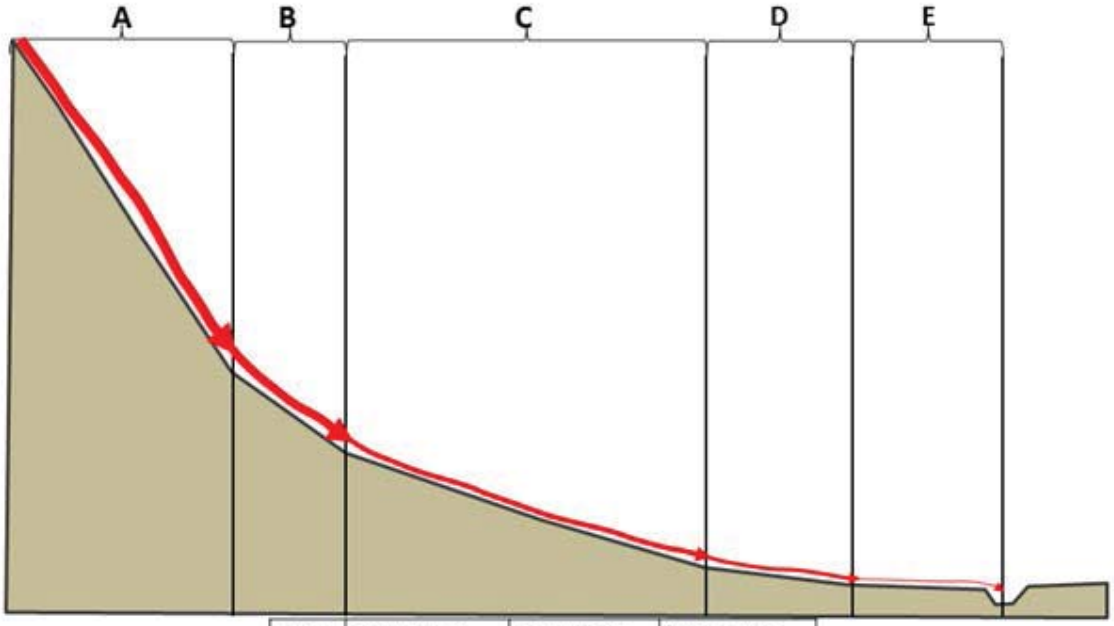

Zone	Accumulated RUSLE (tons/yr)	Accumulated Area (ha)	Average RUSLE (tons/yr)
A	12000	150	80
B	17000	225	75
C	19000	600	31
D	21000	800	26
E	22000	1000	22

Figure C–8 Example of an area-weighted RUSLE sediment yield raster

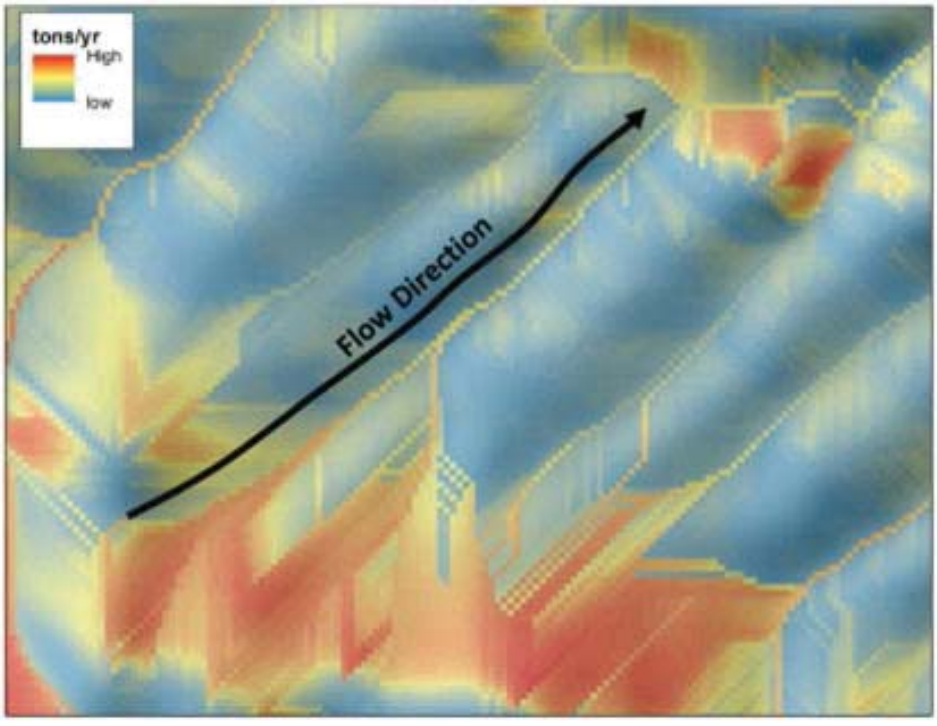

Results and Discussion

Hydrologic modeling was performed to develop estimates of increased flood hazard and erosion potential for streams draining the West Fork Complex wildfire. For several key catchments, at locations where there are threats to residences, hydrographs such as in figure C–9 show the expected response to a 25-year rainfall depth over each entire catchment. Substantially increased flow peaks, runoff volumes, and sediment were estimated. Using a map presentation style (fig. C–10) that is simple for planners, designers, and emergency response officials to utilize, results were provided at pour points throughout and downstream of the fire extents. Results were also provided as attributes in ArcGIS shapefiles. For detailed results, refer to the project report (Yochum and Norman 2014).

Figure C–9 Example of estimated pre- and post-fire hydrographs for the 25-year event

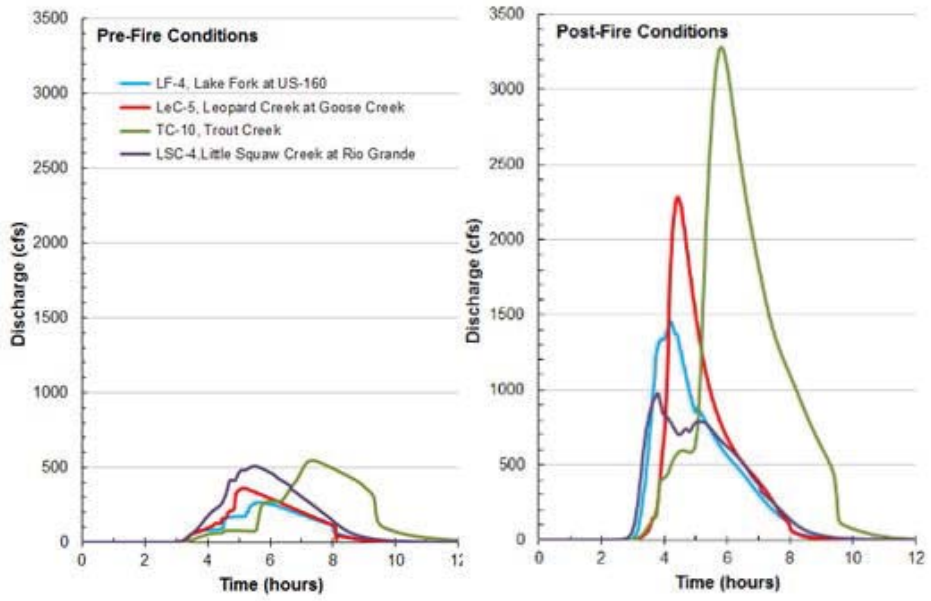

Figure C–10 Map providing pre- and post-fire flood predictions for South Fork Rio Grande

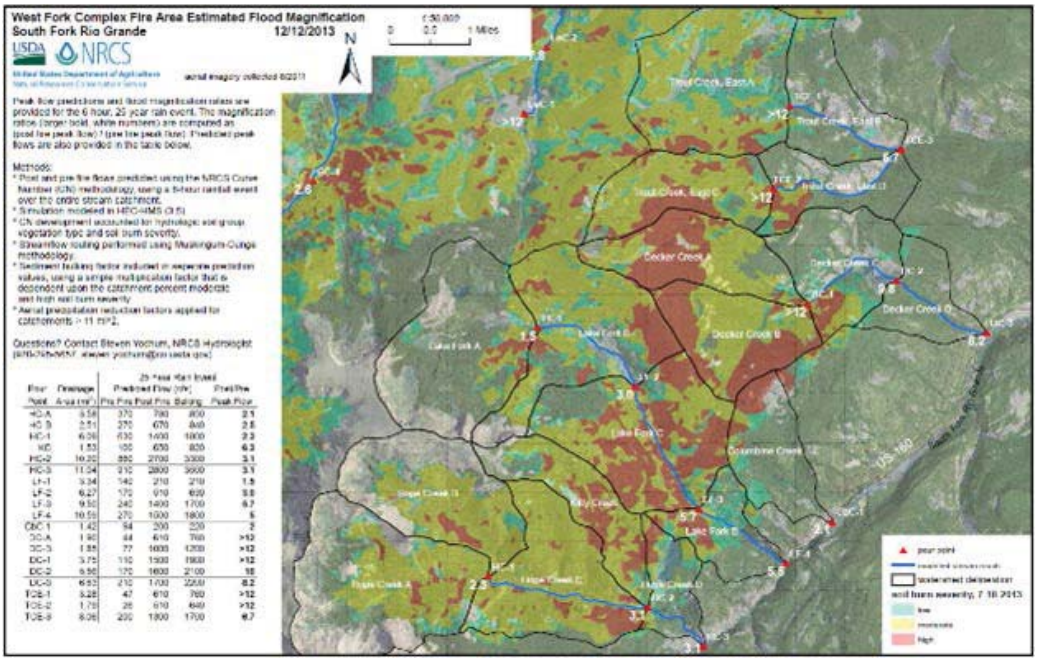

Runoff Modeling Results

In many catchments, post-fire conditions are predicted to cause a 50- or 100-year (pre-fire) flood to result from a 10-year rain event on burned landscapes, similar to actual measured fire runoff responses (Conedera et al. 2003). Peak flow magnification ratios for the 25-year rainfall event are provided (fig. C–11). These ratios are computed as the post-fire peak flow divided by the pre-fire peak flow; a value of three indicates that three times the peak flow is predicted from the burned landscape for the identical rain event.

The fire results in a 41-percent risk that a 10-year rain event will cause runoff that, pre-fire, would have been 50- to 100-year in recurrence. These substantial fire impacts on runoff may persist for at least 5 years. However, as catchment size increases, the small spatial extent of typical convective storms will reduce the severity of the flood effects from these storms.

Figure C–11 Peak flow magnification ratios for the West Fork Complex wildfire

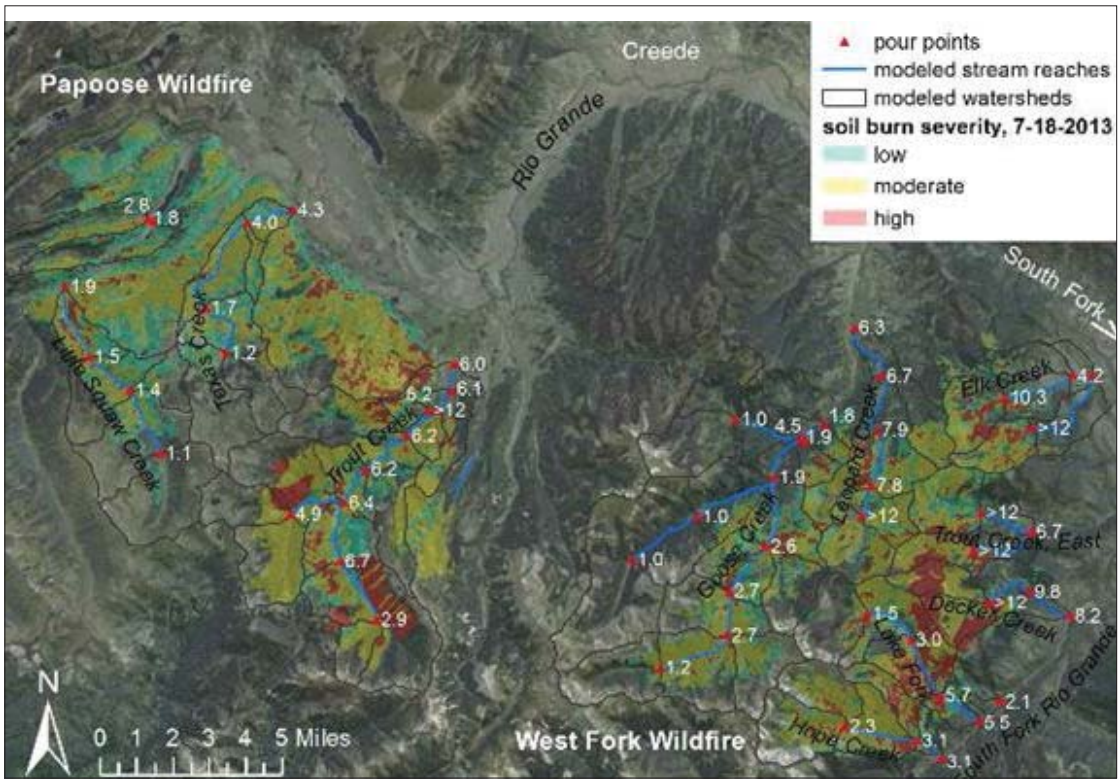

Sediment Modeling Results

Sediment modeling was intended to provide estimated sediment magnification ratios at hydrologic pour points, as well as approximations of sediment yield. Sediment magnification ratios were calculated by taking the ratio between the predicted post- and pre-fire sediment flux values (tons/yr) to compute the magnitude of change. The true magnification ratios and quantities for the pre- and post-fire scenarios are unknown, and these estimates are based on a lumped modeling approach (RUSLE) that provides values with substantial expected error. However, the results do provide a reasonable framework for making management decisions. An overview of the sediment magnification ratios is provided in figure C–12.

The sedimentation analysis for the entire West Fork Complex wildfire predicts that the Upper Rio Grande River will experience on average 130 times more sediment annually above pre-fire conditions (approximately 1,030,000 tons per year). This is based on sediment rates estimated for the 27 outlet pour points that are hydrologically connected to the burn area. These pour point estimates account for all sediment production and transport that occurs upstream of them. The Papoose wildfire accounts for 65 percent of the total

sediment yields in the West Fork Complex, with 70 percent of its outlets having sediment magnification ratios greater than 100. The West Fork wildfire area has lower sediment magnification ratios, with 50 percent of its outlets having ratios higher than 100; but it has the highest yielding catchment (Hope Creek HC), which accounts for about 18 percent of the total sediment yield of the entire West Fork Complex fire area.

The majority of sediment produced by the Papoose wildfire area is from two large catchments (Little Squaw Creek and Trout Creek), which together account for about 50 percent of its total sediment yield. The other 17 outlet pour points do not account for as much sediment on an individual basis, but several (CIC-1, PC-1, UN-1, UN-2 and WC-1, in fig. C–4) have sedimentation magnification rates that exceed 500 times pre-fire conditions. These catchments are small but have steep slopes with high proportions of moderate and high burn severities, which could pose a mass movement risk. The pour points that make up Trout Creek all have sediment magnification ratios greater than 100 with TC-6 (fig. C–4) having the highest sedimentation rate. The Little Squaw Creek catchment of the Upper Rio Grande has magnification ratios that increase dramatically downstream with a large bump in sediment yield at the outlet point (LSC-4). The Texas Creek catchment has magnification ratios that increase up to the midpoint of the catchment (TxC-3) and then decreases to the outlet point with sediment yields still increasing steadily downstream.

The majority of sediment produced by the West Fork wildfire is dominated by two catchments (Goose Creek and Hope Creek) that together produce 75 percent of the total sediment yield. The analysis for Hope Creek predicts sediment magnification ratios greater than 400 with a peak ratio of 605 at HC-2, dropping back to 483 at the outlet. This catchment, along with LF-4, CbC-1, and DC-3 (fig. C–4), connects to the South Fork of the Rio Grande River, which will increase its sediment yield by approximately 250,000 tons annually. The Goose Creek analysis predicts that sediment magnification ratios and yields increase dramatically to pour point GC-4 and then decrease by half at the outlet pour point at Lake Humphreys, where a post-fire sediment yield of approximately 85,400 tons per year was simulated. The other four outlets, DC-3, TCE-3, EC-3, and Lec-5, have moderately low sediment magnification ratios, with a total yield of approximately 390,000 tons per year.

Figure C–12 Sediment magnification ratios for the West Fork Complex wildfire

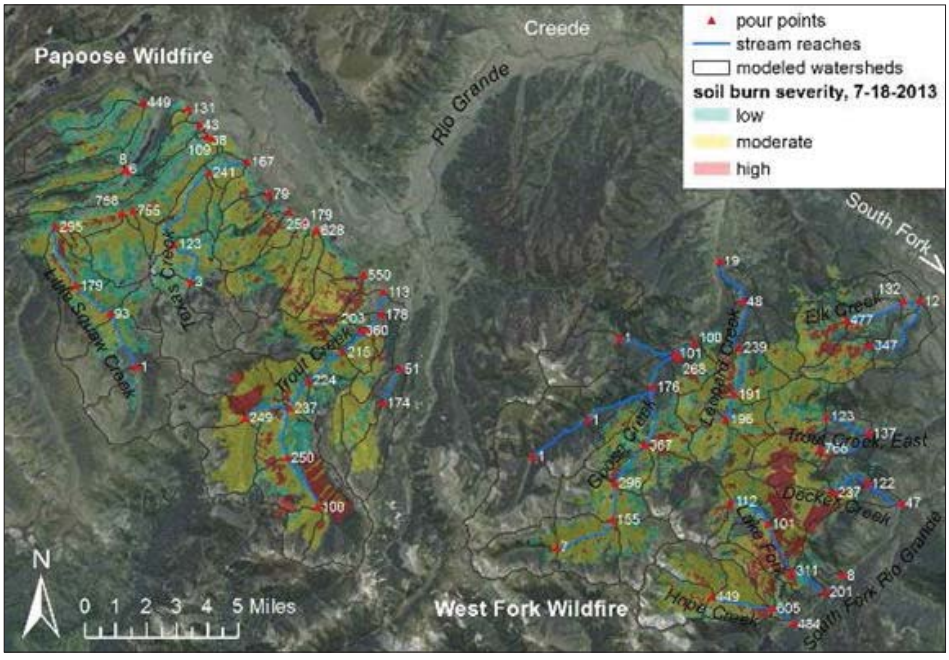

Modeling Limitations

As with all hydrologic modeling, the results provided by these rainfall-runoff and sediment models are approximate. The best use of these results is on a comparative basis, to help identify points of concern and develop mitigation priorities. Absolute values of runoff and sediment yield are approximate and use of these values for infrastructure sizing and estimating reservoir sedimentation rates should be done with caution. Specific limitations in the modeling methods are discussed below.

Rainfall-Runoff Modeling Limitations

Post-fire runoff prediction using the CN technique is hampered by the very limited field data available from which to reliably select CN values from measured rainfall and runoff in burned catchments. With CN values for burned conditions primarily compiled from various grey literature and unpublished sources, they should be considered approximate. As a result, consistent application of these values result in model results that are more dependable in a comparative manner. Catchment-scale research of wildfire-impacted areas is needed to develop more robust post-wildfire CN estimates.

An additional complication arises from the peak rate factor imbedded in the NRCS dimensionless unit hydrograph method. Within HEC-HMS, this peak rate factor cannot be altered from the default value, despite an understanding that this factor tends to increase with steeper watersheds. The ability to adjust the peak rate factor (an option in WinTR-20) would be a valuable addition to HEC-HMS. For more information, see sesection "NRCS dimensionless unit hydrograph" earlier in this technical note.

Most fundamentally, the reliability of the CN method for predicting peak flow from forested, mountainous watersheds is questionable. Forested watersheds in unburned conditions may be dominated by saturation-excess overland flow (fig. C–13) where runoff is produced from relatively small and variable portions of a catchment when rainfall depths exceed the soil capacity to retain water. Newly burned catchments, on the other hand, may be dominated by infiltration-excess (Hortonian) overland flow, where surface runoff is generated when rainfall intensity is greater than soil infiltration capacity, and flow runs down the hillslope surface. Evidence of this surface runoff is provided by such features as surface rilling on freshly-burned hillslopes. Rainfall-runoff modeling performed in the San Dimas Experimental Forest (Chen et al. 2013) found that pre-fire runoff predictions were more accurate using the CN method, while KINEROS2 performed better for post-fire conditions. These results suggest fundamental shifts in runoff mechanisms between pre- and post-fire conditions, complicating modeling strategies.

Despite this shortcoming, due to its relative simplicity and achievable data requirements on large scales, as well as reasonable results when qualitatively compared to actual post-fire runoff events, the CN method is often considered a preferred tool for predicting flow response of wildfire areas. Alternatives approaches can

Figure C–13 Overland flow, infiltration excess vs. saturation excess (Lab. of Ecohydrology)

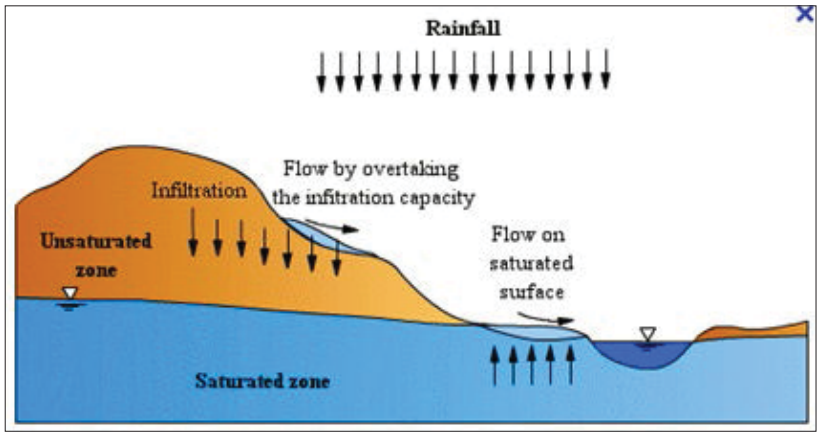

be problematic, due to the need to quantify infiltration rates, the effects of soil litter and hydrophobicity on retention and infiltration for pre- and post-fire conditions, as well as vegetation canopy rainfall interception. This accounting would need to be performed at a spatial resolution appropriate for obtaining the needed flood predictions throughout the entire wildfire extent, which can be a very challenging task with the limited time and resources allotted to practitioners for prediction.

Sediment Modeling Limitations

The ATREW method used to estimate pre- and post-fire sediment yields was originally developed to estimate sedimentation rates to riparian areas based on different land use and climate change scenarios for the Western United States (Theobald et al. 2010.) This scaling issue along with limited information on parameterizing *C* factors for burned vegetation, inherent errors associated with the spatial data and the lumped approach of the RUSLE equation makes predicted sedimentation rates unreliable. This was evident when Larsen et al. (2007) evaluated spatial versions of RUSLE and WEPP performance using established plots for fires on the Front Range of Colorado and found that the models performed poorly due to unaccountable variability not incorporated into the models. To address this weakness, it is preferred that sediment yield modeling focus on the magnitude of change in soil loss and not just to amount produced post fire. The magnitude values are based on an annual average increase in sediment yields for 30 years. This means that actual sediment yields for a given year will fluctuate around the predicted value, but over 30 years may be close to the predicted annual increase in sediment. Nevertheless, the ATREW method, used to estimate pre- and post-fire sedimentation rates and the magnitude of sedimentation post fire, provides a robust framework for managers to help prioritize and guide timely post-fire mitigation activities.

Conclusions

Using the CN and RUSLE methods, peak flow and erosion potential predictions were made for streams draining the West Fork Complex wildfire area, for both pre- and post-wildfire conditions. Watershed maps for each modeled watershed were developed, illustrating pour points, peak discharges, peak flow and sediment magnification ratios, soil burn severity, and stream outlet hydrographs. While many relevant hydrologic mechanisms were simulated in the rainfall-runoff modeling, including rainfall depth and spatial extent; variation in runoff by soil burn severity, vegetation type and soil conductivity; variable lag times; and stream attenuation, the questionable reliability of the CN method in forested watersheds, for both post- and pre-fire conditions, adds a level of undefined uncertainty to the estimates.

The pre- and post-fire sedimentation analysis used landcover solely as a proxy for changes in soil erodibility, rainfall erosivity, and cover post fire. This allows for a rapid response in estimating sediment related issues post fire, but could be enhanced if soil erodibility and rainfall erosivity were incorporated. Additional research is needed to address these uncertainties, especially since lives are often at risk. In the meantime, wildfires will occur and methods need to be available to predict the expected flood response and sediment release from burned watersheds. This case study provides examples for simulation approaches that can be relatively rapidly deployed after a wildfire.

Acknowledgements

Appreciation is expressed to Dan Moore, Hydraulic Engineer, West National Technology Support Center, for peer review. Appreciation is also expressed to Rodney Clark, NRCS area engineer, and Beau Temple, NRCS soil conservation technician, for field data collection activities documenting channel condition for the modeled streams. Additionally, thanks to the FS for providing heat perimeter and soil burn severity mapping data.

References

Benavides-Solario, J.D., and L.H. MacDonald. 2001. Post-fire runoff and erosion from simulated rainfall on small plots, Colorado Front Range. Hydrological Processes, 15, 2931–2952.

Breiby, T. 2006. Assessment of soil erosion risk within a subwatershed using GIS and RUSLE with a comparative analysis of the use of STATSGO and SSURGO soil databases. Volume 8, Papers in Resource Analysis. Saint Mary's University of Minnesota Central Services Press. Winona, MN. 22 pages.

Capesius, J.P., and V.C. Stephens. 2009. Regional Regression Equations for Estimation of Natural Streamflow Statistics in Colorado. U.S. Department of Interior, U.S. Geological Survey, Scientific Investigations Report 2009–5136.

Chen, L., M. Berli, C. Karletta. 2013. Examining modeling approaches for the rainfall-runoff process in wildfire-affected watersheds: using San Dimas Experimental Forest. Journal of the American Water Resources Association 1-16.

Conedera, M., L. Peter, P. Marxer, F. Forster, D. Rickenmann, and L. Re. 2003. Consequences of forest fires on the hydrogeological response of mountain catchments: A case study of the Riale Buffaga, Ticino, Switzerland. Earth Surface Processes and Landforms 28, 117–129.

Dawen, T., K. Shinjiro, O. Tailkan, K. Toshio, and M. Katumi. 2003. Global potential soil erosion with reference to land use and climate changes. Hydrologic Processes 17, 2913–2928.

Desmet, P.J.J., and G. Grovers. 1996. A GIS procedure for automatically calculating the USLE LS-factor on topographically complex landscape units. Journal of Soil and Water Conservation 51(5):427–433.

Elliot, W.J., A.V. Elliot, W. Qiong, and J.M. Laflen. 1991. Validation of the WEPP model with rill erosion plot data, paper presented at the 1991 ASAE International Winter Meeting, Am. Soc. Of Agric. Eng., Chicago, IL, Dec. 1991.

Guobin, T., C. Shulin, and M.K. Donald. 2006. Modeling the impacts of no-till practice on soil erosion and sediment yield with RUSLE, SEDD, and ArcView GIS. Soil & Tillage Research 85, 38–49.

Hudak, A.T., P.R. Robichaud, J.S. Evans, J. Clark, K. Lannom, P. Morgan, and C. Stone. 2004. Field Validation of Burned Area Reflectance Classification (BARC) Products for Post Fire Assessment. Remote Sensing for Field Users: Proceedings of the Tenth Forest Service Remote Sensing Applications Conference, Salt Lake City, UT, April 5–9 2004.

Huffman, E.L., L.H. MacDonald, and J.D. Stednick. 2001. Strength and persistence of fire-induced soil hydrophobicity under ponderosa and lodgepole pine, Colorado Front Range. Hydrologic Processes, 15, 2877–2892.

Larsen, I. J., and L.H. MacDonald . 2007. Predicting postfire sediment yields at the hillslope scale: Testing RUSLE and Disturbed WEPP, Water Resources Res., 43 (W11412): 1–18.

Litschert, S.E., D.M. Theobald, and T.C. Brown. 2014. Effects of climate change and wildfire on soil loss in Southern Rockies Ecoregion. Catena 118, 206–219.

Maidment, D.R. 1992. Handbook of Hydrology McGraw-Hill, Inc.

McCuen, R.H. 1998. Hydrologic analysis and design. Second edition. Prentice-Hall, Inc., Upper Saddle River, NJ.

Miller, J.F., R.H. Frederick, and R.J. Tracey. 1973. Precipitation-Frequency Atlas of the Western United States. U.S. Department of Commerce, National Oceanic and Atmospheric Administration, National Weather Service, NOAA Atlas 2, Vol 3, Silver Spring, MD.

Nearing, M.A. 1997. A single continuous function for slope steepness influence on soil loss. Soil Science Society of America 61(3): 917–919.

Perica, S., D. Martin, S. Pavlovic, I. Roy, M. St. Laurent, C. Trypaluk, D. Unruh, M. Yekta, G. Bonnin. 2013. NOAA Atlas 14 Volume 8 Version 2, Precipitation-Frequency Atlas of the United States, Midwestern States. NOAA, National Weather Service, Silver Spring, MD.

Rallison, R.E. 1980. Origin and Evolution of the SCS Runoff Equation. Proceedings of the Symposium on Watershed Management; American Society of Civil Engineers, Boise, ID.

Renard, K.G., G.R. Foster, G.A. Weesies, D.K. McCool, and D.C. Yoder. 1997. Predicting soil erosion by water: A guide to conservation planning with the revised universal soil loss equation (RUSLE), Agric. Handb. 703, 404 pp., USDA, Washington, DC.

Renschler, C.S. 2003. Designing geospatial interfaces to scale process models: The GeoWepp approach, Hydrol. Processes, 17, 1005–1017.

Robichaud, P.R. 2000. F ire effects on infiltration rates after prescribed fire in northern Rocky Mountain forests, USA, J. Hydrol., 231–232, 220–229.

Stoof, C.R., R.W. Vervoort, J. Iwema, E. van den Elsen, A.J.D. Ferreira, C.J. Ritsema. 2011. Hydrological response of a small catchment burned by an experimental fire. Hydrology and Earth System Sciences Discussions 8, 4053–4098.

Theobald, D.M., D.M. Merritt, and J.B. Norman, III. 2010. Assessment of threats to riparian ecosystems in the Western U.S. A report presented to The Western Environmental Threats Assessment Center, Prineville, OR, by the USDA Stream Systems Technology Center and Colorado State University, Fort Collins, 61p.

Toy, T.J, and G.R. Foster, co-editors. 1998. Guidelines for the use of the Revised Universal Soil Loss Equation (RUSLE) version 1.06 on mined lands, construction sites, and reclaimed lands. Office of Surface Mining and Reclamation (OSM). Western Regional Coordinating Center, Denver, CO.

USDA-NRCS (Department of Agriculture-Natural Resources Conservation Service), 2004a. NRCS National Engineering Handbook, Part 630 Hydrology, Chapter 9, Hydrologic Soil Cover Complexes.

USDA-NRCS (Department of Agriculture-Natural Resources Conservation Service), 2004b. NRCS National Engineering Handbook, Part 630 Hydrology, Chapter 10, Estimation of Direct Runoff from Storm Rainfall.

USDA-NRCS (Department of Agriculture-Natural Resources Conservation Service), 2010. NRCS National Engineering Handbook, Part 630 Hydrology, Chapter 15, Time of Concentration.

USGS (U.S. Geological Survey) National Gap Analysis Program. 2004. Provisional digital land cover map for the Southwestern United States. Version 1.0. RS/GIS Laboratory, College of Natural Resources, Utah State University.

Winchell, M.F., S.H. Jackson, A.M. Wadley, and R. Srinivasan. 2008. Extension and validation of a geographic information system-based method for calculating the Revised Universal Soil Loss Equation length-slope factor for erosion risk assessments in large watersheds. Journal of Soil and Water Conservation 63(3): 105–111.

Woodward, D., R. Hawkins, R. Jiang, A. Hjelmfelt, Jr., J. Van Mullem, and Q. Quan. 2003. Runoff Curve Number Method: Examination of the Initial Abstraction Ratio. World Water & Environmental Resources Congress 2003: pp. 1–10.

Yochum, S., and J. Norman. 2014. West Fork Complex Fire: Potential Increase in Flooding and Erosion. USDA Natural Resources Conservation Service, Colorado State Office, Denver, CO.

Appendix D: Case Study 4:
Whitewater Creek, Gila Wilderness, New Mexico

Background

Lightning sparked several outbreaks of wildfires in May 2012 that joined to become the largest in New Mexico's recorded history. Lack of road access and the steep terrain of the Gila Wilderness (fig. D–1) hampered containment efforts, allowing the individual fires to grow rapidly. By the end of May, they had become one large wildfire known as the Whitewater-Baldy Complex.

The rugged landscape was not the only reason these fires escaped control. The watershed had already been under extreme drought conditions, with the two previous winters recording very low snowfall. Air temperatures at the time of the outbreak were well above average, and high winds contributed to the merging of the fires. In early June, the Whitewater-Baldy Complex was only about 18 percent contained. By mid-June containment increased to 56 percent. For about 3 months, the wildfire burned Ponderosa, Pinon-Juniper, and mixed conifer forests with relatively low burn temperatures. Rainfall in mid-July finally helped fire fighters gain momentum, with 95-percent containment attained in late July.

The wildfire had burned about 465 square miles (fig. D–2, D–3 and D–4). The USDA Forest Service (FS) estimated the final burn severity to be 14 percent high, 12 percent moderate, 55 percent low or unburned, and 20 percent unknown (due to inadequate satellite imagery).

This case study presents a hydrologic analysis of the flood potential of Whitewater Creek and possible hazard to the community of Glenwood, NM. As shown in figure D–5, Glenwood is located near the confluence of Whitewater Creek and the San Francisco River. Considering the drainage area upstream of Glenwood, the percent of the watershed burned was 34 percent high severity, 21 percent medium severity, and 13 percent low severity.

Figure D–1 Burned trees near Hummingbird Saddle, Gila National Forest

Photo by Mike Sanders, USGS

NRCS Involvement

The NRCS Emergency Watershed Protection (EWP) Program was implemented for the installation of monitoring gages in the Whitewater-Baldy Complex burn area, to provide early warning to downstream communities of flood potential. The intensity of the wildfire and its large area prompted the FS, in cooperation with the U.S. Geological Survey (USGS), to seek EWP funding from NRCS. The NRCS New Mexico State office worked with the New Mexico Department of Homeland Security and Emergency Management, which acted as the EWP local sponsor.

Figure D–2 New Mexico county boundaries. National forest in green, wilderness area in yellow (inset shown in fig. D–3)

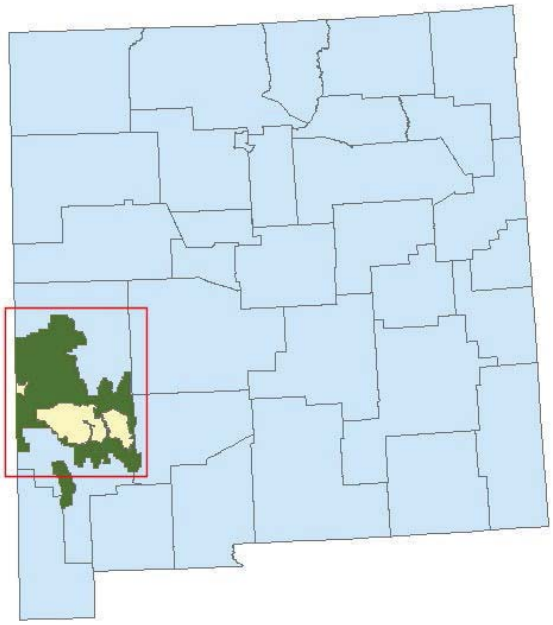

Figure D–3 Gila wilderness in yellow, Whitewater-Baldy complex fire extent in red (inset shown in fig. D–4

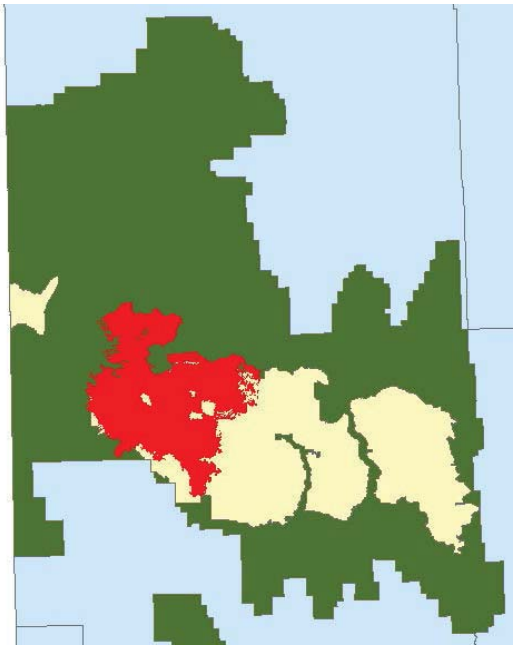

Figure D–4 Local area, with fire extent in red, nearby communities, and highways

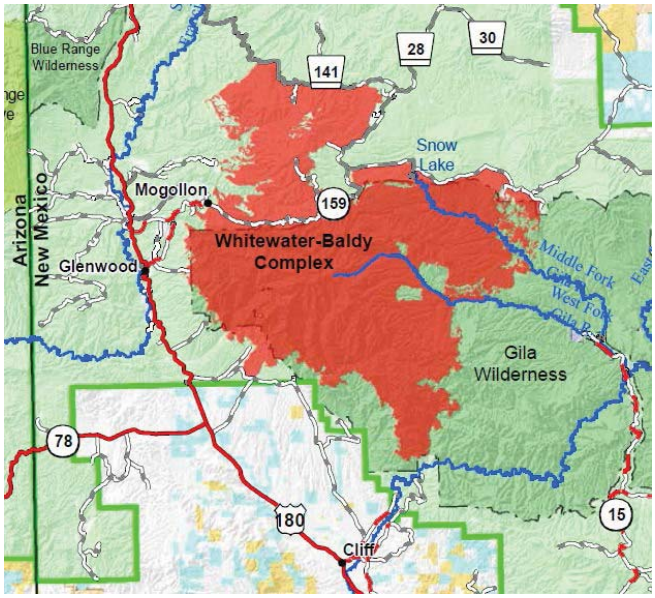

Map provided by the USGS Gila National Forest

Figure D–5 Whitewater Creek watershed and the community of Glenwood, NM

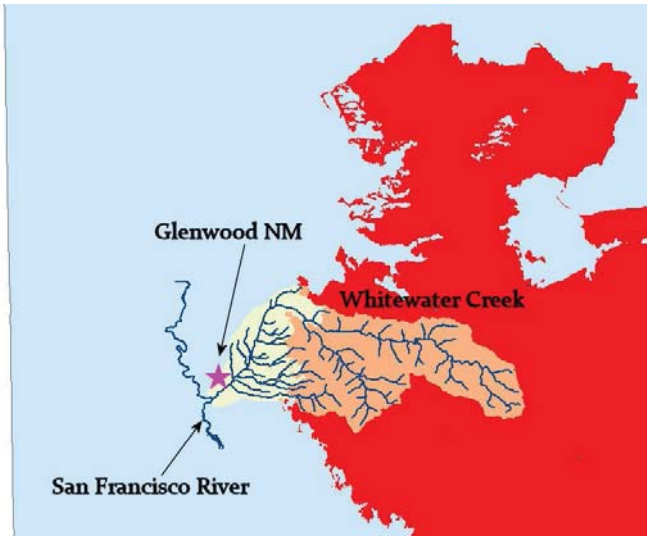

USGS installed a streamflow gage on Whitewater Creek, near the Catwalk Recreational Area (fig. D–6). That station also received a precipitation gage. The existing NRCS Snotel site is shown in figure D–6, along with additional newly installed gages.

NRCS performed a hydrologic analysis to assess flood potential for the community of Glenwood. In recent years, New Mexico residents had witnessed flash flooding after wildfire. The watersheds of the 2011 Las Conchas fire near Los Alamos experienced monsoon rains within weeks of the end of the fire, which sent floodwater, sediment, and debris rapidly downstream. That wildfire burned 245 square miles and held the record for the largest in recorded New Mexico history, until eclipsed by the Whitewater-Baldy Complex wildfire, which was almost twice as large.

The FS, through the BAER team process, also provided a hydrologic assessment. In addition, the USGS held a workshop in early July 2012 for Glenwood residents to learn how to access the early warning data from the new gages. The data are on the Web from USGS New Mexico.

The NRCS hydrologic modeling effort, documented in this case study, examined pre-fire floods and post-fire floods, both immediately after the fire and 1 year later. Data from the newly installed precipitation and streamflow gages was used to verify that the hydrologic model produced reasonable results.

Figure D–6 Gages in the vicinity of Whitewater Creek

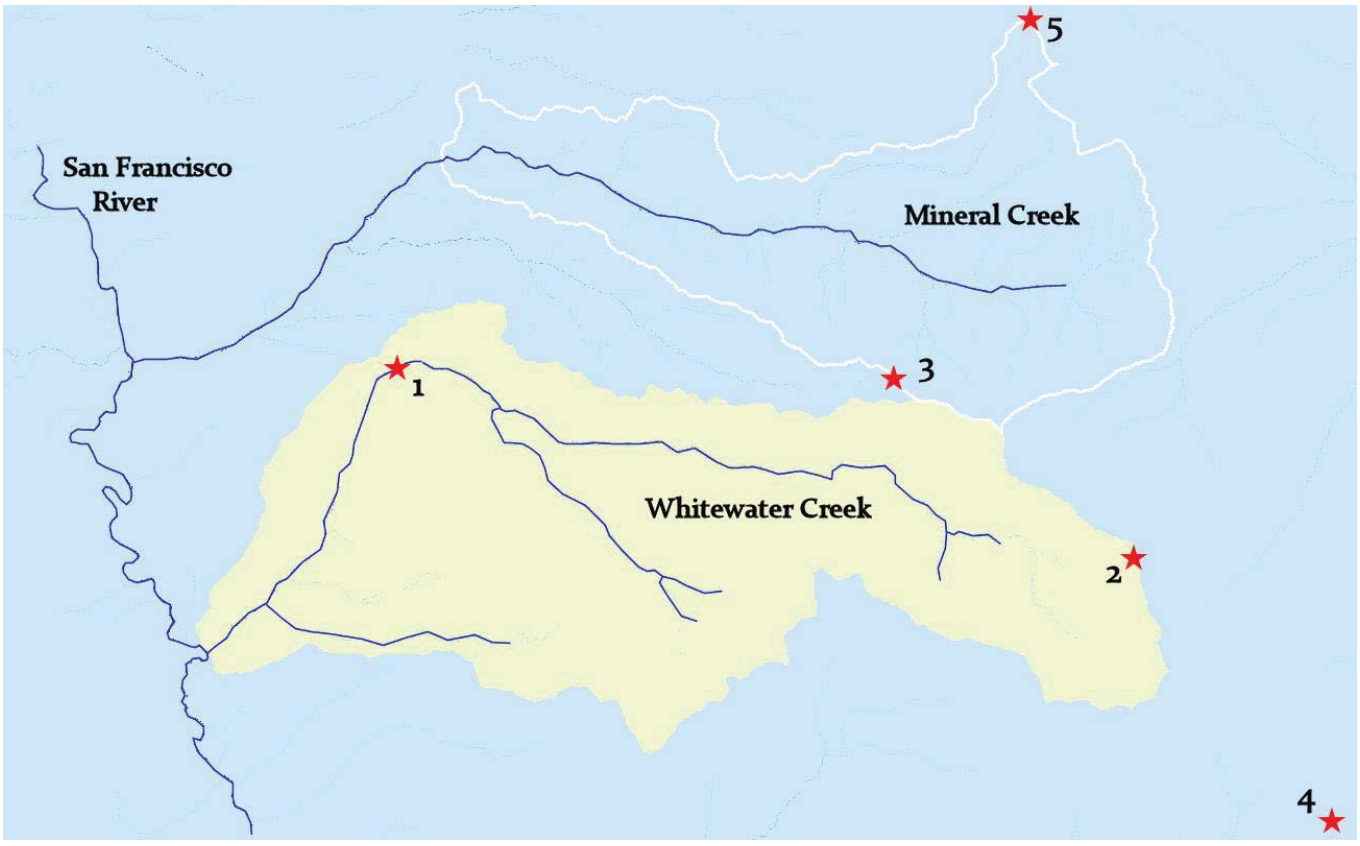

1 = Catwalk streamflow and precipitation (activated 4 July 2012 by USGS)
2 = Hummingbird Saddle precipitation (activated 29 June 2012 by USGS)
3 = Silver Creek Divide SNOTEL site (activated 1 Oct 1978 by NRCS)
4 = Mogollon Baldy Lookout precipitation (activated 28 June 2012 by USGS)
5 = Bear Wallow Lookout precipitation (activated 29 June 2012 by USGS)

Methods and Application

As an alternative to the often-used runoff curve number (CN) method, this case study modeled infiltration of rainfall by the process-based Green and Ampt (GA) method. Both the CN and GA methods are discussed in the main body of this technical note. These two methods are not strictly comparable, since the CN runoff equation accounts for more phenomena than infiltration. These include losses due to transpiration and surface ponding, which, if using GA, must be modeled separately.

In this case study, runoff transformation was also performed differently than the NRCS dimensionless unit hydrograph (UH). The standard NRCS UH peak rate factor of 484, determined with equation 9 in the technical note, is often too low for mountain streams. Title 210, National Engineering Handbook, Part 630, Hydrology, Chapter 15 (USDA-NRCS 2010), provides dimensionless unit hydrographs for peak factors up to 600, which may be used in the hydrology program WinTR-20. Peak factors in mountain watersheds may tend toward the higher end of this spectrum, and the effect of wildfire to drive them up further.

Although runoff transformation for Whitewater Creek also used the unit hydrograph technique, the shape and peak of the UH were determined with time-area histograms. Neither peak factor nor time of concentration were needed. The hydrology model HEC-HMS (USACE-HEC 2013) accepts input of user-derived unit hydrographs, as well as the GA infiltration method. The following list summarizes the modeling options used in this case study:

- Choice of hydrologic computer model—HEC-HMS (USCOE-HEC 2013)
- Runoff transformation—synthetic UH derived by GIS analysis of time-area histograms
- Infiltration loss method—GA equation
- Initial abstraction, ponding—estimates of loss due to vegetation canopy, surface detention
- Baseflow—pre-flood estimates based on subarea size, post-flood estimates based on exponential recession curve
- Rainfall events examined—2-year, 25-year, and 100-year, under three scenarios (pre-fire, post-fire immediately, and post-fire 1 year later)
- Sediment bulking estimated

Choice of Hydrologic Computer Model: HEC-HMS

The model HEC-HMS (USACE 2013) features many options for estimating flood hydrographs. The runoff transformation options include the NRCS dimensionless UH, with the latest version providing selection of peak factors other than the standard 484. Additional synthetic UH options are the Snyder and Clark UHs, which require some form of peaking factor estimation. This case study demonstrates a user-derived synthetic unit hydrograph, in the S curve format. (See fig. D–7 for the HEC-HMS input window, which summarizes the modeling options.)

The Whitewater Creek watershed upstream of Glenwood, NM, is shown in figure D–8. For each of the 41 subareas shown, a GIS time-area analysis was performed. More detail is provided for a single subbasin (fig. D–9, the red inset of fig. D–8)

Time-Area Histogram and Synthetic UH Estimation

Determining runoff depth over time at the outlet of a given subarea requires an estimate of flow travel time from every part of the drainage area. Even small subareas vary considerably in flow slopes, flow cross-sectional areas, and surface roughnesses. Travel time computation requires spatial accounting of these variables as they affect flow velocity, and then the accumulation of time as flows with these varying velocities traverse the distances to the outlet.

Figure D–7 HEC-HMS input window for modeling options in a single subbasin

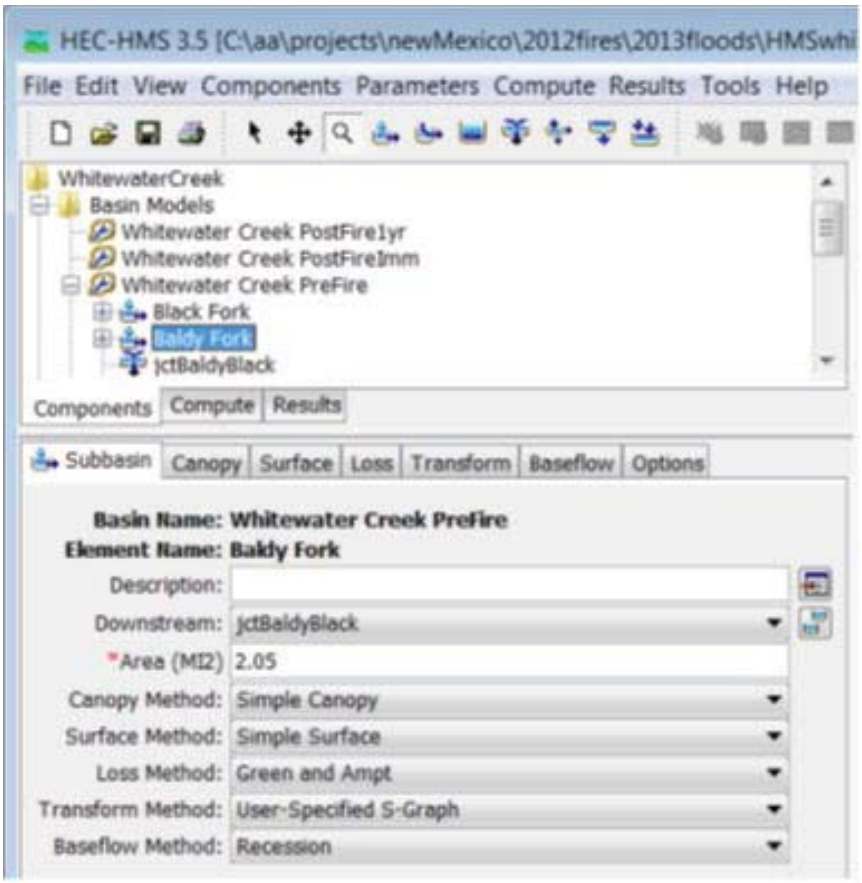

Figure D–8 Whitewater Creek hydrologic subareas

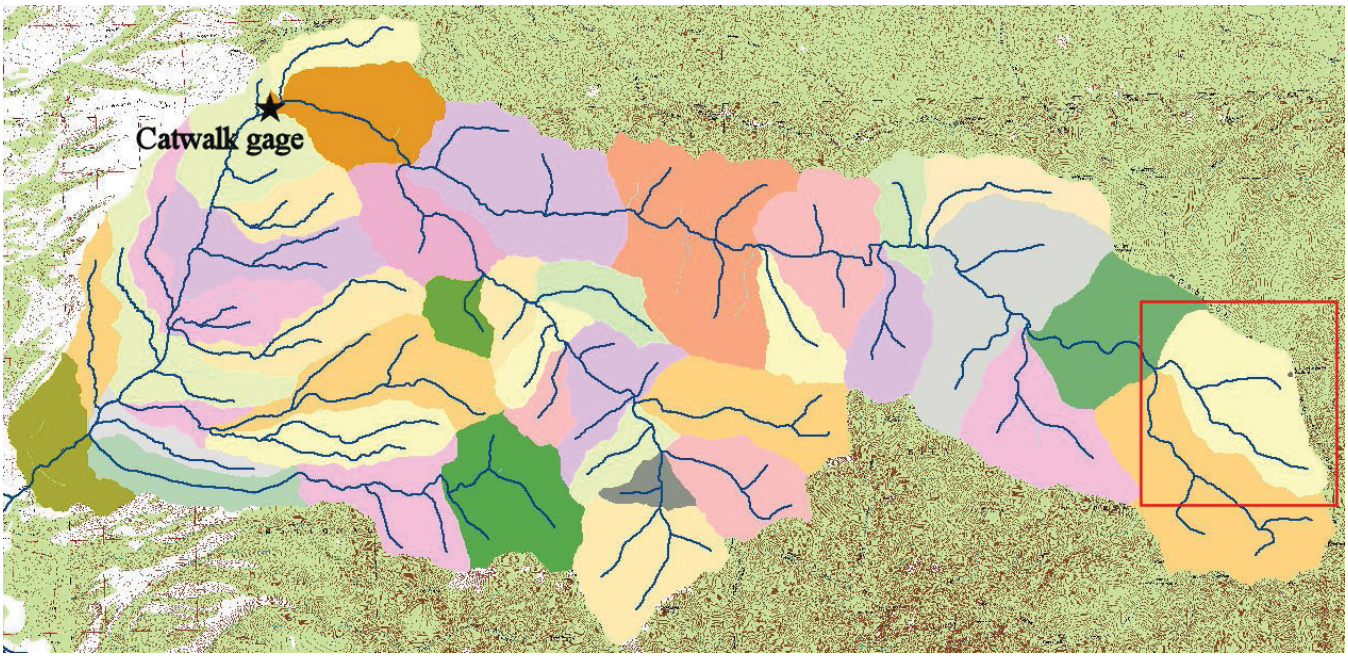

Given the three standard flow segment types (overland, shallow-concentrated, and stream channel), equations and tables from the technical note on the velocity method may be used. A time-area histogram, however, requires not merely time of concentration, but flow time estimation from many subdivisions of the drainage area. Such an analysis is greatly facilitated by the use of GIS.

To develop a time-area histogram for Baldy Fork (fig. D–9) using GIS, the flow time from each GIS raster cell in the subarea to the outlet was determined. The cells were grouped into 5-minute time bands. Flow velocity in each cell depended on whether the flow segment type was primarily overland, shallow-concentrated, or stream channel. Within these segment types, surface roughness was specified. To create a unit hydrograph the time band GIS attribute data was copied into a spreadsheet, as will be detailed below.

Roughness in GIS

The land roughness was determined, given pre-fire land cover and post-fire burn severity, as shown in tables D–1 through D–3. For typical overland and shallow-concentrated flow roughness values, see tables 10 and 11 in this technical note, respectively. Three roughness rasters were created, one for each fire condition. The raster grid sizes, based on the available digital elevation model (DEM) were 10 meters square.

Figure D–9 Upper Whitewater subarea (called “Baldy Fork”)

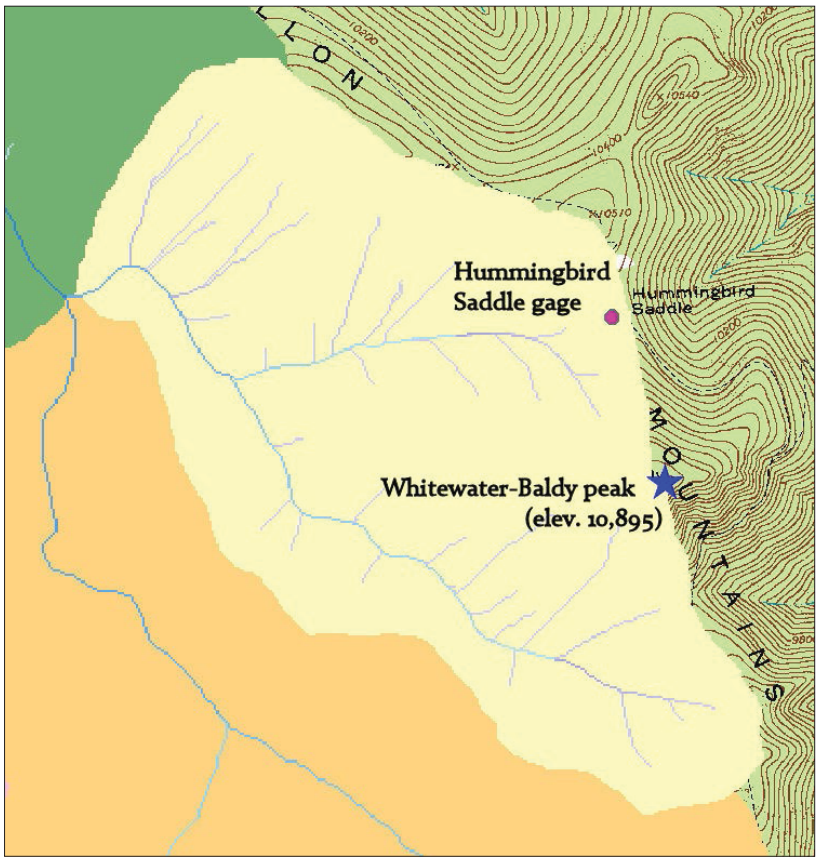

Table D–1 Pre-fire roughness assumptions

Flow segment	Land-use assumptions	*n* value
Overland	Grass, short-grass prairie	0.15
Shallow-concentrated	Steep, rocky, less depth flow	0.08
Channel	Steep, rocky, less debris	0.045

Table D–2 Post-fire (immediately) roughness assumptions

Flow segment	Land-use assumptions	n value
Overland	Bare ground (severe, moderate burn)	0.011
	Bare ground (low burn)	0.08
	Bare ground (no burn)	0.15
Shallow-concentrated	Steep, rocky, more depth flow	0.06
Channel	Steep, rocky, more debris	0.05

Table D–3 Post-fire (1 year) roughness assumptions

Flow segment	Land-use assumptions	n value
Overland	Bare or short grass (severe, moderate burn)	0.03
	Bare or short grass (low burn)	0.10
	Bare or short grass (no burn)	0.15
Shallow-concentrated	Steep, rocky, more depth flow	0.06
Channel	Steep, rocky, more debris	0.05

To set the flow segment type of each raster cell, the typical GIS hydrologic function flow accumulation was used. In GIS, the flow accumulation value of each cell is the number of cells upstream of it (which therefore drain to it). The flow segment type for each 10-meter square cell was determined using the following assumptions:

- Overland flow extends for about the first 100 feet of drainage (three cells).
- Shallow-concentrated flow extends for the next 1,000 feet (thirty cells).
- Channel flow is assumed for any flow accumulation more than 33 cells.

These GIS operations are performed with the raster calculator in ArcMap (ESRI 2010). An example of a raster calculator command is shown in figure D–10, circled in red. Note that the function *Con* is short for *Conditional* (an *if* statement). Given the flow accumulation layer *flowAcc*, the command may be translated into plain English, as follows: "If *flowAcc* is less than or equal to three (an overland flow segment) then set the roughness to 0.15. Otherwise, if *flowAcc* is less than or equal to 33 (a shallow-concentrated flow

segment), set roughness to 0.08. If neither of those two conditions exists (*flowAcc* is greater than 33, a channel flow segment), then set the roughness to 0.045. Note in figure D–10 that the output raster is named "roughPreFire".

To assess the burn condition of each raster cell, the burn severity shape file provided by FS was transformed into a raster layer within GIS. In that layer, (fig. D–11) each cell with a high severity is assigned the number 4, medium 3, low 2, and unburned 1. For the pre-fire condition, using the data in table D–1, the ArcMap raster command is shown in figure D–10. Note that the roughness layers may be created for the entire watershed, not each subarea separately.

For the condition immediately post-fire, using table D–2, the raster command slightly more complicated:

Con("rufPreFire" == 0.08,0.06,Con("rufPreFire" == 0.045,0.05,Con("burnRaster" >= 3,0.011,Con("burnRaster" == 2,0.08,"rufPreFire"))))

In plain English, this command says, "If the roughPreFire cell is 0.08 (i.e., a shallow-concentrated flow cell) then set the roughness to 0.06, otherwise, if the cell in roughPreFire is 0.045 (i.e., a channel cell) then set the roughness to 0.05. If neither of those conditions is true, then if the burn raster cell is greater than or equal to 3 (moderate or severe) then set the roughness to 0.011; otherwise, if the burn raster cell is 2, then set the roughness to 0.08. Finally, if none of those conditions is true, then set the new raster value to the same as the old raster value (unburned overland flow cells).

Figure D–10 ArcMap raster calculator expression creating a pre-fire roughness layer

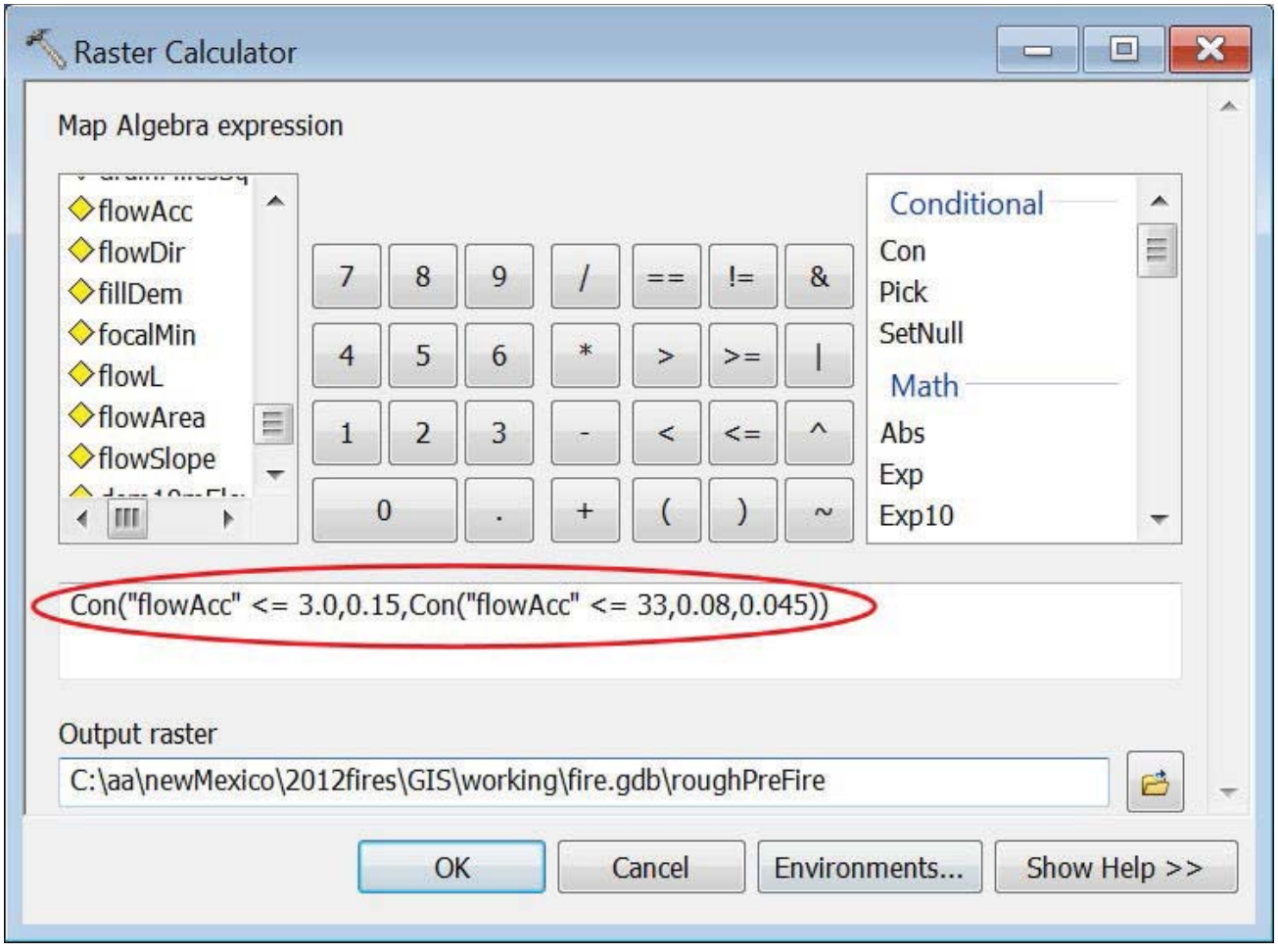

Flow Slope in GIS

ArcMap (ESRI 2010) has a surface slope function that does not produce flow slope because it uses average elevations in a raster cell neighborhood. To obtain flow slope for each cell, the required information is elevation drop from that cell to the lowest neighbor, and the flow length between the two cells. Since flow in a three-by-three neighborhood of cells (fig. D–12) may be either straight or diagonal, the flow length is one of two values. To create a flow distance raster in feet, given a 10-meter DEM, the two length values are either 46.40 feet (diagonal) or 32.81 feet. Figure D–12 shows the cell values created by the hydrology command *flow direction*. The following raster command to obtain flow length examines the flow direction raster for whether the flow is straight or diagonal:

```
Con("flowDir" == 1,32.81,Con("flowDir" == 4,32.81,Con("flowDir" == 16,32.81,Con("flowDir" == 64,32.81,46.4))))
```

Figure D–11 Burn raster (Red = High, Orange =Medium, Yellow = Low, Green = No Burn)

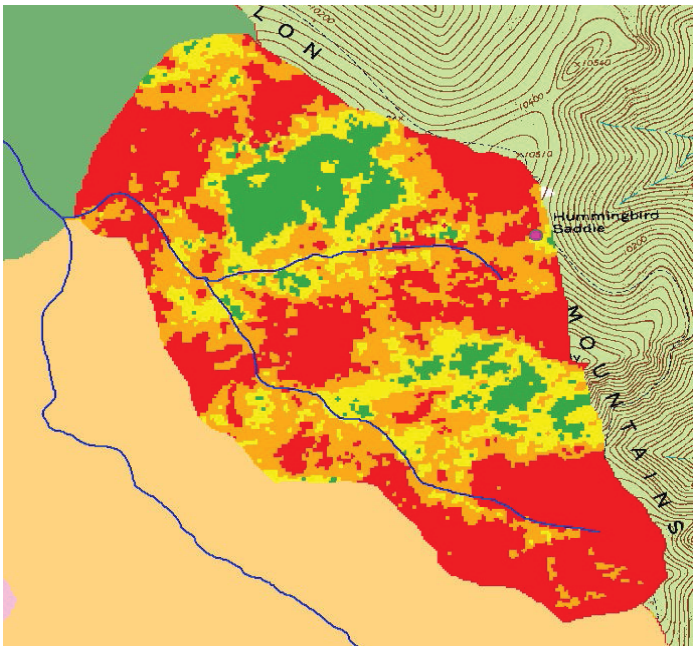

Figure D–12 Flow directions codes

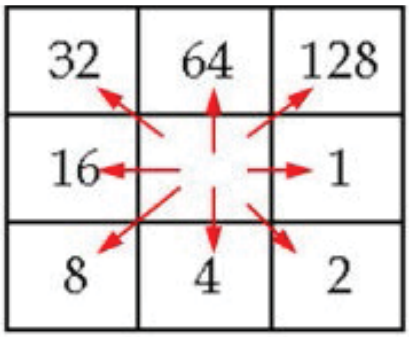

To obtain elevation difference, the ArcToolbox function "Focal Statistics" may be used. Among the available statistics is the elevation drop to the lowest neighbor. Then a flow slope raster is obtained with a raster calculation dividing that elevation difference by the flow length. One final procedure is to prevent zero slopes by evaluating the flow slope raster and setting any zeroes to some minimum value.

Velocity Relationship Derivations

In addition to the velocity methods discussed in the technical note, other references such as USACE (2013) and MacArthur and DeVries (1993) discuss flow velocity calculations for different channel segment types. Considered in the general category of *kinematic wave routing*, these techniques transform Manning's equation into the general form shown in equation 1, where y is flow depth in feet, a is flow cross-sectional area in square feet, S is flow slope, and n is Manning's roughness coefficient:

$$Q = ay^{5/3} \qquad \text{where—} \quad a = \frac{1.486\sqrt{S}}{n} \qquad \text{eq. D–1}$$

Given possible flow areas, often estimated by assuming a flow width, equation D–1 can, for overland flow, be formulated as equation D–2:

$$V_{overland} = \frac{\phi\sqrt{S}}{n} \qquad \text{where:} \quad \phi = \frac{1.486y^{2/3}}{w} \qquad \text{eq. D–2}$$

Note that the velocity equations in technical note table 11 are also given in this form. Table D-4 shows the range of phi values for overland flow.

Table D–4 Values of φ, given assumptions of overland flow width and depth

y *(in)*	*W* *(ft)*	*φ*
0.25	2.0	0.056
0.25	2.5	0.045
0.25	3.0	0.038
0.25	3.5	0.032
0.25	4.0	0.028
0.50	2.0	0.089
0.50	2.5	0.071
0.50	3.0	0.060
0.50	3.5	0.051
0.50	4.0	0.045

For shallow-concentrated flow (collector channels), assuming a triangular channel shape, MacArthur and DeVries (1993) develop an equation in the same form (eq. D–3).

$$V_{shallow} = \frac{\phi\sqrt{S}}{n} \qquad \text{where—} \qquad \phi = 0.94A^{1/3}\left(\frac{z}{1+z^2}\right)^{1/3} \qquad \text{eq. D–3}$$

Table D–5 shows the range of phi values for shallow-concentrated flow, given side-slope *z* in length horizontal divided by length vertical.

Table D–5 Shallow-concentrated flow parameters

Y *(ft)*	*Z* *(H:V)*	*φ*
0.5	3	0.572
0.5	4	0.580
0.5	5	0.584
1.0	3	0.908
1.0	4	0.921
1.0	5	0.928

For channel flow segments, assuming a trapezoidal shape, MacArthur and DeVries (1993) developed an equation of similar form, but more complicated because trapezoidal flow area is dependent on both channel bottom width and side slopes, in addition to depth. Since the equation is also being applied to various locations in a watershed, the flow area increases with drainage area. In kinematic wave routing models, the flow depth and area are computed along the channel, with a time-step change in flow depth. For a time-area histogram, an overall velocity for each cell is needed, regardless of what time during a storm. (Recall the UH assumption that the time is independent of the depth of direct runoff.)

One way to estimate flow area for any given GIS raster cell is to use regional regression equations, if available. For many areas of the country equations which relate bankfull flow area to watershed area have been developed. For the Gila Wilderness region Moody, Wirtanen, and Yard (2003) derived the following:

$$A = 4.78B^{0.512} \qquad r^2 = 0.9163 \qquad \text{eq. D–4}$$

where— A = flow cross-sectional area (ft^2) B = watershed area (mi^2)

Although the equation has a relatively high correlation, the authors included their data, which shows that many much larger watersheds were used than the subarea sizes within Whitewater Creek. To obtain a more applicable equation for such small subareas the authors' data was culled for only the small watershed sizes, 23 total, and the following equation derived, for use in Whitewater Creek (where A and B are as defined above):

$$A = \exp\left(0.5036 \ln B + 1.595\right) \qquad r^2 = 0.88 \qquad \text{eq. D–5}$$

Having channel cross-sectional area is not enough information to estimate velocity using the MacArthur and DeVries trapezoidal equation, unless further simplifying assumptions are made about how flow width and depth vary. By assuming that, for smaller mountain channels, flow velocity can be estimated from a rectangular flow area with a width-depth ratio of two, equation D–6 can be used.

$$V_{channel} = \frac{0.94\sqrt{S}}{n} A^{0.257} \qquad \text{with } A \text{ from regional regression} \qquad \text{eq. D–6}$$

Velocity Relationships Used in Whitewater Creek

Variations in estimated flow depth have a relatively minor effect on velocity, especially in comparison to the effect of roughness. For Whitewater Creek, overland flow depth was assumed 0.25 inches, width 3 feet. With these assumptions, equation D–2 becomes equation D–7 below:

$$V_{overland} = \frac{0.038\sqrt{S}}{n} \qquad \text{eq. D–7}$$

For the shallow-concentrated flow segments, depth was assumed to be 0.5 feet and z was assumed to be 4, which yields (from eq. D–3 and table D–5) equation D–8:

$$V_{collector} = \frac{0.58\sqrt{S}}{n} \qquad \text{eq. D–8}$$

For the channel flow segments, a separate raster layer for flow cross-sectional area was obtained using equation D–5. Then, channel velocity was estimated using equation D–6.

When creating the velocity rasters, the possibility exists that velocity will come out unreasonably high due to very steep slopes, such as vertical drops, or zero due to flat slopes. A better travel time estimate was obtained for Whitewater Creek by restricting the maximum and minimum velocities to 15 and 0.10 feet per second, respectively.

Travel time in GIS

In ArcGIS, the hydrology tool Flow Length is used to obtain the flow travel time of any cell to its outlet. This is possible because the tool can apply an optional weight raster, which may contain such parameters as unit conversions and channel sinuosity, as shown in equation D–9. The time in minutes is obtained using a weight raster that includes a sinuosity of 1.1, a conversion of meters to feet (since the tool is using the 10m DEM), and from seconds to minutes.

$$time = flowLength * weight$$

$$\text{where— } weight = \frac{1.1 * 3.28083}{flowVelocity * 60} \qquad \text{eq. D–9}$$

The resulting time raster can then be reallocated to group the cells into time bands of, say, 5 minutes. The 5-minute time band raster for Baldy Fork subarea is shown in figure D–13.

The attribute table shows the number of cells in each of 21 time bands in Baldy Fork. Since there are 21 5-minute bands the longest drainage time (or time of concentration) may be estimated at 1 hour and 45 minutes. However, the hydrologist can note the number of cells in those later time bands. Sometimes they become so few that a better estimate of time of concentration is taken to be earlier. For Baldy Fork, one might select timeband 18, or 90 minutes, because later time bands have only a total of 61 cells among them. Note that a separate travel time raster is produced for the three scenarios, pre-fire, post-fire immediately, and post-fire after 1 year.

Figure D–13 Twenty-one 5-minute travel time bands for Baldy Fork, with attribute table

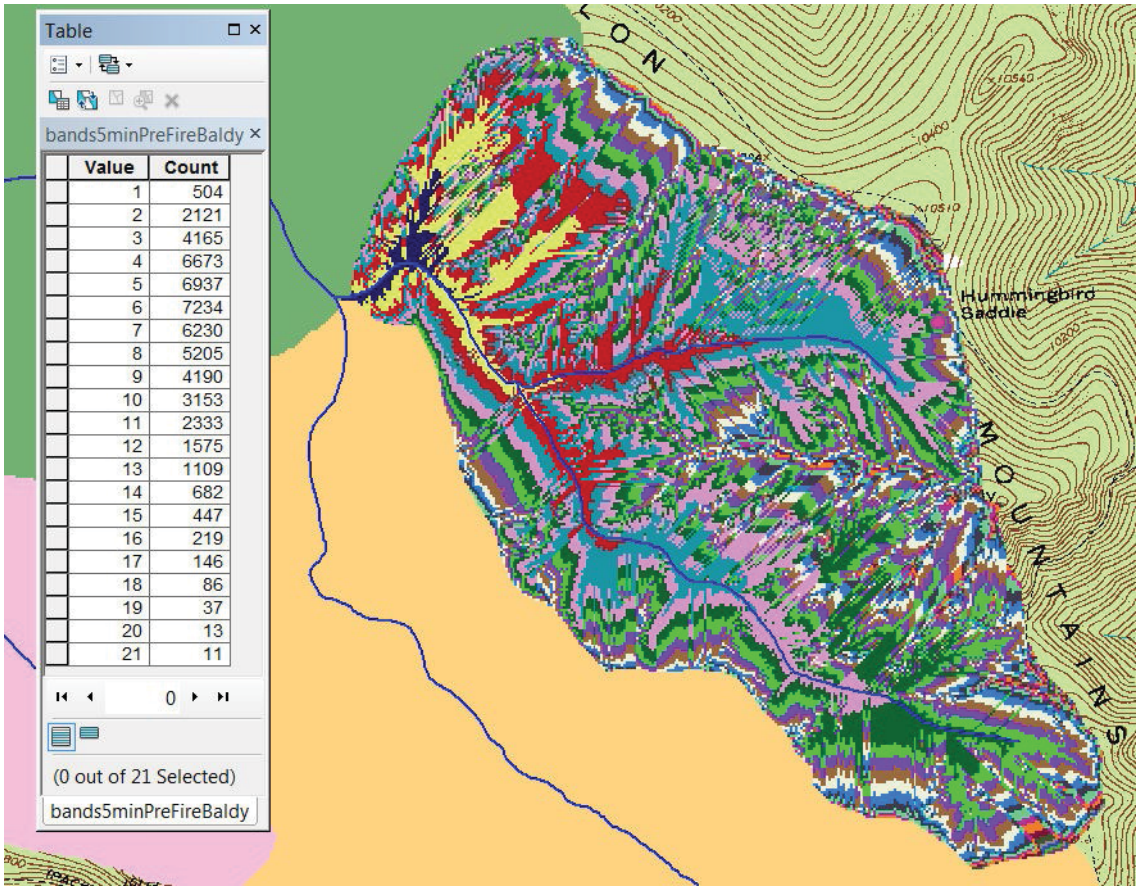

Spreadsheet Derivation of Time-Area Histogram and Unit Hydrograph

To obtain a time-area histogram the 5-minute time band attribute table is copied into a spreadsheet. This procedure is described in many hydrology textbooks, including Bedient, Huber, and Vieux (2012). Since the cells are 100 square meters each, the area drained by each time band can be converted to any convenient unit, such as acres, in the spreadsheet. The resulting time-area histogram for Baldy Fork pre-fire is shown in figure D–14. To obtain a unit hydrograph, a duration must be chosen and 1 inch of effective rainfall applied within that time frame. The runoff from each time band is computed, lagged, and summed.

A screenshot of the spreadsheet is shown in figure D–15. The flow values in column G, in acre-inches, are obtained by summing the lagged flow values in columns K through P. Those flow values are obtained by multiplying the 5-minute increment of effective rainfall (0.167 inches) by the area in acres of each time band (from the GIS attribute table, column B). Then, in column H, the flow is converted to cfs. The 30-minute unit hydrograph peak (cell H14) is 1817 cfs, the peak that would be expected from Baldy Fork if 1 inch of effective rainfall was evenly distributed over the subarea in 30 minutes. Figure D–16 shows the 30-minute unit hydrographs for Baldy Fork under the three scenarios.

Figure D–14 Pre-fire time-area histogram for Baldy Fork

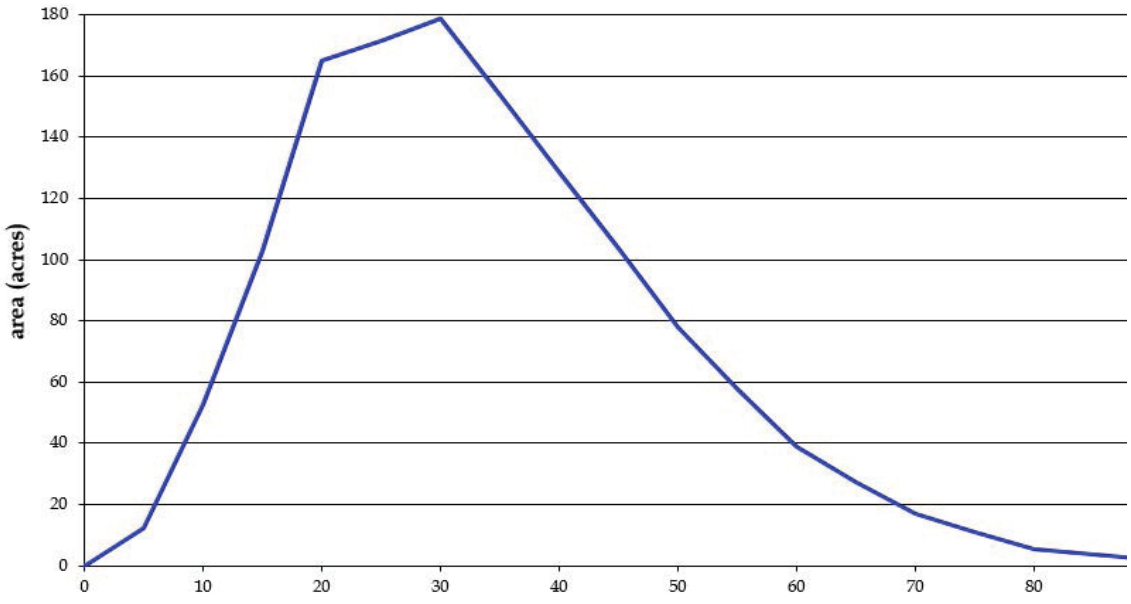

Figure D–15 Pre-fire spreadsheet (30-minute unit hydrograph in column H)

BaldyCkUH.xlsx - Excel

	A	B	C	D	E	F	G	H	I	J	K	L	M
1	time	timeband	5	cellsize	100	UH	0.5						
2	to outlet	cells	area	area		time	flow	flow	rainfall	area	time --------->		
3	(min)	(#)	(ac)	(m^2)		(min)	(ac-in/timeband)	(cfs)	(in)	(ac)	5	10	15
4	histogram	preFire					30-min UH:		1.0000				
5	0	0	0	0		0	0.00	0.00	0.16667	0.00			
6	5	504	12.5	50400		5	2.08	25.12	0.16667	12.45	2.08		
7	10	2121	52.4	212100		10	10.81	130.81	0.16667	52.41	8.74	2.08	
8	15	4165	102.9	416500		15	27.96	338.37	0.16667	102.92	17.15	8.74	2.08
9	20	6673	164.9	667300		20	55.45	670.91	0.16667	164.89	27.48	17.15	8.74
10	25	6937	171.4	693700		25	84.02	1016.60	0.16667	171.42	28.57	27.48	17.15
11	30	7234	178.8	723400		30	113.81	1377.09	0.16667	178.76	29.79	28.57	27.48
12	35	6230	153.9	623000		35	137.39	1662.44		153.95	25.66	29.79	28.57
13	40	5205	128.6	520500		40	150.09	1816.12		128.62	21.44	25.66	29.79
14	45	4190	103.5	419000		45	150.20	1817.37		103.54	17.26	21.44	25.66
15	50	3153	77.9	315300		50	135.70	1641.96		77.91	12.99	17.26	21.44
16	55	2333	57.7	233300		55	116.74	1412.53		57.65	9.61	12.99	17.26
17	60	1575	38.9	157500		60	93.43	1130.52		38.92	6.49	9.61	12.99
18	65	1109	27.4	110900		65	72.34	875.32		27.40	4.57	6.49	9.61
19	70	682	16.9	68200		70	53.71	649.93		16.85	2.81	4.57	6.49
20	75	447	11.0	44700		75	38.30	463.40		11.05	1.84	2.81	4.57
21	80	219	5.4	21900		80	26.21	317.19		5.41	0.90	1.84	2.81
22	85	146	3.6	14600		85	17.21	208.20		3.61	0.60	0.90	1.84
23	90	86	2.1	8600		90	11.07	134.00		2.13	0.35	0.60	0.90

dataPreFire | histogramPreFire | 30min UH | S curve | dataPostFireImm

Figure D–16 Unit hydrographs, 30-minute duration for Baldy Fork

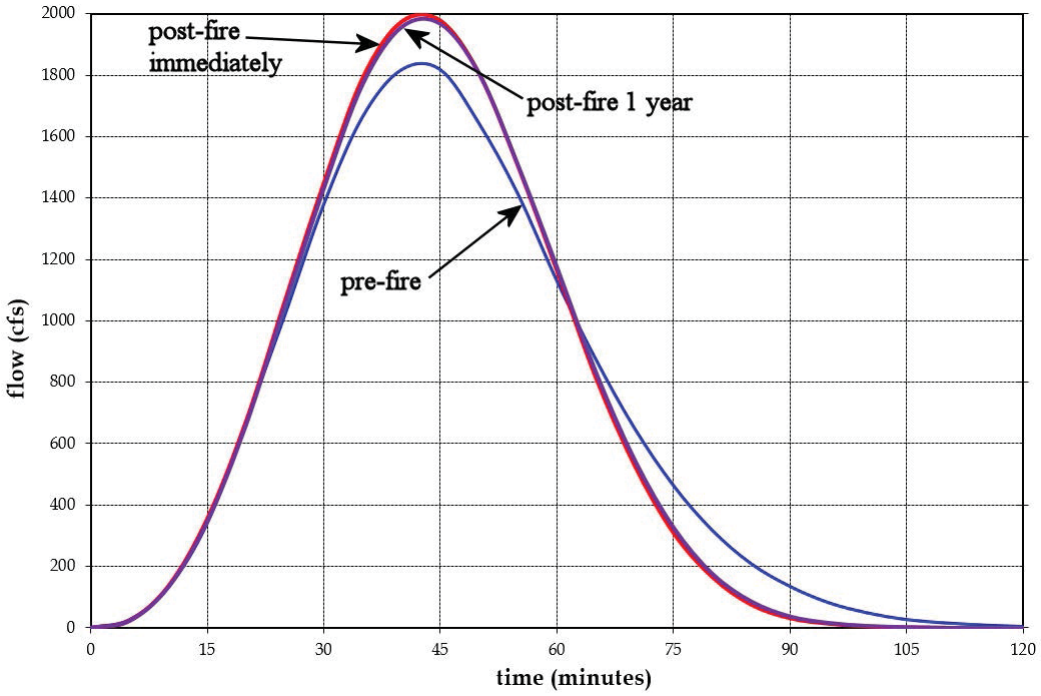

The 30-minute unit hydrograph is applicable when the duration of excess rainfall from a given event is 30 minutes long. To enable a unit hydrograph compilation to apply for any duration of excess rainfall, a so-called S-curve is derived by lagging the 30-minute unit hydrographs in successive 30-minute periods, as shown in figure D–17.

Figure D–17 S-curve from lagged and summed 30-minute unit hydrographs

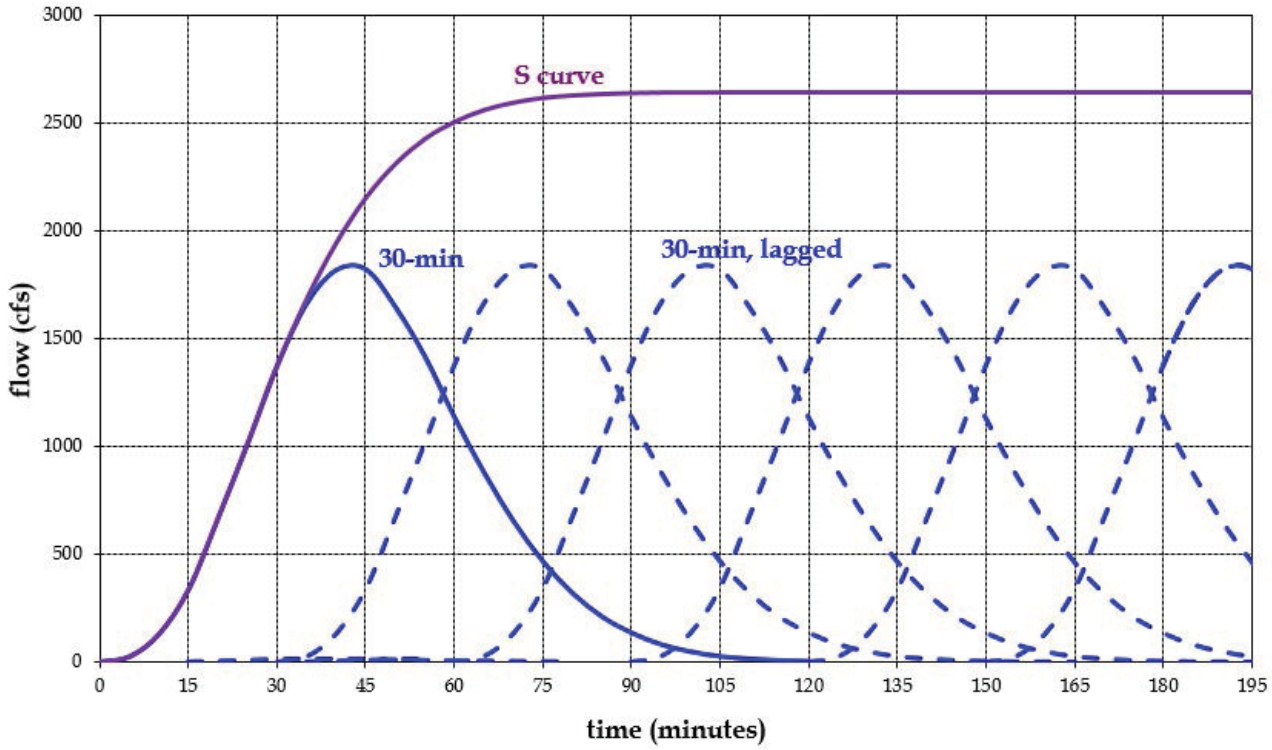

The maximum of the S-curve is the *unit flow* for the subarea—the amount of runoff if a full inch of effective rainfall runs off the entire watershed area in 30 minutes. In the case of Baldy Fork, since the total area is 57,124,070 square feet the unit flow is—

$$\frac{57{,}124{,}070\ ft^2 \times 1\ in}{30\ min} \times \frac{1\ ft}{12\ in} \times \frac{1\ min}{60\ sec} = 2{,}644\ cfs$$

The hydrology model HEC-HMS requires the S-curve to be given as a percent of lag versus percent of unit flow. Watershed lag is the time from the center of the effective rainfall duration to the runoff peak. The lag for Baldy Fork can be seen from the 30-minute unit hydrograph, figure D–16, to go from 15 minutes (center of rainfall) to 45 minutes (peak) or 30 minutes. The S-curve, reformulated for input into HEC-HMS is shown in figure D–18. The values along the x-axis come from the times of figure D–17 divided by the lag time, and the values of the y-axis come from the flow values of figure D–17 divided by the unit flow.

This section has shown the development of the UH S-curve input to HecHMS one subarea in the Whitewater Creek watershed. The same procedures were followed to produce S-curves for every subarea in the model for the three scenarios.

Figure D–18 Baldy Fork S-curves for HecHMS, three scenarios

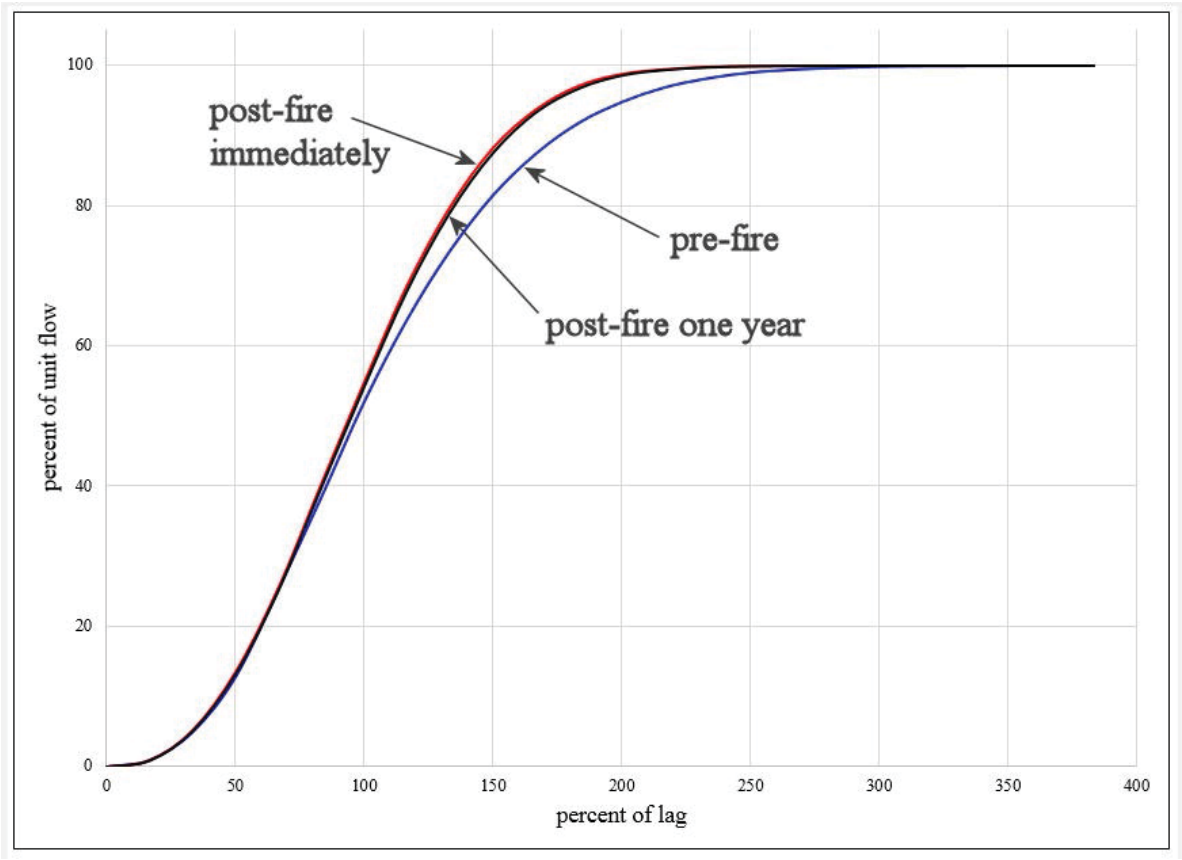

Infiltration Loss Method: Green and Ampt Equation

The process-based (GA) method of infiltration uses soil properties to model progressive loss of surface water into the soil and the change in soil moisture capacity. Although GA is a point-model, the more spatially homogeneous the soil in a given subarea the more applicable this method. HEC-HMS does have the ability to do a grid-based GA infiltration, modeling from cell to cell within a subarea, but this requires more data than is available for the Whitewater Creek basin. Being within the Gila Wilderness, spatially distributed soil data is not available. For the entire watershed, the GA parameters were estimated based on soil type and using the technical note table 12. The assumed soil texture was "sandy loam" with porosity of 0.41 cubic inches of pore space per cubic inch of soil. The initial moisture content was assumed to be near "field capacity" or 15 percent of the porosity. Converting from the metric units of table 12, the wetting front suction was estimated at 4.33 inches and the hydraulic conductivity 0.86 inches per hour.

A final specification for this method is the percent impervious surface of the subarea. This was set at zero for the pre-fire condition. For post-wildfire conditions, the percent imperviousness was used as a way to account for soil hydrophobicity. However, water-repellent soil is not the same as a parking lot pavement. It is consistent in neither spatial extent, nor depth nor layer thickness. In addition, higher rainfall rates can sometimes penetrate hydrophobic soils and infiltrate more than lower rainfall rates. The hydrophobicity will then generally return upon drying. Finally, high soil burn severity is not a fool-proof predictor of the location of hydrophobic soil.

For modeling soil hydrophobicity in the Whitewater Creek watershed, the percent imperviousness for the immediately post-fire condition for each subarea was set to 65 percent of the high soil burn severity area for the 25-year and more frequent rainfall events. For the 100-year rainfall event, the imperviousness was set to 30 percent of the high burn severity area. For the post-fire 1-year later condition, the imperviousness was set to 45 percent of the high burn severity for the 25-year rainfall and more frequent events. For the 100-year rainfall event, the imperviousness was set to 15 percent of the high burn severity.

Initial Abstraction, Surface Ponding, Canopy Loss

The CN method includes an initial abstraction, which is considered to represent interception by vegetation, surface storage, and infiltration prior to runoff. This initial abstraction is not changeable by the user and is a function of the potential maximum loss to infiltration, ultimately a fraction of the user choice of CN. While the CN method is provided as an option by HEC-HMS, the program also provides explicit canopy loss and surface loss methods. Since the GA loss method was chosen for the Whitewater Creek analysis, further losses due to vegetation and surface depressions needed to be modeled.

The options for these losses are not highly sophisticated in HEC-HMS. A maximum retention is specified by the user and an initial condition. The HEC-HMS user manual (USACE-HEC 2013) states that use of a canopy method is generally not necessary for storm events, whereas continuous simulation modeling would take into account the evaporation of intercepted moisture between storms. However, forest canopy is not an insignificant moisture interceptor. The flashiness of Southwestern United States storm events contributes to raising the significance of canopy. In addition, for wildfire events in forests the near total loss of canopy represents a widespread landscape change. For Whitewater Creek pre-fire conditions, the canopy initial storage was set to zero and the maximum storage set to 0.05 inches. For post-wildfire conditions, the canopy interception was set to none.

Surface storage is a separate option in HEC-HMS, represents loss of incoming rainfall to surface depressions, and may be used to represent the retention of moisture in the forest litter or duff layer. For Whitewater Creek pre-fire conditions, the initial storage was set to zero and maximum loss set to 0.03 inches. For post-fire conditions, the maximum loss was set to 0.01 inches.

Baseflow

HEC-HMS provides several options for modeling baseflow. The recession method is common for flood simulations, by which the initial baseflow is specified, along with a constant to modify the rate of exponential recession, and a threshold at which the baseflow is reset after the event. In the arid Southwest United States, baseflow is generally less significant when the concern is storm-event flood peaks. However, the Whitewater Creek analysis included the recession baseflow option, with the initial baseflow set to 0.25 cfs per square mile of subbasin drainage area.

Rainfall Events Examined

The NOAA National Weather Service Precipitation Frequency Data Server (NOAA 2013a) was recently updated for New Mexico. The Web site (see reference) allows the user to select a given precise location on a map and provides the total storm values for various recurrence intervals and durations. Often the 24-hour duration values are used. In the flashy thunderstorm-prone Southwestern United Sates, a shorter duration may be more applicable. Since the BAER hydrologic analysis for the Gila Wilderness used a 6-hour duration, this was selected for the current analysis.

The total rainfall values shown in table D–6 show that there is some orographic effect within the watershed, lowering rainfall values with descending elevation toward the outlet. The first flood hydrograph analysis of this case study assumed that these rainfall amounts would fall on all subareas at the same time. This is unrealistic but provides conservatively high peaks and larger volume hydrographs.

Table D–6 Whitewater Creek watershed 6-hour duration storm totals

Watershed area	2-year (in)	25-year (in)	100-year (in)
Upper Whitewater	1.54	2.73	3.49
SF Whitewater	1.42	2.49	3.19
Lower Whitewater	1.20	2.12	2.73

A second and third set of flood hydrograph analyses considered the three recurrence interval 6-hour rainfalls from table D–6 with smaller storm areal extents. These analyses examine 5-kilometer (km) and 6-km storms, which are centered as shown in figure D–20, with the rainfall amount from the areal reduction applied to the subbasins within the storm circumference.

The areal reduction (fig. D–19), developed for Walnut Gulch, AZ, is assumed applicable to Whitewater Creek, in the same geographic region, about 180 miles away. As Whitewater Creek is about 23 km wide, east to west, the areal reduction from figure D–19 is significant. The largest area on the graph is 300 square km, which corresponds to a radius of about 10 km. Therefore, many of the subbasins of Whitewater Creek will be farther away from the storm center than can be analyzed with the figure. Rather than reduce the rainfall of more remote subareas to zero, the analyses applied minimum values from figure. The selected storm centerings for the areally reduced analyses are shown in figure D–20. The red star marks a 5-km centering and the black star shows a 6-km radius storm centered slightly differently.

To distribute the rainfall totals over time, the standard SCS Type II rainfall distribution, considered applicable in New Mexico, was used. Although the standard distribution pertains to a 24-hour duration, it is easily modified by proportioning for shorter durations, including the 6-hour.

Figure D–19 Areal reduction factors developed for 6-hour duration storms at Walnut Gulch, AZ, experimental watershed (modified, from Osborn, Lane, and Myers 1980)

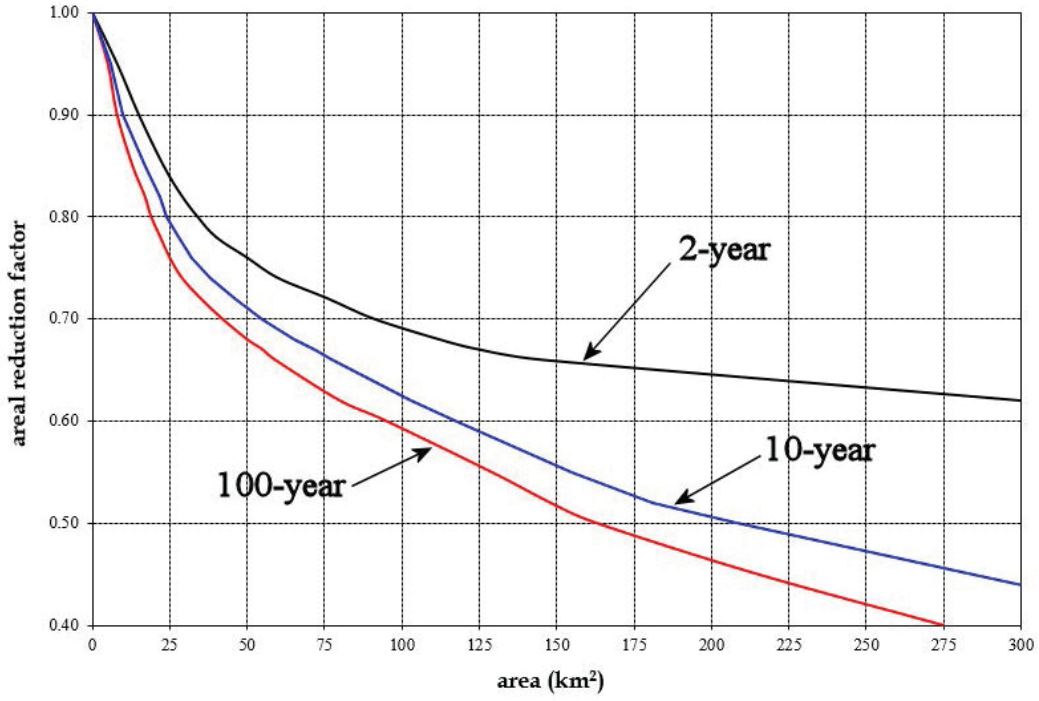

Figure D–20 Two storm centerings for Whitewater Creek, varying areal reduction

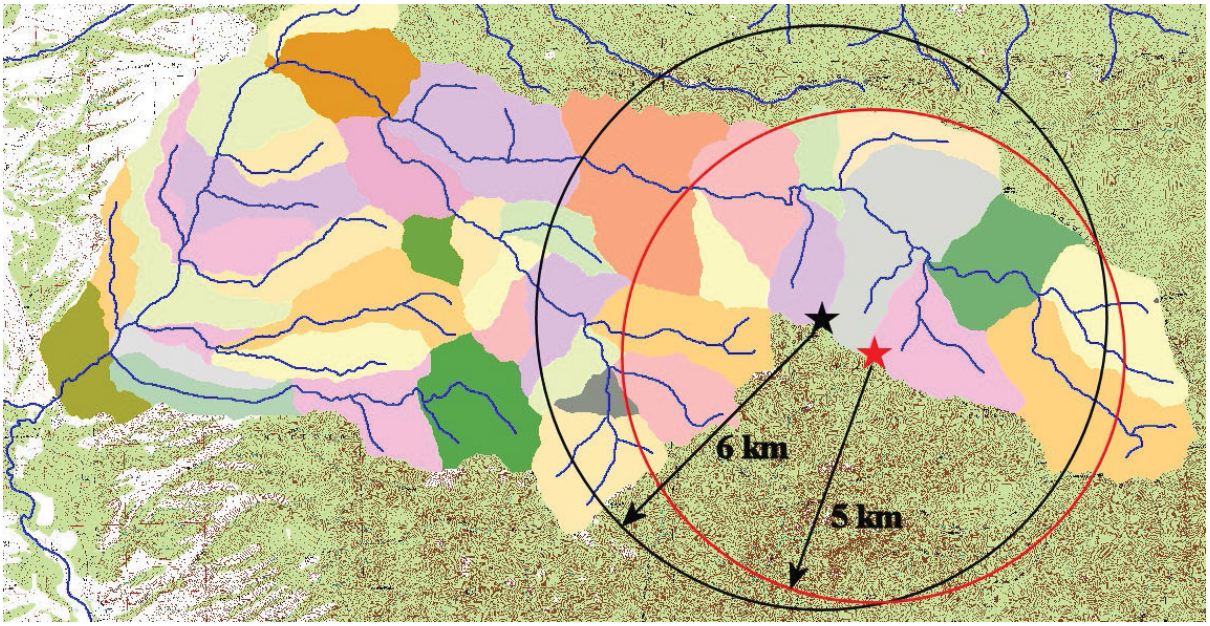

Sediment Bulking

This analysis did not attempt to model sedimentation. As discussed in the main body of the technical note, the maximum sediment concentration short of "debris flow" is considered about 20 percent. A USGS report specifically concerning the Whitewater Baldy Complex wildfire (Tillery, Matherne, and Verdin, 2012) estimated high probabilities in Whitewater Creek of debris flows from 30-minute duration rainfall events for recurrence intervals of 2 years, 10 years, and 25 years. A shorter duration storm of higher intensity is generally required to generate debris flow.

Figure D–21 is a screenshot from plate 3 of Tillery, Matherne, and Verdin (2012) which shows their overall debris flow hazard findings for Whitewater Creek. Notice the main channel of Whitewater Creek in blue and the community of Glenwood at the downstream end circled in red. Subbasins labeled 92 and 93 are the upper Whitewater, subbasin 91 is the SF Whitewater, and subbasin 90 is the upper Little Whitewater.

Figure D–21 Whitewater debris flow hazard (Tillery, Matherne, and Verdin (2012))

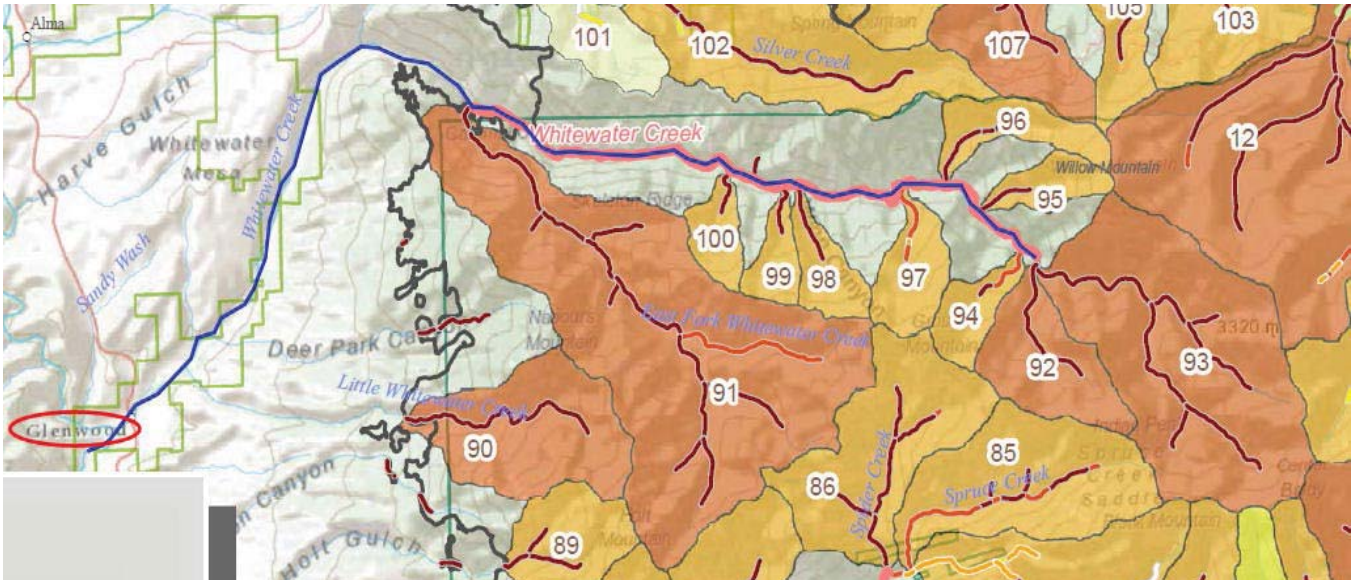

These of brown color are the highest hazard for debris flow in response to a 25-year 30-minute rainfall event (a total storm rainfall of about 1.54 inches).

As a conservative estimate of possible sediment bulking for the events examined in this analysis, with 6-hour duration, the subbasins in brown from figure D–21 were considered 20 percent bulked and the subbasins in yellow, 10 percent bulked.

Results and Discussion

Figure D–22 shows the four locations for which modeling data are reported herein. The HEC-HMS model can produce results for the outlet of any subbasin (shown in the figure by different pastel colors). The output is reported for three recurrence intervals, 2-year, 25-year, and 100-year, for the three scenarios, pre-fire, post-fire immediately, and post-fire 1 year later.

Figure D–22 Locations of reported HEC-HMS modeling output

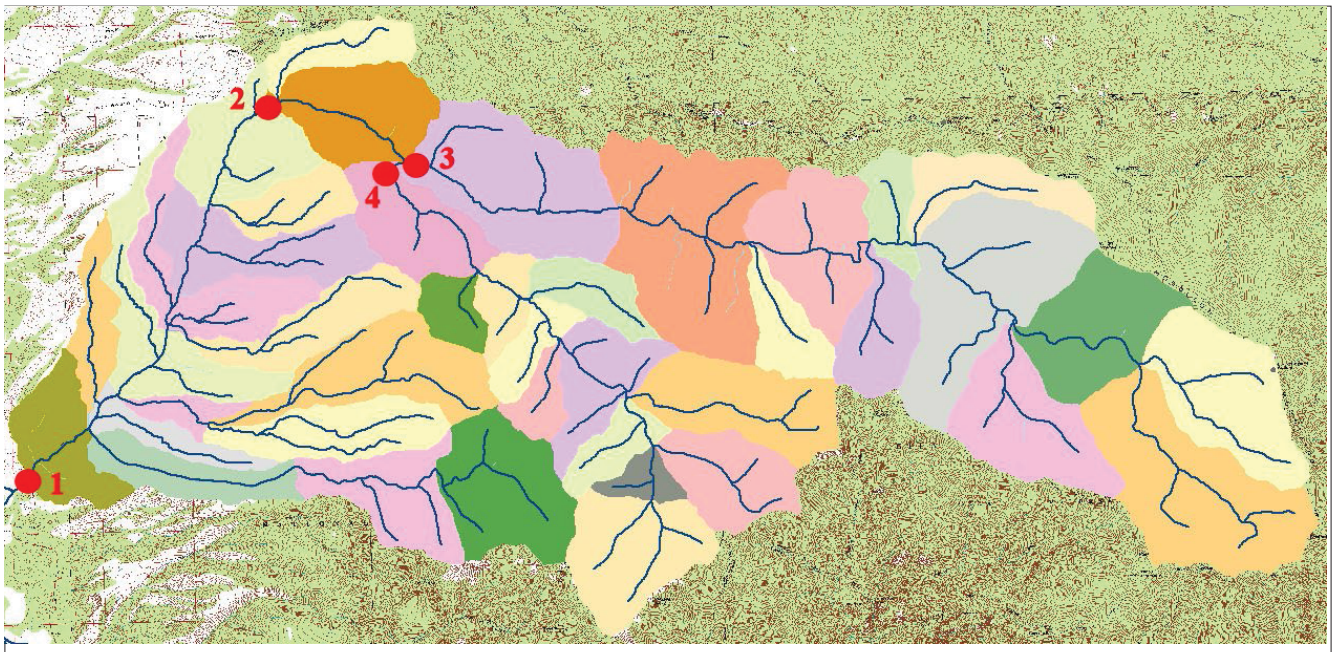

1 = Whitewater Creek outlet at Glenwood NM
2 = USGS gage “Whitewater Creek at Catwalk” (installed 2012)
3 = Upper Whitewater Creek just above the confluence of SF Whitewater
4 = SF Whitewater just above the confluence of the Whitewater

Table D–7 shows HEC-HMS modeling results for the rainfall events with no areal reduction. (These runs include the slight reduction, shown in table D–6, due to the fact that the data provided by NOAA, for three general areas of the watershed, lessens for each recurrence interval as location changes toward the west.

These peaks are considered conservatively high, since no areal reduction was applied and the nature of storms in the Gila Wilderness area is more localized convective thunderstorms. In addition, although the unit hydrographs did change between the two post-fire scenarios, due to the consideration of some vegetation regrowth, the majority of the drop in the peak for the 1-year later condition came from assumptions about

the reduction in hydrophobic soils. No field verification was completed for this analysis and the BAER report (USDA FS 2012) did not discuss the extent of hydrophobic soil. Estimates for this analysis were made using the soil burn severity GIS shapefiles and from the findings of Tillery, Matherne, and Verdin (2012). Figure D–23 shows the full hydrographs for the 100-year no areal reduction scenario at the Whitewater Creek outlet, near Glenwood.

Table D–7 HEC-HMS output: hydrograph peaks (cfs) at four locations (no areal reduction)

Storm	Location (see fig D–22)	Pre-fire peak discharge (cfs)	Post-fire peak discharge (cfs) (immediately following the fire)	Post-fire peak discharge (one year after the fire)
100-yr	abv SF	14,306	20,853	19,318
	SF at mouth	6,158	7,971	7,843
	gage	19,170	27,236	25,548
	Glenwood	21,967	30,937	29,368
25-yr	abv SF	6,848	13,331	11,680
	SF at mouth	2,644	4,404	4,270
	gage	8,976	16,486	14,692
	Glenwood	8,994	17,315	15,647
2-yr	abv SF	3,950	9,294	7,943
	SF at mouth	2,153	3,900	3,724
	gage	5,881	12,279	10,891
	Glenwood	6,655	13,804	12,470

Figure D–23 HEC-HMS results, 100-year storm peaks at Glenwood (no areal education)

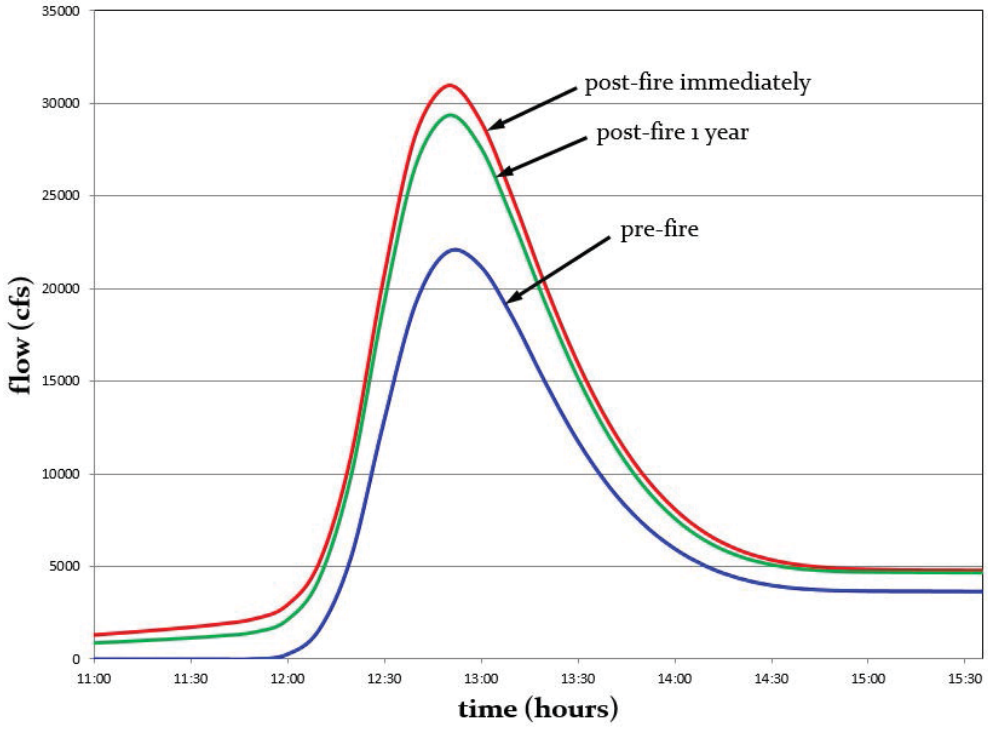

The areal reductions, as discussed above came from Osborn, Lane, and Myers, (1980), in particular their examination of Walnut Gulch, AZ. That paper also examined a watershed near Alamogordo, NM, which showed less areal reduction than Walnut Gulch. However, the Gila Wilderness area is considered closer geographically to Walnut Gulch than to Alamogordo.

Nevertheless, the areal reductions may be less at Whitewater Creek than what were applied for the results reported in table D–8. Note that the 100-year pre-fire peak at Glenwood between tables D–7 and D–8 drops from 21,967 cfs to 8776 cfs (6 km centering) or 7916 cfs (5 km centering). The post-fire reductions in peak due to areal reduction are similar. The post-fire immediately peak at Glenwood dropped from 30,937 cfs to about 14,000 cfs. Figure D–24 shows the areally reduced 100-year 6-km centering.

Table D–8 HEC-HMS output: hydrograph peaks (cfs) at four locations (areal reductions applied with centerings as shown in figure D–20)

Storm	Location	Centering (km)	Pre-fire peak discharge (cfs)	Post-fire peak discharge (cfs) (immediately following the fire)	Post-fire peak discharge (one year after the fire)
100-yr	abv SF	6	7,164	12,566	11,254
		5	7,797	13,026	11,873
	SF at mouth	6	2,731	4,306	4,242
		5	1,693	2,611	2,458
	gage	6	10,149	15,734	14,623
		5	9,246	15,052	13,500
	Glenwood	6	8,776	14,391	13,245
		5	7,916	13,899	12,431
25-yr	abv SF	6	3,173	7,731	6,647
		5	3,882	7,741	6,893
	SF at mouth	6	1,478	2,300	2,255
		5	869	1,088	1,107
	gage	6	4,384	9,703	8,696
		5	4,589	8,654	7,765
	Glenwood	6	3,854	8,713	7,674
		5	3,934	7,919	7,060
2-yr	abv SF	6	33	3,683	2,372
		5	54	3,420	2,203
	SF at mouth	6	3	845	569
		5	3	314	219
	gage	6	31	4,346	2,878
		5	56	3,723	2,405
	Glenwood	6	31	4,121	2,734
		5	46	3,555	2,308

Figure D–24 HEC-HMS results, 100-year peaks at Glenwood, areal reduction 6-hm centering

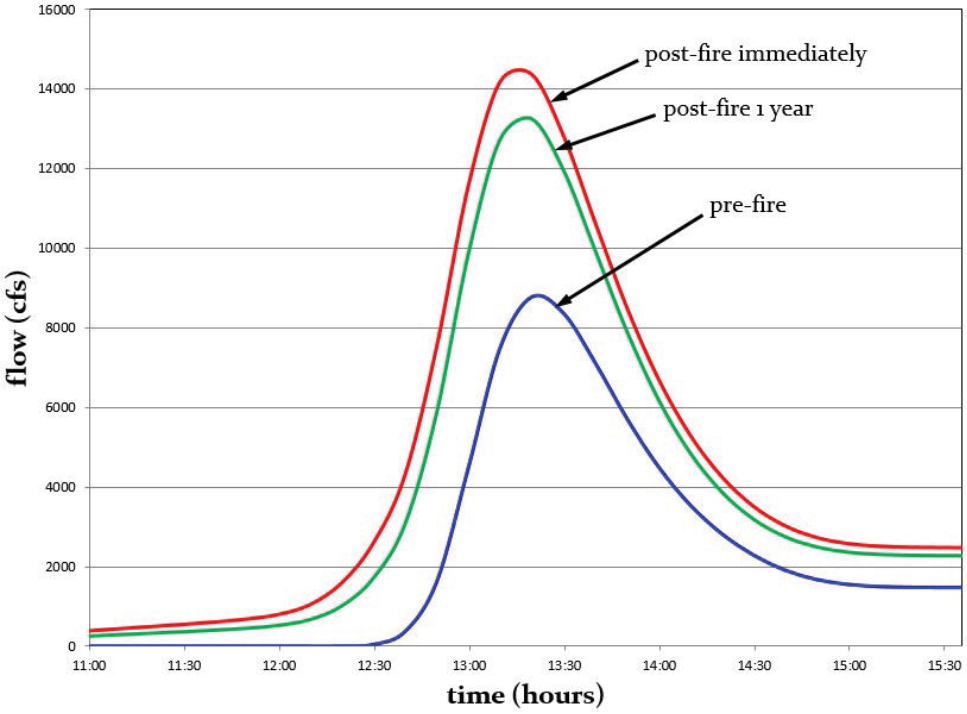

Figure D–25 shows the post-fire results for the 100-year peaks at Glenwood under both centering conditions. Figure D–26 shows the same results for the 25-year recurrence interval. Note the change in the timing of the peak. For the 100-year flood the 5-km centering peaks earlier, but for the 25-year event the 5-km centering peaks later. (The difference is only about 15 minutes either way.)

Figure D–25 100-year post-fire hydrographs at Glenwood

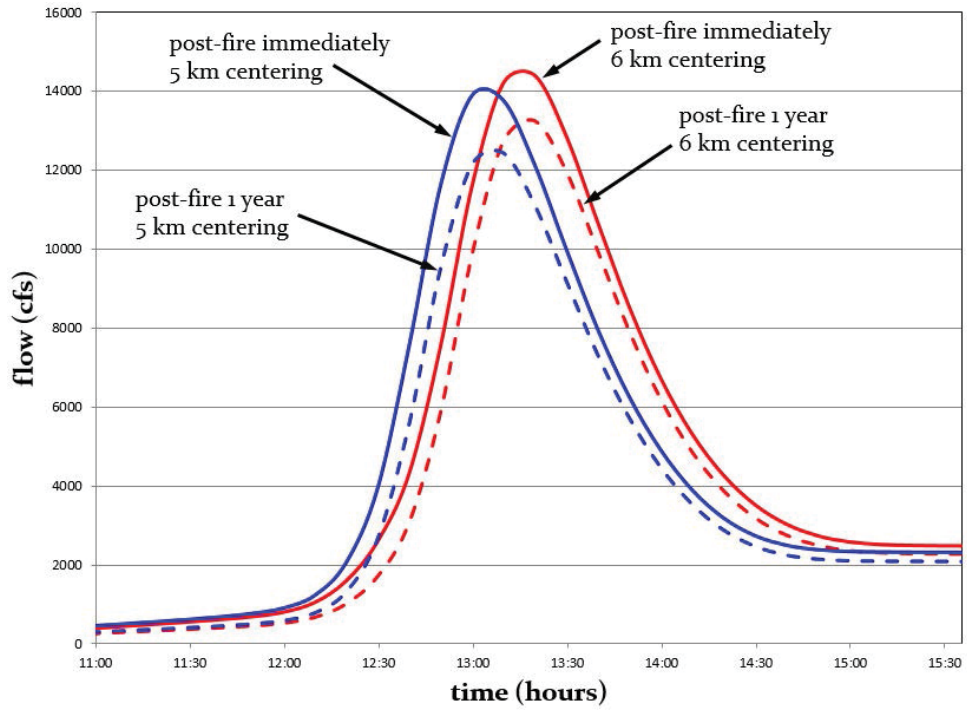

Figure D–26 25-year post-fire hydrographs at Glenwood

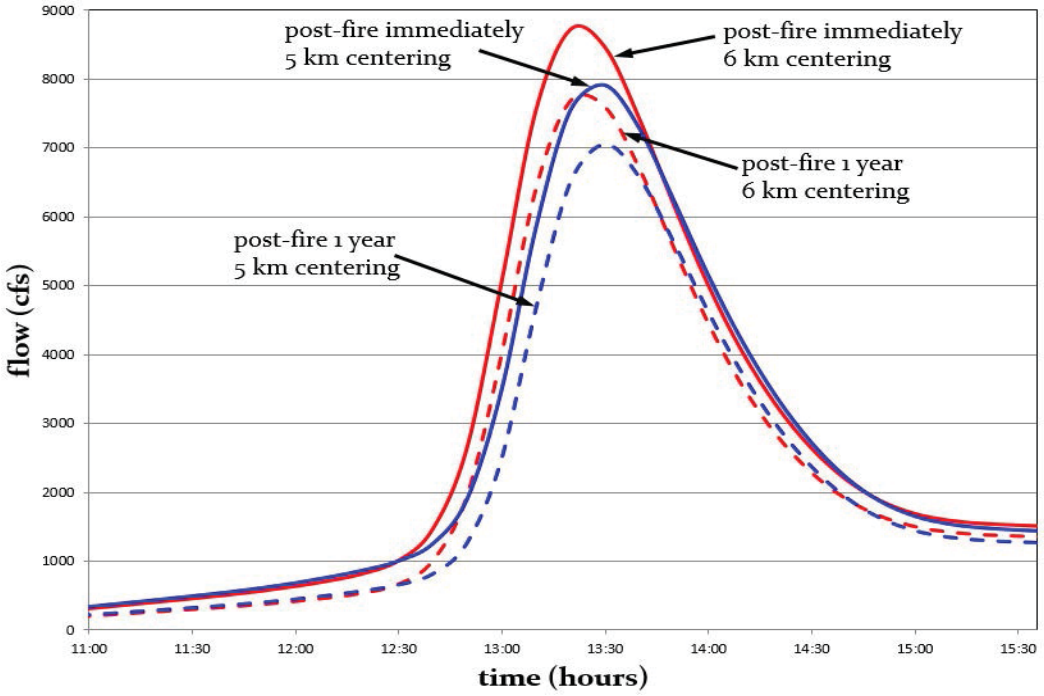

Sediment bulked peak flows have been computed as mentioned above, with the upstream end (about one third) of the Upper Whitewater subbasin contributing a 20 percent sediment discharge, the lower end 10 percent, and the entire SF Whitewater subbasin contributing 20 percent. These results are shown in table D–9.

Table D–9 Sediment bulked peak flows (cfs) for Whitewater Creek

Storm	Location	6 km centering		5 km centering	
		Post-Fire (immediately following the fire)	**Post-Fire** (one year after the fire)	**Post-Fire** (immediately following the fire)	**Post-Fire** (one year after the fire)
100-yr	abv SF	14,325	12,042	14,850	12,704
	SF at mouth	5,167	4,666	3,133	2,704
	gage	18,354	15,835	17,398	14,577
	Glenwood	17,011	14,457	16,245	13,508
25-yr	abv SF	10,328	15,517	8,825	7,376
	SF at mouth	2,760	2,481	1,306	1,218
	gage	11,245	9,387	9,955	8,358
	Glenwood	10,255	8,365	9,220	7,653

Peak Rate Factor Discussion

As discussed in the technical note section on the NRCS dimensionless unit hydrograph, the standard peak rate factor may not be applicable to steeper mountain streams. The GIS time-area histogram approach used in this case study precludes the need to determine peak rate factors. But the resulting unit hydrographs can be compared to NRCS dimensionless unit hydrographs of any given peak rate factor. The dimensionless UH is made dimensional using the subbasin drainage area and time of concentration. For the Baldy Creek subbasin, the GIS derived UHs show that the proper peak rate factor would have to be over 700 (fig. D–27).

Modeling Observed Data

September 2013 brought heavy rainfall to the Rockies from Wyoming to New Mexico. The extensive damage in and around Boulder, Lyons, and Estes Park, CO was documented in national headlines. Storms of similar magnitude also visited the Gila Wilderness watersheds that had been previously damaged by the Whitewater-Baldy Complex fire. Figure D–28 shows the NOAA 5-day precipitation forecast for the region, which shows that the storms were large enough to cover not only the Colorado Front Range, but also to reach as far as southwestern New Mexico (NOAA 2013b).

The largest rainfall totals in the Whitewater Creek watershed were recorded between September 14 and 15, 2013. The NOAA Precipitation-Frequency data server (NOAA 2013a) data for a storm centering over the confluence of the SF Whitewater is shown in table D–10, along with the rainfall totals (in blue) for the event recorded at the Catwalk gage.

For all four durations shown in the table the event was more rare than a 1,000 year recurrence. Evidence of storm areal extent is provided by the fact that the Hummingbird Saddle gage during this event received minimal precipitation. Between 9 p.m. and midnight, while the Catwalk gage was recording 6.10 inches of rainfall, the Hummingbird Saddle gage recorded zero. For the 3 hours after midnight, rainfall at Catwalk dropped off considerably (0.75 inches, total) and Hummingbird Saddle recorded a similar total (0.93 inches). Figure D–29 shows the storm event for which modeling results are presented below.

Figure D–27 Baldy Fork GIS-derived 30-minute unit hydrographs with an NRCS UH

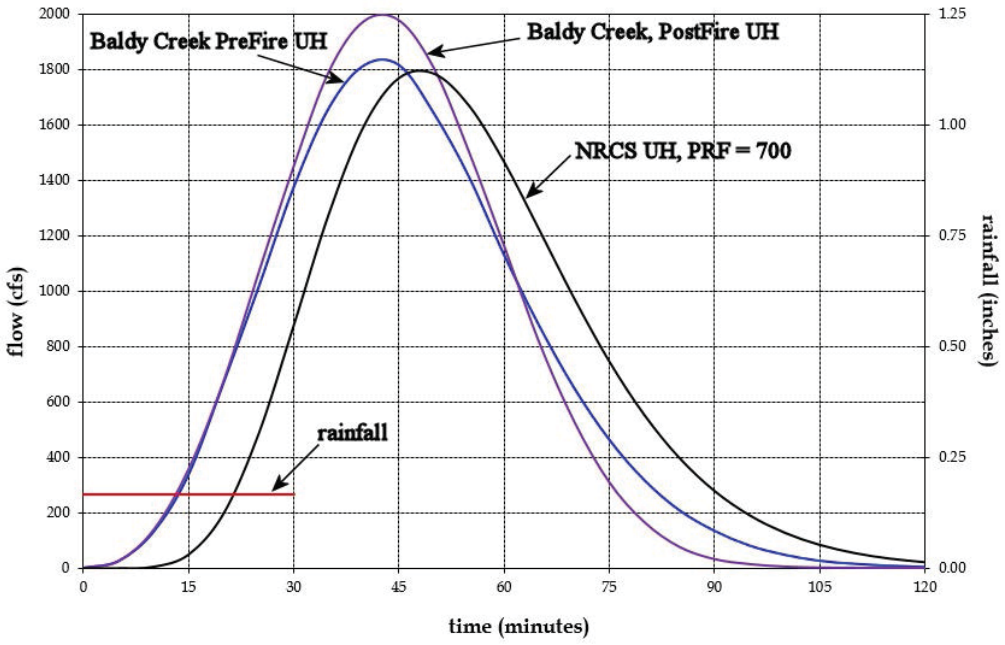

Figure D–28 NOAA National Weather Service 5-day forecast issued September 9, 2013 (NOAA 2013b)

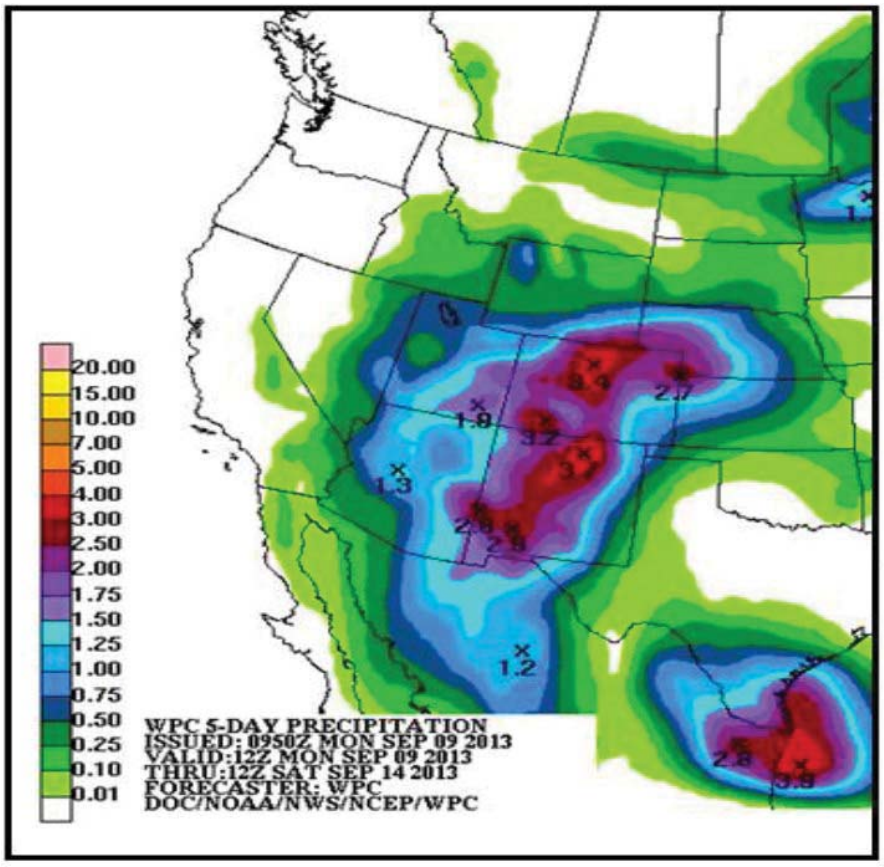

Table D–10 NOAA precip-frequency values and September 2013 rainfall event from Catwalk gage

Storm centering at SF Whitewater confluence (rainfall in inches)							
Duration	Recurrence Interval-->						
	50-year	100-year	200-year	500-year	1000-year	Gage	14–15 Sep 2013
1-hour	1.83	2.04	2.24	2.5	2.71	**3.01**	9–10 p.m.
2-hour	2.02	2.27	2.52	2.86	3.14	**4.09**	9–11 p.m.
3-hour	2.12	2.38	2.66	3.04	3.35	**6.10**	9–midnight
6-hour	2.48	2.8	3.14	3.61	3.99	**6.85**	9 p.m.–3 a.m.

Figure D–29 Whitewater Creek, NM, flood event of September 14–15, 2013, gaged rainfall and streamflow

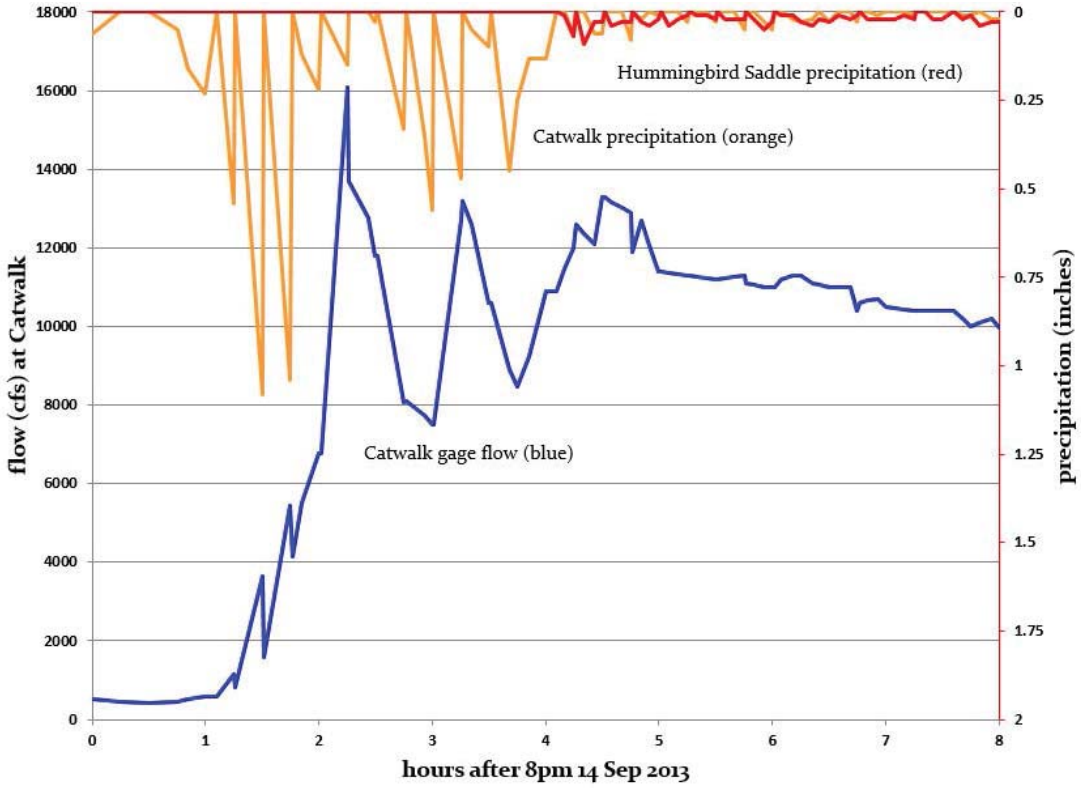

To have two gages in a post-wildfire watershed may be considered a great luxury, but the data will be far from adequate to calibrate a hydrologic model. However, such data can be used to show whether the hydrologic model is reasonable. For example, three runs with different assumed storm centerings were made for this event. The same areal reduction factors as shown in figure D–19 were used (although the rarest event on that graph is 100-year, compared to the observed event, more rare than a 1000-year recurrence). The areal reduction for the observed event could be expected to show a steeper drop off than the 100-year event in the figure. This is not contradicted by the concurrent rainfall at Hummingbird Saddle. To estimate sediment bulking, the extreme rarity and magnitude of the event was considered to justify a 20-percent estimate for both brown and yellow subwatersheds from figure D–21. The event occurred about a year after the wildfire, so some healing could have occurred. However, this event could have produced debris flow, and uncertainty of sediment transport may be considered significant for this observed event.

To create sediment hydrographs, the Data Storage System (DSS) functionality of HEC-HMS was employed. A separate program HEC-DSSVue provides hydrograph manipulation tools, with which sediment hydrographs were made by multiplying individual subbasin flow hydrographs by 20 percent. The database preserves the timing, so that the subbasin bulked hydrographs can be summed for an outlet such as the Catwalk gage. Only two subwatershed sediment hydrographs were required (as can be seen by examining fig. D–21), one for the upper Whitewater and one for the entire SF Whitewater. These were combined to create a total sediment hydrograph at the gage. Figure D–30 shows modeled versus observed flows.

Figure D–30 Whitewater Creek flood September 14–15, 2013, observed and modeled

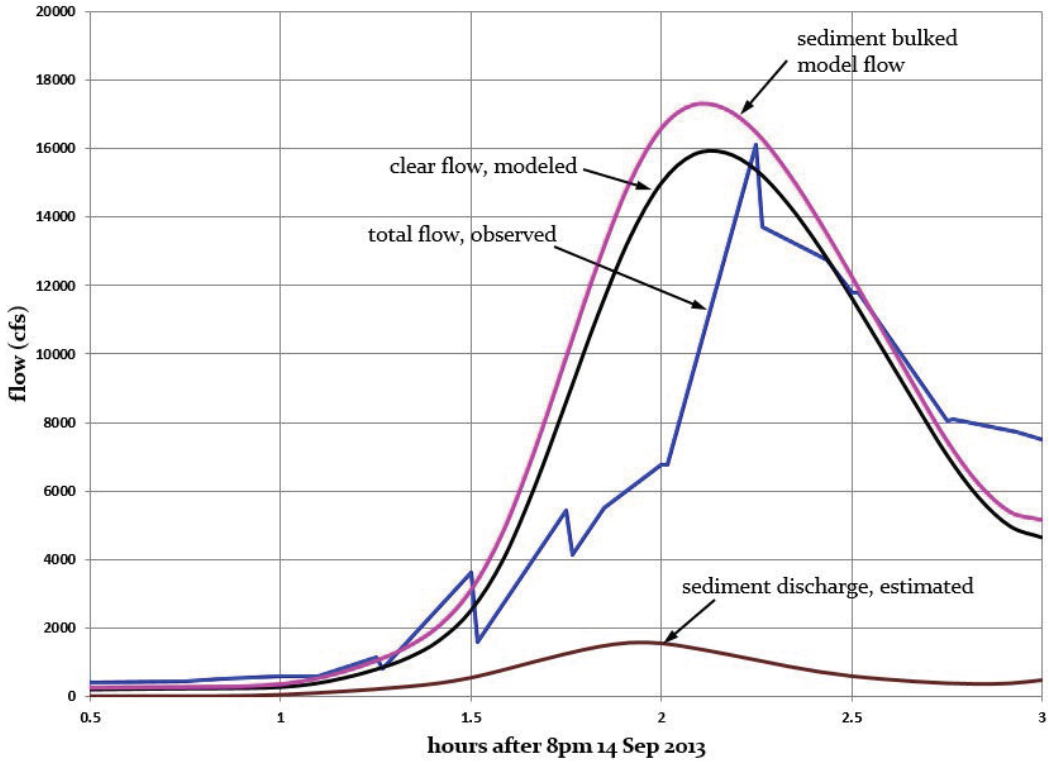

Conclusions

The post-fire hydrograph results are highly dependent on the amount of hydrophobic soil and the timing of its breakdown and return to pre-fire conditions. This is impossible to predict accurately without extensive field investigation. The burn severity mapping can be considered to at least rule out hydrophobicity in unburned and low burned areas. The extent to which hydrophobicity truly excludes infiltration in highly burned areas should be investigated. Although the findings of the research literature indicate that post-wildfire hydrophobic soils can persist for over 5 years, critical questions remain for hydrologic modeling. For example, does hydrophobicity immediately post-fire completely cover a landscape or only partially? And does the breakdown of hydrophobic effects on runoff occur more rapidly than the complete disappearance of the phenomenon because of the nonhomogeneity on a landscape?

The second major issue for hydrologic modeling, particularly in the arid Southwestern United States, is the extent of areal reduction in any given area. A literature search for this analysis turned up very little, and studies by NOAA that were scheduled to be underway by 2006 apparently have not been completed.

In considering the methodology differences between this case study and others, which use NRCS CN and dimensionless unit hydrographs, a number of salient points arise. Practitioners accounting for high burn severity and/or hydrophobicity have found that CN values should be set very high, usually around 95. See tables 5, 7, 8, and 9 in the technical note. This need to approach the very upper limit of CNs may have been necessary not only because hydrophobicity does, indeed, somewhat mimic a pavement, but also because the standard NRCS peak factor was not adjusted. As shown in figure D–27, the standard peak factor may be much too low for steep mountain streams. However, the practice of running up the CN to account for

hydrophobicity has no less scientific merit than setting subbasin percents of imperviousness, as was done in this case study. The need for some way to rapidly assess hydrophobic effects becomes apparent.

Although the time-area histogram methodology demonstrated in this case study precludes the need to determine peak factors, the GIS manipulations require analysis time, which can be a function of the GIS experience of the hydrologist. Perhaps scripts could be written to speed the process, but the greater the number of subareas the more analysis time needed to create time-area based UHs. However, the numerous GIS layers available for use in post-wildfire analyses, especially regarding soil burn severity, should encourage the hydrologist to increase GIS proficiency.

References

Bedient, P.B., W.C. Huber, and B.E. Vieux. 2012. Hydrology and Floodplain Analysis, Prentice Hall, NJ, 5th Edition, 801 pages.

Beven, K.J. 2001. How far can we go in distributed hydrologic modelling? Hydrology and Earth Systems Sciences 5, 1-12.

ESRI (Environmental Systems Resource Institute). 2010. ArcMap 10.0 ESRI, Redlands, CA.

MacArthur, R., and J.J. DeVries. (1993) Introduction and application of kinematic wave routing techniques using HEC-1. U.S. Army Corps of Engineers Hydrologic Engineering Center, Davis, CA, 68 pages.

Moody. T., M. Wirtanen, and S.N. Yard. (2003) Regional relationships for bankfull stage in natural channels of the arid Southwest. Report from Natural Channel Design, Inc., Flagstaff, AZ, 38 pages.

NOAA National Weather Service Precipitation Frequency Data Server 2013a. Available at http://dipper.nws.noaa.gov/hdsc/pfds/. Accessed Sep 2013.

NOAA National Weather Service, 2013b. Service Assessment, The Record Front Range and Eastern Colorado Floods of September 11-17, 2013b.

Oreskes, N., K. Shrader-Frechette, and K. Belitz. (1994) Verification, validation, and confirmation of numerical models in the earth sciences. Science 263, 641-646.

Osborn, H.B., L.J. Lane, and V.A. Myers. (1980) Rainfall/watershed relationships for Southwestern Thunderstorms. Transactions ASAE 23(1), 82-91.

Tillery, A.C., A.M. Matherne, and K.L. Verdin. (2012) Estimated probability of postwildfire debris flows in the 2012 Whitewater-Baldy fire burn area, Southwestern New Mexico. USGS Open File Report 2012-1188, 11 pages.

USACE-HEC (U.S. Army Corps of Engineers, Hydrologic Engineering Center), 2013. HEC-HMS Technical Reference Manual. Accessed in April, 2013.

USDA Forest Service (2012) Glenwood, Reserve and Wilderness Ranger Districts, BAER Report Executive Summary for the Whitewater Baldy Complex fire, including hydrology appendices.

USDA-NRCS. 2010. NRCS National Engineering Handbook, Part 630 Hydrology, Chapter 15, Time of Concentration.

USDA-SCS. 1985. Soil Survey of Catron County, New Mexico, Northern Part, 199 pp.

This page intentionally left blank

Appendix E: Case Study 5:
Saratoga Springs, Utah

Predicting and Comparing Measured Bulking and Peak Discharge Using Multiple Methods for Post-Fire Hydrologic and Sedimentation Analysis on the Dump Fire in Saratoga Springs

Background

In late June 2012, wildfire burned the watershed above the Utah communities of Saratoga Springs and Eagle Mountain, about 40 miles south of Salt Lake City. Reported to have been sparked by target shooters, the fire burned approximately 5,500 acres and required the evacuation of an estimated 9,000 residents. No serious injuries or damages were reported as a result of the event, which became known as the Dump Fire. Local residents protested the name, which came about because the fire was started near an old dump. This case study will refer to the event as the Saratoga Springs fire. See figure E–1 for location.

The wildfire prompted the City of Saratoga Springs to request assistance from the NRCS through the Emergency Watershed Protection Program (EWP). Storm damages following an early September rainfall event (2 months after the fire) occurred before countermeasures could be installed.

Figure E-1 State of Utah and fire location, about 40 miles south of Salt Lake City

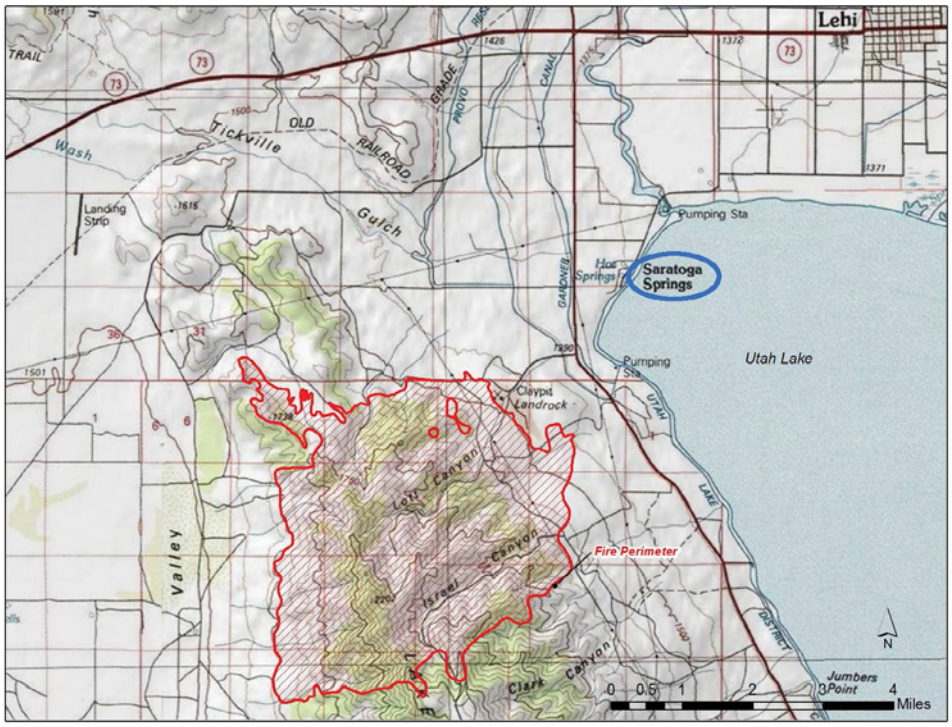

NRCS performed a post-fire hydrologic analysis in support of the design of a sediment basin to protect residents from the accelerated erosion and sedimentation caused by the fire. Figures E–2 and E–3 illustrate the burning watershed from the point of view of the community of Eagle Mountain.

The storm of September 1, 2012, was centered over an unnamed tributary and Israel Canyon, which drain into Saratoga Springs. Local officials reported that the rainfall was 1.25 inches over a 25-minute duration. NRCS engineers estimated that the subsequent runoff deposited a bedload estimated at 70,000 tons. The mud slurry damaged houses, inundated basements, and filled and overtopped a small debris basin. The event was comparable to two times the 100-year (1-percent-chance event) flow.

Figure E–2 Burning watershed from Eagle Mountain, UT, 9/21/2016

Photo by Cindi Braby, Eagle Mountain, UT

Figure E–3 Burning watershed from Eagle Mountain, UT, 9/22/2012

Photo by Cindi Braby, Eagle Mountain, UT

The flow direction into the residential areas of Saratoga Springs is shown in figure E–4. The drainages discharge onto an alluvial fan that slopes into residential development where mud slurry, small boulders, cobbles, and gravel were deposited during the storm (fig. E–5 and E–6). This debris damage was caused by the vulnerability of the watershed immediately following the fire, which increased erosion and mudflows in the steep gradient alluvial fan.

Figure E–4 Burned watershed flow direction into Saratoga Springs from September 2012 event

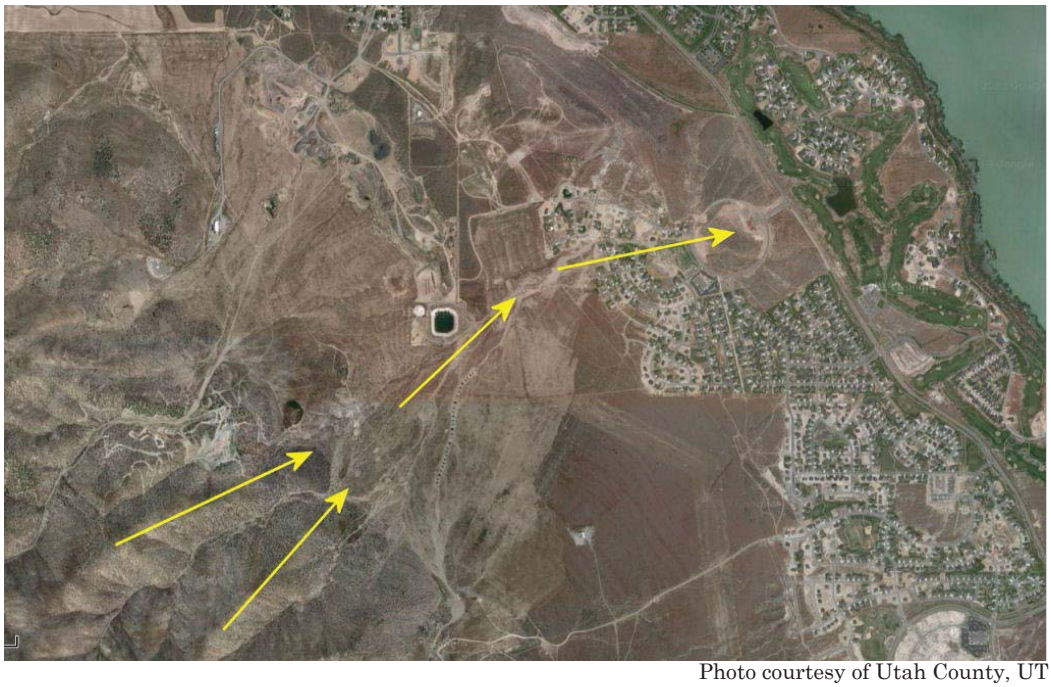

Photo courtesy of Utah County, UT

Figure E–5 Sediment-laden flow through residential neighborhood

Photo courtesy of City of Saratoga Springs, UT

Figure E–6 Typical sediment composition in residential area

Photo courtesy of City of Saratoga Springs, UT

Methods

As part of the post-fire hydrologic analysis for the Saratoga Springs fire, a number of computer programs were used. Runoff hydrographs were determined using the NRCS hydrology program WinTR-20 (USDA-NRCS(a) 2004). The model Automated Geospatial Watershed Assessment Tool, or AGWA, (Goodrich et al. 2006 and USDA-ARS 2014) was used to determine sedimentation rates. AGWA was created by the USDA Agricultural Research Service's Southwest Watershed Research Center in Tuscon, AZ. It combines previously existing models KINEROS2 (Smith et al. 1995, Woolhiser et al. 1990) and SWAT (Arnold et al. 2012).

The runoff CN and derived hydrologic characteristics from local stream gage networks and regression equations (USGS StreamStats) were used to determine the logical pre-fire inputs. NOAA Atlas 14 rainfall distribution and modified cumulative Kirpich time of concentration methods were also used.

Changes to the time of concentration (T_c) and CN inputs into WinTR-20 and AGWA were based on past studies for post-fire analysis. Goodrich et al. (2005) provides support for modification of CN values, given reduction of cover and burn severity. McLin et al. (2001) provides a method to estimate change in lag time associated to relative increases in CN.

Two methods were used to analyze the viability of derived post-fire peaks and debris flow volumes. These include the Cannon and Gartner (2005) regression equations for estimating peak debris flow, given burn area and lithology of burn area, basin gradient, and storm rainfall, and the Gartner et al. (2008) regression equations for estimation of debris flow volumes.

Typically, the ratio of sands and colloidal grain sizes to bedload is estimated at 10:1 or 3:1 ratios. Since the AGWA value was within reason for the total sediment and sands as a percentage (i.e., 10 percent), it was assumed to be comparable to total bedload in this case.

For the hydrologic analysis of the burned watershed above Saratoga Springs, the entire watershed was assumed to have experienced moderate burn severity.

An initial estimate of pre-fire sedimentation conditions was made using the map of Bridges (1973) which shows estimated yearly sediment yield and a breakdown between sheet and rill erosion versus channel and gully erosion. For the Saratoga watershed, pre-fire sediment yield is estimated to range between 0.1-0.2 acre-feet per square mile per year, with sources being 60 percent sheet and rill and 40 percent channel and gully.

Pre-Fire Flow Ranges

The first step in estimating the pre-fire watershed condition was to review existing gages in the area to determine reasonable pre-fire flows for the 25-, 50-, and 100-year (4-percent-, 2-percent-, and 1-percent-chance) events. After this was completed, WinTR-20 was used with NOAA Atlas distributions and a modified cumulative Kirpich equation. Runoff CNs were modified between ground cover conditions and used Title 210, National Engineering Handbook (NEH), Part 630, Hydrology, Chapter 9, Hydrologic Soil-Cover Complexes (USDA NRCS(b), 2004); the U.S. Geologic Survey (USGS) National Land Cover Database (NLCD) (Fry et al. 2011); and the NRCS SSURGO database (USDA-NRCS(c) 2012).

Stream Gages

Six nearby stream gages were analyzed to help estimate peak flows for the pre-fire watershed above Saratoga Springs. The stream gages are listed in table E–1 and are shown on the figure E–7 map. Their statistics were taken from the StreamStats report appendix (Kenney et al. 2007). Discharge per unit area (cubic feet per second per square mile, CSM) was computed for each probability and graphed (fig. E–8).

Of the six nearby gaged watersheds, numbers 1 through 3 (table E–1) are most similar in drainage area, although the modeled watershed area above Saratoga Springs is 2.5 square miles, which is about half the size of three nearby gages. In figure E–8, the graphs of those three gages are the higher ones: blue, green, and violet.

Table E–1 Six stream gages near Saratoga Springs, UT

Number on figure E–8	USGS #	Drainage (sq. mi.)	Gage Name
1	10172790	5.77	Settlement Canyon near Tooele, UT
2	10172805	5.38	N. Willow Creek near Grantsville, UT
3	10172800	4.19	S. Willow Creek near Grantsville, UT
4	10166430	26.5	W. Canyon Creek near Cedar Fort, UT
5	10172765	6.7	Clover Creek above Big Hollow near Clover, UT
6	10172910	16.8	Settlement Creek above Reservoir near Tooele, UT

Figure E–7 Location of stream gages and study area

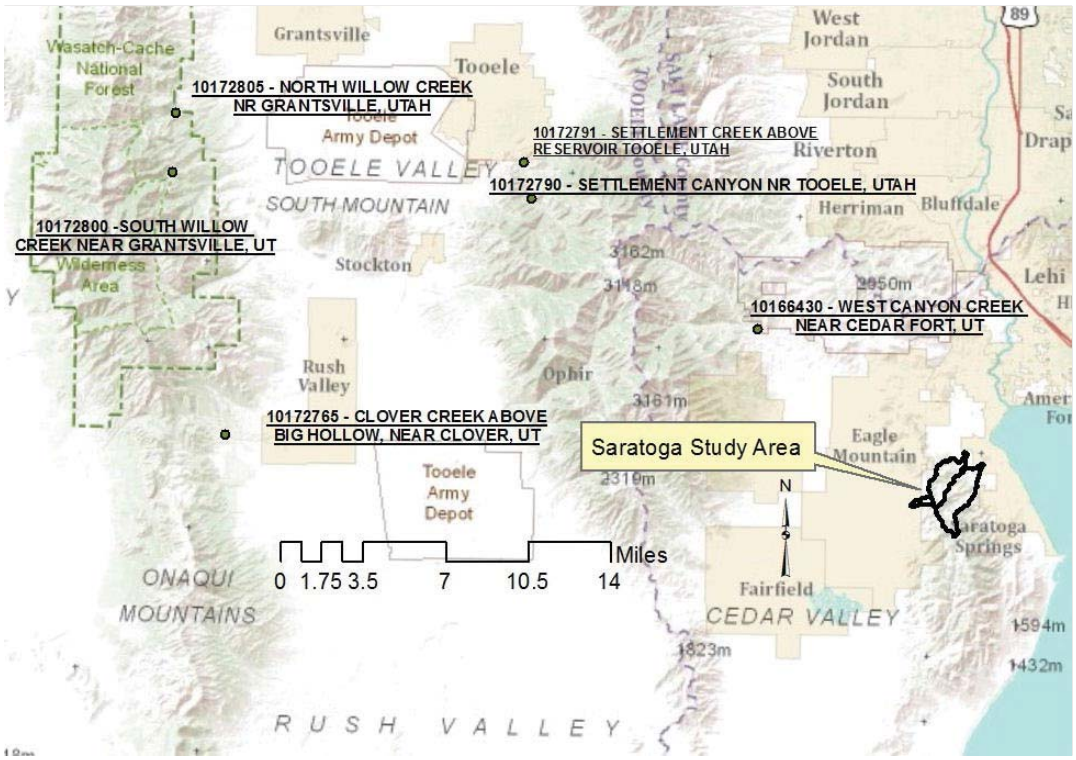

Figure E–8 Stream gage regression output converted to discharge per unit area

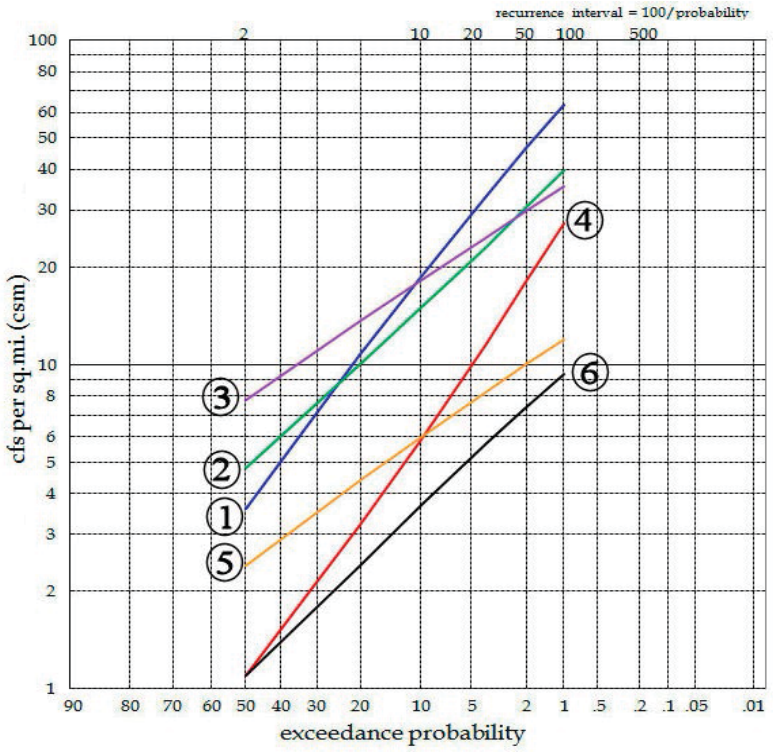

Pre-Fire T_c

The upper range CSM exceedance probability was used to determine the pre-fire inputs into WinTR-20. The T_c was estimated to be 1 hour, or an average velocity of 6.0 feet per second. The upper elevation of the watershed is 7,500 feet above mean sea level, the watershed outlet is at 4,875 feet above mean sea level, and the longest flow path is 3.8 miles in length.

Pre-Fire CN

The CN lookup values were adjusted pending 210-NEH, Part 630, Chapter 9, ground cover conditions (USDA-NRCS(b), 2004) based on NLCD and SSURGO data. The generated T_c, adjusted CN, and NOAA Atlas 14 rainfall distribution were entered into WinTR-20. The CN was adjusted until the WinTR-20 output and calculated CSM matched the range of CSM of nearby stream gages.

Post-Fire Peaks and Volumes of Sediment

The burned watershed above Saratoga Springs has a total drainage area of 4.91 square miles. For WinTR-20 analysis, the burned area was divided into three subareas, as shown in figure E–9. Subareas 1 and 2 converge and provide outlet to the Saratoga Springs residential areas shown in figures E–4 through E–6. Subarea 1 is known as Israel Canyon. See tables E–2 and E–3 for WinTR-20 basic input related to these subareas, including selected pre-fire and post-fire CN.

Figure E–9 Burned zone (red) and subareas upstream of Saratoga Springs

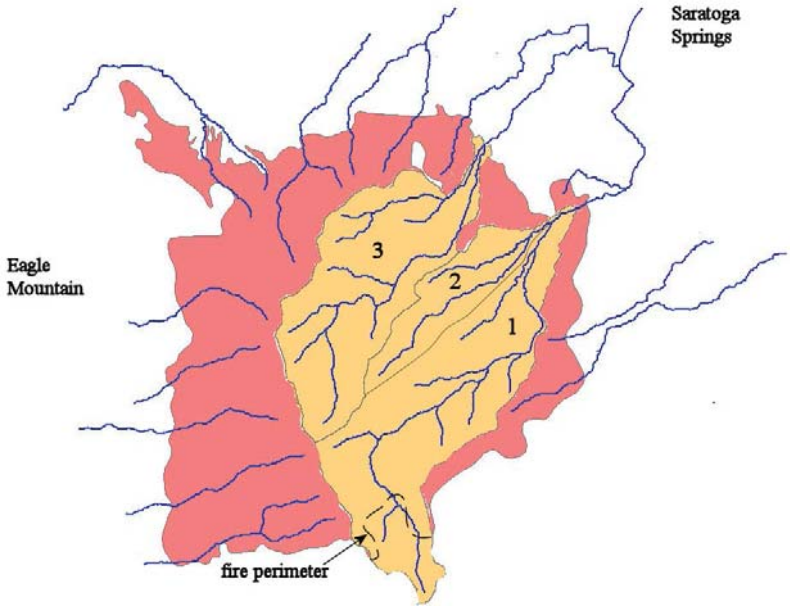

Table E–2 Burned watershed subarea input to WINTR-20

Subarea	Drainage (mi^2)	CN (Pre-fire)	CN (Post-fire)	T_c (Pre-fire) (hrs	T_c (Post-fire) (hrs)
1	1.81	62	74	0.92	0.85
2	0.60	74	80	0.40	0.37
1 + 2	2.50	65	75	1.00	0.92

Post-Fire CN Modification

Post-fire CNs were selected based on Goodrich et al. (2005), which stated that, "there [is] a 15-percent reduction in cover for low-severity burns, a 32-percent reduction for moderate-severity burns, and a 50-percent reduction for high-severity burns" (fig. E–10).

Table E–3 shows the CN increase from pre-fire to post-fire CN used in this study. The table associates these with the standard National Land Cover Dataset (NLCD) and hydrologic soil groupings (hsg).

Table E–3 Increase in runoff CN from pre-fire to post-fire conditions

Burn severity	NLCD	Cover name	HSG A	HSG B	HSG C	HSG D
Low	41	Deciduous forest	4	5	3	2
	42	Evergreen forest	4	16	10	8
	43	Mixed forest	4	5	3	2
	51	Shrubland	2	2	1	1
Moderate	41	Deciduous forest	10	10	5	5
	42	Evergreen forest	10	21	12	11
	43	Mixed forest	10	10	5	5
	51	Shrubland	5	5	3	2
High	41	Deciduous forest	15	16	8	7
	42	Evergreen forest	15	27	15	13
	43	Mixed forest	15	16	8	7
	51	Shrubland	10	11	6	3

Figure E–10 CN from cover, for hydrologic soil groups (Goodrich et al. 2005)

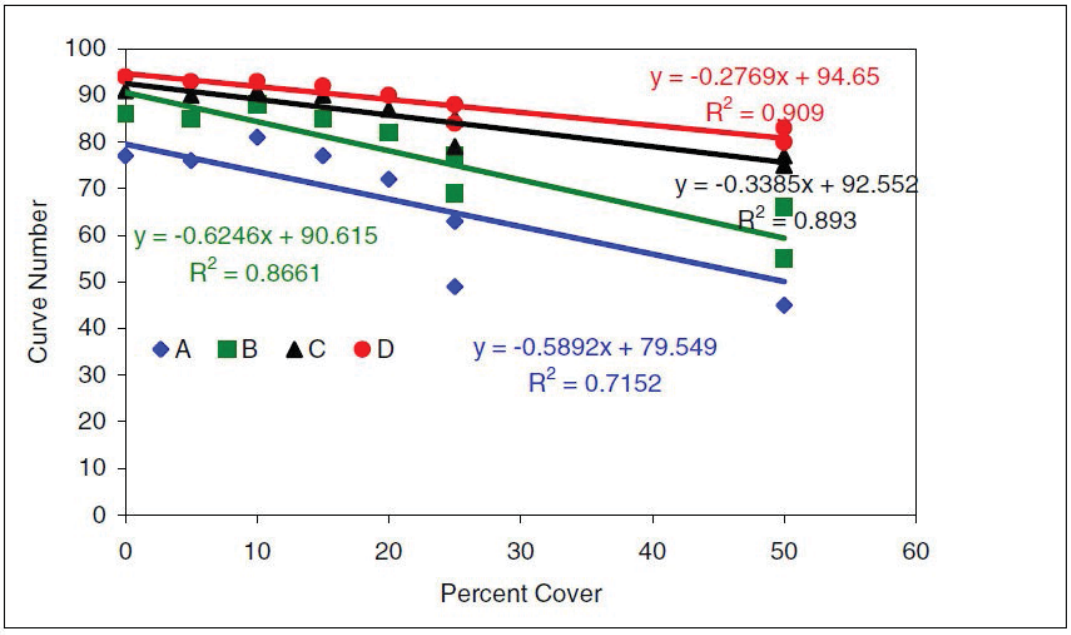

Post-Fire T_c ModificationT_c was adjusted using McLin et al. (2001), which suggest that lag time decreases from the pre-burn to post-burn condition as a result of increase in CN (fig. E-11). Note that this depends on channel blockages caused by the fire, and frequency that the watershed experiences wildfire. Channel blockages can possibly increase lag times. In this case, however, the watershed cover is generally mixed with deciduous forest and low-lying shrubs and no channel blockages were assumed. Furthermore, the roughness of the watershed was assumed to decrease as a result of fire. For this case study, the following rule of thumb was adopted for changes in runoff velocity and associated change in time of concentration: velocity increases 0.5 feet per second for low severity burns, 1.0 feet per second for moderate severity burns, and 1.5 feet per second for high severity burns.

AGWA

The AGWA model was used to model sediment rates. AGWA has a GIS interface and uses one of two routines to route runoff using the kinematic wave equation in the submodel KINEROS2. In AGWA the landscape, including land uses and management practices, are handled by the submodel SWAT. Table E–4 shows output parameters for KINEROS and SWAT. Although AGWA produces both flow hydrographs and sedimentation rates, only the latter was used for the current study.

Figure E–11 Interdependency of CN and lag time, Cerro Grande wildfire (McLin et al. 2001)

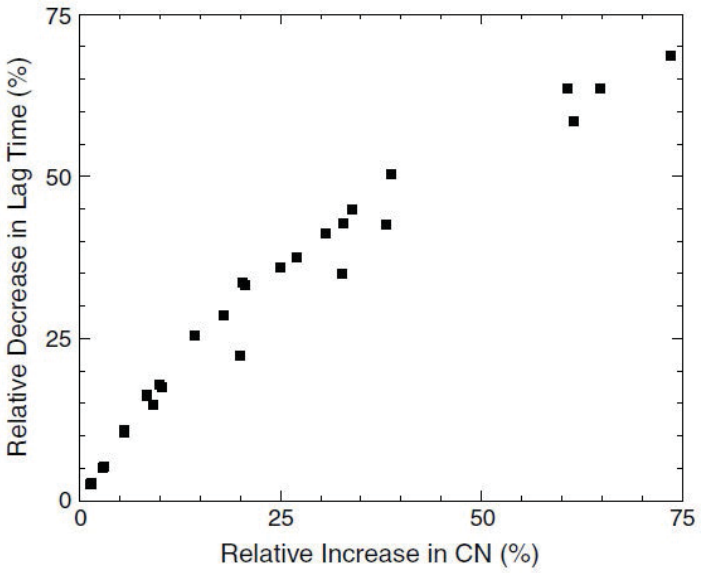

Table E–4 Output variables available in AGWA

KINEROS - ■ Infiltration (mm; m3/km), ■ Infiltration (in; ac-ft/mi), ■ Runoff (mm), Runoff (m3), ■ Sediment yield (kg/ha), ■ Peak flow (m3/s), Peak flow (mm/hr), ■ Sediment discharge (kg/s)	SWAT-■ Channel Discharge (m3/day), ■ ET (mm), ■ Percolation (mm), Surface runoff (mm), ■ Transmission loss (mm), ■ Water yield (mm), ■ Sediment yield (t/ha), ■ Precipitation (mm)

Bulking

Another way to estimate sedimentation is to consider typical runoff bulking factors for recently burned watersheds. This was done to further support concentration volumes that were deposited on the alluvial fan. Considering a 20-percent bulking factor, an event sedimentation volume can be estimated and applied to WinTR-20 post fire-results.

Western Regional Equation

The empirical Western United States regression model to estimate fire-related debris-flow volumes (Gartner et al. 2008) was used to estimate post fire sediment. The equation used is presented below (eq. E–1). The Western United States regression model to estimate fire-related debris-flow volumes (Gartner et al. 2008) was taken from the Giraud and Castleton (2009) investigation.

$$\ln V = 0.59 \ln S + 0.65\sqrt{B} + 0.18\sqrt{R} + 7.21 \qquad \text{eq. E–1}$$

where—V= volume (cubic meters)

S= basin area with slopes great than or equal to 30 percent (square kilometers)

B = basin area burned at moderate and high severity (square kilometers), and

R = total storm rainfall (millimeters)

Comparative Analysis to Existing Studies

Figure E–12 from McLin et al. (2001) illustrates that the change in peak discharge per unit area caused by wildfire can be quite large, therefore the pre- and post-fire ranges from figure E–12 were considered.

Figure E–12 Comparison of observed and simulated pre-fire and post-fire peak discharges per unit drainage basin area in New Mexico (McLin et al. 2001)

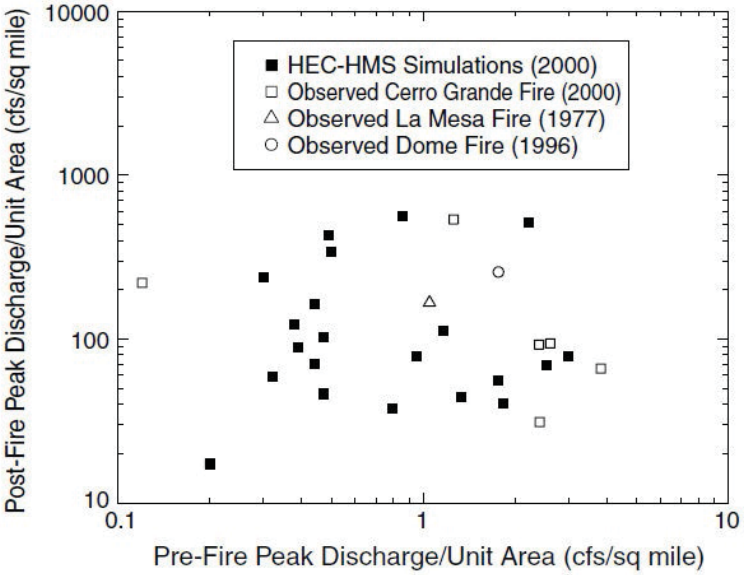

Regional Equations

The regression equations of Cannon and Gartner (2005) were also used to estimate post-fire flow. Since the Saratoga Springs watershed is sedimentary, the regression equation (eq. E–2) from Cannon and Gartner (2005) was used to compute an estimated peak discharge. Since the equation units are SI, conversions are required. For the Saratoga Springs watershed, 2.5 square miles converts to 6.47 square kilometers.

$$Q_p = 17 A_b^{0.4} \qquad r^2 = 0.42 \qquad \text{eq. E–2}$$

Bridges Map

The Bridges (1973) map entitled "Estimated Sediment Yield Rates for the State of Utah" references many data sources as part of the map, including the following:

- Great Basin Upper Colorado and Lower Colorado Regions, Comprehensive Framework Study, Appendix VIII, "Water Management," June 1971, Pacific Southwest Inter-Agency Committee/Water Resources Council
- Utah State soils map and soil descriptions
- Reservoir surveys by SCS and USBR
- Suspended load measurements by USGS, USGR, and SCS
- Watershed studies by SCS
- General knowledge of the State from regular SCS program work, in which the author notes, "Do not use these rates to determine sediment yields at specific sites. Large variations in sediment rates may occur within the delineated areas."

According to the USDA Soil Conservation Service map (Bridges 1973), the sediment yield for the Saratoga watershed ranges between 0.1-0.2 acre-feet per square mile per year with 60 percent sheet and rill erosion and 40 percent channel and gully erosion.

The range of erosion rates for the Saratoga Springs watershed from the 1973 map are plotted (fig. E–13). On the graph, the red squares represent the acre-feet per square mile per year rate that correlates to the tons for 2.5 square miles, burn condition. The blue diamonds on the graph show values assuming a 0.45 acre-feet per square mile per year rate plotted in total tons, a conservative pre-fire condition. Finally, the green triangles represent the breakdown of erosion types (60 percent sheet and rill erosion, 60 percent other colloidal material, 40 percent channel and gully erosion), a post-fire condition.

Figure E–13 Range of annual erosion rates from Bridges (1973)

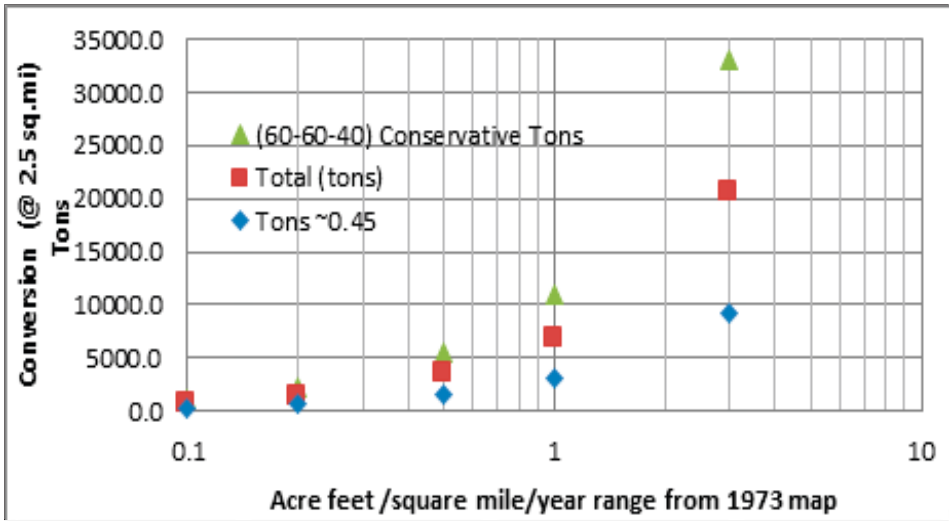

Results

WinTR-20 Pre- and Post Fire—The WinTR-20 provides pre-fire flow calculations that correlated well to the USGS stream gages CSM provided in figure E–8. Table E–5 below illustrates these results. The less frequent return intervals from WinTR-20 pre-fire results are higher and the more frequent return intervals are lower than USGS calculated CSM. For estimation purposes, the upper results for the 25-year (4-percent chance), 50-year (2-percent chance) and 100-year (1-percent chance) events will be focused on during the rest of the paper. Table E–6 reflects the pre- and post- fire peak discharges.

The WinTR-20 output in figure E–14 shows the considerable increase in runoff peaks and volumes due to the fire. The peaks are predicted to more than double, with the 25-year (4-percent chance) event (red dashed for post-fire versus black dashed for pre-fire) rising from 71 cfs to 342 cfs. The runoff volume (represented by the area under each curve and in table E–7) is predicted to increase runoff from the pre-fire to post-fire event, 192 percent to 122 percent for the 25-year to 100-year events.

Table E–5 CFS per square mile (CSM) from WinTR-20 pre-fire results and selected stream gages

	2-year (50%-chance) (CSM)	5-year (20%-chance) (CSM	10-year (10%-chance) (CSM)	25-year (4%-chance) (CSM)	50-year (2%-chance) (CSM)	100-year (1%-chance) (CSM)
WinTR-20 pre-fire	0	2.5	6.8	28.4	58	100.8
Observed CSM from figure 8	~5	12	<20	30	45	60

Table E–6 Burned watershed pre-fire and post-fire peak flow output from WinTR-20

Subarea	2-year (cfs)	5-year (cfs)	10-year (cfs)	25-year (cfs)	50-year (cfs)	100-year (cfs)
1 (pre-fire)	0	0	0	25	65	127
1 (post-fire)	14	57	118	234	359	514
2 (pre-fire)	6	29	62	126	195	280
2 (post-fire)	39	92	149	248	347	466
1+2 (pre-fire)	0	6	17	71	145	252
1+2 (post-fire)	26	92	179	342	516	728

Figure E–14 Burned watershed pre-fire and post-fire hydrograph from WinTR-20

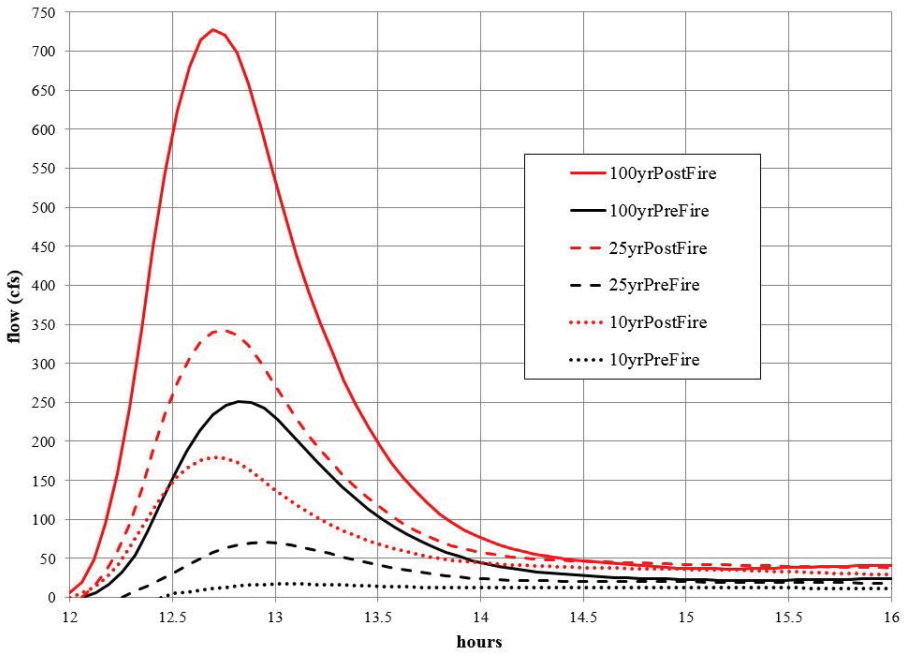

Table E–7 Storm totals runoff for various recurrence intervals, input to WinTR-20 and post-fire runoff values for subarea 1+2

Percent Chance	2-year (50%-chance)	5-year (25%-chance)	10-year (10%-chance)	25-year (4%-chance)	50-year (2%-chance)	100-year (1%-chance)	200-year (0.5%-chance)	500-year (0.2%-chance)
Pre-fire run-off (inches) Subarea 1+2	0.01	0.03	0.07	0.13	0.19	0.27	0.35	0.48
Post-fire run-off (inches) Subarea 1+2	0.09	0.17	0.25	0.38	0.48	0.60	0.73	0.92
Pre-fire run-off in acre feet over 2.5 sq. mi	1	4	9	17	25	36	47	64
Post-fire run-off in acre feet over 2.5 sq. mi	12	23	33	51	64	80	97	123

AGWA

The sediment for the 25-year (4-percent chance) storm was estimated to be 10,303 tons and the 100-year (1-percent chance event) storm was estimated to be 27,897 tons.

Bulking

An event sedimentation volume was estimated considering a 20-percent bulking factor on the WinTR-20 post-fire results. The information in table E–8 was derived by taking the post-fire clear flow hydrographs of figure E–14, from WinTR-20, and considering the event sedimentation rate to be 20 percent at each time-step. The area under the sedimentation hydrograph provided a volume, which was converted to tons by assuming a sediment unit weight of 108 pounds per cubic foot in table E–8.

Western United States Regression Model

The empirical Western United States regression model to estimate fire-related debris-flow volumes (Gartner et al. 2008) was estimated to be between 34,550 to 51,182 tons for the 2- to 100-year (50-percent to 1-percent chance) rainfall events. These numbers are high, since the model assumes that watersheds typically have moderate to high severity burns.

Table E–9 shows the WinTR-20 pre-fire and post-fire peaks (in cfs per square mile) for comparison with figure E–12. The current case study results would plot generally lower on the figure than the New Mexico watersheds, the WinTR-20 results are considered reasonable.

Regional Equations

The regression equations of Cannon and Gartner (2005) after inserting 6.47 as Ab into the equation results in a Qp of 35.88 cubic meters per second, or a Qp of 1267 cfs after converting to English units. This results in 506 CSM, and the WinTR-20 post-fire result is 728 cfs or 291 CSM.

Table E–8 Burned watershed post-fire event total sediment runoff in tons

Event totals	25-year (4% chance) (tons)	50-year (2% chance) (tons)	100-year (1% chance) (tons)
Sediment	23,705	29,943	37,429

Table E–9 Saratoga Springs burned watershed pre-fire and post-fire peaks (CSM) from WinTR-20

Flood	25-year (4% chance)	50-year (2% chance)	100-year (1% chance)
Pre-Fire (CSM)	28.4	58	100.8
Post-Fire (CSM	136.8	206.4	291.2

Conclusions

Pre-fire runoff modeling with WinTR-20 was an iterative process, making CN modifications and considering data from USGS stream gages in the region. Post-fire CNs were then applied and time of concentration lowered. These post fire impacts resulted in both higher peaks and larger volumes of runoff. AGWA, a 20-percent bulking to WinTR-20 post fire results, and the Western Regional Equation overall correlated well. These results were compared to McLin et al. (2001) pre- and post-fire peak discharges per unit drainage basin area and to a range of potential erosion values on the Bridges sedimentation map (1973).

Typically, one would think of using the peak discharge of post-fire analysis using WinTR-20, while increasing the CN and decreasing time of concentration. The peak discharge during the flood event and high water marks were observed as being in range for the post-fire WinTR-20 results. The Cannon and Gartner (2005) estimate of over 1,200 cfs may be reasonable and could be used for preliminary or lower and upper bound limits; the lower limit at 75 percent of the total, and the upper at 100 percent of the total.

The range of sediment, bulking and mud slurries were in a range of 10,000 tons to over 50,000 tons for the post-fire 25- to 100-year (4-percent to 1-percent chance) events. The AGWA range is between 10,000 and 28,000 tons for the 25- to 100-year (50-percent to 1-percent chance) post-fire event. The bulking at 20 percent is 23,000 to 37,000 tons for the post-fire event. The western regional equation produced a number of 34,600 to 51,200 tons. Between the sand, colloidal, and bedload the percentages can vary. For the sediment, sand and colloidal the numbers above could still be a low estimate. Bedload at either 1:3 or 1:10 ratio could be still be small. However, due to the system being flushed by previous storm events, these ratios may be accurate. A range of 5,000 to 17,000 tons could be accounted for bedload.

References

Arnold, J. G., D. N. Moriasi, P. W. Gassman, K. C. Abbaspour, M. J. White, R. Srinivasan, C. Santhi, R. D. Harmel, A. van Griensven, M. W. Van Liew, N. Kannan, M. K. Jha, SWAT: Model Use, Calibration and Validation. Transactions of the ASABE. 55(4): 1491-1508.

Bridges, B.L. 1973. Map: Estimated sediment yield for the State of Utah. Erosion and Sedimentation, Western U.S. Water Plan, prepared by SCS August 1973.

Cannon, S.H. and J.E. Gartner. 2005. Wildfire-related debris flow from a hazards perspective, in Jakob, M. and Hungr, O., Debris-flows hazards and related phenomena: Chichester, United Kingdom, Springer-Praxis Books, p. 362–385.

Fry, J., G. Xian, S. Jin, J. Dewitz, C. Homer, L. Yang, C. Barnes, N. Herold, and J. Wickham, 2011. Completion of the 2006 National Land Cover Database for the Conterminous United States, PE&RS, Vol. 77(9):858-864.

Gartner, J.E., S.H. Cannon, P.M. Santi, and V.G. deWolfe. 2008. Empirical models to predict the volumes of debris flows generated by recently burned basins in the western U.S. Geomorphology, 96, 339-354.

Giraud, R.E., and J.J. Castleton. 2009. Estimation of Potential Debris-Flow volumes for Centerville Canyon, Davis County, Utah. Report of Investigation 267 Utah Geological Survey, Utah Department of Natural Resources, Salt Lake City, UT.

Goodrich, D.C., H. E. Canfield, I.S. Burns, D.J. Semmens, S.N. Miller, M. Hernandez, L.R. Levick, D.P. Guertin, and W.G. Kepner. 2005. Rapid Post-Fire Hydrologic Watershed Assessment using the AGWA GIS based Hydrologic Modeling Tool. Proc. ASCE Watershed Manage. Conf., July 19-22, Williamsburg, VA.

Kenney, T.A., C.D. Wilkowske, and S.J. Wright. 2007. Methods for estimating magnitude and frequency of peak flows for natural streams in Utah: U.S. Geological Survey Scientific Investigations Report 2007-5158, 28 p.

McLin, S. G., E.P. Springer, and L.J. Lane. 2001. Predicting floodplain boundary changes following the Cerro Grande wildfire. Hydrological Proc., 15(15): 2967-2980.

Smith, R.E., D.C. Goodrich, and J.N. Quinton. 1995. Dynamic, distributed simulation of watershed erosion: The KINEROS2 and EUROSEM models, Journal of Soil and Water Conservation, 50(5): 517-520.

USDA-ARS (U.S. Department of Agriculture-Agricultural Research Service). 2014. AGWA (Automated Geospatial Watershed Assessment Tool) Web site, through the ARS Southwest Watershed Research Center, Tuscon, AZ, http://www.tucson.ars.ag.gov/agwa/.

USDA-NRCS(a) (U.S. Department of Agriculture-Natural Resources Conservation Service), 2004. WinTR-20 User Guide. Available at http://go.usa.gov/KoZ/. Accessed in April 2013.

USDA-NRCS(b), 2004. National Engineering Handbook, Part 630 Hydrology, Chapter 9, Hydrologic Soil-Cover Complexes.

USDA-NRCS(c), 2012. Soil Survey Geographic (SSURGO) Database. Available online at http://sdmdataaccess.nrcs.usda.gov/. Accessed (2012).

Woolhiser, D.A., R.E. Smith, and D.C. Goodrich. 1990. KINEROS, A kinematic runoff and erosion model: Documentation and User Manual. U.S. Department of Agriculture, Agricultural Research Service, ARS-77, 130 pp.